The University Of Sheffield.

Staphylococcus aureus cell and infection dynamics: The road to novel prophylaxis and therapy

By:

Oliver T Carnell BA (Hons), MRes.

(University of Oxford, University of Manchester)

A thesis submitted for the degree of Doctor of Philosophy

September 2020

Department of Molecular Biology and Biotechnology, University of Sheffield,

Firth Court, Western Bank, Sheffield, S10 2TN

Abstract

Staphylococcus aureus remains a leading cause of nosocomial infections and sepsis and is becoming increasingly difficult to treat due to antimicrobial resistance. Development of novel antibiotics is hampered by insufficient understanding of *S. aureus* cell components as potential targets. Prevention of infection by vaccination is an ideal goal. However, natural infection doesn't grant immunity to *S. aureus* and there is no known correlate of protection. Numerous vaccine candidates have reached clinical trials, but all have failed to yield sufficient protection despite promising pre-clinical data. Lack of understanding surrounding *S. aureus* pathogenesis has culminated in this poor translation of pre-clinical models to human infection.

This thesis approaches research for therapeutic development at the level of the bacteria and the host and their interactions. The essential *S. aureus* division protein DivIC was found to bind to wall teichoic acid, through pulldown assays using cell wall preparations from a range of *S. aureus* genetic mutants, and bacterial species. My work indicates this interaction may be important for *S. aureus* cell division and could potentially be a future target for logical antibiotic design.

From the host perspective, the NGF-β immune pathway was found to lack importance in the mammalian infection model, compared to its reported significance in zebrafish, through infection of transgenic mouse lines.

Finally, augmentation of *S. aureus* infection through use of pro-infectious agents such as peptidoglycan was recently reported. This phenomenon was shown to require concomitant administration of peptidoglycan thereby improving our understanding of *S. aureus* pathogenesis. This form of infection was also shown to be immunologically distinct from challenge with bacteria alone which potentially delineates between the models for bacteraemia and sepsis and increases the utility of the mouse as a preclinical model for *S. aureus* vaccine development.

Overall, my multipronged approach has given rationale for DivIC and WTA to be interrogated as potential antibiotic targes (or antigens) and improved upon the mouse model to translate future research into new approaches for controlling this important pathogen.

Acknowledgments

I would like to thank my supervisor, Professor Simon Foster, for guiding me through the PhD process and my funders, the BBSRC, for the incredible opportunity to realise the dream of my high school self in attaining a PhD. Not only has this experience given me a great scientific backing in microbiology, it has left me with skills that will serve me well wherever I end up next.

What I thought was going to be a journey of immunological discovery quickly turned into the trials & (mis)adventures of DivIC, but my PhD has been a thoroughly valuable and enjoyable experience. It has also been difficult and arguably I wouldn't have finished it without a number of people. In this instance my greatest thanks likely have to go to my conference companion and the other half of "Joliver": Josh. Thanks in short for teaching enough microbiology to get started, putting up with my immunological laments and providing pints and a clear head for my melodramatic musing over the logistics of quitting. Also Thank you to pretty much everyone else in the F18 for teaching, helping and drinking with me over the past 4 years. Thank you all for putting up with my untidy bench and the coffees that were clearly too strong for most. I would also like to thank the other mouse people, Josh, Josie & Daria for their company and assistance in long experiments up in the BSU. Thank you also to the team in the biological services unit, without whom none of the mouse work in this thesis would be possible.

My family are a big part of my life and I wouldn't be the person (and scientist) that I am without their lifelong influence. Therefore, I'd like to thank my mum and dad, Ben, Charlotte and the grandparents for their constant emotional (and occasionally financial/alcohol based) support. I'd also like to thank my friends in Sheffield, Holly, Josh, Saira *et al.* who made the city a much more enjoyable place to live. Elsewhere in the country Amanda, David, Paddy, Sam, Becca and co. thank you for providing escape from the Sheffield/PhD bubble and joining me in being drunken reprobates when the occasion called for it.

List of abbreviations

~	Approximately
Alum	Alhydrogel® aluminium based adjuvant
AF647	Alexa Fluor 647
AMR	Antimicrobial resistance
APS	Ammonium persulphate
BSA	Bovine serum albumin
CCL2	C-C motif Chemokine ligand 2
CCL4	C-C motif Chemokine ligand 4
CFU	Colony forming units
ClfA	Clumping factor A
CP5	Capsular polysaccharide serotype 5
CP8	Capsular polysaccharide serotype 8
CpG	deoxy-cytidylate-phosphate-deoxy-guanylate DNA
Cre	Cre recombinase
CXCL1	C-X-C motif Chemokine ligand 1
D-Ala	D-Alanine
dH_2O	Distilled water
DivIC-AF647	Alexa Fluor 647 labelled DivIC
DivIC-Cy2	Cy2 labelled DivIC
DTT	Dithiothreitol
EDTA	Ethylenediamine tetra-acetic acid
GlcNAc	N-acetyl glucosamine
HF	Hydrofluoric acid
Hla	α-Hemolysin
HPLC	High performance liquid chromatography
IFN	Interferon
IL	Interleukin
IPTG	Isopropyl β-D-1-thiogalactopyranoside
Kan	Kanamycin
LB	Luria Bertani broth
LCP	LytR-CpsA-Psr
LTA	Lipoteichoic acid
ManNAc	N-acetylmannosamine
MRSA	Methicillin resistant *Staphylococcus aureus*

MSSA	Methicillin sensitive *Staphylococcus aureus*
MST	Microscale thermophoresis
MurNAc	N-acetylmuramic acid
MWCO	Molecular weight cut off
NF-kB	Nuclear Factor kappa-light-chain-enhancer of activated B cells
NGF-β	Nerve growth factor β
NLRP3	NOD-, LRR- and pyrin domain-containing 3
NMWL	Nominal molecular weight limit
NOD2	nucleotide-binding oligomerisation domain 2
NTML	Nebraska transposon mutant library
OD600	Optical density measured at 600 nm
$p75^{NTR}$	p75-neurotrophin receptor
PAGE	Polyacrylamide gel electrophoresis
PAMP	Pathogen associated molecular pattern
PBP	Penicillin binding protein
PBS	Phosphate buffered saline
PCR	Polymerase chain reaction
PGN	Peptidoglycan
PIA	polysaccharide intercellular adhesin
PRR	Pattern recognition receptor
PVL	Panton-Valentine leukocidin
ROS	Reactive oxygen species
rpm	Revolutions per minute
SDS	Sodium dodecyl sulphate
Spec	Spectinomycin
SSTI	Skin and soft tissue infections
TAE	Tris-acetate EDTA
TES	Tris-EDTA NaCl
TLR	Toll-like receptor
TNF-α	Tumour necrosis factor alpha
Tris	Tris (hydroxyl methyl) aminomethane
TrkA	tropomyosine receptor kinase A
TSA	Tryptic soy agar
TSB	Tryptic soy broth
UV	Ultraviolet
v/v	Volume per volume
w/v	Weight per volume

WTA	Wall teichoic acid
x	Times
xg	Times gravity

Table of Contents

Table of Figures

List of Tables

Table of Supplementary Figures

Chapter 1:
Introduction

1.1 *Staphylococcus aureus*

Staphylococcus aureus is a gram-positive coccus that grows to approximately 1µm in diameter. The name translates to golden grapes, due to how the organism clusters in bunches and the formation of yellow colonies due to the production of the carotenoid pigments such as staphyloxanthin. Staphyloxanthin has a role in the protection of *S. aureus* against reactive oxygen species[1]. *S. aureus* is distinguished from other *Staphylococcal* species through positive DNase and coagulase tests[2].

1.2 *S. aureus* pathology & epidemiology

S. aureus is carried commensally in the nares and on the skin by approximately one third of the human population[3]. When in this commensal niche it is harmless, however, *S. aureus* is an opportunistic pathogen and can thus cause disease when it gains access to other parts of the body. *S. aureus* causes a variety of pathologies such as: sepsis, bacteraemia, pneumonia, skin & soft tissue infections (SSTI), endocarditis, food poisoning, meningitis, osteomyelitis, and toxic shock syndrome [4–7]. *S. aureus* is a leading cause of nosocomial infections[8–10] and from an economic standpoint, hospital acquired infections with *S. aureus* increases the length (and therefore cost) of hospital stay[11]. To this end, being able to effectively treat, or (ideally) prevent, these infections would greatly benefit the respective healthcare service and economy as well as the individual.

1.2.1 Skin & Soft Tissue infections

When *S. aureus* becomes overly prevalent in the skin microbiome or is present on an abrasion then it can cause a skin infection such as folliculitis and more invasive skin and soft tissue infections (SSTI) which can present as cutaneous abscesses, cellulitis, impetigo and even necrotizing fasciitis[7]. Incidence of SSTI due to *S. aureus* is on the increase with about a three-fold increase in both the USA[12] and UK[13] between the 1990s and mid 2000's. *S. aureus* establishes itself in SSTI through the expression of numerous virulence factors. Production of Panton-Valentine leukocidin (PVL) causes

lysis of neutrophils that infiltrate the cutaneous tissue in response to infection and has been linked to the ability of an *S. aureus* strain to establish SSTI[14]. However, this does not correlate well in animal models[15,16] but this could be due to the species specificity of *S. aureus* toxins[17]. Another important virulence factor in *S. aureus* SSTI is α-Hemolysin (Hla) which recognises the ADAM10 receptor on endothelial cells, keratinocytes and immune cells. Hla is a pore forming toxin which induces caspase-I mediated pyroptosis in keratinocytes which contributes to *S. aureus* invasion and penetration through keratinocytes[18]. Levels of Hla production have also been correlated with severity of *S. aureus* skin infections in mice[19] and rabbits[15]. Phenol soluble modulins (PSM) are another virulence factor that can perturb the eukaryotic membrane due to their amphipathic nature[20], the α-PSM is so potent it can cause lysis of immune cells in the sub-micromolar range[21]. PSM have also been implicated in SSTI severity in animal models[21,22] and *S. aureus* clinical isolates from SSTI have higher PSM expression characteristics than strain-matched clinical isolates from pneumonia[23].

1.2.2 Bacteraemia & sepsis

Bacteraemia refers to infection with the presence of viable bacteria in the bloodstream and is one of the most infamous incidences of *S. aureus* infection due to its potential to result in huge immune reaction, sepsis, and multiple organ failure. Despite the rates of MRSA bacteraemia falling thanks to increased surveillance[24] and control measures[25], the leading gram-positive causative agent of bacteraemia is still *S. aureus*[26–28]. Bacteraemia can occur whenever bacteria gain access to the bloodstream with incidence increasing with the onset of medical practices involving catheterization. Free *S. aureus* in the bloodstream are mostly taken up by the Kupffer cells, which are macrophages of the liver[29]. The majority of the bacteria are cleared but those that survive within the macrophage can escape and either grow extracellularly and form a micro-abscess or be phagocytosed by other immune cells which *S. aureus* can use to disseminate throughout the host[29–31]

S. aureus further dysregulates haemostasis through initiating extraneous blood clotting. It does this through secretion of two factors: coagulase (Coa) and von Willebrand factor (vWbf). These secreted proteins bind host prothrombin activating the clotting cascade which leads to the formation of fibrin clots to which *S. aureus* can bind via ClfA thereby forming infectious microthrombi[32]. These fibrin clots further protect *S. aureus* from

opsonisation but also provide a potential vehicle for dissemination throughout the organism should a thrombus become an embolus. This scenario is aggravated as the previously mentioned pore-forming Hla can bind to the ADAM10 receptor on endothelium which causes leaky vasculature[33]. A counter-intuitive effect of the bacterially-mandated clotting is a greater propensity for haemorrhage during bacteraemia because the clotting components have been depleted[34]. This allows for systemic spread of *S. aureus* which can lead to multiple organ failure. The continued presence of bacteria and their PAMPs in the bloodstream and endothelial damage releasing damage associated molecular patterns (DAMPs) over activates the immune system resulting in conflicting anti- and pro-inflammatory signalling which is a signature of sepsis[34].

1.3 *S. aureus* antimicrobial resistance (AMR)

Treating bacterial infections, including *S. aureus* infections, has become increasingly difficult due to the emergence, and spread of AMR (Fig 1.1). There has been speculation that society is entering a post-antibiotic era with very few new classes of antibiotics reaching clinical trials[35] and estimates of 10 million deaths from antibiotic resistant infections by 2050[36]. This is arguably because production of a new antibiotic is an economically thankless task; given the threat of resistance, proper antimicrobial stewardship would dictate that a novel class of antibiotics would only be used as a last resort thereby reducing financial return during the lifetime of a patent. In addition, antibiotics tend to be a short course of treatment further reducing the economic incentive for the pharmaceutical companies which might develop novel antibiotics to do so[37,38].

The antibiotic resistance issue became apparent in *S. aureus* after clinical introduction of the first beta lactam antibiotic: penicillin[39]. The beta-lactam class of antibiotics work by blocking the transpeptidase activity of PBP2. Penicillin resistance was discovered in 1942 shortly after the clinical introduction of the antibiotic[39]. The resistance mechanism was a beta-lactamase enzyme that cleaved the beta-lactam ring of penicillin, this led to research which developed methicillin which could kill penicillin resistant bacteria. Methicillin resistant *S. aureus* (MRSA) was first described in the 1963 despite methicillin only coming into clinical use in 1959[40,41]. It was subsequently discovered the mechanism of resistance to methicillin was conferred by mobile genetic elements

including *mecA*, which encodes the alternative PBP2a which the beta-lactam antibiotics cannot inhibit. This resistance is clearly an issue as meta-analysis has shown there is a greater risk of mortality due to infection with MRSA than methicillin-sensitive *S. aureus* (MSSA)[42].

Another antibiotic choice for the treatment of *S. aureus* is vancomycin which also targets cell wall synthesis by binding to the D-ala-D-ala motif of lipid II thereby blocking peptidoglycan cross-linking by binding to the necessary moiety and inhibiting transglycosylation through steric hindrance[43]. This clearly bypasses MecA induced antibiotic resistance by targeting the substrate of transpeptidation rather than the transpeptidase enzyme. However, fully vancomycin resistant *S. aureus* was described in 2003 with the *vanA* cassette that altered the peptide stem to have a D-ala-D-lactate motif[44]. Of special concern is the fact this cassette was discovered in *Enterococci* previously[45], thereby highlighting the risk of horizontal gene transfer for the spread of antibiotic resistance even between genera. Beta lactam antibiotics and glycopeptides like vancomycin, are some of the conventional treatment choices for *S. aureus* infection, yet resistance against these is becoming increasingly widespread as is resistance to the variety of other antibiotic classes. However, antibiotic discovery has slowed with the majority of new compounds in the last few decades being synthetic alterations or reformulations of existing antibiotics.

There was renewed hope in novel antibiotic development due to the recent discovery of teixobactin[46] which was made possible through new methods of culturing soil bacteria such as *Eleftheria terrae* which produces teixobactin. Teixobactins mechanism of action is to bind to lipid II and potentially form aggregates within the bacterial membrane[46,47] and this molecule has shown great antibiotic action against gram-positive pathogens including MRSA[46]. Given the microbial origins of teixobactin it is tempting to assume resistance mechanisms have also co-evolved and these would be selected for with increased medicinal use. This likelihood is supported by the fact that recently identified resistance cassettes can also be identified in a range of historically preserved bacterial DNA samples which predate clinical antibiotic use[48,49]. There is also cause for concern in the development of synthetic antibiotics as most compound libraries for drug screening are stacked towards molecules that fit criteria set out by Lipinski *et al*. that dictate suitability for oral availability[37] despite Lipinski *et al*. stating these chemical

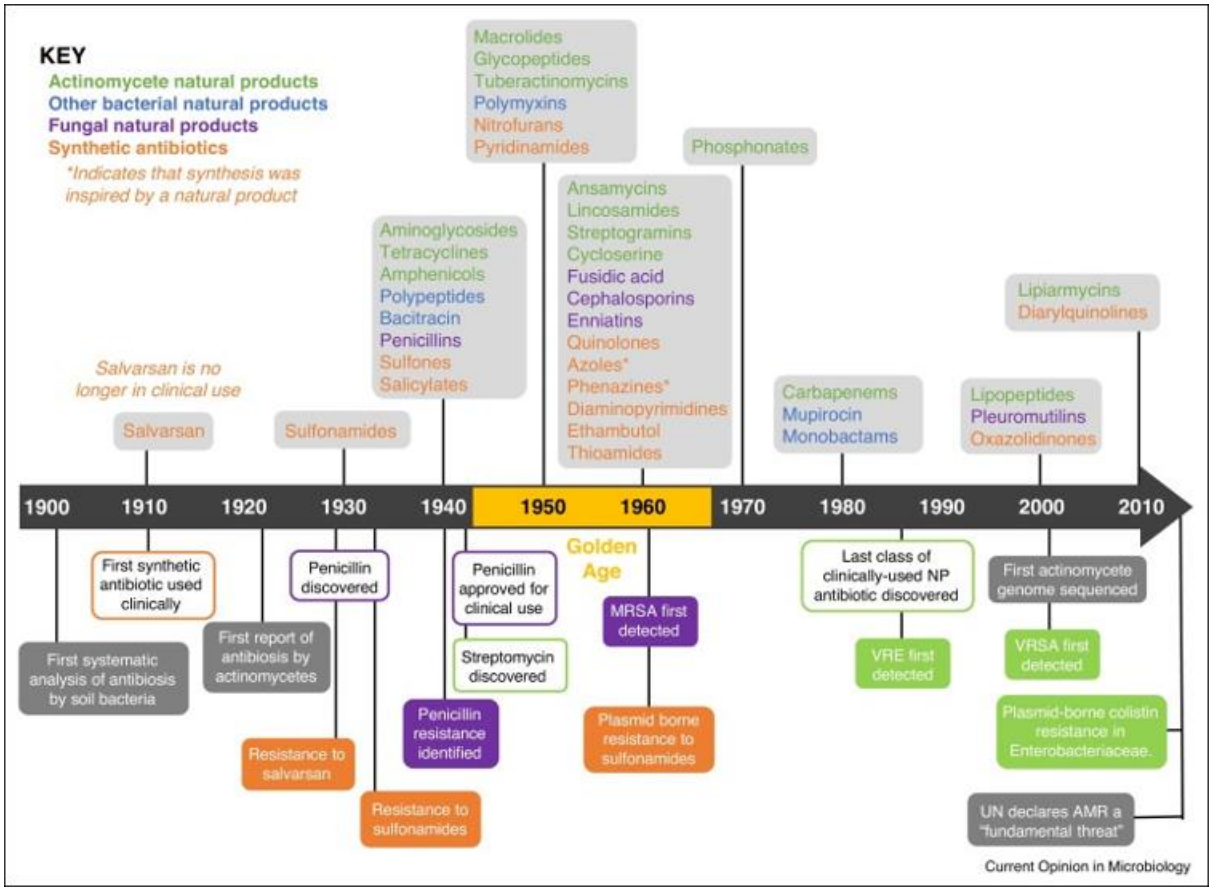

Figure 1.1 Antibiotic discovery and antibiotic resistance timeline.
Timeline showing discovery and introduction of new antibiotic to the clinic and documented emergence of resistance. Methicillin-resistant *S. aureus* (MRSA), vancomycin-resistant enterococci (VRE), vancomycin-resistant *S. aureus* (VRSA) and plasmid-borne colistin resistance in Enterobacteriaceae. Taken from Hutchings *et al.* (2019)[50].

restrictions were not suitable for antibiotics[51]. There is even some evidence that certain bacteria are developing increased tolerance to alcohol based disinfectants[52].

Antibiotics as a therapeutic route are arguably doomed to fail eventually, simply because our rate of innovation and antibiotic discovery will never be able to keep pace with evolution in an organism which has a generation time of 30 minutes. Therefore, we as a scientific community need to change our approach to antimicrobial development to make drugs which will stop bacterial colonisation and pathogenesis without inducing a large evolutionary selection pressure. This approach is confounded by our lack of understanding surrounding the precise details of bacterial physiology and cell cycles. Greater study of the plethora of cell division proteins in *S. aureus* might allow us to select better targets for logical antibiotic design.

1.4 Cell envelope

The morphology, maintenance of viability and interaction of *S. aureus* with its environment is governed by its cell wall. The cell wall is made of various constituents, the synthesis of which must be coordinated (Fig 1.2A). Furthermore, this is the part of the bacterium that interacts with the environment and can thus be easily targeted by both antibiotic therapies and the immune system.

1.4.1 Peptidoglycan

S. aureus possesses a thick peptidoglycan cell wall and a single phospholipid cell membrane as opposed to two membranes with a thin, periplasmic, peptidoglycan cell wall as seen in Gram-negative bacteria. The glycan backbone of the peptidoglycan is made up of N-acetylglucosamine (GlcNAc), N-acetylmuramic acid (MurNAc) repeating units[53]. In *S. aureus* these glycan backbones are on average 6 disaccharides long[54], but glycan length varies between bacterial species. The GlcNAc and MurNAc are linked through 1,4-glycosidic bonds and the MurNAc residues carry L-alanine, D-glutamine, L-lysine, D-alanyl-D-alanyl pentapeptide side chains[55]. The glycan backbones are crosslinked via a pentaglycine bridge between the 4th (D-alanine) residue on one chain and the 3rd (L-lysine) residue on another chain.

The precursors for peptidoglycan are synthesised in the cytoplasm (Fig 1.2B). This begins with MurA and MurB acting in conjunction to convert UDP-GlcNAc to UDP-

MurNAc[56]. MurC-F then perform peptide synthesis independently of ribosomes to form the peptide stem. This UDP-MurNAc with a pentapeptide stem is then loaded onto undecaprenol as a lipid carrier by MraY. The precursor at this stage is referred to as lipid I and synthesis continues anchored to the interior leaflet of the cell membrane.

MurG ligates a GlcNAc to the MurNAc of lipid I thereby forming lipid II[57]. Lipid II is then modified by the FemXAB enzymes which sequentially build the pentaglycine bridge on the 3rd residue on the peptide stem[53,58]. The pentaglycine modified lipid II is then translocated to the exterior leaflet of the cell membrane by MurJ[57]. From the external leaflet of the cell membrane pentaglycine lipid II is incorporated into the glycan backbone of peptidoglycan by transglycosylation activity of PBPs and other transglycosylases such as SgtA[59,60]. The pentaglycine is crosslinked between peptide stems to become the pentaglycine bridge by the transpeptidase activity of PBPs and other potential transpeptidases[60,61]. This cross-linked peptidoglycan mesh surrounds the cell, resisting intracellular turgor pressure both providing the cell shape and stopping osmotic lysis[63]. The peptidoglycan framework can also be modified and functionalised through addition of chemical moieties which alter the surface properties of the bacterium.

A

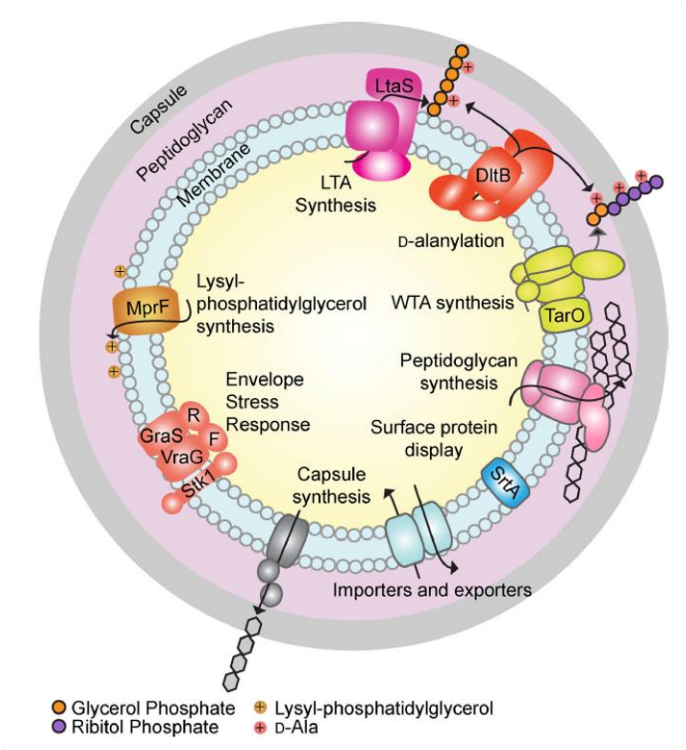

B

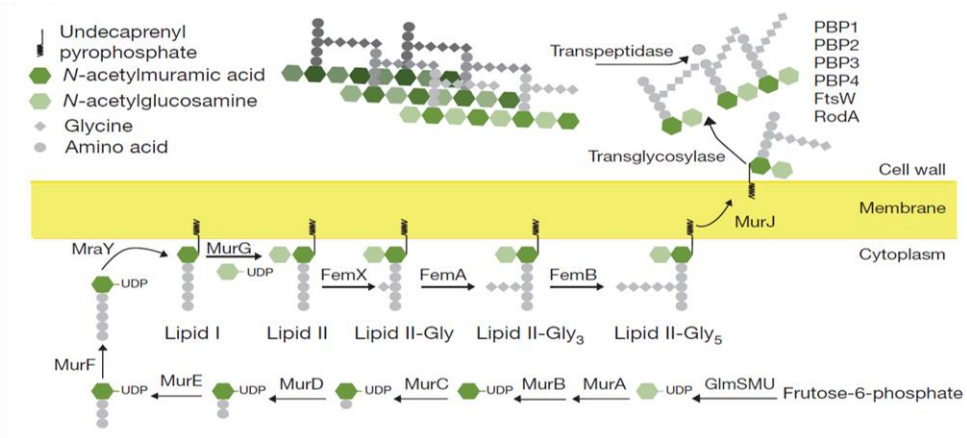

Figure 1.2 Cell envelope structure and peptidoglycan synthesis in *S. aureus*

A) The complex cell envelope is the first line of *defence* for the *S. aureus*. Major pathways involved in the synthesis of the cell envelope include capsule, peptidoglycan, and teichoic acid synthesis. *S*urface protein display systems function to tether proteins to the cell membrane or cell wall, which perform important roles in adhesion and interaction with the environment*.* Taken from Rajagopal & Walker (2017)[62].

B) Peptidoglycan is synthesised on the interior leaflet of the membrane using undecaprenol as a lipid carrier, then translocated to the exterior leaflet by MurJ before being incorporated into the cell wall by PBPs. Taken from Monteiro *et al*. (2018)[55].

Peptidoglycan is specific to bacteria and thus its synthesis makes a great target for antibiotics but also constitutes a source of pathogen associated molecular patterns (PAMPs) to be recognised by the pattern recognition receptors (PRRs) of the immune system during infection[64]. Cytoplasmic fragments of gram-positive peptidoglycan are recognised by the nucleotide-binding oligomerisation domain 2 (NOD2) of the host which induces NF-kB dependent inflammation via the Myd88 pathway[65]. Disruption of the lysosome by particulate peptidoglycan or perception of peptidoglycan breakdown products such as GlcNAc by hexokinase on the mitochondrial membrane can also activate the NOD-, LRR- and pyrin domain-containing 3 (NLRP3) inflammasome which induces pyroptosis and IL-1β secretion via the caspase pathway[66,67]. Furthermore, mammalian endothelial and innate immune cells secrete soluble peptidoglycan recognition proteins which have bactericidal effects[68–70].

1.4.2 Cell wall proteins

The peptidoglycan-based cell wall is functionalised through the addition of many cell wall proteins. Proteins which are covalently bound to the cell wall are attached by sortase enzymes[71] to the free amino group of the pentaglycine cross-bridge[72]. The major cell wall sortase in *S. aureus* is sortase A (SrtA) which ligates proteins to the cell wall through cleavage of an LPXTG motif[73], whereas sortase B (SrtB) recognises a NPQTN sorting signal[74]. The export and attachment is further regulated with some LPXTG containing proteins also possessing a YSIRK-G/S motif which targets them for export at the mid-cell during cell division[75]. Many of the cell wall anchored proteins such as ClfA, FnBPA and IsdB have roles in adhesion[76,77], colonisation[78] and pathogenicity[79,80]. This involvement with *S. aureus* pathogenesis and their surface localisation, making them amenable to targeting by antibodies, has led to cell wall anchored proteins such as these to be assessed as vaccine antigens[81,82].

1.4.3 Wall teichoic acids

Wall teichoic acids (WTA) are cell wall polysaccharides that, in *S. aureus*, are synthesised by the Tar proteins (Fig 1.3A). Synthesis of the polymer on an undecaprenol lipid carrier, on the internal leaflet of the cell membrane is initiated by TarO[83–85]. The completed WTA is exported to the external leaflet of the cell membrane by TarGH[86] and once in the periplasmic space the WTA is ligated onto MurNAc

residues of the glycan backbone by the LytR-CpsA-Psr (LCP) proteins[87–89]. The linkage unit which is ligated to the MurNAc on the peptidoglycan consists of GlcNAc, N-acetylmannosamine (ManNAc) and two glycerol moieties phosphate linked to the sugar backbone of the molecule[90,91]. The main backbone of WTA is 40-60 ribitol phosphate repeats in *S. aureus*[90]. This backbone can be modified by TarM and TarS or the Dlt proteins during production. These enzymes add α-GlcNAc, β-GlcNAc[92,93] and D-alanine[92,94] modifications respectively to the ribitol sugars in the backbone. WTA synthesis can be inactivated by the ablation of *tarO* or *tarA,* but mutations in the remainder of the pathway are conditionally lethal based on the presence of the initial TarO step[95]. This is because undecaprenol is also used in the peptidoglycan synthesis pathway and TarO in WTA synthesis commits this molecule to WTA leading to the undecaprenol becoming sequestered in a non-functional synthetic pathway if the downstream synthesis is interrupted.

WTA in *S. aureus* can make up to half the dry weight of the cell wall[91]. Numerous functions have been suggested for WTA in *S. aureus*. The ribitol phosphate backbone is anionic and is therefore suggested as being involved in scavenging cations[96]. WTA also protect the underlying peptidoglycan framework as they have been shown to be involved in resistance to β-lactam antibiotics[97] and to resist cleavage by peptidoglycan hydrolases[98,99]. WTA have also been implicated in regulating cell shape in rod-shaped bacteria whereby a loss of WTA causes them to become spherical[100–102]. And more recently and importantly WTA have been proposed to help coordinate cell division and peptidoglycan synthesis in *S. aureus* as PBP4-based crosslinking seems to be controlled by WTA[103].

WTA also play a significant role in the pathogenesis of *S. aureus*. WTA are involved in colonisation of commensal spaces such as the nares but has also demonstrated roles in *in vivo* adhesion with WTA-deficient strains less able to colonise the heart valves and cause endocarditis in rabbits[104]. WTA also contribute to the spread of antimicrobial resistance and virulence cassettes as they are the ligand to which many phages bind. Phages can directly facilitate horizontal gene transfer.

S. aureus WTA are clearly immunogenic as purified WTA or synthetic tetrameric ribitol-phosphate can induce abscess formation[56] or IL-6 production respectively[55,] . D-alanylation of the synthetic ribitol phosphate tetramer was necessary for IL-6 production

but this cytokine production was blocked by addition of a β-GlcNac motif[107]. The β-GlcNac modification is recognised by langerin[108] and mannose binding lectin[109]. Therefore, there is an interesting interplay between the presence of this molecule reducing inflammation but also allowing *S. aureus* to be perceived by the immune system.

This moiety is shown to be important for *S. aureus* in infection as a strain that expressed mostly α-GlcNAc modified WTA *in vitro* switched to expression of mostly β-GlcNAc modified WTA *in vivo* in an animal model of infection[92]. This shows that *S. aureus* is dynamically altering WTA in response to the host environment. It has also been found that *S. aureus* can alter the amount of WTA in the cell wall in an Agr & TarH dependent fashion[110]. This study also demonstrated that cell walls from WTA^{High} strains induced bigger abscesses and that overexpression of WTA in WTA^{Low} strains caused a WTA^{High} phenotype and a concomitant increase in virulence. Thus, dynamic alterations in WTA also cause alterations in *S. aureus* pathogenicity.

Furthermore, an alternative, prophage-encoded TarP enzyme has been identified in some healthcare-associated MRSA clones[111]. This TarP ligates GlcNAc to a different hydroxyl group than TarS and resulting in WTA that is much less immunogenic.

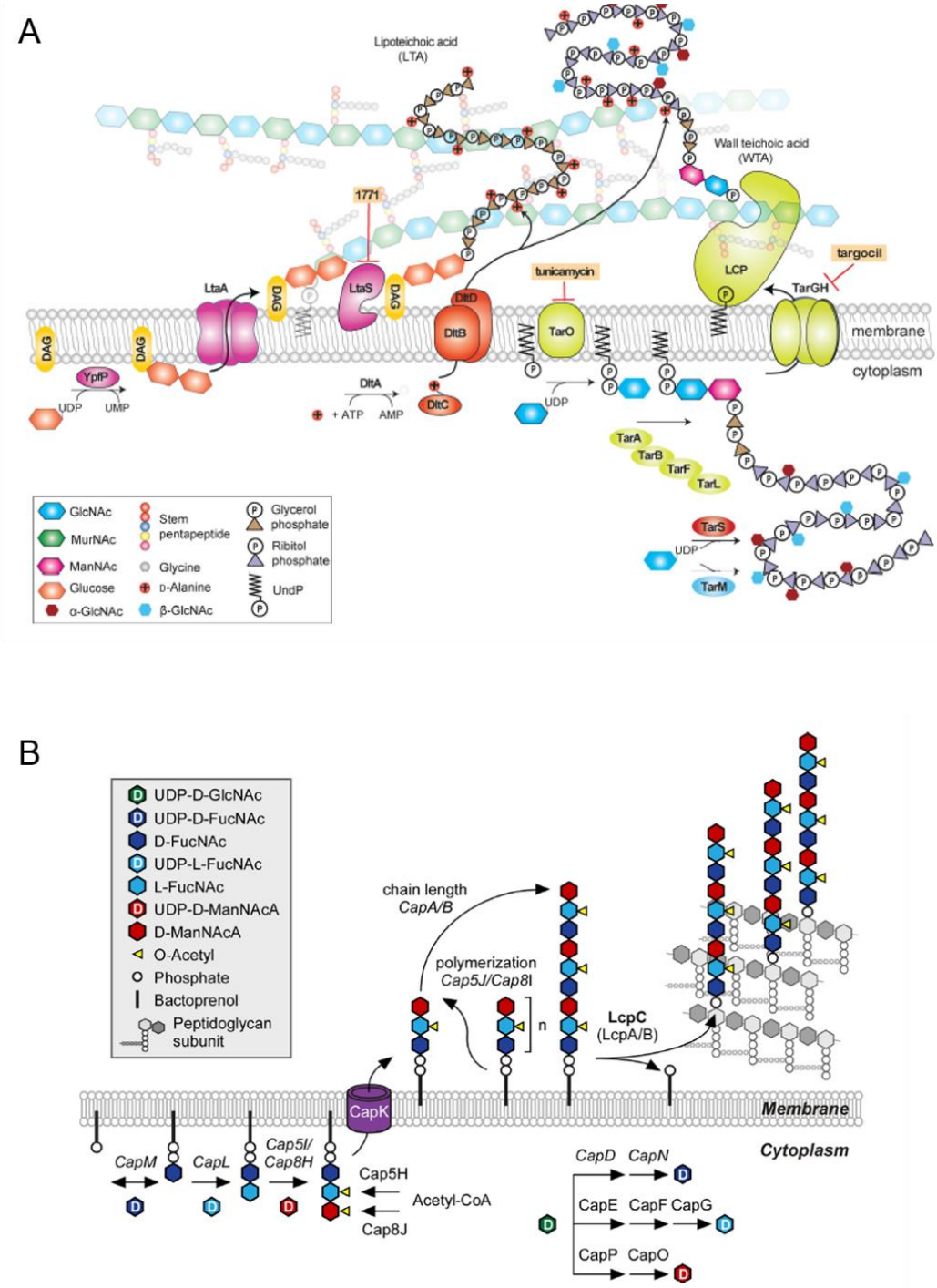

Figure 1.3 Teichoic acid and capsule synthesis pathways of *S. aureus*
A) Diagram depicting different synthetic pathways and common Dlt-mediated alanyl modification of LTA and WTA polymers in *S. aureus.* Taken from Rajagopal & Walker (2017)[62]
B) Diagram depicting synthesis of capsule in *S. aureus*. CP5 or CP8 specific enzymes are shown. Taken from Gar-Yun Chan *et al.* (2014)

1.4.4 Lipoteichoic acids

Lipoteichoic acids (LTA) have a separate synthetic pathway to WTA. LTA are membrane bound but have a long glycerol phosphate backbone which is approximately 25 repeats long in *S. aureus*, therefore, LTA are long enough to interact with the cell wall[112]. LTA synthesis differs from WTA in a few key parts, for instance, the double glucose linkage unit of LTA is constructed by YpfP on diacylglycerol as a lipid carrier compared to undecaprenol. This linkage unit is exported to the external leaflet of the cell membrane by LtaA and then the glycerol phosphate sugar backbone of LTA is built in the periplasmic environment by LtaS[113] (contrary to intracellular poly-ribitol phosphate synthesis of WTA). The glycerol phosphate backbone of LTA can be decorated with GlcNAc residues and D-alanylation in a similar fashion to WTA[114,115].

S. aureus can produce LTA polymers in the event that *ltaA* or *ypfP* are disrupted but the glycerol phosphate repeats are attached directly onto diacylglycerol of cell membrane without a linkage unit and the resulting polymer is much longer[116]. These mutants with longer LTA, which lack the diacylglycerol anchor, have defects in cell division in that they grow much larger before dividing. It has been argued that YpfP activity acts as a measure of nutritional availability thereby controlling the onset of cell division[117]. The exact function of LTA is unknown, however, along with WTA it is conditionally essential in the fact that these molecules cannot be knocked out or interrupted at the same time without loss of viability[118,119]. Thus, is could be that LTA and WTA have some functional redundancy but mutants in synthesis pathways for either molecule give distinct attenuated phenotypes[95,97,120]. LTA also seems to be an immunogenic PAMP with evidence linking LTA and lipopoteins to the ligation of TLR2[121].

1.4.5 Capsule

The majority of *S. aureus* pathogenic clonal lineages fall into two capsule serotypes: CP5 and CP8. The fact that capsule is typeable through antibody binding demonstrates it has antigenic capacity. Capsule is involved in endothelial adherence[122] and protects *S. aureus* from opsonophagocytosis[123,124] thereby enhancing virulence. Capsule synthesis enzymes are encoded by the *cap* genes and synthesis strikes a balance between traits of both LTA and WTA pathways. Capsule synthesis uses undecaprenol as a lipid carrier like WTA whereby the repeat unit (D-N-acetylfucosamine, L-N-acetylfucosamine, ManNAc) is constructed on the interior leaflet of the cell membrane.

These single repeats are exported to the exterior leaflet by the CapK transporter and it is here that chain polymerisation takes place (similar to LTA synthesis). Once complete the capsule chains are ligated onto the cell wall by the LCP proteins (Fig 1.3B). Capsule is not essential for *S. aureus*[125] as demonstrated by the fact that SH1000 and Sa113 strains used in this thesis are not capsule competent whereas JE2 and Reynolds strains are[126–128].

1.4.6 Polysaccharide intercellular adhesin (aka poly-N-acetylglucosamine)

Polysaccharide intercellular adhesin (PIA) is a secreted polysaccharide that is a β-1-6 linked polymer of GlcNAc and has been most well studied in *Staphylococcus epidermidis* (*S. epidermidis*). However, PIA has also been shown to be an important component in *S. aureus* biofilms[129], although PIA-independent mechanisms of biofilm formation are known to exist which rely in part on teichoic acids[130]. PIA is synthesised by the enzymes of the *ica* operon with the polymerisation performed intracellularly by IcaA/IcaD and export to the extracellular space by IcaC. IcaB is known to de-N-acetylate some of the GlcNAc residues within the PIA chain. Loss of IcaB in *S. epidermidis* causes a loss of PIA surface association[131] implicating the cationic charge introduced through de-N-acetylation as important to maintain ionic adherence of PIA to the cell wall. PIA has been shown to be immunogenic[132]. This polysaccharide was conjugated to ClfA and shown to elicit anti-PIA antibodies that, when passively administered, were protective in the murine intravenous *S. aureus* sepsis model[133].

1.5 *S. aureus* cell division

The cell envelope is an extensive molecular complex that allows *S. aureus* to survive as a single celled organism. However, the synthesis of this complex structure requires significant coordination to allow for proper growth and cell division. Bacterial cell division requires growth, DNA replication, separation of cytoplasmic resources, septation and daughter cell separation. Many bacteria have morphology or a clear orientation which grants a clear midpoint where septation should occur. However, *S. aureus* is a prolate spheroid and therefore has infinite planes in which it could theoretically divide but it coordinates division in three perpendicular planes. *S. aureus* utilises a plethora of division proteins the exact functions of which are still being deciphered. Bacterial two hybrid analyses of the *S. aureus* division proteins (selected for their homology to known *B. subtilis* division proteins) show that there are numerous

interactions with few proteins having less than two interactions[134] (Fig 1.4A). These proteins are collectively referred to as the divisome (Fig 1.4B).

The site of *S. aureus* cell division is demarcated by the formation of the z-ring made up of FtsZ, which is a bacterial homologue of mammalian tubulin and is essential for septum formation[135]. FtsZ is one of the earliest cell division proteins and its ring formation is stabilised by GpsB[136]. Z-ring formation sets off sequential recruitment of other early division proteins such as FtsA, ZapA, SepF and EzrA. Work in *E. coli* and *B. subtilis* has led to the assertion that FtsA and ZapA potentiate the ability of the Z-ring to interact with the membrane[137]. Also FtsA and ZapA are essential in *E. coli* for recruitment of FtsK[138], the *S. aureus* homologue of which is important for transporting DNA away from the septum[139]. EzrA may be important in the connection between the cytoplasmic Z-ring and the membrane associated divisome components as loss of EzrA results in lack of septal localisation of divisome proteins[134].

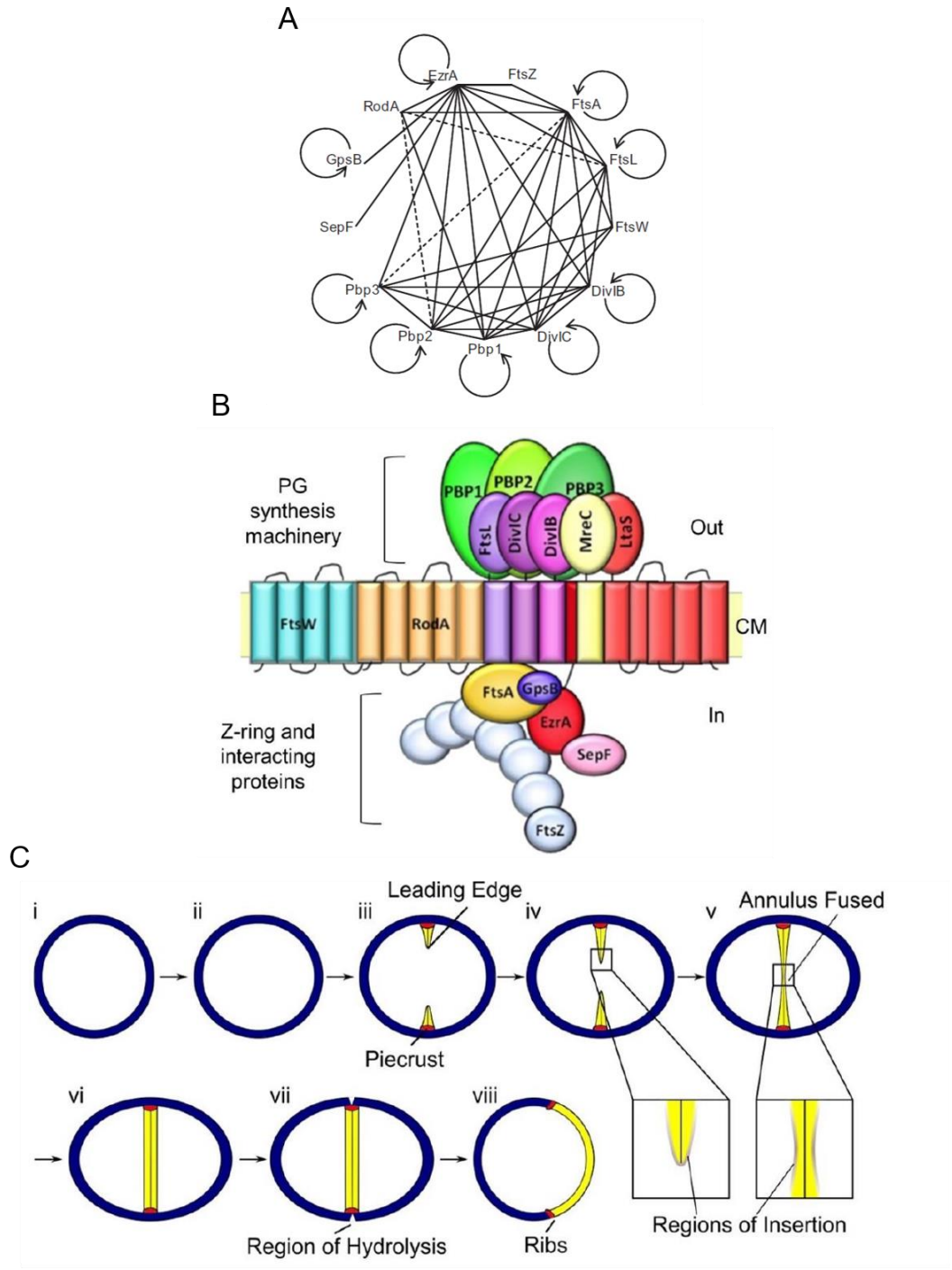

Figure 1.4 Illustration of *S. aureus* divisome and cell division
A) Schematic illustrating cell division machinery from *S. aureus*. CM, cytoplasmic membrane. Taken from (Bottomley, 2011).
B) Map of cell division protein interactions as determined by two-hybrid analysis. Positive interactions are shown by a solid line and putative interactions with a dashed line. Homodimerization is indicated by a circular arrow. Taken from (Steele *et al*. 2011)
C*)* Model of *S. aureus* cell cycle and peptidoglycan insertion. Cell division begins with an increase in cell size followed by insertion of peptidoglycan to the midcell to form a septum with final uniform thickness. Following completion of the septum, the daughter cells separate from each other. Taken from *(Lund et al., 2018)*

The late stage, membrane associated divisome proteins: DivIC, DivIB, FtsL, FtsW and PBPs, are involved in coordinating the localised synthesis and remodelling of new peptidoglycan which forms the septum which in turn drives membrane invagination. PBP1[140] and PBP2[141] are essential for septum formation and progression whereas PBP3 complexes with RodA for off septal peptidoglycan synthesis[142] and PBP4 is the only low molecular weight PBP and is involved in facilitating the increased cross-linking seen in *S. aureus* peptidoglycan[143,144].

DivIC, DivIB and FtsL (FtsB, FtsQ and FtsL in gram-negative bacteria) are thought to form a heterotrimer in a variety of bacterial species[145–147], the stability of DivIC being dependent on FtsL and FtsL stability being dependent on DivIB. Regardless of their specific function, it has been demonstrated via mutagenesis studies that DivIC and DivIB act through their extracellular domains in *B. subtilis*[148]. It was suggested that these proteins form a scaffold to regulate "the assembly of membrane-associated division proteins"[149] but it was recently shown that DivIB has peptidoglycan binding function in *S. aureus*[150] which might implicate it as having a more active role in cell division than a scaffold. Since then it has been elucidated that the FtsBQL complex in *E. coli* is capable of inhibiting PBP1b and PBP3[151]. Therefore these late stage divisome proteins potentially act as pacemakers of septum progression, inhibiting peptidoglycan synthesis until the cell is ready or this inhibition is antagonised by accumulation of FtsN and peptidoglycan synthesis continues[152]. Once the septum is complete the nascent peptidoglycan must be digested by hydrolases, such as Atl, to separate the daughter cells. Recent data from atomic force microscopy has elucidated there is a significant difference in peptidoglycan structure at the newly divided septum compared to the older section cell wall[153] which might indicate a difference which allows for controlled cell wall hydrolysis.

Greater understanding of *S. aureus* cell division with focus on the assembly of the cell envelope may provide better rationale for logical target selection for antibiotic development. However, there is also a dearth of knowledge regarding the exact mechanisms of pathogenesis and protection for a wide variety of organisms, especially pathogens such as *S. aureus* which causes many pathologies[3,7]. This is part of the

reason we have yet to successfully induce specific, lasting, evolving protection to *S. aureus* via vaccination.

1.6 *S. aureus* vaccine landscape

1.6.1 History of *S. aureus* vaccine development

Prophylaxis by vaccination has been one of the greatest scientific advances in terms of saving lives since clean drinking water[154]. In simple terms vaccination involves exposing the immune system to a pathogen in a state (e.g. component, dead, attenuated) that the host organism can handle without the occurrence of significant pathology. This teaches the immune system to recognise the pathogen and ideally results in a lasting protection through immunological memory. However, vaccination is far from this simple as exemplified by the fact there are currently no licensed vaccines against *S. aureus* despite numerous candidates progressing to clinical trials as shown in Table 1.1.

It has been shown that natural infection and vaccination with whole cell preparations do not work for *S. aureus*[155] as is the case with other pathogens such as *Bordatella pertussis*[156]. Another vaccination approach is to use a pathogen sub-unit, such as an important protein, which has been successful for diseases which rely on a single protein such as diphtheria[157,158] or tetanus[159] whereby antibodies against their respective toxins ameliorate pathogenicity. However, a single protein has so far proven insufficient for protection against *S. aureus* as demonstrated by the V710 vaccine which infamously led to worse outcomes than placebo[160,161]. There has since been a shift towards multiple antigen formulations in the development of *S. aureus* vaccines[162–165]. This is because *S. aureus* has many different virulence factors allowing disease in many niches and bypassing of immune defences, therefore it seems prudent to seek protection against numerous antigens. It has been shown that combining *S. aureus* antigens in a multivalent vaccine provides better protection from *S. aureus* infection in mice than vaccination with any of the same antigens singly[166].

Capsular polysaccharide alone was shown to be a poor antigen due to its being T cell independent[127]. However, the poor MHC-based recruitment of T cell help has been overcome via conjugation to a protein in numerous successful vaccines against other pathogens such as *Streptococcus pneumoniae*[167,168] and *Haemophilus influenzae*[169]. This is the approach of StaphVAX by Nabi pharmaceuticals which conjugated CP5 and CP8 to mutated non-toxic *Pseudomonas aeruginosa* toxin[170]. Despite this vaccination

resulting in high antibody titres, which lasted up to a year when a vaccine boost had been received, the vaccine gave no protection compared to placebo and was thus a failure[171]. Unfortunately, coupling the capsule conjugate approach with the multivalent antigen approach has also produced limited results in vaccines against *S. aureus*. This includes the most recent *S. aureus* vaccine candidate to fail in clinical trials; the Pfizer Sa4Ag trial, which was halted prematurely as an independent panel deduced the study was unlikely to reach its end points[172].

The successive failure of clinical trials indicates not enough is known regarding how to generate a protective immune response against *S. aureus*. This is despite many preclinical trials yielding promising results in animals, simply demonstrated by the fact any vaccine candidate advanced to clinical trials. There are many potential reasons for this. Chief among them is the fact we lack sufficient understanding of how pathogenesis differs between *S. aureus* infections and it appears the necessary protection differs between pathology. Yet *S. aureus* infections and the assumed necessary protections are often treated as one entity within the literature. Our lack of appreciation for the differences between *S. aureus* pathologies might contribute to potential misinterpretation of animal models of infection that is evident by the fact preclinical successes have failed to translate to success in clinical trials in humans. These issues are further compounded by the lack of any known correlates of protection for *S. aureus*.

1.6.2 Correlates of protection

When vaccinating an individual one hopes for a quantifiable, immunological readout such as antibody titre that can be measured to ensure the vaccine has worked and will provide protection. This measurement is then termed the correlate of protection[173]. However, there is no known correlate of protection for *S. aureus* and without this the only way to assess efficacy is morbidity and mortality rates in a large clinical trial.

One of the most commonly used correlates of protection is a specific antibody titre in response to vaccination or primary challenge[173]. Antibodies are produced in response to colonisation with *S. aureus*, but these are not seen as a correlate of protection. Over 14000 non-bacteraemic, non-surgical patients were screened for nasal carriage of *S. aureus* and carriers had a greater chance of developing bacteraemia but had a reduced mortality as a result of bacteraemia[174]. Another large-scale study of nasal carriage

Table 1.2 Vaccines against *S. aureus* known to have been in clinical development
GSK: GlaxoSmithKline; CP: capsular polysaccharide antigens; Hla: α-haemolysin toxin; ClfA: clumping factor A; Als3p: agglutinin like sequence 3 protein; TSST: toxic shock syndrome toxin; NIAID: National Institute of Allergy and Infectious Diseases, USA; Mnt: manganese transporter protein; S-PVL: Panton–Valentine leukocidin component S; IsdB: iron surface determinant B. Table adapted from Redi *et al.* (2018)[175]

Vaccine	Developer	Target antigen	Immunity	Phase	Status and results
GSK2392103A	GSK	CP5/CP8/Tetanus toxoid/mutated α-toxin/ClfA (Conjugate)	N/a	Phase I	Completed, no further Development.[176]
NDV3 rAls3p-N	NovaDigm Therapeutics	(*C. albicans* surface protein cross reacting with *S. aureus*; Alum adjuvated)	Humoral and cellular	Phase I	Completed, safety and immunogenicity, stopped phase II due to enrolment problems.[177]
SA75	Vaccine Research International	Whole cell vaccine	Humoral and cellular	Phase I	Completed, safety and tolerability, no further development.[178]
N.A.	Integrated BioTherapeutics	Enterotoxins A and C1, TSST (recombinant)	Humoral	Phase I	Completed, safety, evaluating possible phase II trial.[179]
STEBvax	Integrated BioTherapeutics and NIAID	Enterotoxin B (rSEB) (recombinant, Alum adjuvated)	Humoral	Phase I	Completed, safety, demonstrated production of toxin neutralizing antibodies.[180]
SA4Ag (PF-06290510)	Pfizer	ClfA/MntC/CP5/CP8 (Conjugate)	Humoral and cellular	Phase IIb	Discontinued by independent data monitoring committee due to futility.[162,172]
N.A.	Nabi	Hla/S-PVL (recombinant)	Humoral	Phase I	Completed, safety, robust immune response.[181]
StaphVAX	Nabi	CP5/CP8 (purified and conjugated capsular polysaccharides)	Humoral	Phase III	Stopped, no differences between vaccine and placebo in end-stage renal patients[182]
V710	Merck	IsdB (purified surface protein)	Humoral	Phase III	Stopped, increased mortality in vaccinated subjects post cardiothoracic surgery[160,161]
GSK3878858A	GSK	Sa-5Ag (recombinant protein, bioconjugated, adjuvanted)	Unknown	Phase I	Ongoing to assess safety, immunogenicity, and efficacy against SSTI

elucidated that persistent nasal carriers had significantly higher IgG and IgA titres against toxic shock syndrome toxin and *staphylococcal* clumping factor A/B respectively compared to non-carriers[183]. Together these studies demonstrate that antibodies against *S. aureus* virulence factors arising from commensal carriage increase incidence of bacteraemia whilst reducing disease severity. This indicates natural exposure does not provide conventional immunity and is not truly protective. In addition, *S. aureus* has virulence factors to circumvent antibody recognition such as *Staphylococcal* protein A (SpA) which binds the Fc region of antibodies thereby inhibiting their binding capacity and any subsequent opsonophagocytosis[184]. In addition, patients with defects in antibody production such as agammaglobulinemia do not have increased susceptibility to *S. aureus* infection[185,186], a phenomenon mirrored in mice defective in B cell development which are no more susceptible to *S. aureus* infection[187,188]. Furthermore, none of the vaccines which have focused on humoral immunity have led to clinical protection[175]. This leads to the conclusion that antibodies may not be an appropriate correlate on their own in humans.

Given the lack of success focusing entirely on the humoral response, there has been an increased interest on the T cell response to *S. aureus*. CD4+ T helper cells help martial and direct the immune response[189]. Th1 response predisposes to a pro-inflammatory environment and enhances macrophage phagocytosis and bactericidal killing via priming these cells with IFN-γ. Alternatively, the Th2 response predisposes to a more humoral response by helping B cell development. Both of these, and other T helper cell responses, have been shown to be beneficial in protecting against *S. aureus* with each seeming to be beneficial to different types of *S. aureus* infection[190–193]. Furthermore, given the intracellular niche of *S. aureus*[194], the cytotoxic role of CD8+ T cells is deemed to be important in anti-S*. aureus* immunity. However, unfortunately the T cell responses don't produce an easily identifiable marker such as antibodies which makes using them as a correlate of protection much more difficult. Without time-consuming cell sorting the best approximation of the T cell response is to interrogate cytokines, which are chemical messengers, used by the immune system, often found in the blood to coordinate and steer the response to a pathogen.

There are obvious ethical restrictions on manipulating infection in humans, therefore data on the human interaction with *S. aureus* is mostly retrospective and observational based on clinical outcomes. One example of this is cytokine levels during bacteraemia.

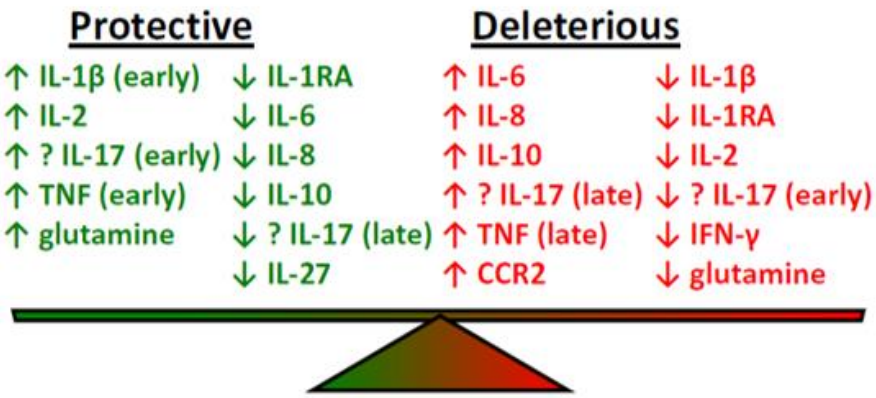

Figure 1.5. Cytokine responses to *S. aureus* bacteraemia in human studies.
Cytokine levels and their associated protective (green) or deleterious (red) clinical outcome in human patients with *S. aureus* bacteraemia. ↑ = relatively increased cytokine level. ↓ = relatively decreased cytokine level. Early is defined as within 3 days of diagnosis of *S. aureus* bacteraemia and late is anything after this 3-day period. Taken from Miller et al. (2019)[195]

As blood is taken to confirm the bacterial species causing bacteraemia, clinical sampling is amenable to also taking cytokine measurements and data is starting to point to cytokines as indicators of probable outcome. These data indicate that there is an immunological distinction between favourable and unfavourable outcomes in bacteraemia. Increased levels of IL-1β, IL-17 and TNF seem to be beneficial for the host, but timing is also important with these being protective during early infection but detrimental as the disease progresses[195]. Whilst cytokine levels are not necessarily correlates of protection they do point towards the type of response that might be protective (Fig 1.5).

Some of these cytokine signatures have also been seen in animal models of *S. aureus* infection, which is encouraging due to the necessity of animal models in the in-depth study of *S. aureus* pathogenicity. Animal models allow much deeper interrogation of immune phenotypes involved in anti-*S. aureus* immunity. For instance animal models of *S. aureus* have determined more recently characterised immune cell type which have been shown to be potentially important in anti-*S. aureus* immunity such as γδ T cells and their subsets[196].

γδ T cells possess a T cell receptor with γδ chains as opposed to the conventional αβ chains and are not MHC-restricted[197]. These cells are also present in a variety of tissues and rapidly proliferate compared to lymphoid resident conventional T cells whilst still having a memory capability[198]. γδ T cells kill intracellular and extracellular pathogens and produce IL-17 which has been shown to be useful in anti-*S. aureus* immunity[199,200]. Moreover, the γδ T cell compartment has been shown to expand in response to host exposure to *S. aureus* and these immune cells have been shown to be important in protecting against *S. aureus* in peritoneal[201], cutaneous[202], respiratory[203], and wound infections[199].

1.7 *S. aureus* animal infection models

Clinical observations of human infections are limited as patients only present at the onset of symptoms and the extent to which the infection can be manipulated/studied is limited due to ethics. Human live challenge models exist, but only where suitable animal models of infection are not available, such as with *Salmonella enterica serovar typhi* (*S. typhi*)[204,205], and these studies are very closely regulated. Infection dynamics can be

interrogated *in vitro* through use of mammalian immune cell culture. Macrophage, neutrophil and dendritic cell cultures have been used to assess the interaction of *S. aureus* with the immune system[206]. Despite advances towards cell cultures with numerous cell types and organoid developments *in vitro* studies will always lack the nuance and complexity of the complete immune system. Study of complete immune pathogen interactions are best facilitated by *in vivo* infection.

For *S. aureus* infection, numerous animal models of infection exist, each with their own merits and shortcomings. Invertebrate models such as *Caenorhabditis elegans*[207], *Galleria mellonella*[208] and *Drosophila melanogaster*[209], have the advantage of being high throughput but lack sophisticated immune systems. Vertebrate models overcome this drawback. Rabbits are used for the study of osteomyelitis and implant/prosthetic infections as their bones are large enough to be manipulated[210]. Cows have been experimentally infected[211] but this is to facilitate the study of bovine mastitis of which *S. aureus* is the major cause[212]. Non-human primates can be colonised by *S. aureus*[213], however due to long generation time and greater ethical considerations there is significance expense in using non-human primates in infection studies and they are often reserved for advanced stage preclinical trials. At the University of Sheffield, the infection models of choice for *S. aureus* are the zebrafish embryo and mouse models.

1.7.1 Zebrafish model

Zebrafish (*Danio rerio*) embryos are commonly used with *S. aureus* injected directly into the circulation valley to give an approximation of sepsis[214]. A major advantage of using zebrafish embryos as an *in vivo* infection model is that their bodies are transparent thereby allowing relatively easy imaging of pathogen immune interactions *in vivo*. Another major advantage of the zebrafish embryo model is the high throughput that can be achieved due to the low cost of upkeep and the short generation time. There is also a growing repertoire of transgenic zebrafish including knockout and reporter lines thereby allowing better dissection of the immune interactions[215].

The primary drawback of this model of infection is that zebrafish embryos only have innate immunity with neutrophils and macrophages developing at 18- and 25-hours post-fertilisation[216–218] respectively. As a jawed fish, zebrafish possess an adaptive immune system, but this develops at later stages post-fertilisation[219] and the advantage of the organism's transparency is often lost by this stage. Despite this immunological

drawback the zebrafish embryo model has proven useful for investigating *S. aureus* pathogenesis. Not only has the model indicated potentially important innate immune pathways[214] it has also shown there is an innate immune bottleneck whereby *S. aureus* can use an intraphagocyte niche to disseminate throughout the host[194]. This process was also shown to be clonal in the zebrafish embryo[29]. Much of this work informed further work and was shown to be mirrored in the murine model of infection.

1.7.2 Mouse

The mouse is the most widely used mammalian model in science. The availability of inbred wildtype strains reduces the variation that is inherent in *in vivo* experimentation[191,220] and allows for better comparison with findings in the literature. Furthermore, the mouse genome was first sequenced in 2002[221], thus the organism is genetically tractable and there are numerous transgenic strains which permit the dissection of biological pathways and their importance in infection.

The mouse has many advantages over the previously mentioned models, first and foremost the vaccination can be tested in mice due to the presence of an adaptive immune system. Also, as a larger organism than invertebrates and fish, with mammalian anatomy, there are more possible routes of administration meaning more types of disease can be modelled. *S. aureus* sepsis can be modelled in the mouse through either intraperitoneal[190] or intravenous injection[222], skin infections via subcutaneous injections[191], wound infections through application of bacteria to superficial wounds[199], gastrointestinal infection by oral gavage or direct jejunal injection[223] and pneumonia[192] through intranasal administration. This versatility within the same organism has demonstrated that different immune responses are triggered in different infection types even when the same host and infectious organisms are used[224].

There are some drawbacks to overcome when modelling *S. aureus* infection in mice. Lab mice can be colonised with *S. aureus* but strains which are pathogenic to humans tend to need a large inoculum to establish disease in mice. This is because human-evolved pathogenic strains have evolved many human specific virulence factors such as leukocyte toxins to which murine leukocytes are resistant[16,17]. Numerous approaches have previously been taken to allow better infection of mice with human pathogens.

Mouse adapted strains of *S. aureus* have been described[225] but these often lack human-specific virulence factors which prophylactic therapy is interested in. In other

infection models mouse specific surrogate pathogens are used, such as when *Salmonella typhimurium* is used as *S. typhi* cannot infect mice. Other approaches have been to humanise the immune system by irradiating the mouse bone marrow and transplanting human haematopoietic progenitors as has been done in HIV infection studies due to the necessity of human $CD4^+$ T cells for infection[226]. This approach has been used successfully for *S. aureus* infection showing greater susceptibility to *S. aureus* pneumonia[227]. However, this model can suffer from chronic inflammation if mouse MHC proteins are not also ablated, which may confound results due to graft versus host effects[226]. A recent advancement in the murine *S. aureus* infection model to reduce the inoculum necessary for establishing infection was inclusion of commensal bacteria or their cell wall material in the inoculum[222]. This allowed reduction of the CFU required for reliable, reproducible pathogenesis by 1000-fold. This also likely replicates natural infection much more closely as natural infection is unlikely to ever be due to homogenous inoculation with one bacterial species.

1.8 Aims of this study

To develop better therapeutics and treatment options for *S. aureus* better understanding is required surrounding the bacterium itself, the host immunological response and the host-pathogen interactions. The overarching aim of this study was to add more understanding in these areas with the more specific objectives to:

- Decipher the role of the division protein DivIC in *S. aureus* cell division as a possible prophylactic/therapeutic target.
- Interrogate the role of the mammalian NGF-β immune response with regards to anti-*S. aureus* immunity.
- Assess improvements to the *S. aureus* intravenous murine sepsis model in its utility to vaccine development.

Chapter 2:
Materials & Methods

2.1 Media

All growth media was autoclaved at 121^{o}C for 20 minutes, then handled under aseptic conditions to prevent contamination. Media containing agar was sterilised in the same manner and allowed to cool to 55^{o}C before addition of any additives such as antibiotics used for selection etc.

2.1.1 Luria Bertani broth (LB)

- Tryptone 10 g/L
- NaCl 5 g/L
- Yeast Extract 5 g/L

1.5%(w/v) bacteriological agar (VWR chemicals) was added for LB agar

2.1.2 Tryptic soy broth (TSB)

- Tryptic soy broth (oxoid) 30 g/L

1.5%(w/v) bacteriological agar (VWR chemicals) was added for tryptic soy agar (TSA).

2.1.3 Nutrient Broth

- Nutrient broth 13 g/L

1.5%(w/v) bacteriological agar (VWR chemicals) was added for nutrient agar.

2.2 Buffers

Buffers were made up dH_2O and made sterile by autoclaving or sterile filtration as necessary then stored at room temperature or 4^{o}C as necessary.

2.2.1 Phosphate buffered saline (PBS)

- Gibco™ Phosphate buffered saline tablets (Thermo) 2 tablets/L

2.2.2 1.5M Tris-HCl

- Tris Base 181.71 g/L

pH was adjusted to 8.8 with HCl before autoclaving

2.2.3 50mM Tris-HCl

- Tris Base 6.05 g/L

The pH was adjusted to 7.5 with HCl before autoclaving

2.2.4 50mM Tris-HCl + SDS + 1.25mM EDTA + 50mM DTT

- Tris-HCl pH 7.5 50 mM
- SDS 3 g/L
- EDTA 372 mg/L
- DTT 7.71 g/L

2.2.5 TES buffer

- Tris base 2.42 g/L
- EDTA 1.86 g/L
- NaCl 5.84 g/L

pH adjusted to 8

2.2.6 EAW buffer

- Ethanol 40%(v/v)
- Acetic acid 5%(v/v)

- dH_2O 55%(v/v)

2.2.7 100mM Sodium Phosphate (NaPO4) buffer

- 1M Na_2HPO_4 31.6 ml
- 1M NaH_2PO_4 68.4 ml
- dH_2O 900 ml

2.2.8 START buffer

- $NaPO_4$ 100 mM
- NaCl 500 mM

Imidazole added to varying concentrations with a top concentration of 500mM for eluting His-tagged proteins off the Histrap column (section 2.24.2).

2.2.9 Sodium Borate buffer 250mM

- Boric Acid (H_3BO_3) 15.46 g/L

Made up with dH_2O then adjusted to pH 9 with NaOH then autoclaved.

2.2.10 Peptidoglycan pulldown/MST binding buffer

- Sodium Citrate 20 mM
- $MgCl_2$ 10 mM
- BSA 10 µg/ml
- Tween 0.5%(v/v)

The pH was adjusted to 5 with HCl.

2.2.11 SDS-PAGE loading buffer (x5)

- Tris-HCl pH 7.5 50 mM
- Glycerol 50%(v/v)
- SDS 2%(w/v)
- Bromophenol Blue 0.5%(w/v)

10%(v/v) 2-mercaptoethanol added immediately prior to use.

2.2.12 SDS-PAGE buffer (x10)

- Tris base 30 g/L
- Glycine 144 g/L
- SDS 10 g/L

2.2.13 Phosphate assay buffers

All receptacles for phosphate assay buffers were thoroughly washed with dH_2O prior to being used for buffer production/storage.

2.2.13.1 $MgNO_3$ 10%(m/v) in 35% Methanol

- $MgNO_3$ 5 mg
- dH_2O 32.5 ml
- Methanol 17.5 ml

2.2.13.2 Ascorbic acid 10%(m/v)

- Ascorbic acid 100 g/L

Made up in dH_2O

2.2.13.3 $(NH_4)2MoO_4$ 0.42%(m/v)

- $(NH_4)_2MoO_4$ 0.432 g
- dH_2O 100 ml
- H_2SO_4 2.86 ml

2.2.14 HPLC buffers

HPLC buffers were made with Milli-Q-filtered, 0.2 µm filtered, de-gassed water and HPLC grade chemicals.

2.2.14.1 Buffer A

- 1ml formic acid (98% purity) added to 1L of Milli-Q water

2.2.14.2 Buffer B

- 250µl formic acid (98% purity) added to 250ml Acetonitrile

2.3 Antibiotics

Antibiotics used in this study are shown in Table 2.1. Antibiotic stocks were prepared and sterile filtered (0.2µm) and stored at -20ºC. Antibiotics were added to media just before use and agar was allowed to cool to 50ºC before antibiotics were added to agar.

Antibiotic	Stock concentration (mg/ml)	Working concentration (µg/ml)	Solvent
Ampicillin (Amp)	100	100	dH_2O
Chloramphenicol (Cm)	30	30	100% Ethanol
Erythromycin (Ery)	5	5	100% Ethanol
Kanamycin (Kan)	50	50	dH_2O
Lincomycin (Lin)	25	25	50%(v/v) Ethanol
Tetracycline (Tet)	5	5	50%(v/v) Ethanol
Tunicamycin (TUN)	1	2	dH_2O
Tarocin	5	2.5	DMSO
Spectinomycin (Spec)	50	100	dH_2O

Table 2.1. Antibiotics and concentrations used in this study

2.4 Chemicals & Enzymes

Chemicals and enzymes used in this study were of analytical grade and were purchased from Fisher Scientific, MP biomedicals or Merck (Sigma-Aldrich) unless otherwise stated.

Chemical/Enzyme	Solvent	Concentration	Storage temperature
Pronase	TES buffer	20mg/ml	-20^{o}C
Mutanolysin	200mM Sodium Phosphate	1mg/ml	-20^{o}C
Lysozyme	dH_2O	10mg/ml	-20^{o}C
Lysostaphin	20mM Sodium Acetate (pH 4.6)	5mg/ml	-20^{o}C
Bovine Serum Albumin (BSA)	PBS	10%(w/v)	4^{o}C
Isopropyl β-D-1-thiogalactopyranoside (IPTG)	dH_2O	1M	-20^{o}C
Ammonium persulphate (APS)	dH_2O	10%(w/v)	-20^{o}C
Cytochrome C	PBS	1mg/ml	-20^{o}C
Alcian Blue 8GX	EAW buffer	0.05%(w/v)	RT
CpG (ODN 2006) (Hycult Biotech)	dH_2O	10mg/ml	4^{o}C

Table 2.2 Chemicals and enzymes used in this study

2.5 Bacterial growth

Unless otherwise stated bacteria were grown according to standard microbiological practices. Bacteria were stored on microbank beads at -80ºC and these stocks were used to streak single colonies on agar plates which were grown at 37ºC overnight. Overnight cultures were made through inoculating 10ml of liquid media (with appropriate antibiotic) in a 50ml Falcon tube and incubating at 37ºC, 250rpm overnight. The next morning this was sub-cultured into fresh media to an OD_{600} of 0.05 and grown at 37ºC, 250rpm and mid-exponential phase growth was considered an OD_{600} of 0.4-0.8.

2.6 Measuring bacterial density

2.6.1 Optical density (OD)

Bacterial cultures were spectrophotometrically measured at 600nm (OD_{600}) in Biochrom WPA Biowave 70 DNA spectrophotometer. These were against growth media blanks and cultures were diluted 10-fold when necessary.

2.6.2 Determining CFU

Cultures were serially diluted (1:10) in sterile PBS to 10^{-8}. 5µl of each dilution was spotted onto agar plates, with relevant antibiotics where necessary, and these were incubated at 37ºC overnight. Colony forming units (CFU) were counted and CFU/ml was calculated based on this.

2.7 Growth curve

Overnight cultures were grown, with antibiotics as necessary, as described in 2.5. These stationary phase cultures were used to inoculate pre-warmed media (without antibiotics used for selection) to an OD_{600} of 0.05. These were grown at 37ºC, 200rpm, until stationary phase was reached (approximately 8 hours). To assess growth rate samples were taken every hour to measure the OD_{600} and take direct CFU counts if necessary.

2.8 *S. aureus* strains used

Staphylococcus aureus strains used are listed below in Table 2.3 and were accessed from Microbank beads stored at -80°C. These stocks were used to grow colonies on tryptic soy agar plates containing antibiotics when necessary which were then stored at 4°C.

SJF#	Background	Relevant geneotype	Source
682	SH1000	Functional *rsbU*+ derivative of 8325-4	[228]
4254	RN4220	Restriction deficient transformation recipient	[229]
4257	RN4220	*ΔtarM, ΔtarS*	[93]
4258	RN4220	*ΔtarM ΔtarS* pRB-tarS (Cm^R)	[93]
2183	RN4220	*srtA::ery*	[230]
4591	SH1000	*lgt::ermB*	Constructed by Emma Johnson, (University of Sheffield)
5159	SH1000	*ΔltaS* (Ery^R), *gdpP::Kan*^{R}	Constructed by Lucia Lafage (University of Sheffield)
56	NCTC 8325		[231]
57	NCTC 8325/4	Cured prophages 011, 012,013	[231]
1028	SH1000	*ΔsigB* (Tet^R), (*rbsU*$^+$)	Constructed by A. Needham (University of Sheffield)
2204	Sa113	Wildtype	[94]
2205	Sa113	*Δdlta* ($Spec^R$)	[94]
2206	Sa113	*ΔtarO* (Ery^R)	[104]
4210	ST121	Wildtype Rabbit strain (mutation causes inactive *rot* gene and 3 SNPs in *dltB*)	[232]

4211	ST121	Rabbit strain *ΔdltB*	[232]
4276	JE2	MRSA & parent strain for NTML	[233]
3160	15981	Clinical Isolate, Biofilm positive, natural agr mutant, metic, sensible	[234]
3161	15981	*ΔtarO*	[235]
5289	SH1000	*tarO ::ermB*	Constructed by Dr Bartlomiej Salamaga (University of Sheffield)
5290	SH1000	*tarO :: ermB*, pCU1-*tarO* (Cm^R)	Constructed by Dr Bartlomiej Salamaga (University of Sheffield)
5172	MSSA112	Clinical isolate, Isogenic strain used for deletion of LCP proteins	[88]
5173	MSSA112	*ΔmsrR* (*ermB)*	[88]
5174	MSSA112	Markerless *sa0908* deletion mutant	[88]
5175	MSSA112	Markerless *sa2103* deletion mutant	[88]
5176	MSSA112	*sa0908/msrR (ermB*) double mutant	[88]
5177	MSSA112	*sa2103/msrR (ermB*) double mutant	[88]
5178	MSSA112	Markerless *sa2103/sa0908* double mutant	[88]
5179	MSSA112	*sa2103/sa0908/msrR (ermB*) triple mutant	[88]
3680	NEWHG	*lysA::kan lysA+*	[236]

2368	Reynolds	Serotype 8 mutant of Reynolds	[128]
2369	Reynolds	Serotype 5 prototype strain	[128]
2370	Reynolds	Capsule-negative mutant of Reynolds, *Emr*	[128]

Table 2.3 *S. aureus* strains used in this study

2.9 Nebraska transposon mutant library *S. aureus* strains used

Strains from the Nebraska transposon mutant library from are in the JE2 background (SJF#4276). Mutants from this library that were used in this study are listed in Table 3.1. Stocks were kept on Microbank beads stored at -80ºC. These stocks were used to grow colonies on tryptic soy agar plates containing antibiotics when necessary which were then stored at 4ºC.

2.10 *E. coli* strains used

Escherichia coli strains were obtained from microbank beads stored at -80ºC. These stocks were used to grow colonies on Luria-Bertani agar plates containing antibiotics when necessary which were then stored at 4ºC

SJF#	Background	Relevant geneotype	Source
3165	Bl21*(DE3)	pALB26: fragment of gene encoding the DivIC extracellular domain (Lys56 to Lys130) with a 6xHis tag ligated into pET21d protein expression vector (Amp^R)	Constructed by Azhar Khabli (University of Sheffield)
3539	XL1 blue	PCF40: Expression of residues 40-559 of ClfA plus N terminal His tag in Qiagen overexpression vector PQE30 (Amp^R)	[237]

Table 2.4 *E. coli* strains used in this study

2.11 Other bacterial strains used

Other bacterial species used in this study are listed below in Table 2.6. The stocks for these bacteria were kept on Microbank beads stored at -80^{o}C. These stocks were used to grow colonies on tryptic soy agar plates (Nutrient broth agar in the case of *Bacillus subtilis*) containing antibiotics when necessary which were then stored at 4^{o}C.

SJF#	Species
1	*Bacillus subtilis* 168 (HR trpC2)
43	*Streptococcus mutans* (LT11)
4393	*Micrococcus luteus* ATCC4698 (spontaneous Rifampicin resistant mutant)
229	*Staphylococcus epidermidis* 138
704	*Enterococcus faecalis* NCTC 775
3535	*Lactococcus lactis* MG1363
449	*Curtobacterium flaccumfaciens pvar poinsettiae*

Table 2.5. Other bacterial species used in this study

2.12 Centrifugation

- Eppendorf microcentrifuge 5424, capacity to 24 x 1.5-2 ml microfuges, maximum speed of 21130 x g (14800 rpm).
- Sigma centrifuge 4K15C with a capacity of 16 x 50 ml falcon tubes, maximum speed 5525 x g (5100 rpm).
- Avanti High Speed J25I centrifuge, Beckman Coulter:
- JA-25.50 rotor with a capacity of up to 6 x 50 ml, maximum speed 75000 x g (25000 rpm)
- Avanti High Speed J-26XP centrifuge, Beckman Coulter:
- JLA 8.1000 rotor with a capacity of 6 x 1000 ml, maximum speed of 15970 x g (8000 rpm)

2.13 Sonication

Sonication was performed using a Soniprep 150 Plus bench-top ultrasonic disintegrator with a probe with a 3mm-tip. The minimum sample volume to be sonicated was 400µl.

Sonication was performed for rounds of 30 seconds with samples incubated on ice between rounds of sonication.

2.14 Cell wall purification

Bacterial cells were grown at 37^{o}C to stationary phase then harvested via centrifugation and resuspended in Tris-HCl before boiling for 7 mins. Cell suspensions were then loaded into FastPrep tubes containing lysing matrix B (MP biomedical) and mechanically lysed through at least 10 cycles of 30 secs at 6.0 m/s in a Fastprep-24^{TM} 5G (MP Biomedical). The samples were put on ice between homogenisation cycles. Fastprep tubes were spun at 100xg in a microfuge to pellet the silica beads allowing the cells to be recovered in the supernatant and check for breakage by light microscopy. Cell walls were resuspended in water before addition of pronase to a concentration of 2mg/ml and incubated at 60^{o}C for at least 1 hour to degrade cell wall protein. Cell walls were then resuspended in 50mM Tris-HCl containing SDS, DTT and EDTA and boiled for 30 minutes to dissociate any remaining lipid-linked molecules or non-covalently bound proteins. The resulting cell walls were then washed with dH_2O until all SDS was removed (approximately 6 times). At this stage cell walls had phosphate linked molecules such as WTA and many preparations were stopped and quantified at this stage. When WTA-negative peptidoglycan was required, cell walls were incubated with 250µl 48 %(w/v) hydrofluoric acid (HF) at 4 °C for 48 hours to remove any phosphate linked molecules. The peptidoglycan was then washed with 50mM Tris-HCl (pH 7.5) and dH_2O in alternating washes until the supernatant reached pH 5 and the sample was considered safe. Both WTA-positive cell walls and WTA-negative peptidoglycan were stored at -20^{o}C.

2.15 Cell wall/Peptidoglycan quantification

Purified cell wall/peptidoglycan was purified by freeze drying a small amount in a pre-weighed Eppendorf. Briefly, 100µl of purified cell wall/peptidoglycan stock in dH_2O was added to a pre-weighed Eppendorf and centrifuged at 20000xg for 10 minutes, supernatant was discarded, and the Eppendorf was frozen to -80^{o}C before an overnight incubation in the freeze drier (ScanVac Cool Safe 55-4 Pro 3800). The next morning the tube was re-weighed, and the amount of cell wall/peptidoglycan stock was calculated in mg before being resuspended in PBS. Freeze-dried samples for quantification were

discarded but this methodology was also used to produce freeze-dried peptidoglycan for *in vivo* challenge as seen in Figure 4.3. In this instance the peptidoglycan was freeze dried as above but in larger quantity before being resuspended in etox PBS and sonicated before addition to inocula.

2.16 Wall teichoic acid (WTA) purification

Purified WTA-positive cell walls as isolated in section 2.15 were incubated in 0.1M NaOH at room temperature for 72hours whilst rotating. Cell wall suspensions were then centrifuged at 20000xg for 10 mins and the supernatant was taken and neutralised with 5%(v/v) acetic acid. The supernatant was then loaded into 0.5-1.0KDa dialysis tubing (Spectrum™ labs) and then dialysed in 2L dH_2O at room temperature. The dialysis liquid was changed at least four times to ensure reduction of salt in the sample. The sample was then extracted from the dialysis tubing into a pre-weighed microfuge tube and frozen at -80^{o}C before overnight incubation in the freeze drier (ScanVac Cool Safe 55-4 Pro 3800). The tube was then weighed again to ascertain the yield of WTA.

2.17 Native PAGE

Two 20%(w/v) Native-PAGE gels were made with:

- 1.5M Tris-HCl (pH 8.8) 3.3 ml
- BioRad 30%(w/v) Acrylamide/Bis solution (35.5 :1) 6.7 ml
- 10%(w/v) ammonium persulphate 100 µl
- Tetramethylethylenediamine (TEMED) 10 µl

400-500ng of polysaccharide sample was loaded onto these gels in 50%(v/v) glycerol. The gels were run at room temperature for ~90 minutes at a constant of 180V in a BioRad Mini-PROTEAN® gel system. These gels were run in 1X Novex™ Tris-Glycine Native Running Buffer.

2.18 Alcian-Silver Stain

Native-PAGE WTA gels were incubated with gentle agitation in Alcian blue stain overnight. Gels were then washed with dH_2O and silver stained with Pierce™ Silver Stain for Mass Spectrometry (Thermo). The manufacturer suggests fixing protein gels 30%(v/v) ethanol/10%(v/v) acetic acid but as this is the solvent for the alcian blue stain

repeating incubation in this buffer was omitted. Apart from this omission the kit was used according to manufacturer's instructions to stain the WTA on the gel. Briefly:

- gels were washed twice for 5 minutes in 10%(v/v) Ethanol,
- washed twice for 5 minutes in ultrapure water,
- incubated for 1 minute in silver stain sensitizer,
- washed twice for 1 minute in ultrapure water,
- incubated for 5 minutes in silver stain with silver stain enhancer,
- washed twice for 20 seconds in ultrapure water,
- incubated in developer solution until bands appear (approx. 2-3 minutes) the reaction is stopped via incubation in 5%(v/v) acetic acid.

The gel was then imaged on Gbox Chemi-XX9 imager (Syngene).

2.19 Flow cytometry

Samples were resuspended in sterile filtered (0.2µm pore) PBS and loaded into a 96 well flow cytometry plate and analysed for forward scatter and side scatter on a Millipore Guava EasyCyte system. *S. aureus* samples used were grown to exponential phase for this analysis and peptidoglycan samples were sonicated (2.13) prior to flow cytometry. 6500 counts were obtained per sample and samples were then gated to against a sterile filtered PBS blank to exclude small events that constitute background noise.

2.20 Cell wall digestion/solubilisation

2mg of purified cell wall/PGN was suspended in 10 µl sodium phosphate buffer (2.2.7), 90µl dH_2O and 50µg mutanolysin and incubated overnight at 37°C. This was then boiled at 100°C to inactivate mutanolysin and soluble cell wall/muropeptides were collected by centrifugation at 20000 x g and the supernatant which contained the solubilised cell wall/PGN was taken forward for further processing

2.21 Reduction of soluble cell wall fraction

Soluble cell wall/muropeptides were mixed in a 1:1 ratio with sodium borate buffer (2.2.9) or until the pH reached 9. Sodium borohydride was added, and the mixture was incubated at room temperature for 15 minutes. The reaction was stopped by addition of

phosphoric acid until the pH reached 4. The pH was then raised to at least 6 using NaOH and sterile filtered (0.2µm) to remove any insoluble contaminants from the sample.

2.22 HPLC muropeptide analysis

Samples were analysed using a Thermo Scientific Hypersil GOLD aQ column (200 x 2.1 mm, 1.9µm particle size), which was pre-equilibrated with Buffer A (2.2.14.1) in a Dionex HPLC system. Soluble cell wall/PGN fractions were eluted from the 200 x 2.1 mm column using a flow rate of 0.3 ml/min, using a multi-step convex gradient over 63 minutes. Elutions of muropeptides or solubilised cell wall were detected by measuring absorbance at 202 nm and analysed using chromeleon version 6.80

Time (min)	% Buffer A	% Buffer B
0	100	0
5	95	5
23	90	10
42	85	15
47	70	30
47.1	0	100
55	0	100
55.1	100	0
63	100	0

Table 2.6 RP-HPLC elution gradient for *S. aureus* muropeptide analysis

2.23 SDS-PAGE

Proteins were separated by Laemmli SDS-PAGE. 12%(w/v) Mini-PROTEAN® TGX™ precast 10-well protein gels (BioRad) were loaded into a Protean II (BioRad) gel tank and submerged in 1x SDS-PAGE reservoir buffer. Protein sample was boiled in 1x SDS-sample buffer to denature the protein and 10-20µl of protein sample per well was loaded onto the gel. The gel was run at 150V until the dye front reached the bottom of the gel (~45 minutes). Samples were run alongside Colour Prestained Protein Standard, Broad Range (NEB) which was used to approximate the size of proteins seen in the sample. Gels were removed from the tank and casting cassette and stained for 30 minutes in Quick-Coomassie (Generon) to visualise the protein bands within the sample.

2.24 Protein production

2.24.1 Protein expression

An overnight culture of the protein production *E. coli* strain was made by inoculating 10ml LB with a single colony and incubating this at 37ºC at 250rpm. The next morning this was sub-cultured into 1L of LB to give an OD_{600} of 0.05. This was grown at 37ºC at 180rpm until OD_{600} reached approximately 0.6, at this point IPTG was added to a final concentration of 1mM. The culture was incubated again at 37ºC, 180rpm for approximately another 6 hours before the culture was harvested via centrifugation at 14000xg for 10 mins; at this point the pellet can be stored overnight at 4ºC. The next day the pellet was resuspended in START buffer and underwent a -80ºC freeze-thaw cycle 3 times then sonicated 3 times for 30 seconds with incubations of ice between sonication. The solution was then centrifuged to pellet insoluble material and the soluble and insoluble material was separated. Each fraction was ran separately on an SDS-PAGE gel to find which fraction had the majority of recombinant protein.

2.24.2 Soluble Protein Nickel affinity purification

The fraction containing recombinant protein was passed through a 0.45µm pore sterile filter. A 5ml HisTrap™ His tag protein purification column was loaded with 5mM $NiSO_4$, excess NiSO4 was flushed out with ultrapure water then attached to a peristaltic pump (BioRad) and equilibrated with START buffer. The protein sample was passed through the column and the flow through was reserved. START buffer containing stepwise increases in Imidazole concentration (10 ml of each: 0mM, 25mM, 50mM, 75mM, 100mM, 125mM, 250mM, 500mM) was passed through the column and each fraction collected. All fractions were run on SDS-PAGE to find the samples with the pure/large amounts of recombinant protein and these fractions were taken forward.

2.24.3 Protein dialysis

Spectra/Por 3 dialysis membrane (3.5KDa MWCO) was washed in dH_2O before loading with selected protein fractions from section 2.24.2. This was then submerged in 2L PBS and stirred at 4ºC for at least 3 hours. PBS was changed at least 4 times in order to remove all residual imidazole in the protein sample. After dialysis protein was stored at -20ºC.

2.24.4 Size exclusion chromatography/Fast-performance liquid chromatography (FPLC)

When further purification was required protein was passed through a Superdex™ 200 10/300 GL column (Tricorn™ high performance columns) by an ÄKTA fast-performance liquid chromatography (FPLC) system (ÄKTA design, Amersham Bioscience). This separated recombinant protein based on size allowing you to analyse the oligomerisation state of purified protein to ensure use of monomers over aggregates. The mobile phase was de-gassed PBS as this was the solvent for the recombinant protein and protein elution was measured by absorbance at 260 nm and 280 nm and size calculated based on elution times of proteins standards of known size (Gel Filtration Standards, GE Healthcare).

2.24.5 Bichinoic acid (BCA) assay

Protein was measured with a Micro BCA™ Protein Assay Kit (Thermo) according to manufacturer's instructions. Briefly, both the unknown protein and a BSA standard were serially diluted in a 96 well plate and the working BCA reagent was mixed from kit components immediately prior to the assay. Then equal volumes of working BCA reagent and protein solution were mixed and incubated at 37^{o}C for an hour. Then the absorbance was measured at 595nm and the unknown protein concentration was calculated from a BSA-derived standard curve.

2.24.6 Protein concentration by ultracentrifugation

Amicon® Ultra 4 mL Centrifugal Filters with a 3000 Nominal molecular weight limit (NMWL) were used in accordance with manufacturer's instructions in order to concentrate protein solutions. Protein solution was loaded into the centrifugal filter which was centrifuged at no more than 4000 x g for 10 minutes. This was repeated until the sample was sufficiently concentrated, the sample was then recovered, and concentration measured by BCA assay.

2.24.7 Protein endotoxin purification

Recombinant protein that was to be used in *in vivo* experiments needed to be free from endotoxin. Therefore, endotoxin was removed with Pierce™ High Capacity Endotoxin Removal Spin Columns with resin containing beads with modified ε-poly-L-lysine with an endotoxin binding capacity of 2000000 Endotoxin Units (EU)/mL. Columns were

used according to manufacturer's instructions. Briefly, columns were centrifuged at 500 x g to remove their storage buffer, incubated in 0.2N NaOH overnight, washed with 2M NaCl and endotoxin-free water, equilibrated in endotoxin-free PBS tree times before being incubated with the sample with end-over-end mixing at room temperature for one hour. Sample was then collected via centrifugation at 500 x g and the column could be regenerated through incubation in 0.2N NaOH.

Endotoxin removal was confirmed via of the Pierce™ Chromogenic Endotoxin Quant Kit (Thermo) used according to manufacturer's instructions.

2.24.8 Mass spectrometry for protein verification

Recombinant protein structure/identity was verified by the Dickman group in the Department of Biological and Chemical Engineering, University of Sheffield. Verification/identification was performed by Trypsin digestion and LCMS as described in Shevchenko *et al*. 2006.

2.25 Cy2 labelling of protein

1mg of protein in PBS was mixed with 1mg Fluorolink Cy^{TM}2 Reactive Dye (Amersham) at room temperature, rotating, in darkness for 5 hours.

The protein-dye conjugate was then loaded into Spectra/Por 3 dialysis membrane (3.5KDa MWCO) and dialysed at 4^{o}C in 2L PBS with 10%(w/v) BSA whereby the BSA could act as a sink for any unbound amine-reactive dye. The dialysis fluid was changed 4 times.

2.26 Cell wall pulldown assay

0.1mg/ml of unlabelled or 500nM of Cy2 labelled DivIC was incubated with various concentrations of cell walls or peptidoglycan in binding buffer (2.2.12) at a total volume of 200µl. The mixture was incubated at room temperature for 5 minutes then centrifuged at 20000xg in a microfuge for 10 minutes. In experiments with unlabelled DivIC, the insoluble cell wall pellet and the soluble supernatant fractions were separated and analysed by SDS-PAGE (2.23). When Cy2 labelled DivIC was used 100µl of the soluble supernatant fraction was measured for Cy2 fluorescence on a Victor^{2}$_{TM}$, Wallac plate reader. The average of the DivIC-Cy2 alone values was set at 100% and the other fluorescence data points are displayed relative to this. In the

instance a DivIC-Cy2 alone control was not available the average of the HF-treated samples was taken the 100%

2.27 Alexa Fluor 647 labelling of protein

0.5mg of Protein was mixed with 100µl of 2mM Alexa Fluor™ 647 NHS Succinimidyl Ester (AF647) (Thermo) and 5µl of triethylamine. This was incubated in the dark at room temperature rotating for 24 hours then left open to the air for 1 hour for excess triethylamine to evaporate.

The protein-dye conjugate was then loaded into Spectra/Por 3 dialysis membrane (3.5KDa MWCO) and dialysed at 4^{o}C in 2L PBS with 10%(w/v) BSA whereby the BSA could act as a sink for any unbound amine-reactive dye. The dialysis fluid was changed 4 times.

2.28 Microscale thermophoresis (MST)

MST was performed on a Monolith NT.115 (Nanotemper) using nanotemper control software. 100-300nM protein conjugated to AF647 (2.34) was mixed with potential binding partners such as WTA in 1x binding buffer and loaded into Monolith NT.115 Premium capillaries (Nanotemper), capillaries were also loaded with AF647 conjugated protein alone in identical buffer to serve as a negative control. Capillaries were placed in the Monolith NT.115 and measurements were made at 21^{o}C, using the red at 10% excitation power and medium MST power. The software was used to run quality control such as checking for aggregation, ligand autofluorescence and starting fluorescent counts being in the correct range. The programmed binding check protocol allowed comparison between protein alone and protein-ligand complex to assess whether binding was taking place.

2.29 Phosphate concentration assay

Varying amounts of sample were added to glass test tubes that had been thoroughly washed with dH_2O to remove residual phosphate. 30µl of 10%(m/v) $MgNO_3$ (in 35%v/v Methanol) was added to each test tube and the liquid was evaporated via gently heating with a Bunsen burner leaving a white/brown powder. 600µl of 0.5M HCl was added to each test tube and these were added to a pre-heated 100^{o}C water bath at rolling boil. The tubes were allowed to cool on the bench. 10%(m/v) ascorbic acid was mixed 1:1

with 0.42%(m/v) $(NH_4)_2MoO_4$ (dissolved in 100ml H_2O and 2.86ml H_2SO_4) which should turn yellow. 1.4ml of the yellow ascorbic/ammonium molybdate mixture was added to each test tube and then incubated at 37°C to produce a colour change to blue in phosphate positive samples. Samples were measured for absorbance at the pink wavelength of 820nm.

Samples were ran along a standard curve of 0.65mM sodium phosphate which was used to calculate phosphate content per sample.

2.30 Murine Infection Model

2.30.1 Generation of inoculum

2.30.1.1 Bacterial

S. aureus (NEWHG) was grown in TSB at 37°C to early stationary phase, washed with sterile, etox PBS and resuspended in sterile, etox PBS with 10%(w/v) BSA. This was aliquoted and stored at -80°C. The CFU/aliquot was established through plating serial dilutions onto TSA and growing overnight at 37°C. Then the correct dilutions to get the desired dose were calculated and verified via serial dilution and plating. Infectious inocula were always retained after infection of experimental animals and checked via serial dilution and plating to verify the infectious dose each animal received.

2.30.1.2 Peptidoglycan

HF-stripped, *M. luteus* peptidoglycan (made as described in section 2.15) was washed once in etox PBS and resuspended in etox PBS at a concentration of 10mg/ml. This was stored at -20°C and once thawed for *in vivo* work was sonicated (section 2.13) to ensure proper solubility before inclusion in any inoculum.

2.30.1.3 Vaccine

Vaccine formulations were made in 1X etox PBS under aseptic technique. Vaccines were used at a final concentration of 1µg/dose recombinant, endotoxin purified, mass-spectrometry confirmed, Clumping factor A (ClfA), 50µg/dose CpG-B DNA (Hycult Biotech), 1%(w/v) Alhydrogel® adjuvant (Invivogen) and, when included, 100µg *M. luteus* peptidoglycan. Vaccines were always administered subcutaneously with initial

vaccination constituting day 0 and vaccine boosters given on day 14 and day 21 post-vaccination. Vaccines were always administered alongside a PBS placebo control group.

2.30.2 Mice backgrounds used

2.30.2.1 Balb/C

Female Balb/C mice were obtained from Charles River so they would be 7-8 weeks old at the start of the experimental procedure.

2.30.2.2 Lox/Cre mice

Mutant mice, in the C57BL/6-129 background, were produced by the Minichiello group at the University of Oxford using *Cre/lox* mutagenesis strategies[238] with the Cre enzyme under the control of the *LysM* gene leading to knockouts specifically in phagocytes. The following mouse lines were created and shipped to Sheffield for *S. aureus* challenge:

- *$Trka^{lox/lox}$; LysM Cre* (*$Trka^{LysMCre}$*)
- *$p75^{NTR\ lox/lox}$; LysM Cre* (*$p75^{NTR\text{-}LysMCre}$*)
- *$Trka^{lox/lox}$ & $p75^{NTR\ lox/lox}$; LysM Cre* (*Trka/$p75^{NTR\text{-}LysMCre}$*)
- *NGF-$\beta^{lox/lox}$; LysM Cre* (*NGF-$\beta^{LysMCre}$*)

Mice were sent to the University of Sheffield when there were enough mutant and wildtype females to carry out an experiment with sufficient statistical power. This led to *LysM Cre* mice having a larger age range than Balb/C experiments, but wildtype controls were littermate controls thus accounting for the greater age range. At the end of each experiment using *LysM Cre* mice, tail biopsies were taken and sent back to the Minichiello lab for genotyping to confirm correct groupings of mutant and wildtype mice.

2.30.3 Intravenous infection/inoculation

Mice were weighed and checked prior to inoculation. Inocula were vortexed prior to loading into insulin injector needles. Mice were warmed in a 37ºC incubator for 10 minutes to encourage their tail veins to dilate. Then mice were place one at a time in a commercial mouse restraint device and injected with a maximum of 100µL in the tail vein. The health status of the mice was then checked twice daily, and they were weighed once daily once on procedure.

2.30.4 Subcutaneous infection

Mice were weighed prior to inoculation. Inocula were vortexed then drawn into the 29G insulin injector needle. Mice were scruffed and restrained by the investigator and injected subcutaneously, dorsally into the scruff behind the head between the forelegs. The maximum volume injected was 100µL per injection. The health status of the mice was then checked twice daily, and they were weighed once daily once on procedure.

2.30.5 CFU enumeration

At the end of an infection experiment mice were culled according to schedule one procedures and dissected. For intravenous experiments liver and kidneys were always taken, the spleen, lungs and heart were also taken periodically. For subcutaneous infections, the cutaneous and underlying muscle tissue at, and surrounding, the site of injection was excised. Tissue was kept on ice during dissection then stored at -20^{o}C for at least two days before processing. Tissues were suspended in sterile PBS (3ml for livers and 2ml for all other tissue types) and homogenised in a Precellys 24 homogeniser. These homogenates were then serially diluted and 5µL spots were plated onto agar and incubated at 37^{o}C overnight to determine CFU per organ.

2.30.6 Blood sampling

Mice were warmed in an incubator at 37^{o}C to encourage tail veins to dilate then restrained whilst Vaseline was applied to their tail before being cut over the tail vein over an Eppendorf and massaged along the tail length to encourage blood flow. Blood was stored on ice and allowed to coagulate before centrifugation to separate the haematocrit and serum. The serum was reserved and stored at -20^{o}C for later cytokine analysis.

2.30.7 Cytokine analysis

Serum was sent to the University of Sheffield Core facilities flow cytometry unit. Here it was analysed by core facility technical staff using BD^{TM} cytometric bead analysis Flex sets using a FACSArray Bioanalyzer (BD BioSciences, USA) in accordance with manufacturer's instructions.

2.31 Ethics

Murine work was carried out according to UK law in the Animals (Scientific Procedures) Act 1986, under Project License PPL 40/3699 and Project License P3BFD6DB9 (*Staphylococcus aureus* and other pathogens, pathogenesis to therapy). Personal license PIL I77FCCCBC (Categories A and B).

2.32 Statistical analysis

All statistical analysis was completed using GraphPad Prism software

For peptidoglycan pulldowns, phosphate concentration assays, flow cytometry and microscale thermophoresis, data were compared by the Student t-test where only two samples were compared. Where more than two samples were compared a One-way ANOVA with Dunnett's multiple comparisons was used to draw comparisons against control samples. In the instance of the cell wall pulldown assay where different cell wall samples were tested in different binding buffers a Two-way ANOVA with Tukey's multiple comparisons was used in order to simultaneously draw comparisons between both variables.

For CFU recovered and percentage of initial weight on the final day of infection, comparison between two groups was carried out via Mann-Whitney U test and comparison by more than two groups was performed by the Kruskall Wallis test with Dunn's multiple comparisons. Pre and post vaccination cytokine data were compared by Kruskall Wallis test with Dunn's multiple comparisons where whereas pre-vaccination and post-infection cytokine data was analysed by Two-way ANOVA and Tukey's multiple comparisons to allow for comparison between both treatment and infection type.

2.33 Collaborative work

Nickel affinity purified DivIC and ClfA was given to Dr Nicola Galley (University of Sheffield) for further purification by size exclusion chromatography (section 2.24.4). The purified ClfA was also verified as ClfA via mass spectrometry by Dr Caroline Evans (Department of Chemical & Biological engineering, University of Sheffield). Dr Galley also assisted by running the flow cytometry of the peptidoglycan samples shown in Figure 4.3. Assistance was provided in Microscale thermophoresis by Dr Nate Adams in terms of teaching me the technique and assisting with the initial optimisation. HF

treatment of bacterial cell walls was carried out by Dr Joshua Sutton, Mr Joshua Hooker or Dr Grace Pidwell (University of Sheffield).

Mouse work was usually carried out with the assistance of Dr Joshua Sutton, Dr Josie Gibson or Dr Daria Shamarina (University of Sheffield) who helped with loading injection needles, culls and dissections. This assistance was reciprocated as requested with their animal experiments. Transgenic mice were generated and bred by the Minichiello group at the University of Oxford before being shipped to the University of Sheffield for the infection experiments detailed in this thesis. Tail biopsies were sent back to the Minichiello group for genotyping to ensure correct stratification before data analysis.

Chapter 3:
WTA binding activity of DivIC

3.1 Introduction

Bacterial cell division is an essential process for bacterial viability. Despite this importance no clinically used antibiotics directly target the cell division machinery other than peptidoglycan biosynthesis. This is in part due to a lack of sufficient knowledge of division proteins. However, the essentiality of division components whilst making them an attractive antibiotic target also makes them more difficult to study genetically. Therefore, to facilitate logical drug design for antibiotic discovery we need to learn more about the cell division machinery of bacteria. Given the increasing emergence of antibiotic resistance and its importance in disease, *S. aureus* is a good bacterium in which to study cell division[44,239,240].

S. aureus division is discussed in Chapter 1.3, here I focus on the divisome complex with specific attention on DivIC. The divisome components DivIC, DivIB and FtsL, form a complex that assembles and provides a link between early and late-stage division, this therefore presents a checkpoint that could be targeted. Furthermore, all three proteins have short cytoplasmic N terminal domains and much larger extracellular C-terminal domains which provides a rationale for thinking that they might present a druggable target. Furthermore, it has been shown that the intracellular N-terminal domains and transmembrane domains of DivIC and DivIB can be substituted in *B. subtilis* with domains from the *E. coli* protein TolR which is not involved in cell division. These mutant cells with hybrid DivIC and DivIB are viable indicating that their transmembrane and cytoplasmic domains are non-essential in *B. subtilis* under conditions where the complete gene is known to be essential[148]. The predicted topology of DivIC is depicted in Figure 3.1 and shows that Q55-K130 (57.7% of the primary sequence length) is extracellular. DivIC in *S. aureus* is thought to be essential due to its absence from *S. aureus* transposon mutant libraries[233,241]. This chapter focuses on the putative essential extracytoplasmic domain of DivIC in *S. aureus*.

A suggested role for the DivIC, DivIB, FtsL divisome complex and its Gram-negative homologue: the FtsQBL complex, is to provide a scaffold for later division proteins. DivIC and FtsL are both small bitopic proteins with a single transmembrane domain. It

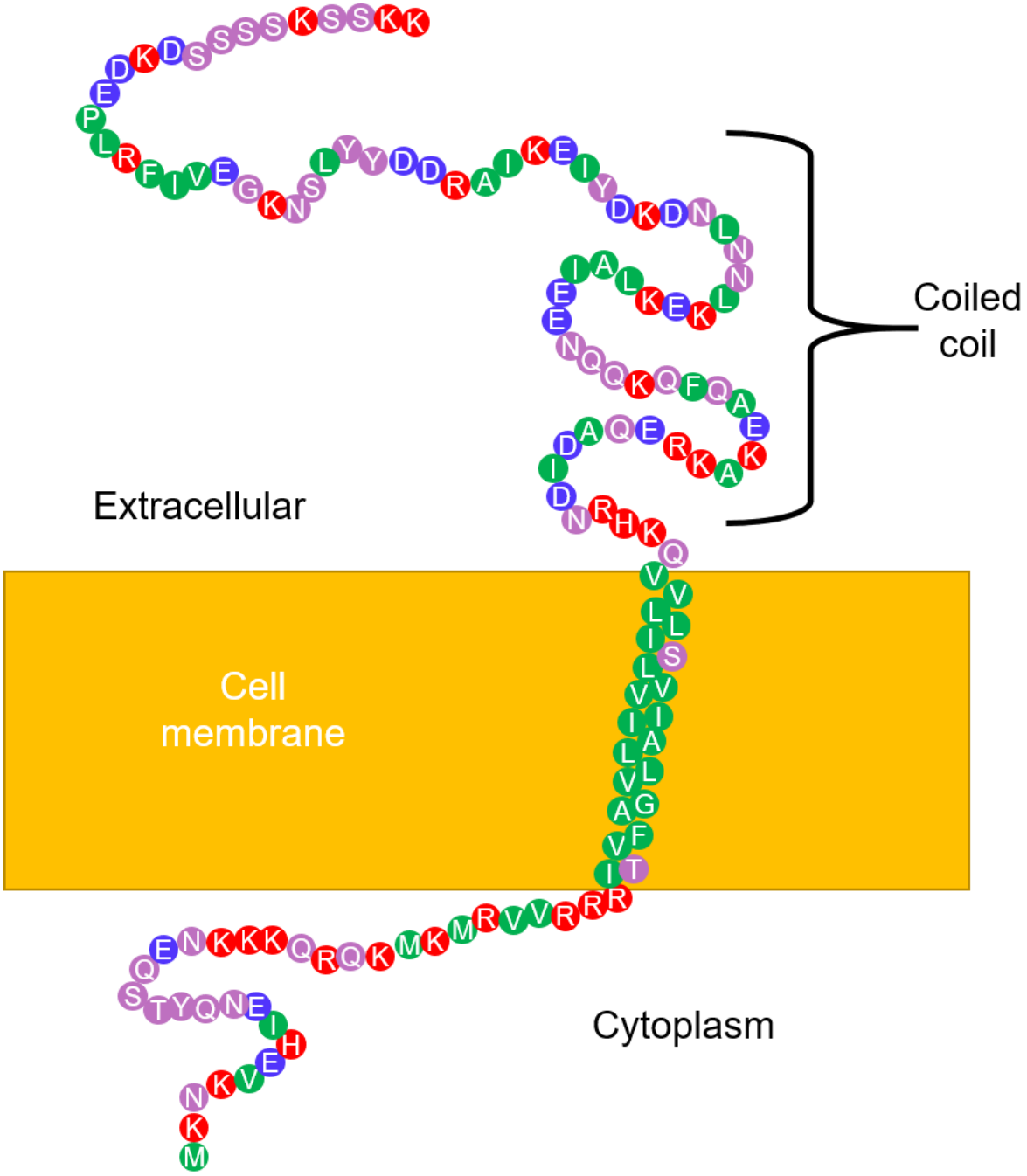

Figure 3.1 Predicted membrane topology of *S. aureus* DivIC
DivIC of *S. aureus* is 130 amino acids long with a predicted transmembrane region from I34-V54. There is little structural data available on DivIC but based on its primary sequence there is a predicted coiled coil region from V54-K94. Amino acids are colour coded based on charge (red; positive, blue; negative) and polarity (green; non-polar, violet; polar).

has been shown in *B. subtilis* that the stability of DivIC is dependent on FtsL[242], however the exact functions of DivIC and FtsL are unknown. Due to their role in cell division, they are not easily genetically tractable. In *Streptomyces coelicolor* (*S. coelicolor*) colony formation is not dependent on cell division and it has been shown that deletion of *divIC* or *ftsL* causes inefficient septation without detriment to cell growth/colony formation[243]. In addition, a *B. subtilis* temperature sensitive *divIC* mutant showed defects in septum formation[244]. Together these studies indicate that DivIC has a role in septation. Furthermore, bacterial two hybrid analyses have demonstrated that DivIC interacts with numerous division proteins[134], WTA biosynthesis machinery[245] and LTA synthesis proteins[245,246] thereby indicating a potential interaction between cell division and teichoic acids. Whilst a direct function for DivIC remains elusive, a role which also points towards septum formation/progression has been found for its divisome partner: DivIB[150].

A conditional lethal construct has been produced in *S. aureus* where *divIB* has been placed under the control of an inducible promotor. When DivIB is depleted in this strain the cell arrests during septation after the initial “piecrust” formation[150]. DivIB was also found to be a peptidoglycan binding protein *in vitro* through pulldown assays using purified, insoluble peptidoglycan. This was also demonstrated *in vivo,* through Western blots of different cell fractions with α-DivIB showing that DivIB, a membrane protein, could be found in the cell wall fraction. This raised questions of whether the other divisome proteins DivIC and FtsL could interact with cell wall components such as peptidoglycan. It was subsequently found that DivIC bound to cell walls before but not after treatment with hydrofluoric acid (HF)[247].

Treatment with HF is the final step in the *S. aureus* peptidoglycan purification process (section 2.14, Figure 3.2). The process progressively removes moieties on the insoluble cell wall until nothing remains except the MurNAc, GlcNAc glycan backbone and peptide side chains crosslinked by pentaglycine bridges. This is the material that makes up the peptidoglycan framework of the cell wall and in this thesis “peptidoglycan” refers to this final material of the purification process shown in Figure 3.2. Azhar Kabli had shown that the final HF treatment step resulted in loss of the cell wall capability to bind DivIC in pulldown assays. Therefore, in this thesis “cell wall” refers to the material just before the HF treatment which consists of only peptidoglycan and phosphate linked

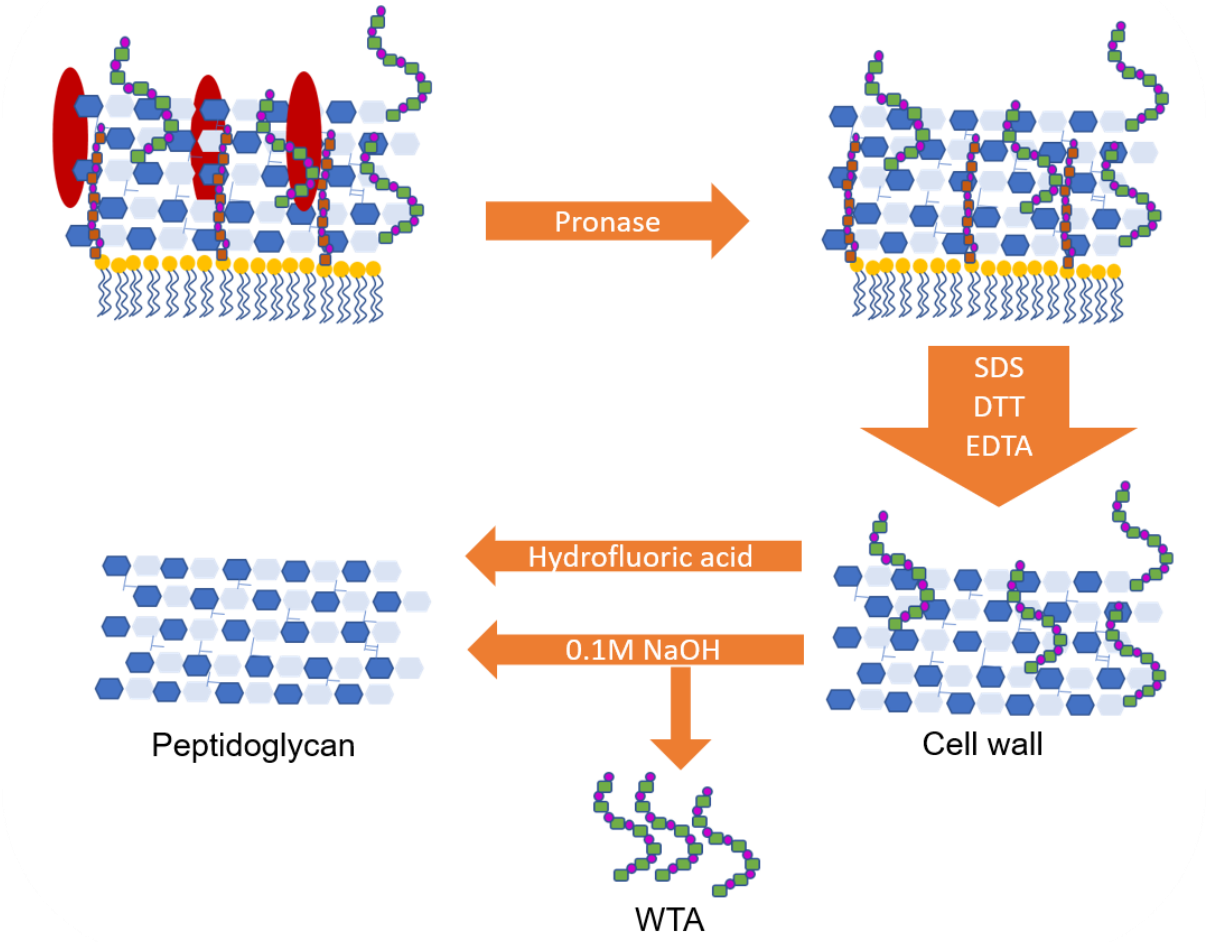

Figure 3.2 Diagram depicting workflow to purify cell walls and peptidoglycan from broken cells. Cells are broken to give fragments of cell wall associated with membrane and cell wall proteins (top left), these are treated with pronase to remove cell-wall associated proteins (top right), then they are boiled in Tris-HCl with SDS/EDTA/DTT to remove lipids, protein remnants, and associated molecules leaving a cell wall with only phosphate linked molecules such as WTA (bottom right). These cell walls can be treated with Hydrofluoric acid (HF) or NaOH to remove phosphate linked molecules leaving pure peptidoglycan (bottom left). After treatment with NaOH peptidoglycan is removed by centrifugation and the supernatant neutralised and dialysed to give WTA (bottom middle).

(likely polysaccharide) molecules as proteins and lipid-linked molecules should have been removed in previous steps as shown in Figure 3.2.

Within the divisome, DivIB binds to peptidoglycan and DivIC binds to something distinct from peptidoglycan within the cell wall. This may indicate that there could be more function to these divisome proteins than mere scaffolding. These proteins could be signalling the status of the cell wall or sensing a specific part of the cell wall where septation and subsequent division should take place. However, to determine the role of DivIC we would first need to establish what it is binding to within the cell wall.

3.2 Aims

Given the seeming essentiality of DivIC, and the proven essentiality of proteins it interacts with such as DivIB, interrupting the function of these proteins has the potential to have antibacterial activity. By elucidating the cell wall binding ligand of DivIC one might begin to be able to interrupt its seemingly essential process with molecules that could eventually become therapeutic antibiotics. Therefore, the works presented in this chapter aimed to:

- Characterise cell wall binding by DivIC by determining the binding ligand within the cell wall.

3.3 Results

3.3.1 Hydrofluoric acid eliminates DivIC binding to the cell wall

A 6xHis tagged, recombinant, extracellular domain of *S. aureus* DivIC (Lys56 to Lys130) was produced in *E. coli* cells containing an IPTG-inducible protein expression construct. Cells were lysed and fractionated then recombinant protein was purified from the soluble fraction by Ni^{2+} affinity chromatography and then further purified via size exclusion chromatography (section 2.25-2.27). Protein purity was ascertained via SDS-PAGE and demonstrated through a single observable peak on the UV spectra from the size exclusion chromatography (Supplementary Figure 1). This extracellular domain of DivIC is the primary DivIC construct used throughout this study and therefore “DivIC” will refer to this recombinant protein unless otherwise stated.

DivIC was shown to bind better to cell walls than peptidoglycan which had been treated with hydrofluoric acid (HF)[247]. This finding was recapitulated here through a pulldown assay. Briefly, 100µg/ml (~10µM) DivIC was mixed with varying amounts of cell wall or

peptidoglycan in binding buffer, this mixture was centrifuged at 14000 x g and soluble and insoluble fractions were separated before protein was analysed by SDS-PAGE (Fig 3.3).

When DivIC was mixed with SH1000 cell walls at greater than 250µg/ml the majority of the DivIC was found in the pellet/insoluble fraction thus indicating that DivIC had bound to the cell wall (Fig 3.3A). In contrast, when mixed with peptidoglycan from SH1000 cells, DivIC could always be found at greater abundance in the supernatant/soluble fraction than the insoluble fraction (Fig 3.3B). DivIC was detectable in the pellet/insoluble fraction but at much lower levels than the supernatant. This provided a qualitative basis from which to characterise the cell wall binding properties of DivIC.

3.3.2 DivIC binds significantly better to cell walls than peptidoglycan

In order to quantify the binding of DivIC to cell walls/peptidoglycan, DivIC was conjugated to a bis-reactive Cy2 fluorophore (section 2.25). This was then mixed in a pulldown assay in binding buffer as previously in section 3.3.1. Once the mixture had been centrifuged, 100µl of supernatant was measured for Cy2 fluorescence thereby quantifying the level of unbound DivIC (Fig3.4A). Thus, in this assay a higher fluorescence signals less binding.

The DivIC conjugated to Cy2 (DivIC-Cy2) was incubated in binding buffer with different concentrations of SH1000 cell wall and SH1000 peptidoglycan and analysed by the pulldown assay. The supernatant was analysed and showed that at all concentrations of cell wall/peptidoglycan used, the cell wall bound DivIC better than peptidoglycan (Fig 3.4B). The implication here is that there is a phosphate linked molecule or a cell wall moiety, that is removed or denatured by HF, treatment which is binding DivIC.

3.3.3 DivIC binding partner is not growth phase specific

S. aureus cell wall composition and architecture can change based on the maturity of the cell[248]. Therefore, to clarify if the DivIC binding partner was growth phase-dependent, cell walls were purified from exponential and stationary phase SH1000 cells and the binding of DivIC-Cy2 to these cell walls were compared via a pulldown assay (Fig 3.4C). There was no significant difference between the capacity of exponential or stationary phase cell walls to bind DivIC-Cy2. Therefore, the DivIC-binding partner on cell walls was present throughout the growth cycle. Due to this discovery, all further cell

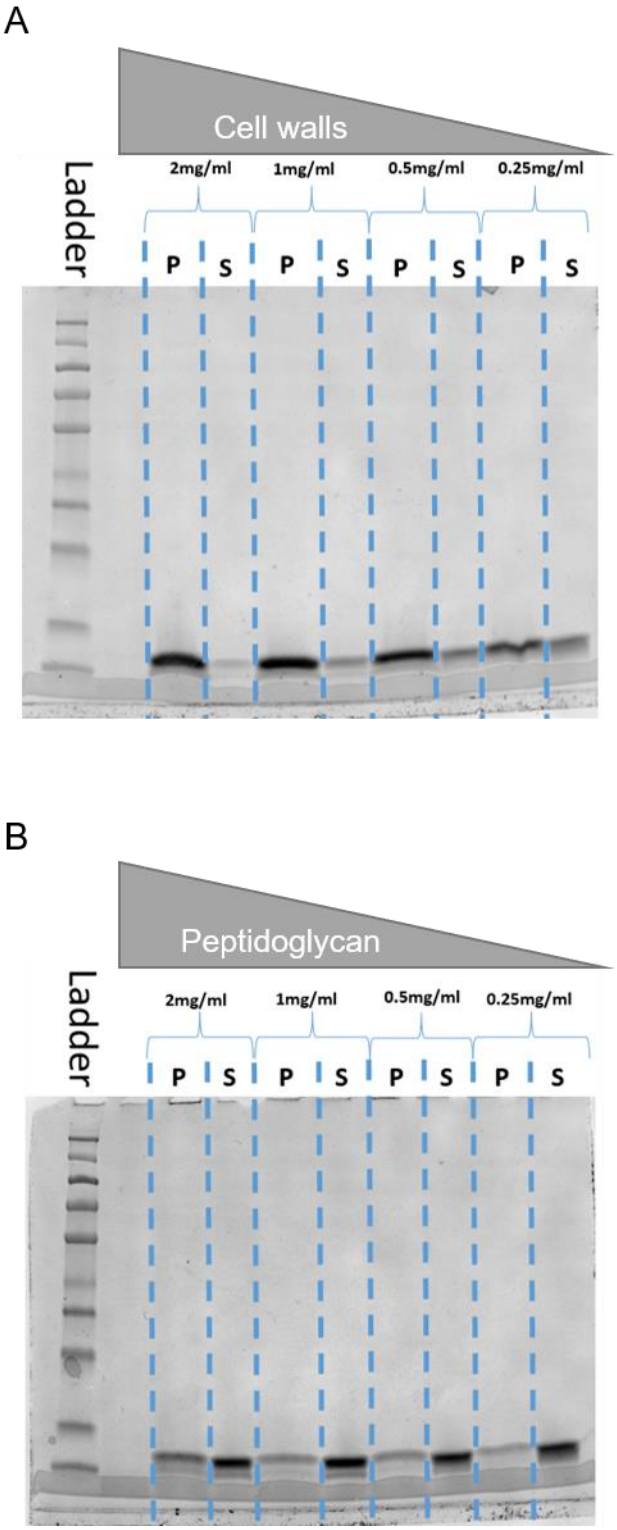

Figure 3.3 DivIC binds preferentially to cell walls compared to peptidoglycan
0.1mg/ml (~10µM) DivIC was incubated with varying concentrations of SH1000 cell wall (A) or HF-treated SH1000 peptidoglycan (B) in binding buffer (20mM sodium citrate, 10mM $MgCl_2$, 0.1%(v/v) Tween, 10µg/ml BSA, pH 5). These mixtures were centrifuged and the insoluble pellet (P) and soluble supernatant (S) fractions were separated, boiled in SDS-PAGE loading buffer containing 10%(v/v) 2-mercaptoethanol and analysed by 12%(w/v) SDS-PAGE.

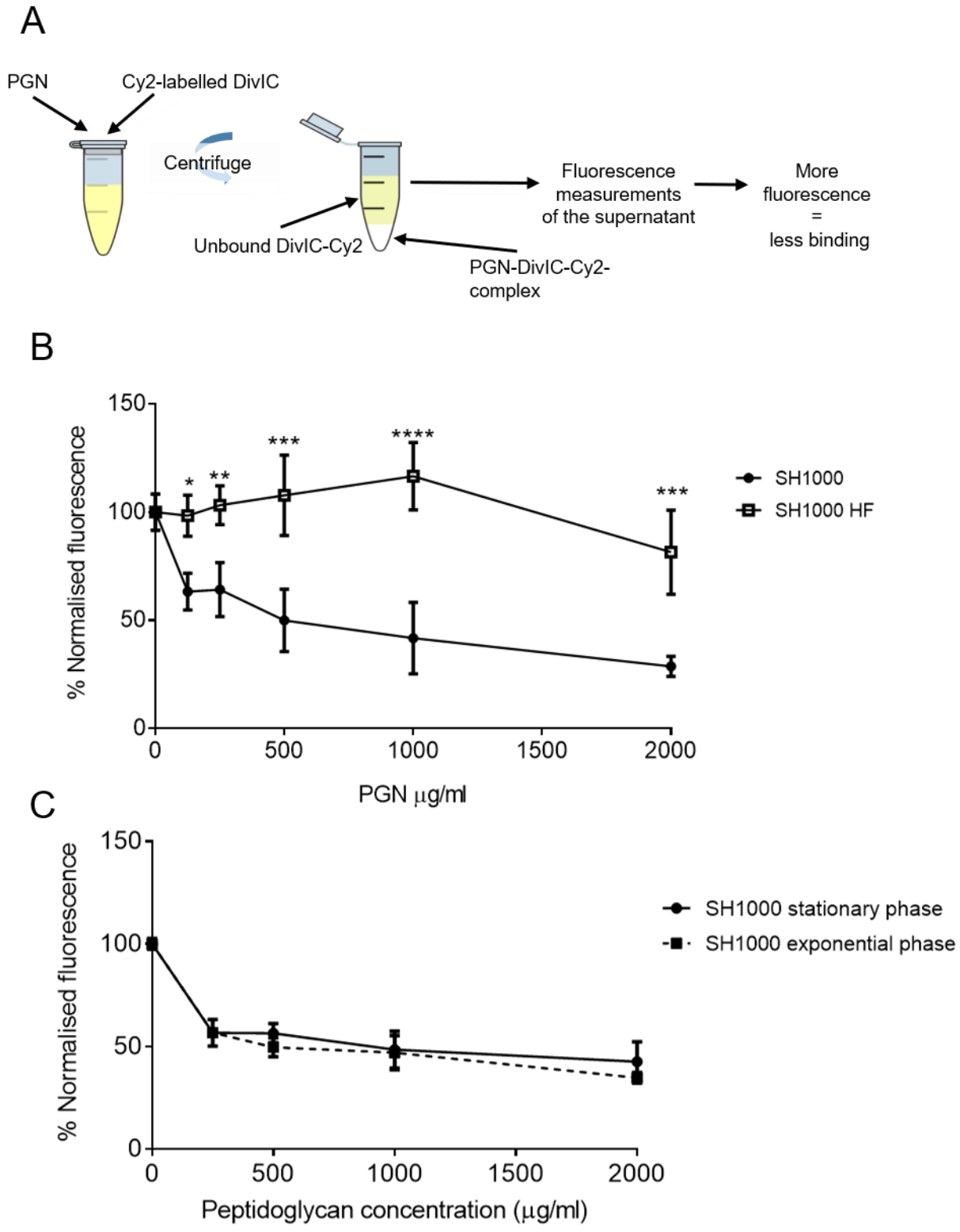

Figure 3.4 DivIC-Cy2 binds better to cell wall than peptidoglycan regardless of cell wall growth phase

DivIC was labelled with Cy2 and analysed by the a pulldown assay with cell walls/peptidoglycan in binding buffer (20mM sodium citrate, 10mM $MgCl_2$, 0.1%(v/v) Tween, 10µg/ml BSA, pH 5) and the supernatant was measured for Cy2 fluorescence (A). This methodology was used to compare DivIC-Cy2 binding to SH1000 cell walls before and after HF treatment (B) and to compare DivIC-Cy2 binding to cell walls from SH1000 stationary phase and exponential phase cultures (C). Data presented as mean and Std Dev. * P<0.05, ** P<0.01, *** P<0.005, **** P<0.001. n= 3 biological repeats.

wall purifications used stationary cell cultures as these gave better yields.

3.3.4 NaOH reduces the ability of cell walls to bind DivIC

HF reduces the ability of cell walls to bind DivIC (Fig 3.3, 3.4). HF is used in peptidoglycan purification as it breaks phosphodiester bonds and therefore removes WTA from cell walls[249,250]. HF is a harsh treatment as it not only strips the WTA from cell walls but has been shown to hydrolyse the high molecular weight WTA backbone to smaller molecules[251]. Therefore, a gentler treatment to remove WTA and phosphate linked molecules and preserve their integrity was required. NaOH was used as this has been previously used to strip intact WTA from cell walls for further analysis[252].

Cell walls were incubated with 0.1M NaOH for various timescales up to 24 hours before being neutralised with 5%(v/v) acetic acid and then compared against untreated and HF-treated cell walls in the DivIC-Cy2 pulldown assay. As seen from Figure 3.5A, cell walls were sufficiently devoid of WTA and phosphate linked molecules after 5 hours incubation with 0.1M NaOH that they bound significantly less DivIC-Cy2 than untreated cell walls. This loss of binding capacity increased the longer the cell walls were incubated with NaOH with greater significant differences seen between untreated cell walls and the cell walls incubated with 0.1M NaOH for 24 hours compared to 5 hours. However, all NaOH treatments up to 24 hours reduced DivIC binding significantly less than treating cell walls with neat HF for 48 hours. Therefore, the timescale of NaOH treatment was extended to 72 hours.

Cell walls which had been incubated with 0.1M NaOH for 72 hours exhibited minimal binding to DivIC-Cy2 in a similar fashion to HF-treated cell walls. As shown in Figure 3.5B the NaOH treated cell walls exhibit no concentration dependent changes in ability to bind DivIC-Cy2. This data implies that treatment with 0.1M NaOH for 72 hours is as effective, if not more so, than the standard 48 hours incubation with HF for removing the ability of cell walls to bind DivIC.

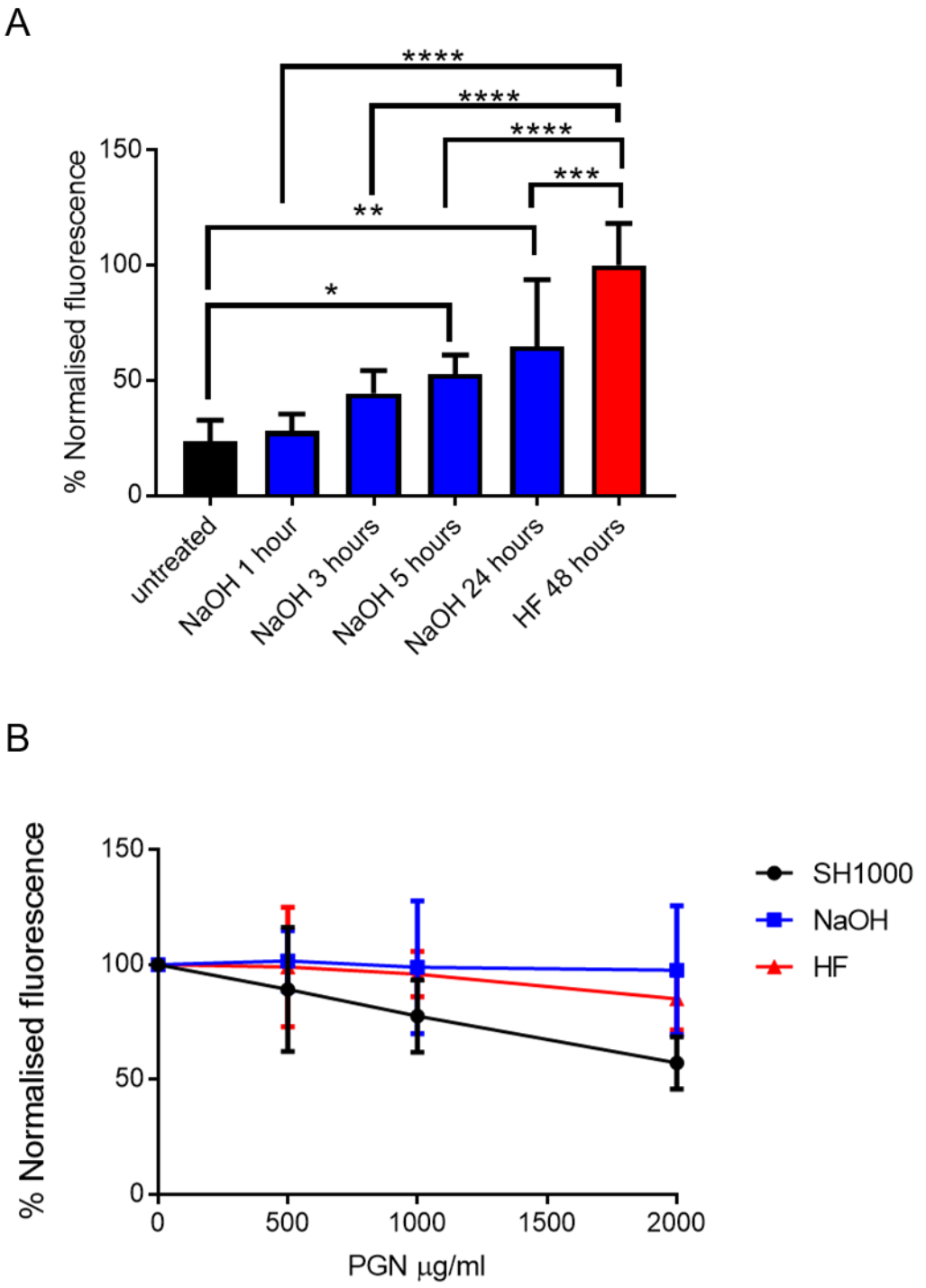

Figure 3.5 Effect of NaOH (0.1M) treatment of cell walls on DivIC binding.
SH1000 cell walls were incubated with 0.1M NaOH for different times up to 72 hours. Samples were neutralised to pH 7 with 5%(v/v) acetic acid. 0.25mg/ml of cell walls incubated with 0.1M NaOH, or cell walls incubated with HF for 48 hours or untreated cell walls were incubated with 500nM DivIC-Cy2 in binding buffer (20mM sodium citrate, 10mM $MgCl_2$, 0.1%(v/v) Tween, 10µg/ml BSA, pH 5). This was centrifuged at 14000 x g and 100µl of supernatant was measured for Cy2 fluorescence (A). 500nM DivIC-Cy2 was incubated with various concentrations of untreated SH1000 cell walls, cell walls treated with HF for 48 hours or cell walls treated with 0.1M NaOH for 72 hours. This mixture was in binding buffer (20mM sodium citrate, 10mM $MgCl_2$, 0.1%(v/v) Tween, 10µg/ml BSA, pH 5). This was centrifuged at 14000 x g and 100µl of supernatant was measured for Cy2 fluorescence (B). Data presented as mean and Std Dev. * P<0.05, *** P<0.005, **** P<0.001. Each point in the pulldown represents a biological repeat.

3.3.5 DivIC binding to cell wall is divalent cation-dependent

DivIC binds preferentially to cell walls over peptidoglycan in pH 5, 20mM sodium citrate, 10mM $MgCl_2$[247]. The pH was chosen as there is extensive evidence of an acidic pH of the exoplasm between the cell membrane and interior leaflet of the cell wall in *B. subtilis*[253,254] and *S. aureus*[255]. Divalent cations such as Mg^{2+} are essential as cofactors in many cellular processes[256]. DivIC-cell wall binding was tested in buffers with different buffer compositions.

500nM DivIC-Cy2 was incubated with 0.25mg/ml SH1000 cell wall or 0.25mg/ml SH1000 peptidoglycan in 20mM sodium citrate buffer with different additional ions. $CaCl_2$, $MgCl_2$, $MgSO_4$ and NaCl were added to binding buffers to a final concentration of 10mM. Binding was compared between cell walls and peptidoglycan as a negative control in the presence of these additional ions. In addition, 0.1%(v/v) Tween and 10µg/ml BSA were added to reduce non-specific binding, to assess if this had any influence of the dependency on divalent cations. Under all conditions, the addition of divalent cations increased binding of DivIC to cell walls but not to purified peptidoglycan (Fig 3.6). The addition of tween and BSA, to remove non-specific binding, exaggerated the role of divalent cations (Fig 3.6C).

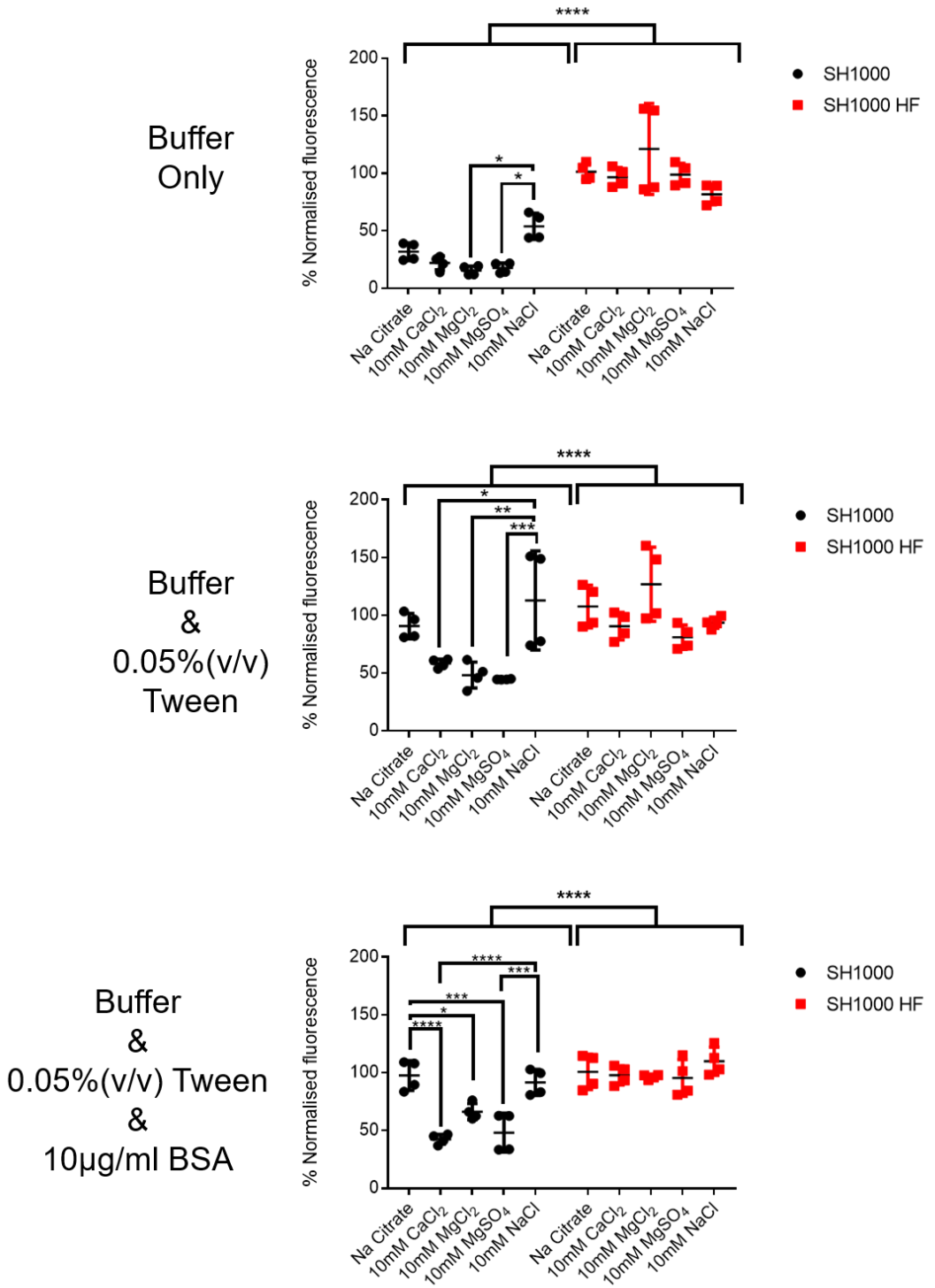

Figure 3.6 DivIC-cell wall binding is divalent cation-dependent
500nM of DivIC-Cy2 was incubated with 0.25mg/ml SH1000 cell wall or SH1000 peptidoglycan in 20mM sodium citrate with or without the addition of 10mM salt ($CaCl_2$, $MgCl_2$, $MgSO_4$ or NaCl). This binding buffer was altered through addition of 0.05%(v/v) Tween or 0.05%(v/v) Tween and 10µg/ml BSA. The mixtures of cell wall/peptidoglycan and DivIC-Cy2 were centrifuged at 14000 x g and 100µl of supernatant was measured for Cy2 fluorescence. Error bars indicate mean and Std Dev. * P<0.05, ** P<0.01, *** P<0.005, **** P<0.001. Each point represents a technical repeat.

3.3.6 Effect of cell wall charge on DivIC binding

To examine the likely role of ionic interaction, DivIC-Cy2 was incubated with SH1000 cell walls in binding buffer with and without the addition of 300mM NaCl (Fig 3.7A). The high salt addition significantly reduced DivIC binding.

To interrogate this further, cell walls were purified from strains with different cell wall charges. WTA represents the largest proportion of charged molecules in the cell wall due to a negatively charged phosphate present in the ribitol phosphate backbone[257,258]. WTA are modified by DltA and DltB which cause the addition of positively charged D-Alanine moieties thereby altering the overall charge of the cell wall. However, loss of *dltA* or *dltB* genes in *S. aureus* had no effect on DivIC binding (Fig 3.7B). Therefore, subtle changes in the charge of the WTA backbone are not enough to negate DivIC binding to cell walls.

3.3.7 DivIC binds to cell walls without O-acetylation

Treatment of cell walls with HF is known to ablate phosphate linked molecules leaving pure peptidoglycan, however, HF also degrades the O-acetylation modification of peptidoglycan[259]. As treatment with HF also reduced the capacity of cell walls to bind DivIC (Fig 3.3, 3.4) O-acetylation was investigated using an *ΔoatA* mutant which lacks O-acetylation (Fig 3.8A). Cell walls from the *ΔoatA* mutant were used in the DivIC-Cy2 pulldown assay and these still significantly bound to DivIC.

3.3.8 DivIC-cell wall binding is not affected by absence of common cell wall contaminants

During the cell wall/peptidoglycan purification (2.14) proteins are degraded by pronase and cell membrane/lipid associated molecules are removed by boiling in SDS/DTT/EDTA. This leaves a cell wall that only has phosphate linked molecules such as WTA and peptidoglycan. However, in order to confirm there were no remaining contaminants that contributed to DivIC binding, cell walls were purified from mutant *S. aureus* strains which lacked common contaminants of cell wall preparations[260].

Cell walls from these mutants lacking lipoprotein (Δ*lgt*), lipoteichoic acid (Δ*ltaS*) and sortase linked proteins (Δ*srtA*) were purified and then incubated at 0.25mg/ml with 500nM DivIC-Cy2 in binding buffer. The mixtures were centrifuged at 14000 x g and

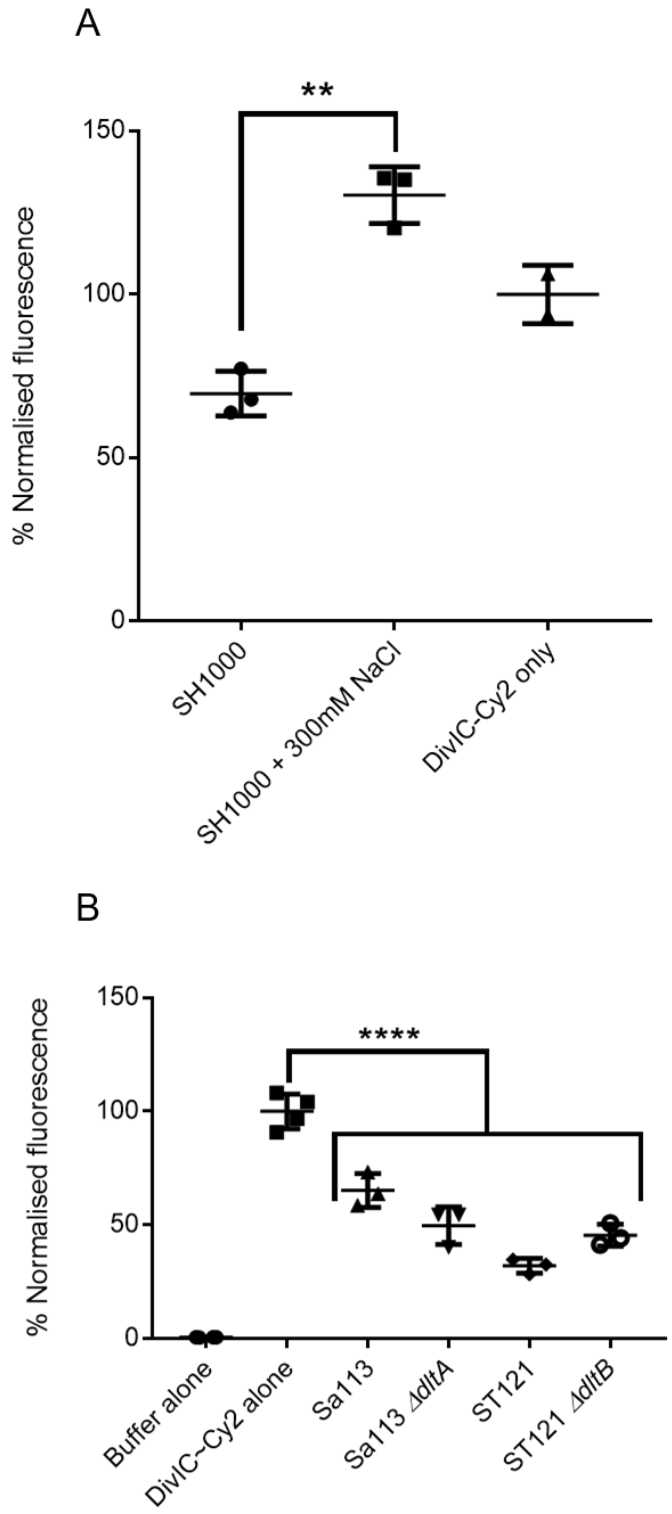

Figure 3.7 Analysis of the role of ionic interaction in DivIC-cell wall binding
SH1000 cell wall was incubated with 500nM DivIC-Cy2 in binding buffer with or without 300mM NaCl and the mixtures were centrifuged at 14000 x g before 100µl of supernatant was measured for Cy2 fluorescence (A). Cell walls from *dlt* mutants were isolated and 0.25mg/ml of cell walls were incubated with 500nM DivIC-Cy2 in binding buffer (20mM sodium citrate, 10mM $MgCl_2$, 0.1%(v/v) Tween, 10µg/ml BSA, pH 5). This was centrifuged at 14000 x g and 100µl of supernatant was measured for Cy2 fluorescence (B). Error bars indicate mean and Std Dev. *** P<0.005, **** P<0.001. Each point represents a technical (A) or biological (B) repeat.

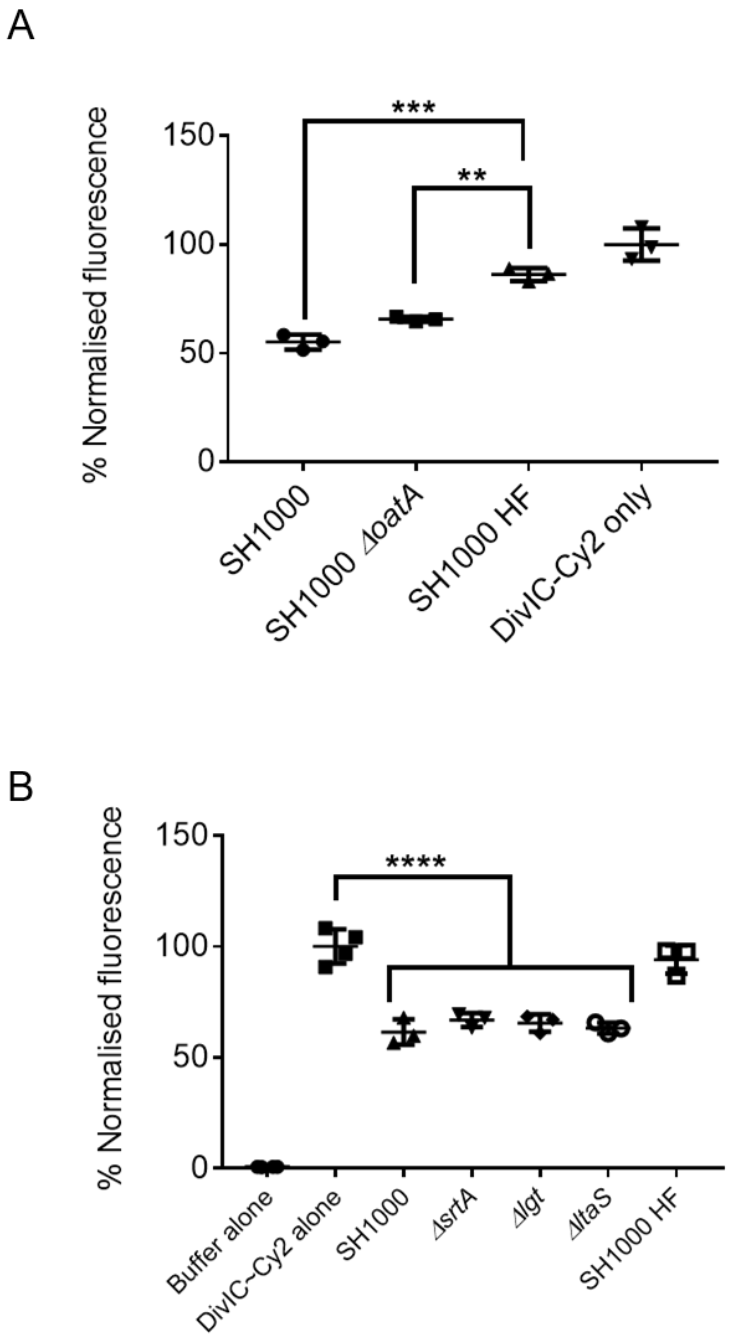

Figure 3.8 Role of cell wall modifications and associated components in DivIC binding
500nM DivIC-Cy2 was incubated with 0.25mg/ml cell walls from SH1000 or mutants deficient in O-acetylation of peptidoglycan (A) or missing lipoprotein (Δ*lgt)*, lipoteichoic acid (Δ*ltaS*) or Sortase A (Δ*srtA*) (B) or with peptidoglycan in binding buffer (20mM sodium citrate, 10mM $MgCl_2$, 0.1%(v/v) Tween, 10µg/ml BSA, pH 5). This was centrifuged at 14000 x g and 100µl of supernatant was measured for Cy2 fluorescence. Error bars indicate mean and Std Dev. **** P<0.001. Each point represents a biological repeat.

100µl of supernatant was measured for Cy2 fluorescence. As shown in Figure 3.8B there is no difference in binding between cell walls from the mutants and the SH1000 cell wall as all bound DivIC-Cy2.

3.3.9 Cell wall binding of DivIC is dependent on TarO

The most abundant phosphate-linked molecule on the peptidoglycan is WTA where it constitutes up to half of the cell wall dry weight[261]. TarO is the enzyme that enacts the first committed in WTA synthesis and one of the only enzymes in the synthesis pathway which can be interrupted and produce a viable knockout mutant[95]. Δ*tarO* mutants were available in three *S. aureus* backgrounds. Cell walls were purified from the SH1000, Sa113 and 15981 strains and their respective Δ*tarO* mutants. These were then incubated with DivIC-Cy2 in binding buffer for the pulldown assay along with a complemented SH1000 Δ*tarO* mutant. As seen in Figure 3.9A there is a significant loss of binding in Δ*tarO* mutants compared to their respective parent and binding can be restored via complementation.

To confirm that these Δ*tarO* mutants did indeed lack WTA, WTA was purified as described in 2.16 and separated by native-PAGE (2.17) and Alcian-silver stained (2.18). As seen in Figure 3.9B there is a clear WTA repeating ladder in all lanes with WTA samples from *tarO* competent strains and a lack of this in *ΔtarO* strains. To further confirm this, the cell walls of the parents and the *ΔtarO* mutants in 15981 and Sa113 were measured for phosphate concentration (2.36). As seen in Figure 3.9C, there is minimal measurable phosphate in the cell walls of the Δ*tarO* strains which further signifies their lack of WTA. The Δ*tarO* strains do not have WTA and their cell walls fail to bind DivIC as effectively as wildtype cell walls.

3.3.10 WTA$^+$ cell wall binding is DivIC specific

To confirm that WTA$^+$ cell wall binding was specific to DivIC, cytochrome-C was used. Cytochrome-C is a membrane protein of similar size and charge to DivIC. 0.1mg/ml (~8µM) Cytochrome-C was incubated with 2, 1, 0.5 and 0.25mg/ml of SH1000 cell wall or HF-treated peptidoglycan and analysed by a pulldown assay whereby the insoluble cell wall/peptidoglycan pellet and the soluble supernatant fractions were analysed by SDS-PAGE. Cytochrome-C was seen in all fractions in both the cell wall and peptidoglycan pulldowns thereby indicating a lack of any concentration dependent, specific binding as seen in the DivIC SDS-PAGE pulldowns (Fig 3.3).

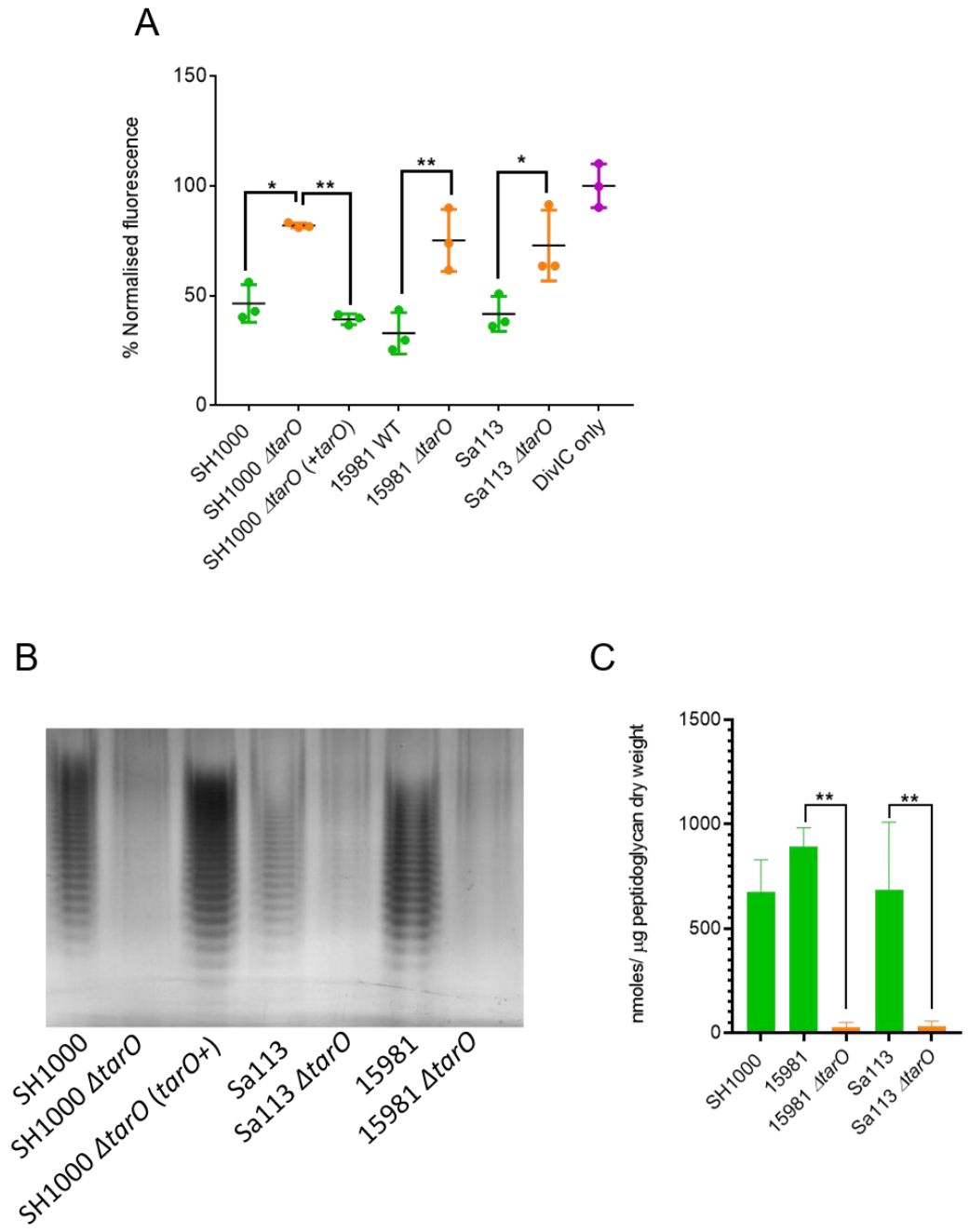

Figure 3.9 DivIC-Cy2 fails to bind to cell walls from Δ*tarO* mutants
Cell walls were purified from SH1000, Sa113 and 15981 *S. aureus* backgrounds and their respective Δ*tarO* mutants. 500nM DivIC-Cy2 was incubated with 0.25mg/ml cell walls in binding buffer (20mM sodium citrate, 10mM $MgCl_2$, 0.1%(v/v) Tween, 10µg/ml BSA, pH 5) and these were centrifuged and 100µl of supernatant was measured for Cy2 fluorescence (A). Cell walls were also incubated with 0.1M NaOH for 72 hours to strip WTA which were neutralised and dialysed in dH_2O before being separated by Native-PAGE and Alcian-silver stained (B). Cell walls were also measured for phosphate content (C). Error bars indicate mean and Std Dev. * P<0.05, ** P<0.01, *** P<0.005. Each point in the pulldown represents a biological repeat.

In addition, 500nM of Cy2-labelled cytochrome-C (Cytochrome-C-Cy2) was incubated in binding buffer with varying concentrations of SH1000 and SH1000 Δ*tarO* cell walls and analysed by a pulldown assay simultaneously with DivIC-Cy2.

As seen in Figure 3.10C the DivIC-Cy2 binds significantly better to SH1000 than Δ*tarO* cell walls, whereas Cytochrome-C-Cy2 shows no difference in cell wall binding regardless of cell wall type (Fig 3.10D). Furthermore, there is no great reduction in supernatant fluorescence due to Cytochrome-C-Cy2 at any cell wall concentration used implying that it is not just failing to bind in a *tarO*-dependent manner, but it does not bind cell walls at all. TarO-dependent cell wall binding is DivIC specific.

3.3.11 Failure to ligate WTA to cell walls results in loss of DivIC binding

The implication of TarO-dependent binding is that the binding of DivIC is to WTA. However, it is possible that TarO/WTA synthesis is required for other cellular processes which might contribute to DivIC cell wall binding. Therefore, to confirm that DivIC cell wall binding is WTA-dependent, another method of interrupting binding without interrupting WTA synthesis was required. WTA are synthesised on the cytoplasmic side of the cell membrane and then need to be translocated across the membrane and ligated to the cell wall by LCP proteins[87–89,262]. Interrupting the WTA synthesis pathway after TarO is toxic leading to non-viable mutants because the synthesis pathway sequesters all the undecaprenol lipid carrier[95]. However, the LCP dependent ligation of WTA to the cell wall can be interrupted thus leaving the WTA synthesis pathway and recycling of undecaprenol intact yet the cell wall is devoid of WTA[88]. It was especially prudent to investigate the LCP proteins as a bacterial two hybrid analysis had shown their interaction with DivIC[245].

S. aureus has three LCP proteins (MsrR/LcpA, sa0908/LcpB and sa2103/LcpC) which are functionally redundant[89], knockout mutants of all the LCP encoding genes and their relevant MSSA background were obtained from the Berger-Bächi/Stutzmann Meier lab and the triple knockout was confirmed by whole genome sequencing. Cell walls were purified from all the mutants and the MSSA112 parent and these were used in a pulldown assay with DivIC-Cy2 (Fig 3.11A). MSSA112 and all single and double LCP mutants showed significant binding to cell walls. Only the LcpABC triple mutant failed to bind cell walls.

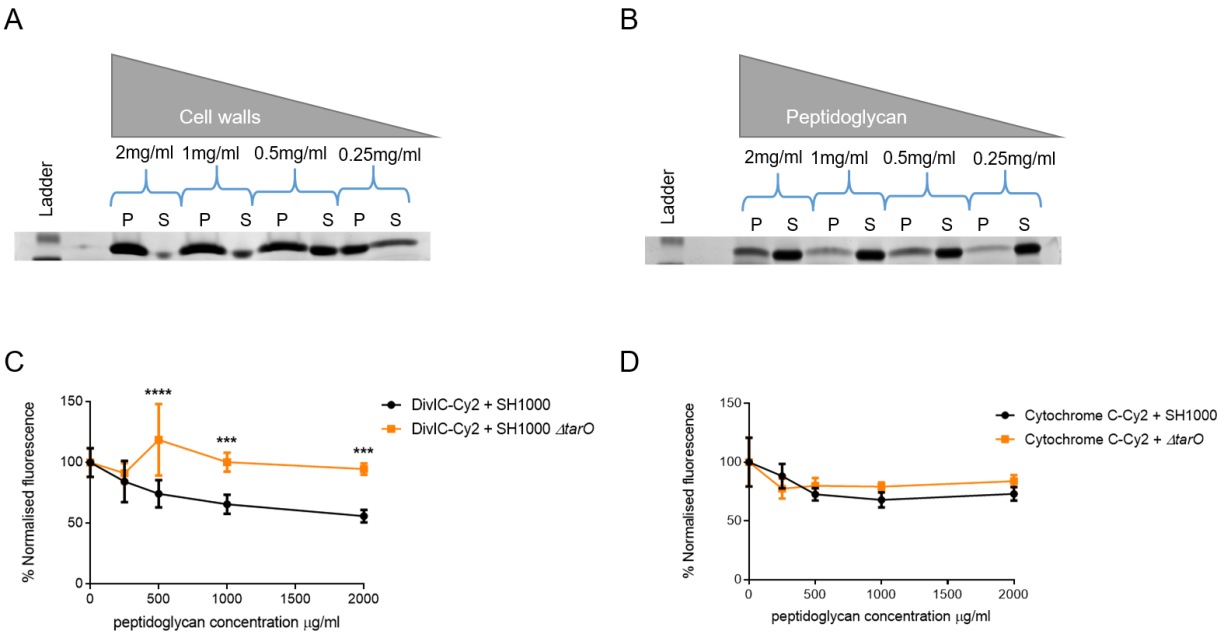

Figure 3.10 Comparison between DivIC and Cytochrome C binding to cell walls
Various concentrations of SH1000 cell walls (A) and HF-treated peptidoglycan (B) were incubated with 0.1mg/ml (~8µM) Cytochrome-C in binding buffer (20mM sodium citrate, 10mM $MgCl_2$, 0.1%(v/v) Tween, 10µg/ml BSA, pH 5). These were centrifuged and the insoluble cell wall pellet (P) and soluble supernatant (S) fractions were analysed by 15%(w/v) SDS-PAGE. Various concentrations of wildtype SH1000 or SH1000 *ΔtarO* cell walls were incubated with 500nM DivIC-Cy2 (C) or Cytochrome-C Cy2 (D) in binding buffer (20mM sodium citrate, 10mM $MgCl_2$, 0.1%(v/v) Tween, 10µg/ml BSA, pH 5) and these were centrifuged and 100µl of supernatant was measured for Cy2 fluorescence. Error bars indicate mean and Std Dev. *** P<0.005, **** P<0.001. Each point in the pulldown represents a technical repeat.

To confirm the triple mutant lacked WTA, the wildtype, double *lcp* mutants and triple *lcp* mutant cell walls underwent the WTA purification procedure (2.16). The WTA samples were separated by native-PAGE and Alcian-silver stained (Fig 3.11B) showing that only the triple *lcp* mutant lacked WTA. This was further confirmed through measuring the same cell walls for phosphate concentration where the triple *Δlcp* mutant had no phosphate (Fig 3.11C). Together with the *ΔtarO* data, there were now two mutant strains which had WTA-deficient cell walls, both of which failed to bind DivIC. Thus, the presence of WTA in the cell wall is important to DivIC binding rather than the WTA synthesis pathway itself.

3.3.12 The involvement of SigB in DivIC-Cell wall binding

Due to the clinical background of the *lcp* mutants it was decided to get the parent wildtype and the triple *lcp* mutant were whole genome sequenced. The genomic sequencing of the triple *lcp* mutant revealed that there was a premature stop codon within the *sigB* gene. SigB acts a regulator for a number of cellular processes including biofilm formation[263] and thus the contribution of SigB to DivIC binding was examined. This was important as our lab strain, SH1000, has a repaired *rbsU*[228] which is a positive regulator of SigB[264]. Therefore, if SigB is important to the lack of binding seen in the triple *lcp* mutant, the *sigB* status in SH1000 might confound findings.

NCTC 8325/4 (*rbsU*) and its parental strain without cured prophages (NCTC 8325) were tested. In addition, the *ΔsigB* derivative of SH1000 was analysed. Cell walls were isolated from these strains and used in a DivIC-Cy2 pulldown assay. It was found that none of them had significantly different binding to DivIC compared to SH1000 cell walls and all of them had significantly better binding to DivIC than HF-treated peptidoglycan (Fig 3.12). Therefore, it seems the activity of *sigB* is not important in DivIC binding.

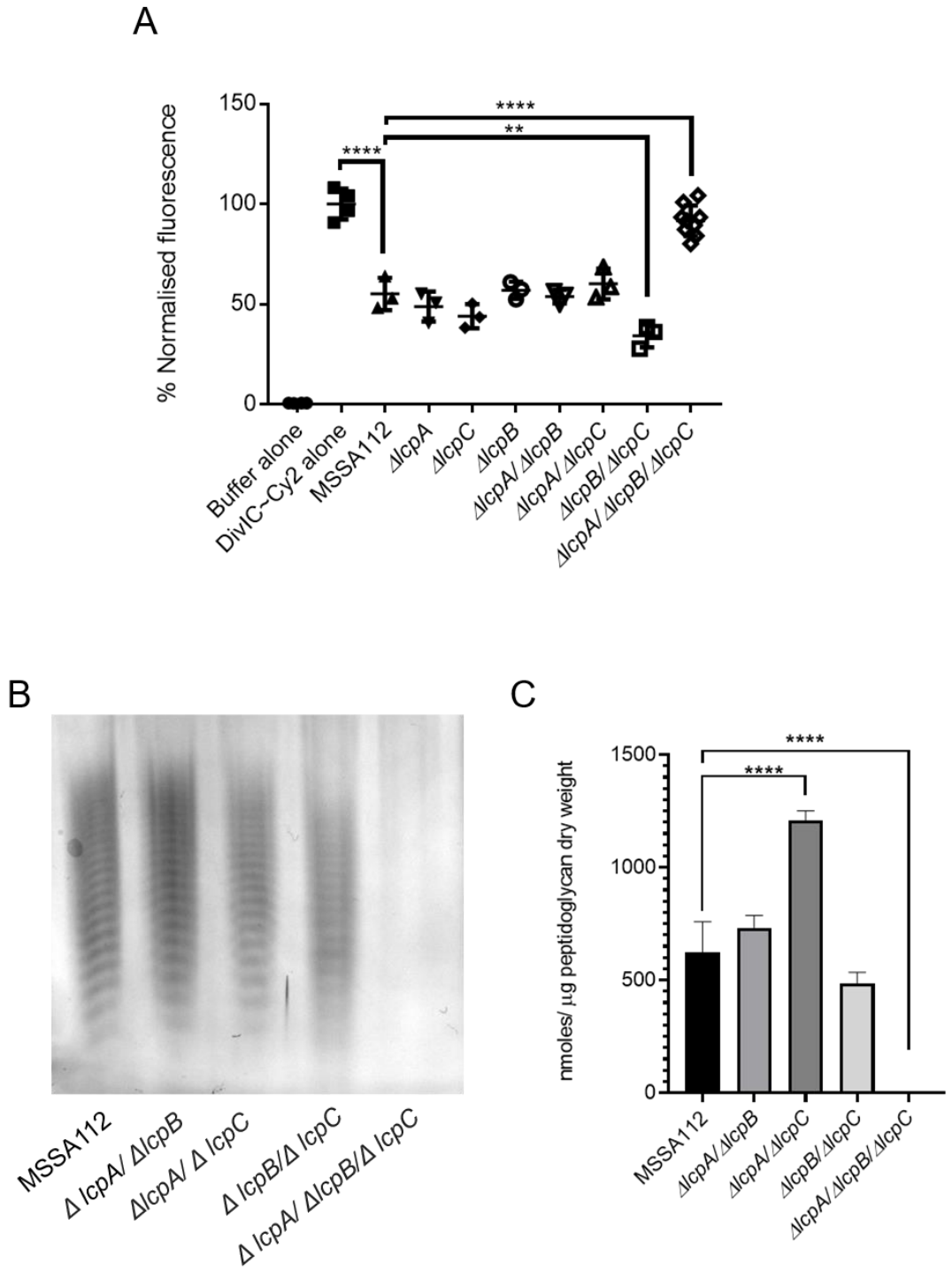

Figure 3.11 Role of LCP proteins in DivIC binding to cell walls
Cell walls were isolated from MSSA112 and all possible combinations of Δ*lcp* mutants in this background. All cell walls were incubated at 0.25mg/ml with 500nM DivIC-Cy2 in binding buffer (20mM sodium citrate, 10mM $MgCl_2$, 0.1%(v/v) Tween, 10µg/ml BSA, pH 5), these mixtures were centrifuged at 14000 x g and 100µl of supernatant was measured for Cy2 fluorescence (A). Cell walls of the wild-type MSSA112 along the double and triple *Δlcp* mutants were also incubated with 0.1M NaOH for 72 hours to strip WTA which were neutralised and dialysed into dH_2O before being separated by a Native-PAGE and Alcian-silver stained (B). These cell walls were also measured for phosphate content (C). Error bars indicate mean and Std Dev. ** P<0.01, **** P<0.001. Each point in the pulldown represents a biological repeat.

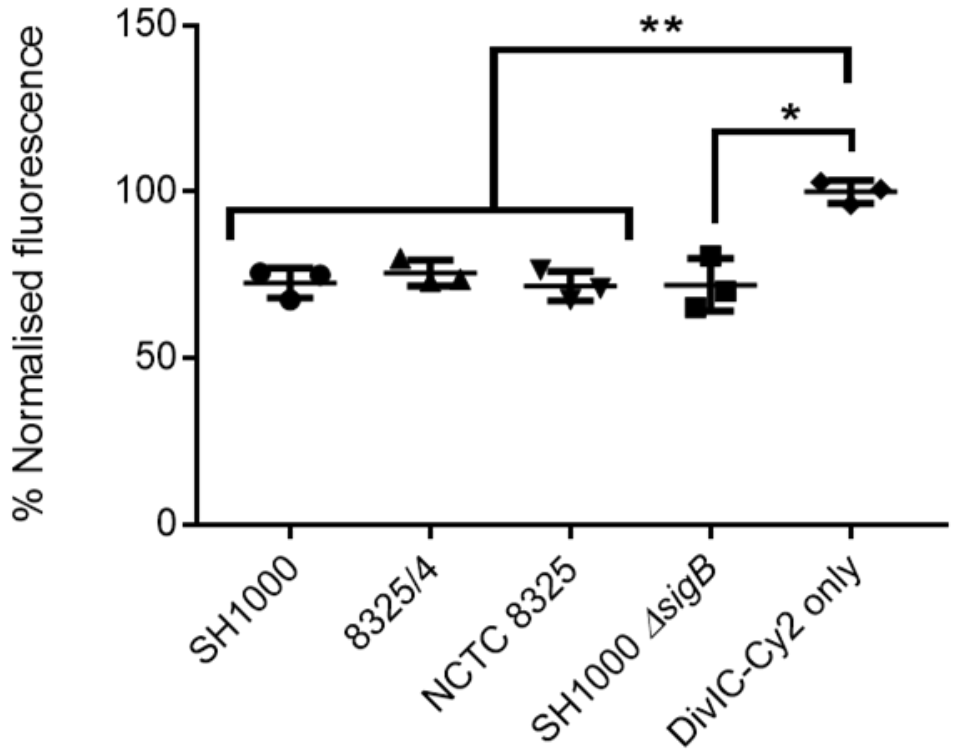

Figure 3.12 Role of SigB in DivIC binding to cell walls
Cell walls were isolated from *S. aureus* strains NCTC 8325, NCTC 8325/4, SH1000 and SH1000 ***ΔsigB.*** 0.25mg/ml of these cell walls were incubated with 500nM DivIC-Cy2 in binding buffer (20mM sodium citrate, 10mM $MgCl_2$, 0.1%(v/v) Tween, 10µg/ml BSA, pH 5), these mixtures were centrifuged at 14000 x g and 100µl of supernatant was measured for Cy2 fluorescence. Error bars indicate mean and Std Dev. * P<0.05, ** P<0.01. Each point in the pulldown represents a technical repeat.

3.3.13 NTML Screening for DivIC binding ligands

DivIC appears to bind to WTA in the cell wall of SH1000, Sa113 and 15981 strains. However, it is important to note that other phosphate linked molecules exist in the cell wall. LCP proteins also play a role in ligating other phosphate linked molecules such as capsule[265,266]. Capsule synthesis is interrupted in SH1000[126] due to a mutation causing an M134R substitution in the active site of Cap5E[267]. As a result of this DivIC may bind to other cell wall components. Therefore, it was important to screen for other potential binding ligands of DivIC in other capsule competent strains such as JE2.

To achieve this, the Nebraska transposon mutant library (NTML) which is a sequence defined *S. aureus* transposon mutant library[233], using a JE2 background, was used. A simple bioinformatics approach was used to select candidates. Given there are likely to only be phosphate linked molecules on the cell wall and phosphate linked molecules are mostly polysaccharides, genes that were annotated as being involved in polysaccharide synthesis were selected. Also, genes involved in the synthesis of known extracellular/cell wall polysaccharides such as capsule or intercellular adhesins were tested. Finally, many genes were selected due to close synteny or positively correlated expression patterns to: *divIC*, *divIB, ftsL, tarO* and the *lcp* genes, as recorded on aureowiki.med.uni-greifswald.de. The list and annotations of NTML mutants selected shown below in Table 3.1. Cell walls were isolated from all the mutants and 0.25mg/ml of cell walls were assessed through the DivIC-Cy2 pulldown assay and compared to JE2 as the parent background of the NTML (Fig 3.13).

All the mutant cell walls assessed had significantly less supernatant fluorescence than in the DivIC-Cy2 alone negative control thus showing they all bound DivIC. The only mutant to show a significant difference from JE2, via a one-way ANOVA with Sidak's multiple comparison test, was NE1384 (SAUSA300_0957: hypothetical protein) and this indicated significantly better binding rather than a loss of binding. This screen indicates none of the genes evaluated were critical for DivIC binding. Therefore, the only genes found to be critical in this respect are *tarO* and the *lcp* genes.

Table 3.1 NTML strains used in this study

NTML#	Gene annotation	Accession number
37	intercellular adhesion protein A	SAUSA300_2600
105	glycosyl transferase, group 1 family protein	SAUSA300_0550
175	glycosyl transferase, group 1 family protein	SAUSA300_0132
246	putative exonuclease	SAUSA300_1970
251	polysaccharide biosynthesis protein	SAUSA300_0482
267	probable transglycosylase	SAUSA300_1676
315	putative membrane protein	SAUSA300_0133
346	putative DnaQ family exonuclease/DinG family helicase	SAUSA300_1346
381	glycosyl transferase, group 1 family protein	SAUSA300_0549
460	autolysin	SAUSA300_0955
461	polysaccharide extrusion protein	SAUSA300_0134
462	putative membrane protein	SAUSA300_0917
480	undecaprenol kinase	SAUSA300_0669
518	glycosyl transferase	SAUSA300_2500
577	PAP2 family protein	SAUSA300_1310
585	NAD-dependent epimerase/dehydratase family protein	SAUSA300_0130
587	prephenate dehydratase	SAUSA300_1896
596	monofunctional glycosyltransferase	SAUSA300_1855
611	glycosyl transferase, group 1 family protein	SAUSA300_0939
620	PAP2 family protein	SAUSA300_0429
766	intercellular adhesion protein C	SAUSA300_2602
792	putative glycosyl transferase	SAUSA300_2583
815	capsular polysaccharide biosynthesis protein Cap5K	SAUSA300_0162
863	30S ribosomal protein S14	SAUSA300_1234
939	UDP-N-acetylglucosamine 1-carboxyvinyltransferase	SAUSA300_2078
942	glycosyl transferase, group 2 family protein	SAUSA300_0252

1022	Fmt protein	SAUSA300_0959
1055	teichoic acid biosynthesis protein X	SAUSA300_0627
1085	segregation and condensation protein B	SAUSA300_1444
1167	intercellular adhesion protein B	SAUSA300_2601
1286	capsular polysaccharide biosynthesis protein Cap1A	SAUSA300_2598
1360	oxacillin resistance-related FmtC protein	SAUSA300_1255
1384	hypothetical protein	SAUSA300_0957
1410	UDP-N-acetylglucosamine 2-epimerase	SAUSA300_2065
1424	conserved hypothetical protein	SAUSA300_2069
1475	putative Bacterial sugar transferase	SAUSA300_0131
1495	UDP-N-acetylglucosamine 1-carboxyvinyltransferase	SAUSA300_2055
1663	diacylglycerol glucosyltransferase	SAUSA300_0918
1728	glycosyl transferase, group 1 family protein	SAUSA300_1349
1778	hypothetical protein	SAUSA300_0958

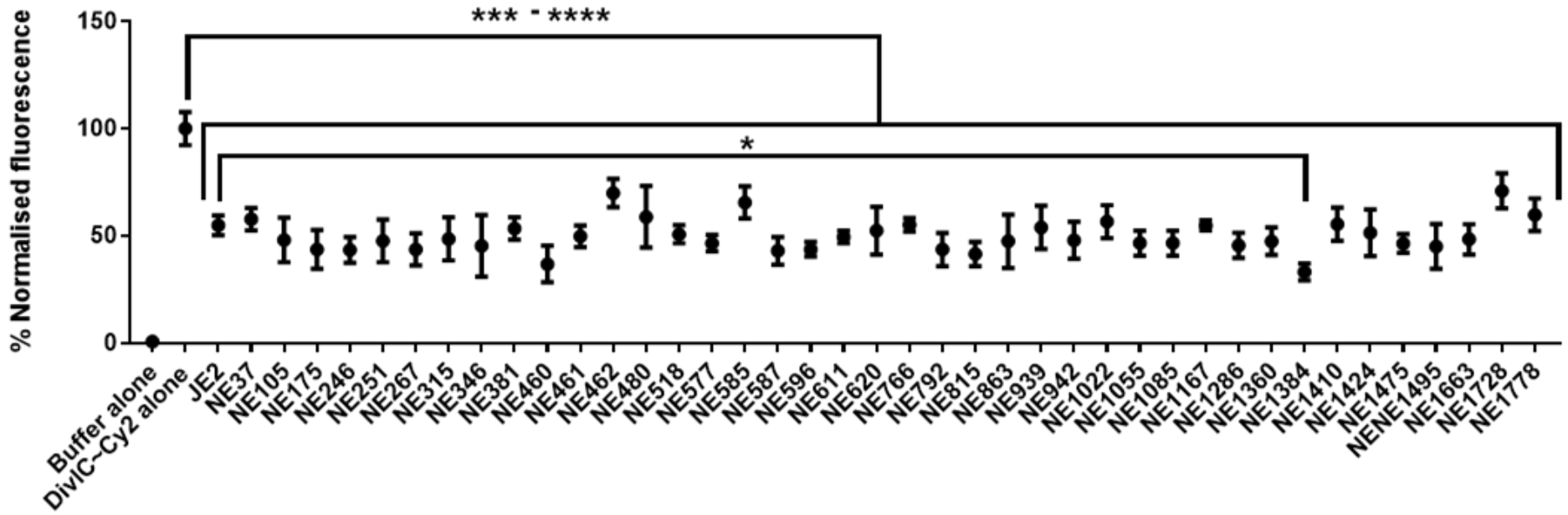

Figure 3.13 Nebraska transposon mutant library screen for components involved in DivIC binding to cell walls
S. aureus strains in the Nebraska transposon mutant library were selected based on basic bioinformatics including synteny and expression similarities with *divIC, tarO* and the *lcp* genes along with any gene annotated as being involved in polysaccharide synthesis. Cell walls were isolated from selected mutants and 0.25mg/ml of cell wall was incubated with 500nM DivIC-Cy2 in binding buffer (20mM sodium citrate, 10mM $MgCl_2$, 0.1%(v/v) Tween, 10µg/ml BSA, pH 5), these mixtures were centrifuged at 14000 x g and 100µl of supernatant was measured for Cy2 fluorescence. Error bars indicate mean and Std Dev. * P<0.05, *** P<0.005, **** P<0.001. Each point in the pulldown represents a biological repeat.

3.3.14 Effect of Tunicamycin and Tarocin on DivIC binding to cell walls

To assess the importance of the interaction between DivIC and WTA *in vivo* it is important to be able to manipulate the level of the binding partners. As DivIC has proven difficult to manipulate genetically, the level of WTA was investigated. Numerous small molecules have been developed in recent years to inhibit WTA synthesis. Tunicamcyin is the most well characterised in the literature and causes division defects similar to those seen in the *ΔtarO* mutant[268]. Tunicamycin inhibits TarO loading undecaprenol with the initial GlcNAc in WTA. At higher concentrations tunicamycin also inhibits MraY which is necessary for peptidoglycan synthesis[268]. Tarocin inhibits TarO in a much more specific manner than tunicamycin[97].

SH1000 cells were grown with 2µg/ml of tunicamycin (Sigma) or 2.5µg/ml tarocin (Sigma) as these are the concentrations shown in the literature[268] to inhibit WTA production without inhibiting peptidoglycan synthesis. This did not inhibit growth compared to untreated cells (Fig 3.14C). Cell walls were isolated from overnight cultures of these drug-treated cells and used in a DivIC-Cy2 pulldown assay. Cell walls from cells treated with tunicamycin or tarocin failed to bind DivIC (Fig 3.14A). This lack of DivIC binding was concomitant with the ability of tunicamycin and tarocin to deplete WTA as shown by cell wall phosphate levels (Fig 3.14B). The lack of WTA was also confirmed by WTA-purification and separation by native-PAGE and Alcian-silver staining (Fig 3.14D). Thus, pharmacological inhibition of WTA production blocks the ability of cells walls to bind DivIC.

For confirmation, the pharmaceutical intervention was repeated using the strain MSSA112. MSSA112 was used as the effect of the compounds could be compared to the loss of 3 LCP proteins in this background. Treatment of MSSA112 cells with tunicamycin or tarocin abolishes DivIC binding to cell walls and does not restore DivIC binding to the cell walls of the triple LCP knockout (Fig 3.15A). Furthermore, these treatments abolish WTA in MSSA112 (Fig 3.15C) without affecting growth (Supplementary Figure 3A).

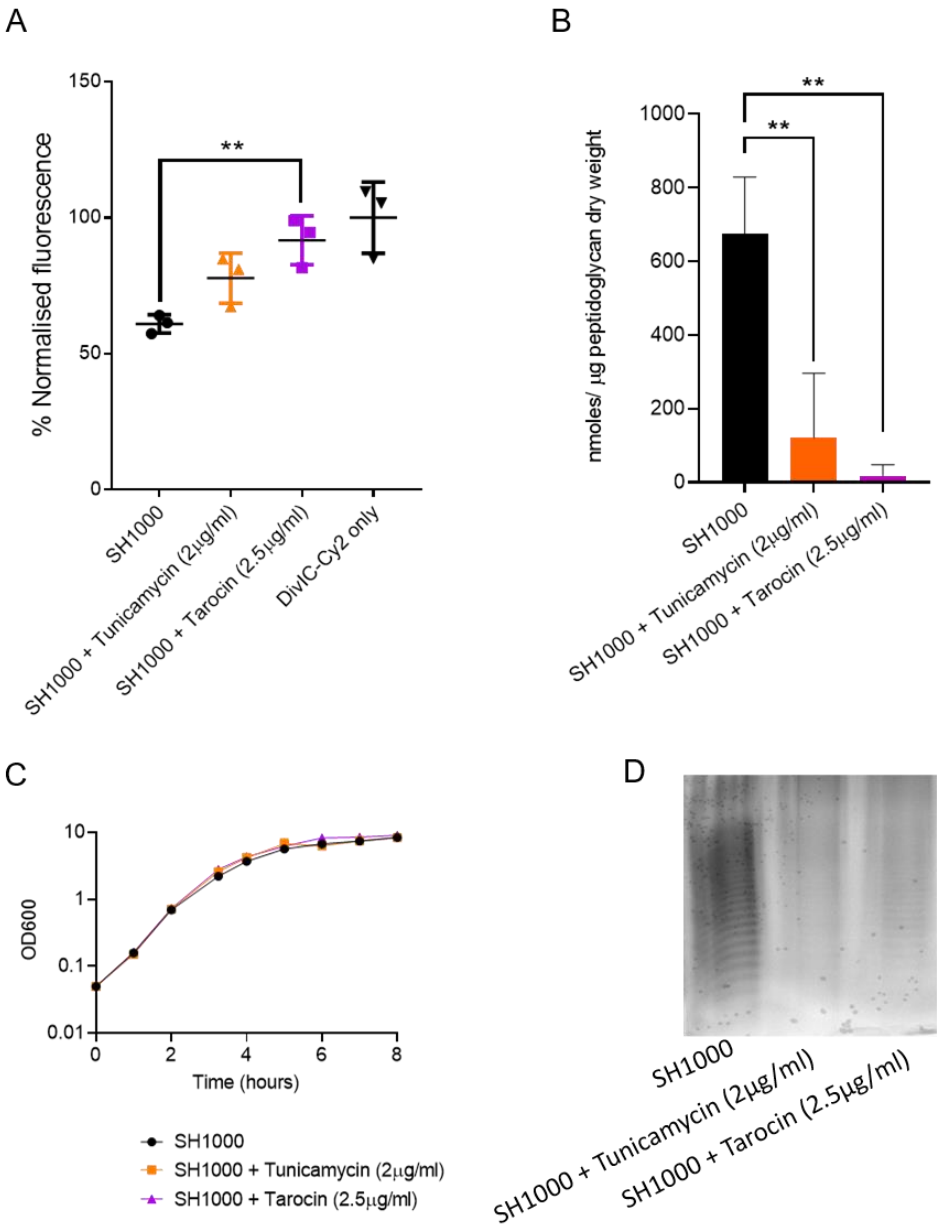

Figure 3.14 Effect of Tunicamycin or Tarocin on DivIC-cell wall binding and WTA production
SH1000 cultures were grown overnight in the absence of drug or in the presence of 2µg/ml Tunicamycin or 2.5µg/ml Tarocin. Cell walls were isolated from these cultures. 0.25mg/ml of these cell walls were incubated with 500nM DivIC-Cy2 in binding buffer (20mM sodium citrate, 10mM $MgCl_2$, 0.1%(v/v) Tween, 10µg/ml BSA, pH 5), these mixtures were centrifuged at 14000 x g and 100µl of supernatant was measured for Cy2 fluorescence (A). Cells walls were measured for phosphate concentration (B) and underwent WTA purification procedures via incubation in 0.1M NaOH for 72 hours, these "WTA" samples were analysed by native-PAGE and Alcian-silver stained (D). An overnight culture of SH1000 was sub-cultured into media containing no drug, 2µg/ml Tunicamycin or 2.5µg/ml Tarocin and the OD_{600} was measured up to 8 hours (C). Error bars indicate mean and Std Dev. ** P<0.01. Each point in the pulldown represents a biological repeat.

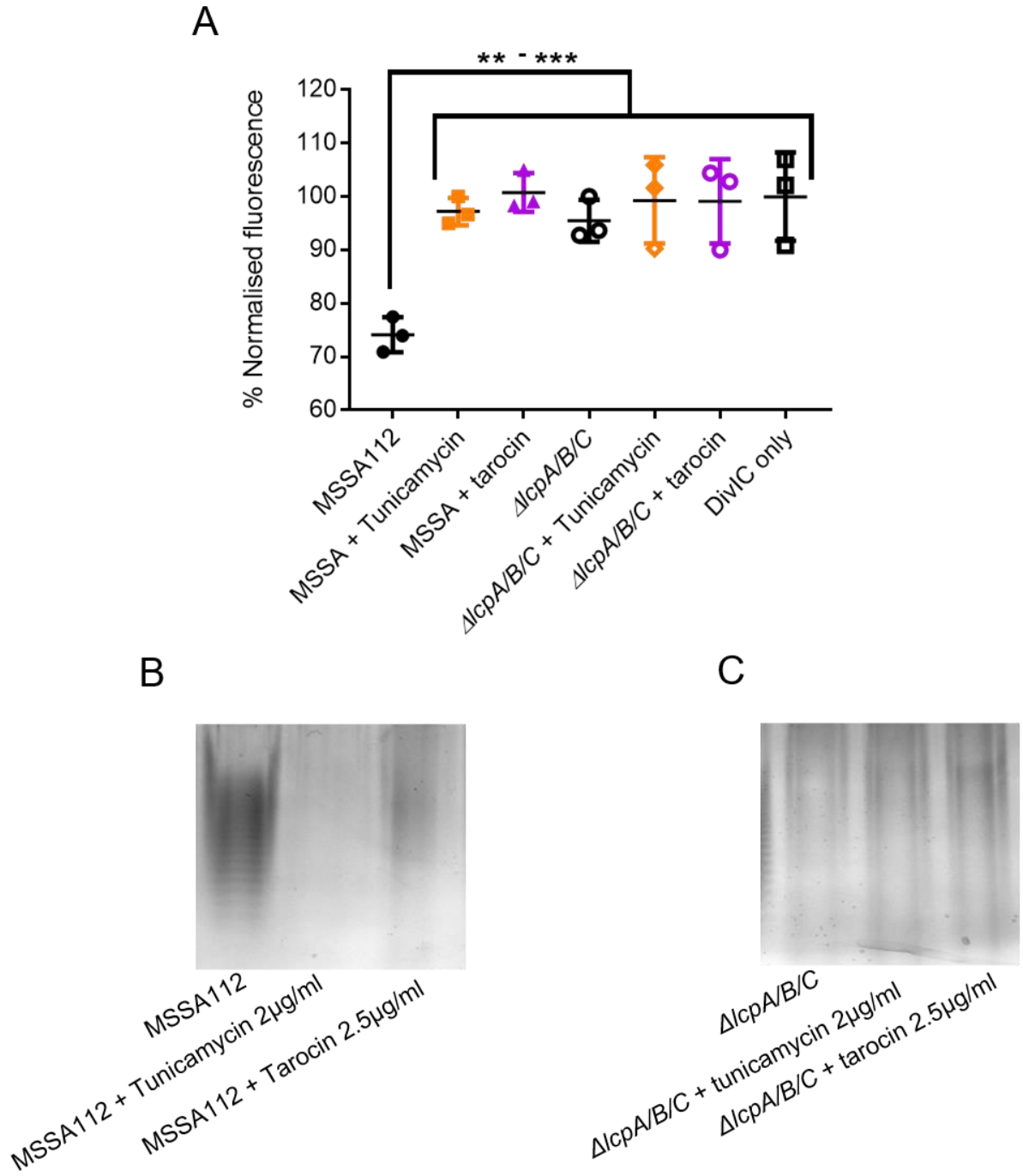

Figure 3.15 Effect of Tunicamycin or Tarocin on DivIC-cell wall binding in MSSA112.

MSSA112 and triple *lcp* knockout cultures were grown overnight in the absence of drug or in the presence of 2µg/ml Tunicamycin or 2.5µg/ml Tarocin. Cell walls were isolated from these cultures. 0.25mg/ml of cell walls were incubated with 500nM DivIC-Cy2 in binding buffer (20mM sodium citrate, 10mM $MgCl_2$, 0.1%(v/v) Tween, 10µg/ml BSA, pH 5), these mixtures were centrifuged at 14000 x g and 100µl of supernatant was measured for Cy2 fluorescence (A). Cells walls isolated from MSSA112 and triple *lcp* knockout cultures underwent alkaline hydrolysis as in the WTA purification procedure and the resulting "WTA" samples were analysed by native-PAGE and Alcian-silver stained (B & C respectively). Error bars indicate mean and Std Dev. ** P<0.01, *** P<0.005. Each point in the pulldown represents a biological repeat.

3.3.15 Role of capsule in DivIC binding to cell walls

To test the potential contribution of capsule to DivIC binding to cell wall, tunicamycin and tarocin were utilised as in Figures 3.14 and 3.15 with an *S. aureus* strain that is known to have the ability to produce large amounts of capsule: Reynolds[127]. A Reynolds strain known to express capsule serotype 5 (CP5) and a mutant expressing capsule serotype 8 (CP8) along with a capsule deficient mutant were grown to stationary phase with and without TarO-inhibiting molecules (2µg/ml tunicamycin or 2.5µg/ml tarocin). Cell walls were isolated from these cultures and used in the DivIC-Cy2 pulldown (Fig 3.16). All cell walls had significantly less ability to bind DivIC-Cy2 if the parent strain had been treated with TarO-inhibiting molecules, regardless of capsule competence or capsule serotype of the *S. aureus* strain. This demonstrates that DivIC is binding to WTA and not capsule.

3.3.16 Do bacteriophage bind to the same cell wall component as DivIC?

DivIC binds to cell walls in a WTA-dependent manner, as do bacteriophage via the phage base plate protein. The base plate of Φ11 was shown to bind to *S. aureus* and invade in a WTA-dependent fashion[269]. This published work also demonstrated that Φ11 binding and subsequent *S. aureus* lysis was dependent on the TarS-mediated modifications of WTA and failed to invade *ΔtarS* cells. TarS and TarM are enzymes that decorate the ribitol phosphate repeating units of WTA with α-GlcNac and β-GlcNac respectively[93].

TarS-dependent modifications represented a genetically tractable target of a known WTA binding protein: the Φ11 base plate. Therefore, cell walls were isolated from RN4220 *S. aureus* cells and a *ΔtarM/ΔtarS* mutant in this background. These cell walls were used in a DivIC-Cy2 pulldown assay alongside those from SH1000. As seen in Figure 3.17 all cell walls, including the *ΔtarM/ΔtarS,* significantly reduced the supernatant fluorescence compared to DivIC-Cy2 alone thus signifying binding. DivIC is therefore binding to a different site on WTA than Φ11.

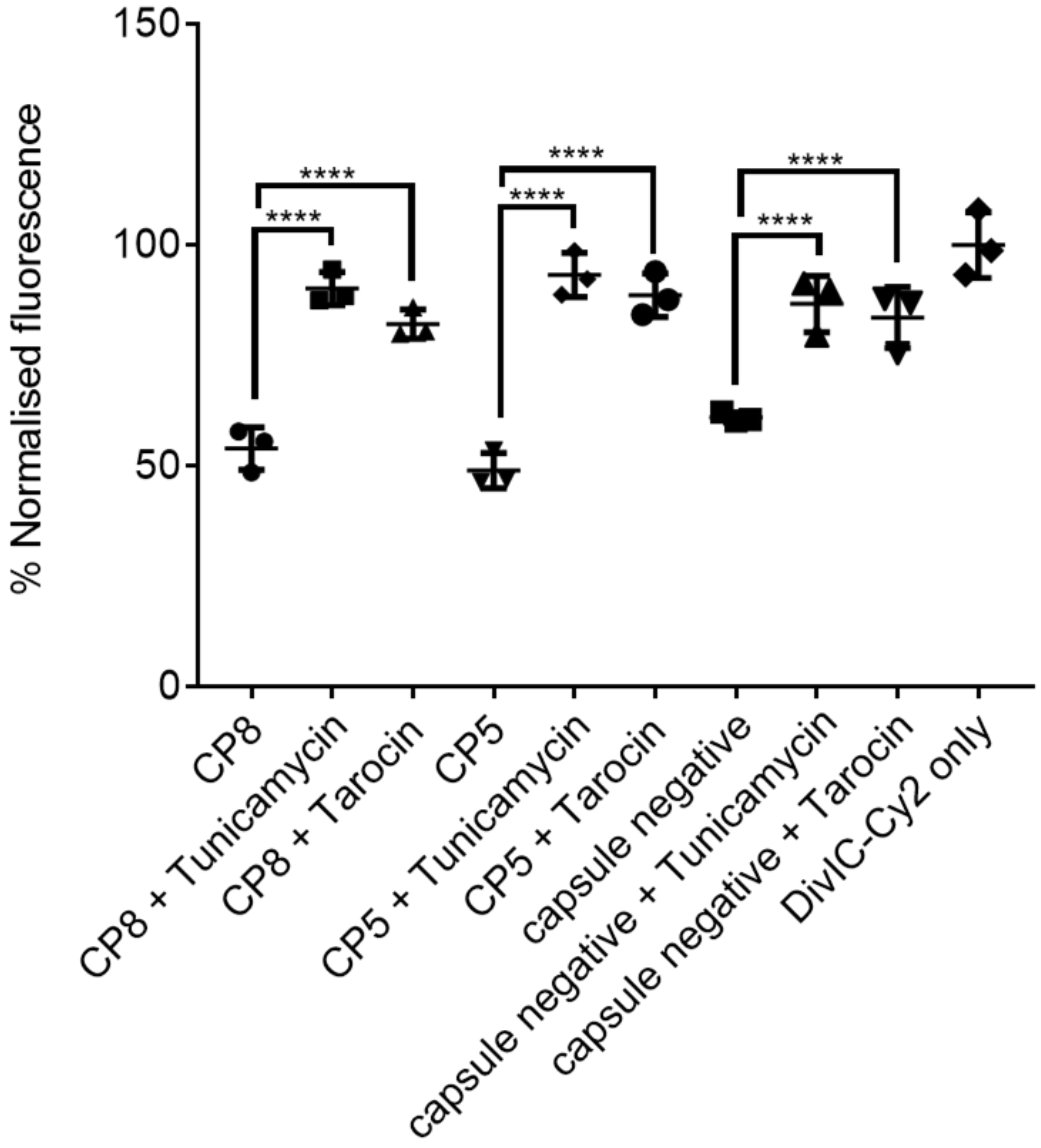

Figure 3.16. Role of capsule in DivIC binding to cell walls
Reynolds CP8, CP5 and capsule negative strains of *S. aureus* were grown overnight in the absence of drug or in the presence of 2µg/ml Tunicamycin or 2.5µg/ml Tarocin. Cell walls were isolated from these cultures. 0.25mg/ml of cell walls were incubated with 500nM DivIC-Cy2 in binding buffer (20mM sodium citrate, 10mM $MgCl_2$, 0.1%(v/v) Tween, 10µg/ml BSA, pH 5), these mixtures were centrifuged at 14000 x g and 100µl of supernatant was measured for Cy2 fluorescence. Error bars indicate mean and Std Dev. *** $p<0.005$, **** $p<0.001$. Each point represents a biological repeat.

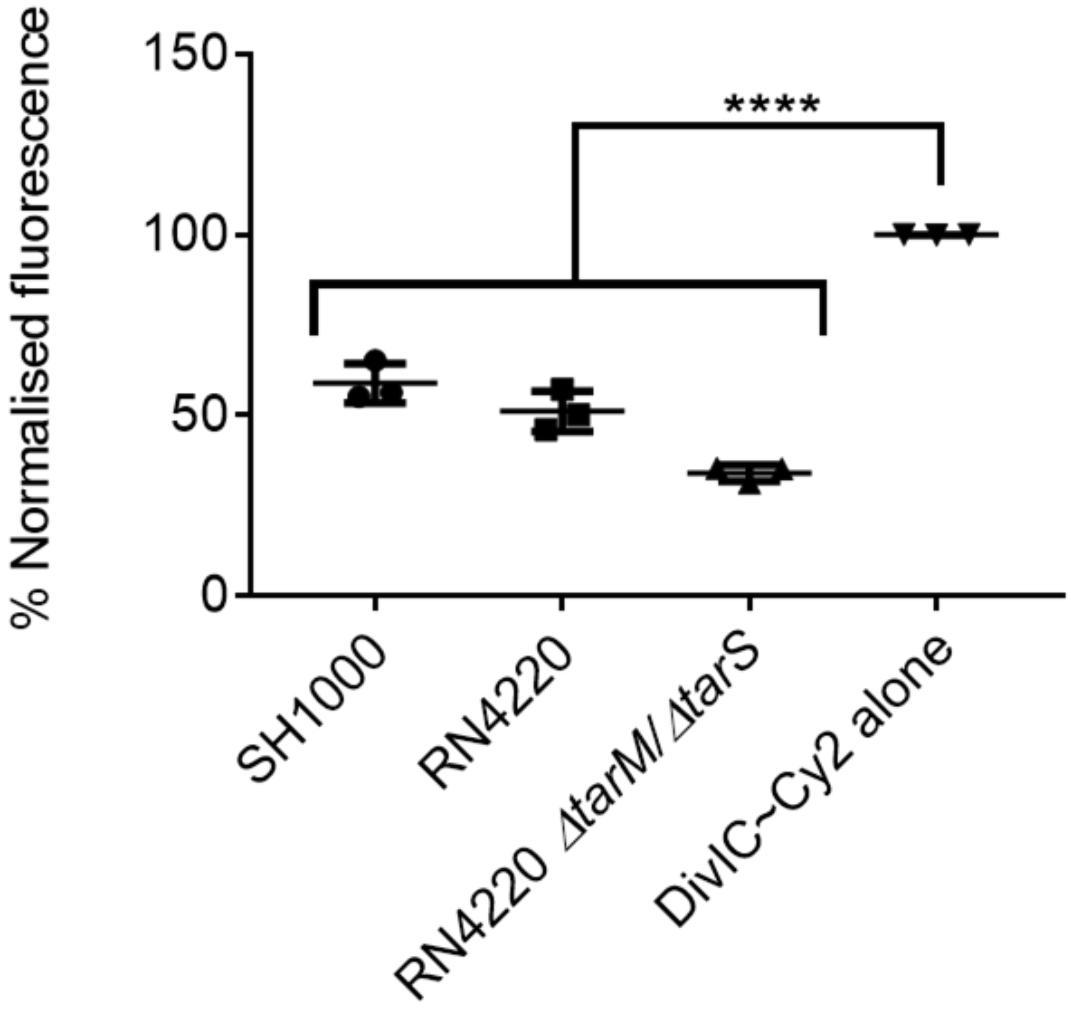

Figure 3.17 Role of WTA glycosylation in DivIC cell wall binding
Cell walls were isolated from SH1000, RN4220 and RN4220 *ΔtarM ΔtarS*. 0.25mg/ml of cell walls were incubated with 500nM DivIC-Cy2 in binding buffer (20mM sodium citrate, 10mM $MgCl_2$, 0.1%(v/v) Tween, 10µg/ml BSA, pH 5), these mixtures were centrifuged at 14000 x g and 100µl of supernatant was measured for Cy2 fluorescence. Error bars indicate mean and Std Dev. **** P<0.001. Each point represents a biological repeat.

3.3.17 Binding of DivIC to cell walls of other bacterial species

The structure of WTA varies between bacterial species, for instance WTA of most *S. aureus* strains has a poly-ribitol-phosphate backbone whereas other species such as *Staphylococcus epidermidis* have a poly-glycerol-phosphate backbone in their WTA[270]. In order to begin to define the molecular constraints of DivIC binding WTA, cell walls from a range of species were used.

Cell walls were isolated from different bacterial species and used in a DivIC-Cy2 pulldown assay alongside *S. aureus* cell walls (Fig 3.18). There was a clear dichotomy between those cell walls that bound DivIC and those that did not. *Staphylococcus epidermidis*, *Bacillus subtilis* (log and stationary phase) and *Curtobacterium flaccumfaciens* cell walls bound DivIC whereas *Streptococcus mutans*, *Micrococcus luteus*, *Enterococcus faecalis* and *Lactococcus lactis* cell walls did not. This shows that DivIC is unlikely to bind the poly ribitol phosphate backbone of WTA as *S. epidermidis* has WTA which have a poly glycerol phosphate backbone. It also indicates that the surrounding cell wall structure may not be important as it bound to cell walls of *C. flaccumfaciens* which has type B2β peptidoglycan[271,272].

Due to a lack of in depth glycomics studies the exact structural differences between *S. aureus* WTA and the WTA in these species is unknown. However, the fact that some species bind *S. aureus* DivIC whereas other do not shows there is a specificity and this DivIC-WTA binding phenomenon might not be limited to only *S. aureus*.

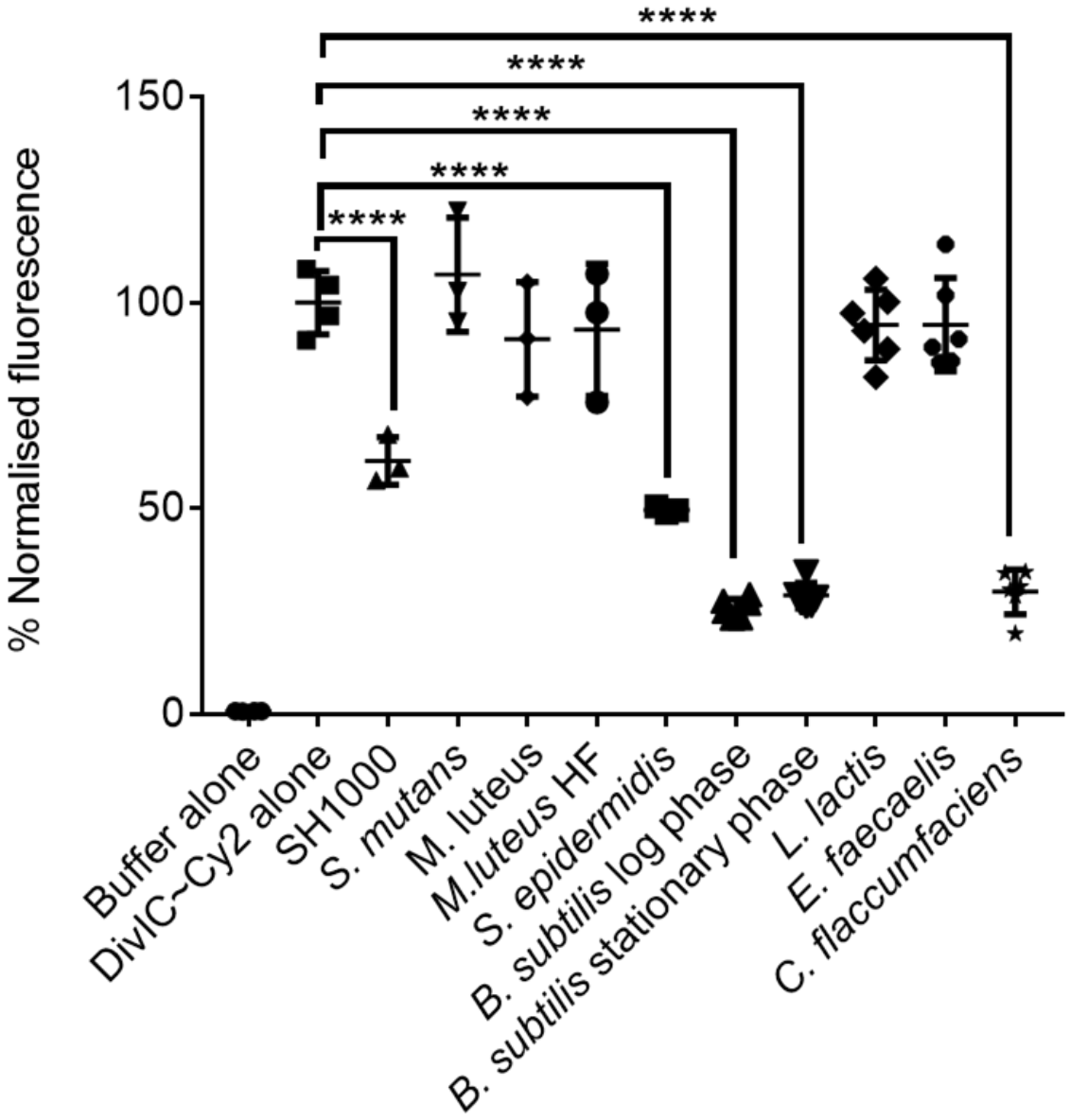

Figure 3.18 Binding of *S. aureus* DivIC to cell walls of bacterial species
Cell walls were isolated from a variety of bacterial species and 0.25mg/ml of these cell walls were incubated with 500nM DivIC-Cy2 in binding buffer (20mM sodium citrate, 10mM $MgCl_2$, 0.1%(v/v) Tween, 10µg/ml BSA, pH 5), these mixtures were centrifuged at 14000 x g and 100µl of supernatant was measured for Cy2 fluorescence. Error bars indicate mean and Std Dev. **** P<0.001. Each point represents a biological repeat.

3.3.18 DivIC binds to soluble WTA in the absence of insoluble cell wall

DivIC binding to the cell wall of *C. flaccumfaciens* (Fig 3.18) showed that the underlying cell wall peptidoglycan structure might not be important for DivIC binding to WTA. Therefore, the ability of DivIC to bind to soluble WTA was assessed via MicroScale Thermophoresis (MST). Put simply, MST works on the principles of thermodynamics where larger molecules move slower down a thermophoretic gradient than smaller molecules (Fig 3.19). An infrared laser heats the buffer in a thin capillary creating a thermophoretic gradient. Fluorescently labelled target molecules move along this thermophoretic gradient from hotter (red) to colder (green to blue) regions and the rate of movement can be measured as a decrease of fluorescence at the hotter region of the thermophoretic gradient. As a protein bound to a ligand will constitute a complex with greater mass than the protein alone it should move slower down a thermophoretic gradient and therefore a slower rate of reduction of fluorescence signifies binding in MST. By varying the concentrations of target to ligand this technique has previously been used to calculate binding stoichiometries and affinities[273]. Here it was used to simply demonstrate that binding occurs between DivIC and soluble WTA.

DivIC was labelled with AlexaFluor647 (AF647) (2.34), subsequently referred to as DivIC-AF647. DivIC-AF647 was incubated in binding buffer with various concentrations (5, 15, 30 and 50 mg/ml) of soluble WTA from SH1000 cell walls and *S. aureus* LTA (Sigma). Approximately 10µl of the mixtures were loaded into a Monolith NT.115 Premium capillary (nanotemper). The capillaries were subsequently placed into the Monolith NT.115 alongside capillaries containing DivIC-AF647 alone and a binding check assay was performed using red excitation at 20% power and medium MST power.

Binding to a ligand would appear as a slower movement along the thermophoretic gradients and a smaller reduction in relative fluorescence compared to DivIC alone. Figure 3.20A shows the raw MST trace where the blue line indicates DivIC-AF647 alone and the other lines represent DivIC-AF647 in the presence of WTA or LTA. This clearly demonstrates that DivIC is moving slower along the thermophoretic gradient in the presence of WTA, this is most clear from the 50mg/ml condition (green).

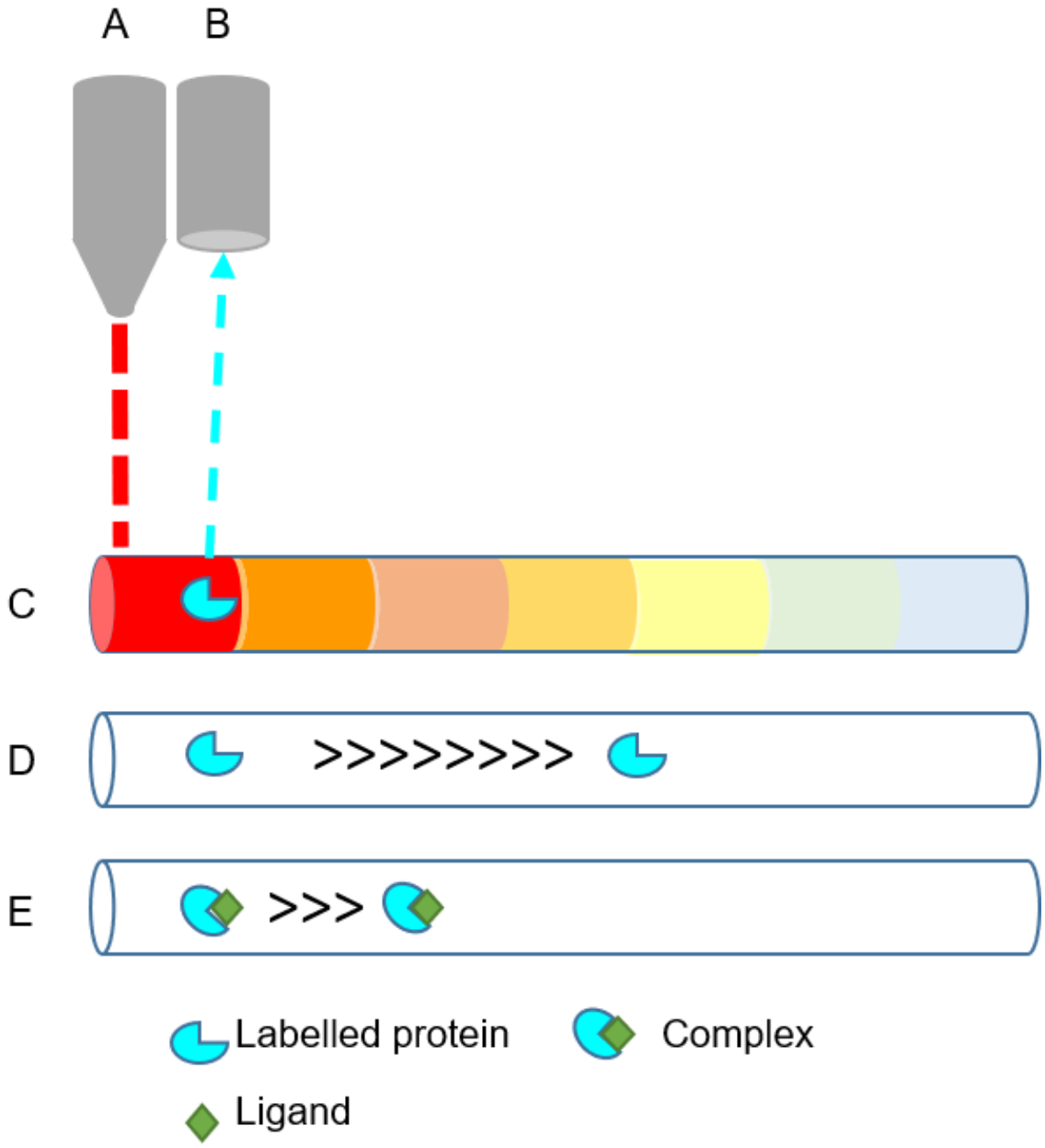

Figure 3.19 Diagram demonstrating the conceptual basis of microscale thermophoresis
Schematic shows the principle of how MST works. An infrared laser (A) heats the buffer in a very thin capillary creating a thermophoretic gradient (C). Fluorescently labelled molecules move down this gradient from hot (red) to colder (green to blue) regions. Labelled molecules are detected by fluorescence (B). Smaller molecules move quicker (D) than larger molecules (E) and as such the reduction in fluorescence in the area measured by the detector is slower when the fluorescent target binds a ligand (forming a complex).

The difference in the relative fluorescence measured at 5 seconds between DivIC and DivIC in the presence of WTA or LTA is shown in Figure 3.20B. The software dictated that the signal to noise ratio was sufficient to determine binding when WTA was present at 15mg/ml or higher, these concentrations of WTA also showed a significant difference in relative fluorescence from DivIC-AF647 according to one-way ANOVA with Dunnett's multiple comparisons. In addition, despite binding failing to reach saturation, there is concentration dependent binding with 50mg/ml WTA condition having significantly higher fluorescence (and binding) than the lower concentrations. Cytochrome-C was also labelled with AF647 and incubated in binding buffer at 100nM with 15mg/ml WTA from SH1000 and this showed no binding which indicates that the WTA binding is a DivIC specific phenomenon (Supplementary Figure 4).

There was no significant binding seen to the LTA at 5mg/ml. LTA was not used at a higher concentration as this was the maximum solubility according to the manufacturers.

3.3.19 WTA samples are free of muropeptides

Given the ability of DivIB to bind peptidoglycan and DivIC to bind cell walls there was a concern that the binding seen in the MST was actually binding to small/soluble remnants of cell wall/peptidoglycan. Given WTA production/purification involved extensive dialysis in 3.5kDa dialysis tubing this should have allowed removal of residual muropeptides and soluble peptidoglycan. However, to check this thoroughly, the WTA sample was subjected to muropeptide analysis (section 2.22).

3mg of WTA and 2mg of cell wall were incubated with mutanolysin to digest and solubilise the peptidoglycan in the sample (section 2.20-2.21) and then analysed for the presence of muropeptides by HPLC (2.22). As shown in Figure 3.21 the only peak present in the WTA sample was at the very beginning (before the elution gradient) (3.21A). There is an apparent absence of a typical muropeptides which are shown very clearly in the cell wall trace (3.21B) with the peaks denoting increasingly cross-linked muropeptides from monomers to oligomers. Integration of the first two major peaks representing muropeptide monomers and dimers indicates there is <1% contamination in the WTA sample due to muropeptides.

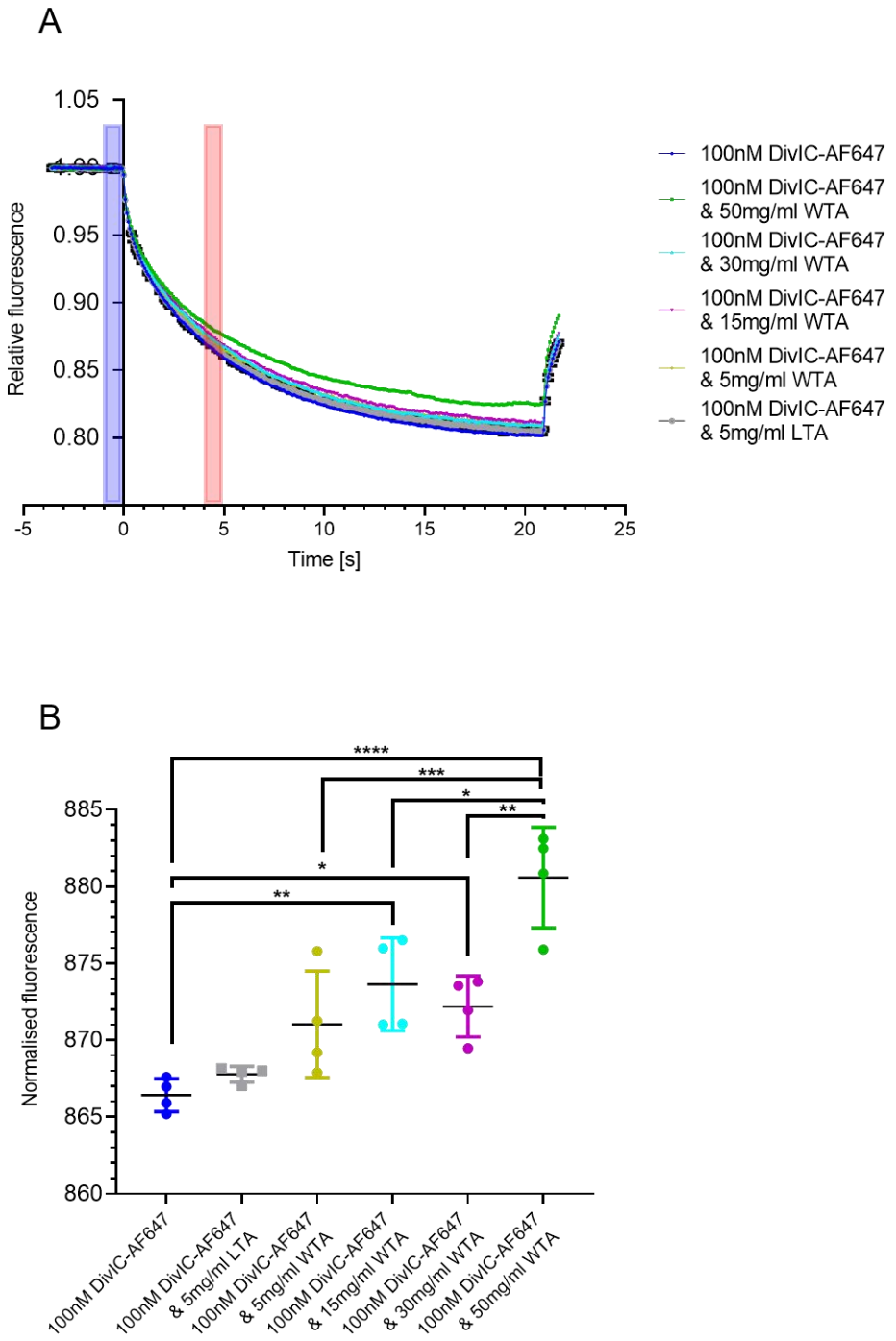

Figure 3.20 Microscale thermophoresis analysis shows DivIC binding to soluble WTA
100nM DivIC-AF647 was incubated in binding buffer (20mM sodium citrate, 10mM $MgCl_2$, 0.1%(v/v) Tween, 10µg/ml BSA, pH 5) with 5mg/ml of LTA (grey) or 5mg/ml (yellow), 15mg/ml (cyan) 30mg/ml (red) or 50mg/ml (green) of WTA isolated from SH1000 cell walls via alkaline hydrolysis. This mixture and DivIC-AF647 alone in the same buffer were loaded into premium capillary tubes in a Nanotemper monolith microscale thermophoresis machine. The binding check protocol was performed with the MST power at medium and red LED-mediated excitation set at 20%. The trace shows the difference between change in detected fluorescence of DivIC-AF647 alone (blue) and DivIC-AF647 with LTA or varying concentrations of WTA over time (A) and the difference in the demarcated 5th second (red) plotted in B. The full trace (A) displays the mean, in B the error bars display the mean ±Std Dev * p<0.05, ** p<0.01, *** p<0.005, *** p<0.001.

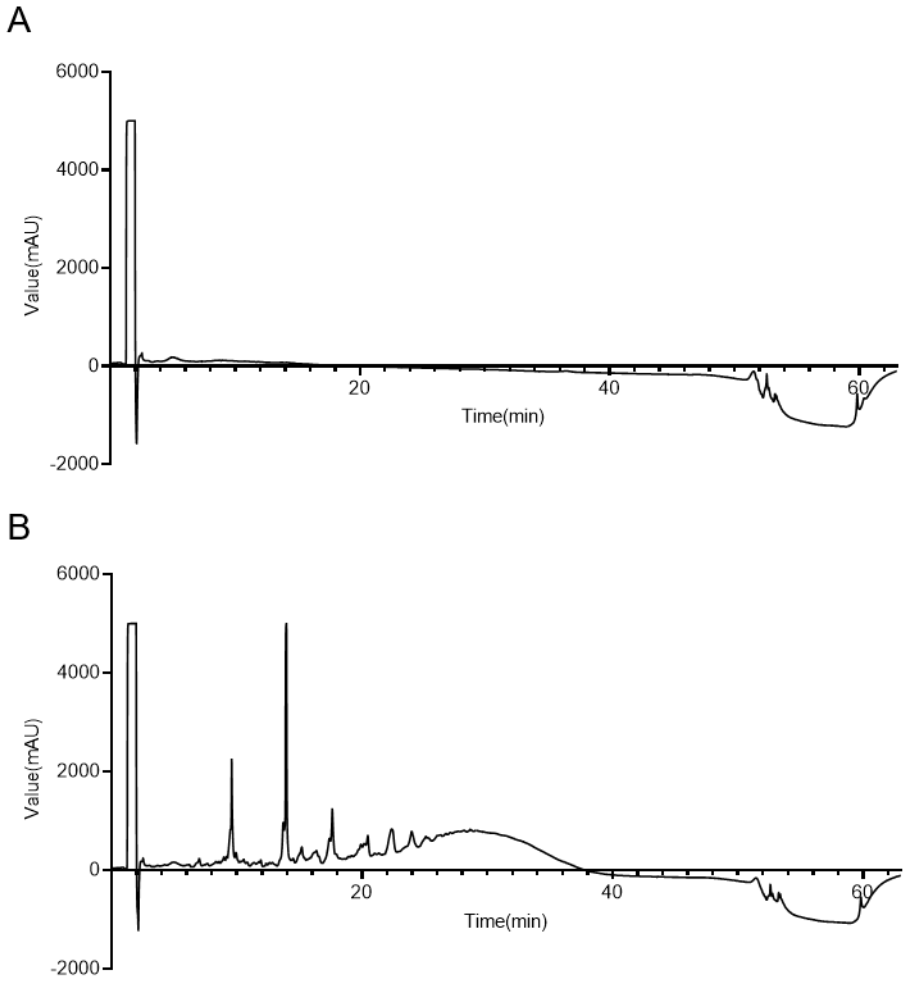

Figure 3.21 WTA samples used in MST are not contaminated with peptidoglycan fragments
3mg of WTA (A) and 2mg of cell walls (B) were incubated with 50µg mutanolysin to digest peptidoglycan. The soluble fraction was reduced through incubation with sodium borohydride. Excess sodium borohydride was degraded with phosphoric acid then neutralised samples were ran through a Thermo Scientific Hypersil GOLD aQ column (200 x 2.1 mm, 1.9µm particle size) with a waters HPLC system. Muropeptides were eluted through increasing percentage of acetonitrile and elutions were measured by absorbance at 202nm.

3.4 Discussion

Peptidoglycan binding proteins involved in cell division have previously been described in species such as *E. coli* and *B. subtilis*, these proteins share a Sporulation-related repeat (SPOR) domain which target them to the septum[274]. However, proteins containing the SPOR domain are not found in *S. aureus*. Proteins which bind to *S. aureus* peptidoglycan include exogenous hydrolases such as lysozyme[275,276] , lysostaphin[277] and endogenous hydrolases SagB[278,279] and Sle1[280] which bind and degrade the cell wall. DivIB was also recently shown to be a peptidoglycan binding protein[150]. This was the impetus for interrogating the cell wall interactions of DivIC as it associates with DivIB and FtsL in the divisome complex. The work described here indicates that DivIC is a WTA binding protein. This is the first data to show that there is a cell division protein that binds WTA in *S. aureus* and this potentially a novel interaction as a target for the development of new antibiotics.

3.4.1 Identification of the DivIC ligand

3.4.1.1 Identification of WTA as binding partner

There are multiple pieces of independent, compounding evidence presented here to demonstrate that DivIC binds WTA in the cell wall:

- Depletion of WTA from cell walls with HF or NaOH reduced the ability of cell walls to bind DivIC and this was shown not to be due to HF-induced structural changes such as loss of O-acetylation.
- The *ΔtarO* mutant studies show that DivIC fails to bind cell walls from mutants genetically incapable of producing WTA.
- The *lcp* mutant experiments show that DivIC fails to bind to the triple *lcp* mutant which cannot ligate WTA onto its cell wall.
- The experiments which pharmacologically inhibited TarO, subsequently blocking WTA production demonstrated that cell walls from strains treated with these pharmacological agents had a reduced capacity to bind DivIC.

Taken together it becomes clear that the presence of WTA within the cell wall is necessary for DivIC to bind cell walls. The MST further demonstrates that DivIC can bind to soluble WTA and WTA therefore represents a ligand of DivIC within the cell wall.

It is also important to discount other molecules as potential binding partners:

- **Purified peptidoglycan** only partially binds at the highest concentrations used and can therefore be largely discounted. Furthermore, DivIC binding to *C. flaccumfaciens* reinforces this message. This is because *C. flaccumfaciens* has B2β type peptidoglycan which ornithine-based interpeptide bridges thus indicating the cell wall context of WTA is not important.
- **Cell wall proteins** are removed by pronase during the cell wall purification process but also cell walls from the *ΔsrtA* mutant which lacks sortase linked cell wall proteins still bound DivIC. This leads to cell wall proteins being discounted as a DivIC ligand.
- **Lipoprotein** constitutes a well-known contaminant of cell wall preparations[260] but DivIC bound to cell wall preparations of *Δlgt* mutants allowing lipoprotein to disregard lipoproteins in DivIC binding.
- **Lipoteichoic acids** should not have been present in the cell wall preparations due to the SDS wash during cell wall purification which removes lipids and associated molecules. But this was also genetically verified through use of cell walls from the *ΔltaS* mutant which bound DivIC. LTA and WTA are structurally quite similar despite different biosynthetic pathways which utilise different lipid carriers[113,258,261]. *S. aureus* WTA has a poly-ribitol phosphate backbone whereas LTA has a poly glycerol phosphate backbone. DivIC also bound to *S. epidermidis* cell walls which contain WTA with a poly glycerol backbone. Furthermore, bacterial two hybrid analysis does show an interaction between DivIC and the LTA synthesis machinery[246]. These facts taken together give us reason to believe it is plausible DivIC could interact with LTA. The data presented here cannot dismiss this possibility, but it does conclusively demonstrate that DivIC binds to WTA. The only difference between *S. aureus* WTA and LTA that is not confounded by DivIC binding to *S. epidermidis* cell walls is the linkage units. The linkage unit of WTA is made of ManNAc and GlcNAc whereas the linkage unit of LTA is made of two glucose moieties[113]. This presence or lack of an N-acetyl amine group might explain any difference in their interactions with DivIC.

3.4.1.2 Other cell wall polysaccharides

Discounting DivIC binding cell wall polysaccharides other than WTA such as polysaccharide intracellular adhesin (PIA) and capsule is a bit more difficult than discounting other types of molecules. Strains Sa113[281] and 15981[234] are PIA-competent and DivIC fails to bind to the Δ*tarO* mutant in this background. This either implies that PIA is not present in cell wall preparations (which is possible as it is not known to be covalently bound to cell walls) or that PIA is not a DivIC binding partner. PIA is evidently not necessary for DivIC-cell wall binding as the NTML mutants NE37, NE461, NE766 and NE1167 have mutations in the individual genes of the *ica* locus responsible for PIA synthesis and the cell walls from all these mutants bound DivIC.

It is possible, although unlikely, that another uncharacterised cell wall polysaccharide exists in *S. aureus*. The NTML screen checked many genes that were annotated as being involved in polysaccharide synthesis and revealed no mutants that failed to bind. This indicates either none of these purported polysaccharides bind DivIC or that WTA is sufficient to bind DivIC in their absence. The NTML screen was also useful in helping ascertain the potential involvement of capsule in binding DivIC.

Strains SH1000 and Sa113 are both derived from the acapsular 8325/4 strain[126], in addition 15981 is an unsequenced clinical strain, therefore the contribution of capsule in the absence of WTA in the *ΔtarO* mutants cannot be assessed from Figure 3.9. Furthermore, LCP proteins are promiscuous in their ligation and have also been shown to ligate capsule to the cell wall[265,282]. Therefore, the triple *lcp* mutant in the MSSA112 background in Figure 3.11 has cell walls deficient in both WTA and capsule. To rule out capsule binding DivIC more conclusively, the experiment was performed with cell walls from the Reynolds *S. aureus* strain which had been grown with and without TarO inhibiting drugs: tunicamycin and tarocin (Fig 3.16). The loss of DivIC binding to cell walls that were capsule competent but TarO-inhibited signifies that DivIC does not bind to capsule.

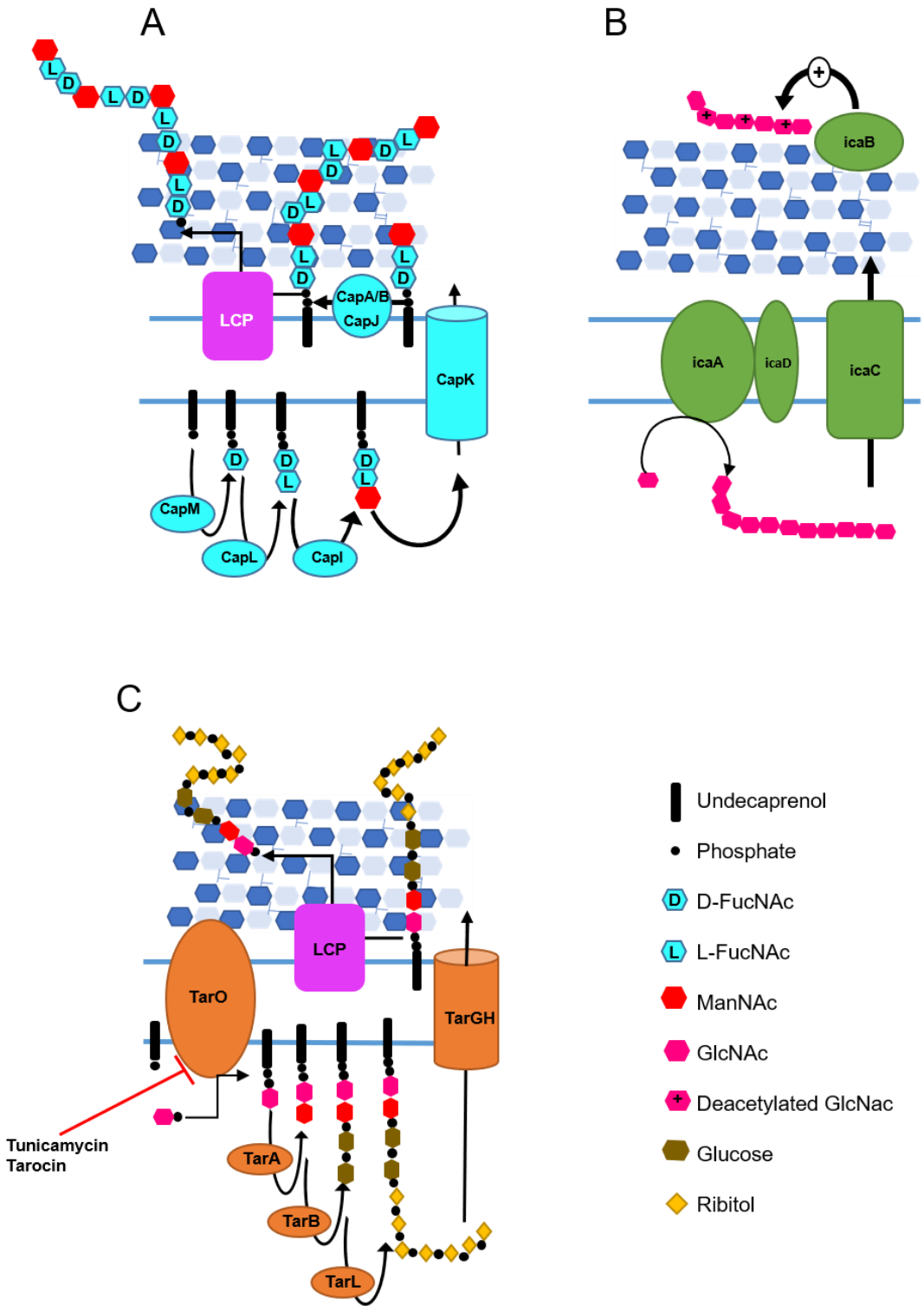

Figure 3.22. Cell wall associated polysaccharide synthesis pathways in *S. aureus*
S. aureus has three well defined cell wall associated polysaccharides: capsule (A), polysaccharide intercellular adhesin (B) and wall teichoic acid (C), which are synthesis by the Cap (cyan), Ica (green) and Tar (orange) enzymes respectively. Capsule and teichoic acids use the undecaprenol lipid carrier (black stick) during synthesis and are ligated onto the cell wall by LCP proteins (purple). Polysaccharide intercellular adhesin does not use the undecaprenol carrier and is not known to be covalently linked to the cell wall but is important in biofilm formation.

3.4.2 DivIC-WTA binding motif

This work has not determined the part of WTA to which DivIC binds but it has narrowed down the possibilities (Fig 3.23). Known exogenous WTA binding proteins include phage base plate proteins, CD207/langerin on Langerhans cells and mannose binding lectins. It was shown that the phage base plate and the dendric cell langerin receptor recognise the β-GlcNAc modifications of WTA[108,269] and Mannose binding lectin also recognises either α-GlcNAc or β-GlcNAc modifications of WTA[109]. The fact DivIC binds the Δ*tarM* Δ*tarS* mutant indicates that DivIC binds to a different part of WTA than CD207, phage base plates and mannose binding lectin. Also, DivIC binds to the cell walls from *ΔdltA* and *ΔdltB* mutants thereby ruling out the D-alanine WTA modification being the binding motif.

Furthermore, the species screen (Fig 3.18) indicates the presence of a ribitol phosphate backbone is not necessary for DivIC binding as it will bind to *S. epidermidis* and *B. subtilis* cell walls which have poly-glycerol-phosphate based WTA[283,284]. This implies the sugar phosphate backbone is not the binding site of DivIC. The only remaining, uninterrogated potential binding motif is the linkage unit.

There may be commonalities between the WTA structures of species the cell walls of which bound DivIC. Based on the arguably limited verifiable structural knowledge of WTA the most likely component is the GlcNAc-ManNAc-GroP linkage unit that attaches the sugar phosphate backbone of WTA to peptidoglycan. There is a rationale to try to construct a mutant that just has this linkage unit on the cell wall. However, the WTA pathway is not easily genetically tractable because it utilises the undecaprenol lipid carrier which is also used in peptidoglycan synthesis. Knocking out *tar* genes downstream of *tarO* sequesters undecaprenol in the WTA synthesis pathway at a stage where it cannot be recycled, leading to a loss of viability. Therefore, the chances of successfully constructing a linkage unit-only WTA mutant are slim. A slightly more feasible approach would be to substitute in an alternative *tarO, tarA or tarB/tarF* enzyme from a species with a different linkage unit to change the GlcNAc, ManNAc or glycerol phosphates respectively.

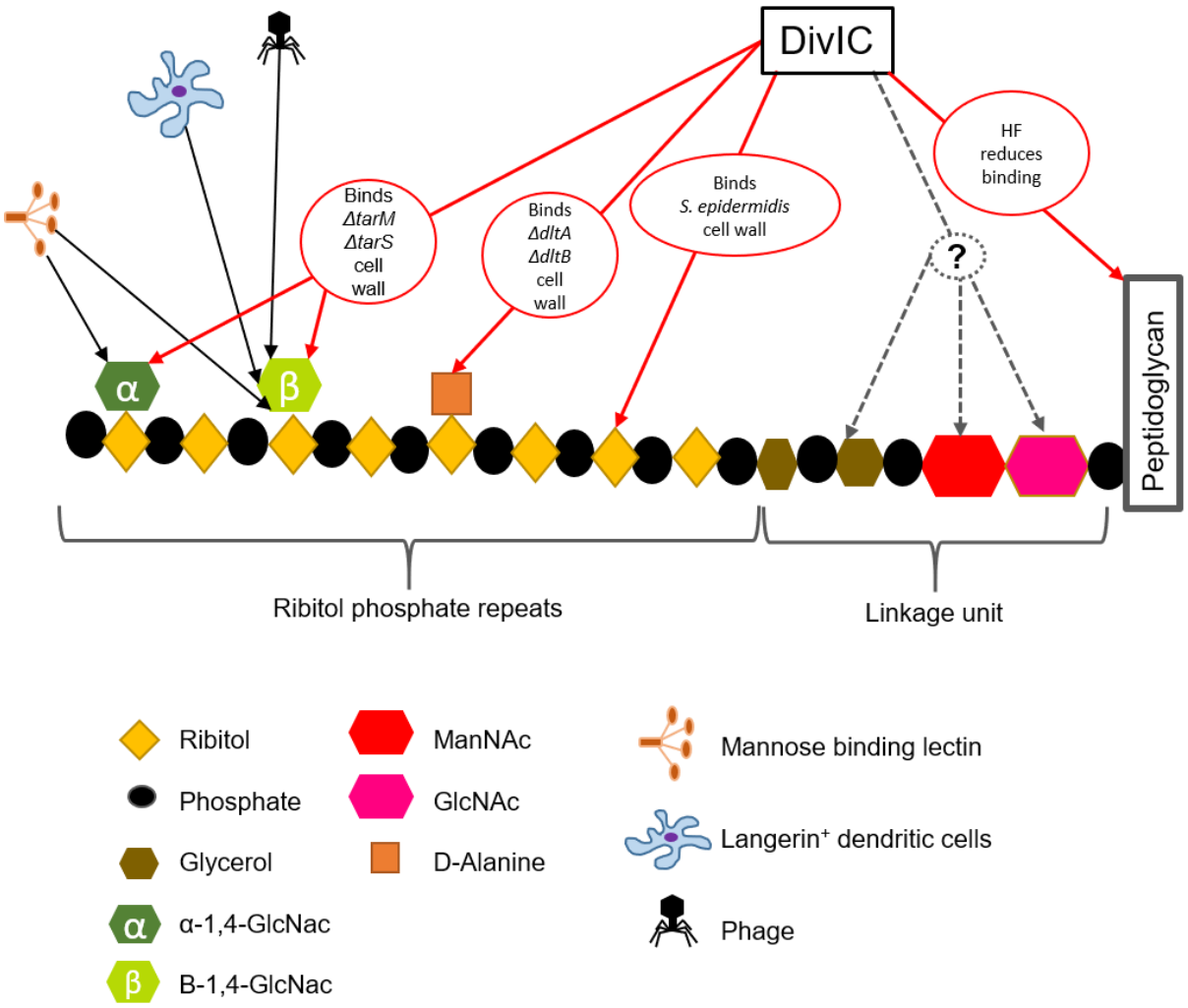

Figure 3.23 Potential binding moieties on WTA
WTA is phosphate(black) linked onto peptidoglycan, the linkage unit consists of GlcNAc (pink), ManNAc (red) and two glycerol(brown) phosphates, there is then a ribitol (yellow) phosphate repeat (n~40) which makes the main sugar backbone of the molecule. This ribitol phosphate backbone is decorated on the ribitol by D-alanine (orange) or α-(dark green) and β- (light green) 1,4-GlcNAc moieties to which phage, langerin and mannose binding lectins bind to as shown by the solid black arrows. DivIC does not bind to any of the moieties indicated by the red arrows as evidenced from the binding behaviour described in the relative red circles. DivIC may bind to any part of the linkage unit as this possible interaction has not been thoroughly interrogated.

3.4.3 Further work

3.4.3.1 Mapping the DivIC WTA binding site

DivIC is a relatively well-conserved protein in Gram-positive bacteria and does have a Gram-negative homologue in the form of FtsB (Fig 3.24). There are conserved residues such as A100, R101, G110 and E111. Furthermore, in the predicted extracellular portion of *S. aureus* DivIC; Q56-K130 (Fig 3.1), there are numerous residues which share physiochemical similarities with over 70% of corresponding residues in homologous proteins of other species. Further work to assess the contribution of these residues will begin with binding checks using truncated versions of the recombinant extracellular domain of DivIC. Through this it could be possible to ascertain which residues are involved in binding WTA and this in turn might help elucidate which moiety on WTA is the binding site. In the fullness of time this may aid logical drug design to target the interaction between DivIC and WTA as a potential therapeutic target for novel antibiotics. Nuclear magnetic resonance (NMR) spectroscopy has previously been used to assess binding of specific residues[285] and this would be another potentially interesting avenue of investigation to assess the binding site.

3.4.3.2 Structural analysis of DivIC

Other methodologies to assess interactions based on structure include X-ray crystallography. The gram-negative homologue of DivIC: FtsB has been co-crystallised with the β sub-unit of the gram-negative DivIB homologue: FtsQ showing an interaction with the 64th and 89th amnio acid of FtsB binding FtsQ[286,287]. However, to date there have been no crystal structures of DivIC and there have been no solitary structures of FtsB without FtsQ. FtsB (and likely DivIC) is unstable without the stabilising presence of FtsL and FtsQ[288] therefore it might be that its structure is not sufficiently stable *in vitro* to be conducive to X-ray crystallography.

Our collaborators in the Han group at Xiamen University have thus far been unable to successfully crystallise any version of DivIC (personal communication). Given the binding of WTA might be part of the function of DivIC, it is plausible that the buffer conditions used in these binding assays (pH 5 and containing divalent cations) might stabilise DivIC. It is also possible that addition of WTA might enhance DivIC X-ray crystallography studies. However, the heterogeneity in the WTA as a sample might

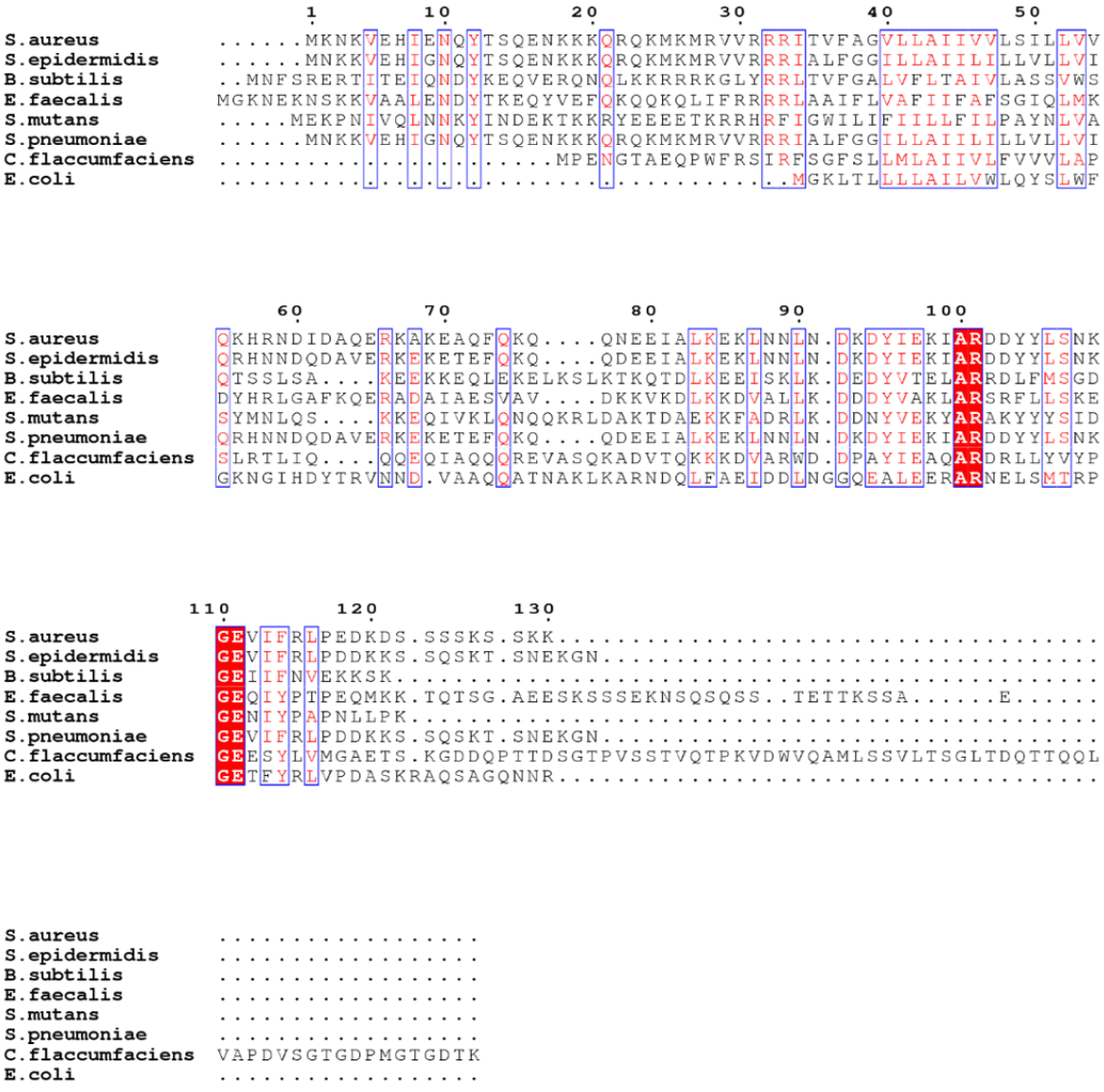

Figure 3.24 Multiple sequence alignment showing homology between DivIC protein primary sequences of bacterial species.
Protein sequences for DivIC (or FtsB in the case of *E. coli*) were aligned using Clustal Omega and this alignment was assessed and plotted using the online ENDscript server[289]. Red highlighted columns have 100% identity and columns in which 70% of residues share physiochemical properties are framed in blue. Residues are numbered according to the *S. aureus* protein.

complicate its use. WTA in *S. aureus* is approximately 40-60 ribitol-phosphate repeat units long[96]. However, WTA is also extremely heterogenous due to the many possible modifications[96].

3.4.3.3 Binding kinetics

WTA heterogeneity limits the ability to determine stoichiometry and binding kinetics through MST as it leads to various molecular masses within a WTA sample which does not allow for accurate molar concentrations to be determined. A chemically defined WTA would be beneficial for study of such interactions. A ribitol phosphate tetramer was chemically synthesised by Jung et al.[105] and shown to be biologically active through its ability to induce IL-6 production in mice. The ribitol phosphate repeat unit is not the important binding moiety given the propensity of DivIC to bind *S. epidermidis* cell walls (Fig 3.18). However, this literature demonstrates that chemical synthesis of WTA-like sugar moieties is possible and should potentially be investigated for the potential of interrogating the linkage unit as the binding moiety.

Unfortunately, a drawback of the MST experiments was a failure to get a good dose response curve reaching saturation. Whilst this wasn't the main objective it would make a more convincing argument for specific binding. It is possible that addition of FtsL and DivIB to form the heterotrimer with DivIC would potentiate the binding leading to binding saturation, this would be an interesting experiment.

3.4.4 Importance of the DivIC WTA interaction

Despite it seemingly being essential, there is no unequivocally defined role DivIC in the literature, but a number of functions or roles have been proposed for WTA. WTA constitute around half the dry weight of the cell wall[83] and deficient strains such as the *ΔtarO* mutant and triple *lcp* knockout have pleiotropic defects[88,268,290]. WTA is involved in regulating the charge of the cell envelope, sequestering ions and virulence[83,96,291]. Recently the Pinho group have suggested WTA has a role in regulating cell division[292]. The evidence reported here supports the proposition that DivIC might provide the missing link in how WTA regulate cell division.

Other bacterial proteins which bind to WTA have been described such as the Choline-Binding Protein L (CbpL) of *S. pneumoniae* which binds the choline residue

of *S. pneumoniae* teichoic acids and is purported to be involved in pathogenesis[293]. WTA binding has also been described more broadly in terms of hydrolysis such as teichoicases used during phosphate starvation, for example GlpQ of *S. aureus* [294] and GlpQ and PhoD of *B. subtilis*[295] which degrade polyglycerol phosphate. Evidence also suggests interaction with the choline residues of *S. pneumoniae* is required for proper function of its autolysin[296,297]. The presence of WTA has also been shown to alter autolytic amidase activity in *B. subtilis*[298]. WTA in *S. aureus* have previously been implicated in targeting AtlA-driven cell wall hydrolysis through blocking hydrolysis where WTA is present[98], potentially through sequestering H^+ ions and lowering pH to a non-permissive acidity for Atl[99]. This role may be fulfilled by choline-containing lipoteichoic acids in *S. pneumoniae* as they seem to inhibit streptococcal autolysin[299]. Furthermore, export of Atl in *S. aureus* has been shown to be dependent on WTA export and inhibited by targocil[86]. Interestingly there may also be a section of the septum that is devoid of WTA as shown by non-uniform electron density in the septum seen by electron microscopy[300]. This would potentially stratify sections of the septum based on their susceptibility to hydrolysis. Thus, WTA and (to a lesser extent) LTA may coordinate cell division through controlling cell wall hydrolysis. The different sugar phosphate backbones in the WTA of these species may also provide specificities to their own hydrolysis machinery or protect against secreted teichoicases such as GlpQ.

A model of how DivIC and its interaction with WTA may fit into the cell division machinery is portrayed in Figure 3.25. DivIC is stabilised through its interaction with DivIB and FtsL[288]. DivIB is a peptidoglycan binding protein[150]. Therefore, peptidoglycan synthesis devoid of WTA might be what recruits DivIB to the septum. This is made more plausible when considering the formation of the piecrust which begins septum formation is possible without DivIB but progression to a complete septum is not[150]. Therefore, this model assumes that DivIB is localised through its interaction with nascent peptidoglycan at the piecrust. This localisation of DivIB would stabilise DivIC and allow the septal plate to be formed.

In addition, it has also been shown that TarO is present at the septum in *S. aureus*[292], as are TarG and TarH in *B. subtilis*[301] implying WTA are not only synthesised but also exported at the septum. A bacterial two hybrid analysis also shows that DivIC interacts with TarO, LcpA and LcpC[245]. Therefore, DivIB and DivIC

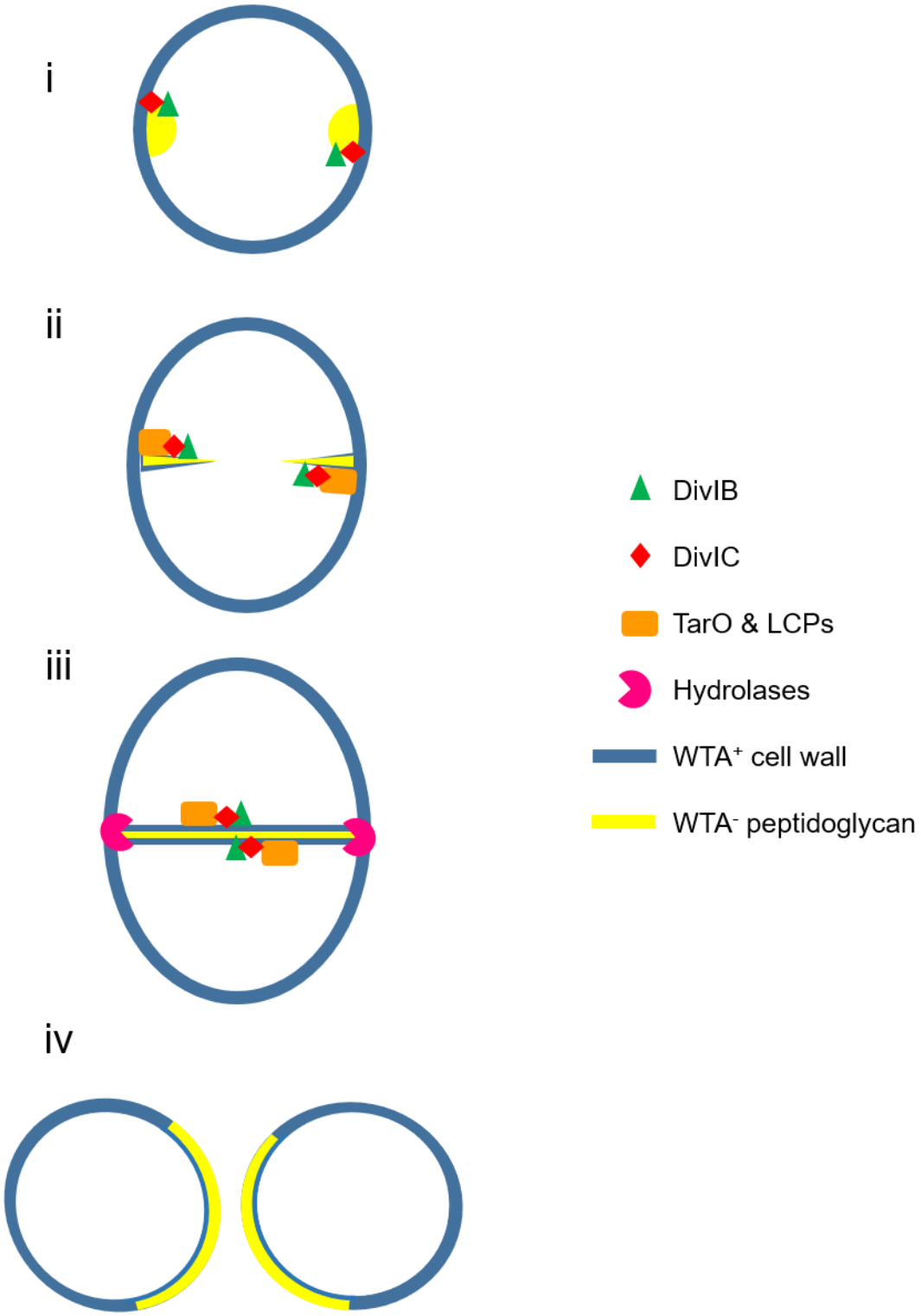

Figure 3.25 Model of DivIC in *S. aureus* cell division
i) DivIB (green) associates with the nascent peptidoglycan (yellow) which has formed at the site of septum formation, forming the “piecrust”. DivIC (red) is stabilised through its interaction with DivIB. DivIC also interacts with WTA synthesis machinery (orange). ii) Peptidoglycan synthesis at the leading edge of the septum directs DivIB and DivIC which in turn, through binding to WTA+ cell wall and interacting with TarO & the LCP proteins, directs the WTA synthesis machinery along the invaginating septum. iii)This process leaves peptidoglycan in the interior of the septum devoid of WTA and liable to be hydrolysed by cell wall hydrolases such as Atl (pink). iv) This allows separation and the completion of division forming two daughter cells which will have smooth rings of nascent peptidoglycan on one face of their exterior.

bound together in the divisome could be providing a directionality to the division machinery through DivIB binding nascent peptidoglycan at the leading edge of the septum and DivIC binding to cell wall as it is decorated with WTA. This would result in a process as is described in Figure 3.25. As the WTA synthesis machinery is dragged along behind the leading edge, the entire septum would become WTA^+ but due to the rapid advancement this WTA decoration would not encompass the entire width of the septum between the soon-to-be two daughter cells. This WTA^- peptidoglycan, which is sensitive to hydrolysis[98,292,302], would be liable to be cleaved by cell wall hydrolases such as Atl resulting in separation and completion of cell division. A clear difference in cell wall architecture between the two faces of the nascent septum has recently been demonstrated in support of this hypothesis[248]. Furthermore, it has recently been described that the FtsQBL complex partially inhibits PBP activity[151] thereby supporting a pacemaker role in septum progression, allowing peptidoglycan and WTA synthesis to be coordinated which in turn would protect the dividing cell from premature or excessive hydrolase activity.

This model could help explain the aberrant misplacement of septa in WTA deficient strains[268,303]. Whilst a Δ*divIC* mutant remains elusive, if this model is correct the expected phenotype would be similar to the Δ*divIB* mutant which can begin a septum but not complete it[150], as seen in the *S. coelicolor* Δ*divIC* mutant[243]. However, many questions remain as WTA synthesis in itself is not required for septal synthesis.

3.5 Conclusion

The data presented in this chapter present strong genetic and biochemical evidence to support the hypothesis that DivIC is a WTA-binding protein. This is an important finding as an essential division protein has not previously been described with these properties in bacteria. The fact that DivIC binds to WTA will likely add to the long-standing debate on the function of WTA. However, as DivIC is thought to be an essential division protein[233,241], its binding to WTA implicates WTA as having a role in cell division, potentially through coordinating cell wall hydrolysis. With further work this could dramatically improve our understanding of bacterial cell division and further inform the model (Fig 3.25) on the role of DivIC and WTA in *S. aureus* cell division.

Additionally, by demonstrating that DivIC binds WTA this chapter potentially provides a novel target for anti-*S. aureus* therapeutic development. Whilst the exact binding

moieties on DivIC and WTA remain to be elucidated there is a clear way forward discussed in section 3.4.3. Elucidating the binding site would provide a target for logical antibiotic design. If the binding site could be discovered and DivIC proven to be essential for *S. aureus* this could present a convincing argument for DivIC and other divisome proteins to be considered as potential vaccine antigens.

Chapter 4:
The augmented infection model of *S. aureus* sepsis: mechanistic insights and potential applications

4.1 Introduction

S. aureus presents a particular challenge in developing new immunotherapies due to its ability to colonise humans and exist in a commensal niche. This continued exposure to the human organism has likely contributed to the evolution of an extensive armoury of virulence factors and immune evasion techniques with which *S. aureus* can cause pathology when it gains access to the body[304–306]. This *S. aureus* immune survival kit allows it to opportunistically infect many compartments of the body and results in a wide variety of pathologies such as: skin and soft tissue infections, osteomyelitis, endocarditis, pneumonia, and sepsis[7]. One organism having such a varied pathological diversity confuses our understanding of *S. aureus* pathogenesis and makes for a difficult moving target.

Numerous studies use the mouse to model human infection as it has been widely used in biological research with a lot of published literature from which to draw comparisons. Furthermore, this is enhanced by the wide variety of transgenic mice available and a wealth of available knowledge on the murine immune system[307,308]. The mouse has been used to model *S. aureus* pneumonia[192], skin and soft tissue infections[309], osteomyelitis[310] and sepsis[29,190,222]. The work presented in this chapter will focus on a model of *S. aureus* sepsis. Our current understanding of *S. aureus* sepsis is largely developed from *in vivo* studies of intravenous and intraperitoneal infections of mice. We primarily use the intravenous route of infection, which closely mimics bloodstream infection that induces bacteraemia, endocarditis and sepsis.

The infection dynamics of the intravenous sepsis model has been recently mapped where, upon introduction into the bloodstream, the majority of *S. aureus* are taken up by macrophages in the liver, called Kupffer cells[29,222]. This initial phagocytosis event represents the first immunological bottleneck of infection where most *S. aureus* cells are neutralised by the phagocytes. However, some *S. aureus* survive within Kupffer cells which eventually lyse releasing free bacteria into the surrounding tissue and bloodstream. Free *S. aureus* are taken up by neutrophils[29] (and peritoneal macrophages in the case of peritoneal sepsis[31]) which can serve to disseminate the

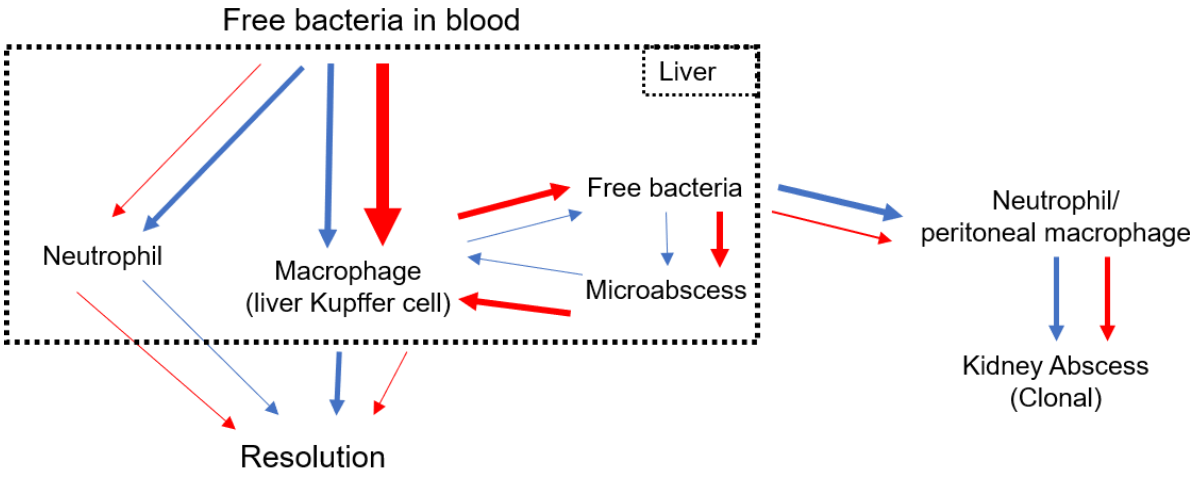

Figure 4.1. Diagram of infection dynamics in *S. aureus* intravenous mouse infection
During intravenous infection with *S. aureus* alone (blue) or *S. aureus* with augmenting material (red), most bacteria are taken up by Kupffer cells in the liver. Many of the bacteria are cleared when internalised by the phagocytes but some escape and form microabscesses. Bacteria can be re-phagocytosed from these abscesses and cleared or survive within phagocytes such as neutrophils which allows dissemination throughout the body. During augmented infection (red) a greater amount of bacterial survival and persistence within the liver. This is through increased uptake survival into and survival within the Kupffer cells and formation of hepatic microabscesses. Adapted from Pollitt *et al.* (2018).

infection. Free *S. aureus* can also proliferate to cause microabscesses with a central nidus of bacteria ring-fenced by an eosinophilic pseudo capsule and neutrophils[79]. This extracellular local concentration of bacteria can act as a source of new spread, increased immune stimulation and subsequent inflammation. This systemic spread and cycling of free bacteria within the vasculature throughout the body leads to pro-coagulation inflammation and endothelial damage which in turn leads to infectious thrombi and haemorrhages[34], ultimately resulting in multiple organ failure and death.

Despite the understanding which has come from infection studies in mice, there are several drawbacks to animal models which have led to a lack of translation from preclinical to clinical trials in vaccines. One of the chief drawbacks among these is that in order to successfully establish infection a large dose of *S. aureus* is required. However, this has been overcome in a recent study which utilised the contribution of the commensal flora to augment infection and allow the infectious dose to be reduced by up to 1000-fold[222]. Given *S. aureus* exists commensally on the skin and in the nose[311,312], natural *S. aureus* infections would not begin with exposure to a homogenous, mono-species challenge. Augmentation of *S. aureus* infection by commensal skin organisms only benefits *S. aureus* with the commensal organisms being effectively cleared[222]*.* Furthermore, isolated bacterial components, such as purified cell wall peptidoglycan can also augment infection. It is also interesting to note that this augmentation of infection somehow alters the infection dynamics by shifting the epicentre of infectious load to the liver (Fig 4.1).

The mechanism of augmentation has yet to be elucidated but given purified peptidoglycan can augment infection[222] it would make sense that there was an immune component as the immune system recognises microbial components such as peptidoglycan as signatures of exposure. Peptidoglycan acts on the immune system primarily through ligation of the PRRs of the innate immune system (including NOD1, NOD2, NLRPs and arguably TLR2)[64]. Contrastingly to its apparent role in augmentation peptidoglycan[313] and *S. aureus*, cell wall ghosts[314] have also been suggested as protective agents which induce immunity in proposed anti-*S. aureus* vaccines. However, neither of these vaccine formulations or any others that were successful in previous, preclinical animal models have passed scrutiny of clinical trials.

This augmented infection model is exciting in allowing a reproducible infection with a human pathogen but also the reduction of the required inoculum indicates it might inform our understanding of *S. aureus* pathogenesis. Not only would this help our therapy development in terms of providing more relevant insights to pathogenic mechanisms but if proven to be closer to *S. aureus* sepsis in humans this model could prove to be invaluable in preclinical evaluations. As it stands there have been many successful *S. aureus* vaccines in preclinical mouse studies but no successful clinical trials, thus if this model can be optimised and shown to be valid it may help this preclinical to clinical translation process.

4.2 Aims

The work in this chapter will seek to aid in this process by investigating the parameters of augmentation and assess its utility in the setting of preclinical vaccine evaluation. The aims of this chapter were to:

- Interrogate the mechanism of infection augmentation by peptidoglycan.
- Assess the utility of the augmentation model in testing of vaccines.
- Investigate the effects of peptidoglycan as an adjuvant in a vaccine formulation.

4.3 Results

4.3.1 Peptide mimics of peptidoglycan do not augment intravenous *S. aureus* infection.

The mechanism by which peptidoglycan augments staphylococcal infection has yet to be determined[222]. The host response to peptidoglycan may induce immunological changes which leaves the host less able to combat *S. aureus* infection. Peptide mimics of peptidoglycan can be recognised by anti-peptidoglycan monoclonal antibodies[315] and have been tested as a vaccine and shown to protect against mice against *S. aureus* infection[316]. Therefore, the peptide mimics may react with the immune system in a similar way to peptidoglycan.

The peptidoglycan peptide mimic shown in Figure 4.3A was synthesized by Peptide Protein Research Ltd., with the structure used in Wang *et al.*[316]. This peptide was chosen as it was very reactive with peptidoglycan mAb in their intial peptide mimic screen[315] and was the peptide they carried forward to their vaccine study[316]. A dosing study was carried out where groups of 2 mice each received escalating doses (10µg,

50µg, 100µg, 200µg) of this peptide mimic via intravenous injection. The mice were monitored for adverse effects or weight loss for 3 days after injection (Fig 4.3B) and there was no significant weight loss compared to PBS injected control mice. Therefore the peptidoglycan peptide mimic was considered safe to take through to infection experiments.

Mice were intravenously injected with $1x10^6$ CFU *S. aureus* (NewHG) alone or with 100µg or 200µg of the peptidoglycan peptide mimic. The group receiving 100µg of peptide mimic with *S. aureus* was injected before the group receiving 200µg peptide mimic in order to assess any immediate adverse reactions, of which there were none. On day 3 post-infection mice were culled and their livers and kidneys harvested for CFU enumeration. There was no significant differences between groups in the CFU measured in the kidneys or livers (Fig 4.3C & 4.3D respectively). There was also no significant difference observed in weight loss (Fig 4.3E).

Thus, the peptidoglycan peptide mimic did not augment *S. aureus* infection. This could be due to lack of uptake of the soluble peptide as soluble peptidoglycan has previously been shown to fail to augment *S. aureus* infection[222]. The lack of particulate properties could be a confounder since these are important in the host response to peptidoglycan[317].

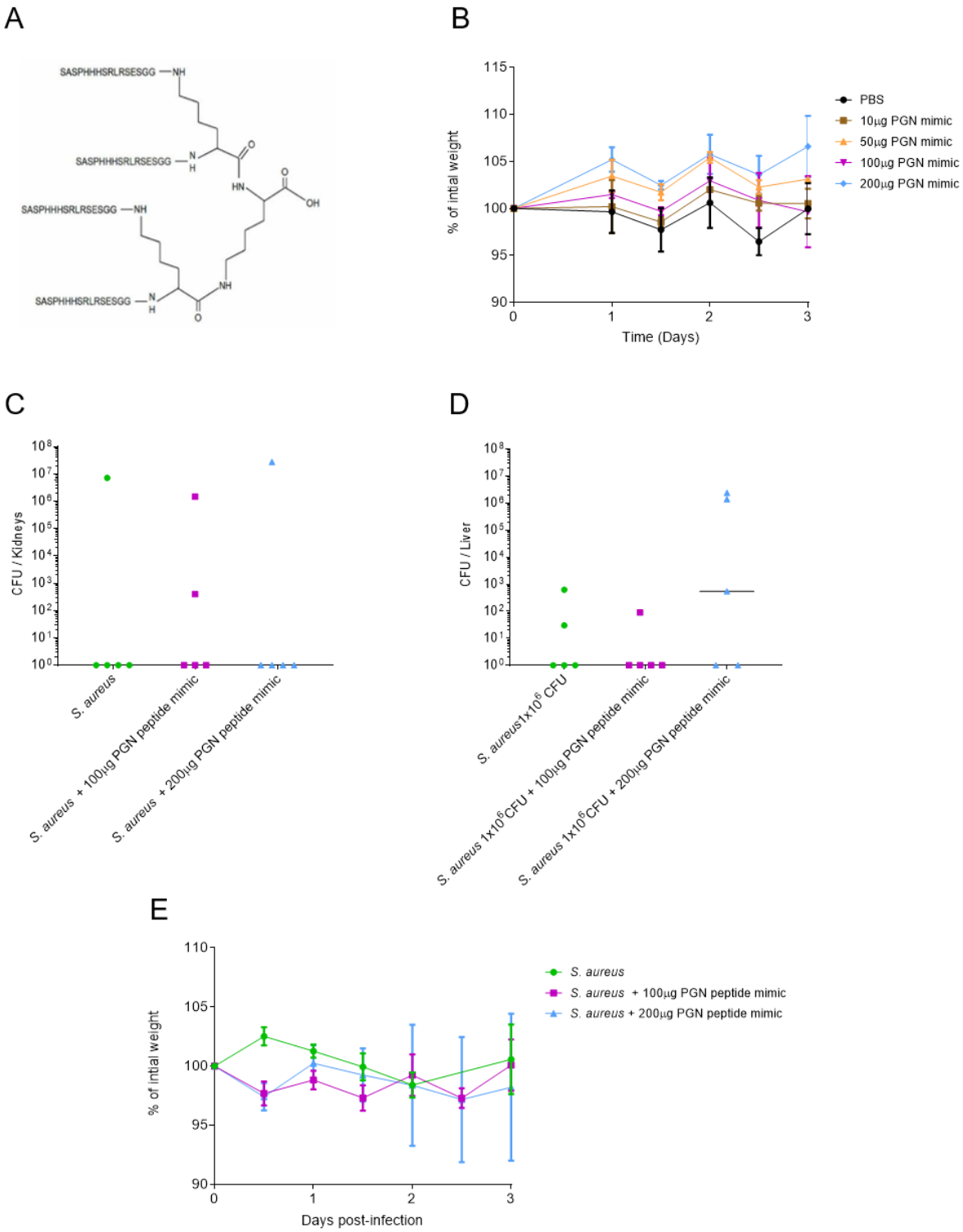

Figure 4.2 A peptide mimic of peptidoglycan does not augment intravenous *S. aureus* infection.
To find a safe dose, mice were intravenously infected with different amounts of the peptidoglycan peptide mimic (SASPHHSRLRSESGG)4-K2-K (A), weighed and monitored over the course of 3 days to check for adverse effects (B). Failing to see any adverse effects 100µg or 200µg of the peptidoglycan peptide mimic was co-injected intravenously with $1x10^6$ CFU *S. aureus* (NewHG). On day 3 post-infection mice were culled and the kidneys (C) and livers (D) were harvested for CFU enumeration. Mice were weighed daily throughout the course of infection (E). CFU shown as median, weights shown as mean and Std Dev. No significant differences were seen ($p>0.05$).

4.3.2 The role of the physical properties of components capable of augmenting *S. aureus* infection

M. luteus peptidoglycan was freeze-dried to alter its physical properties. This was then analysed by flow cytometry and compared to peptidoglycan that had not been freeze-dried and *S. aureus* cells. All samples were sonicated before flow cytometry to break apart clumps/aggregates. Samples were gated based on a PBS blank (Supplementary Figure 5). Flow cytometry, at its most basic, measures forward scatter which gives an indication of cell/particle size and side scatter which gives an indication of the granularity of cells/particles.

The process of freeze-drying peptidoglycan significantly increased its size and significantly decreased its granularity (Fig 4.3). Both peptidoglycan samples were significantly smaller and less granular than intact *S. aureus* cells. However, the peptidoglycan that had not been freeze-dried had a granularity much closer to *S. aureus* cells than the freeze-dried peptidoglycan. Therefore, freeze drying peptidoglycan significantly alters the physical properties of peptidoglycan making it larger and less granular.

As it was possible to verify a physical change in peptidoglycan including a change in granularity, this was taken forward to *in vivo* challenge. A dosing study was carried out to check the safety of freeze-dried versus untreated peptidoglycan. As at 500µg the untreated peptidoglycan could cause some weight loss (Supplementary Figure 5), a dose of 250µg was used for the augmentation/infection study.

Mice were intravenously injected with $1x10^6$ CFU *S. aureus* (NewHG) alone or with 250µg freeze dried or non-freeze-dried *M. luteus* peptidoglycan. Mice were monitored and weighed daily for 2 days before being culled on day 2 post-infection whereupon kidneys, livers, lungs, spleens, and hearts were harvested for CFU enumeration (Fig 4.4).

Both types of peptidoglycan caused significantly more weight loss in combination with *S. aureus* compared to bacteria alone (Fig 4.4F). Untreated peptidoglycan gave significant augmentation of *S. aureus* CFU in the liver, lungs, spleen and heart compared to bacteria alone. However, this augmentation was lost in all organs other than the liver if the peptidoglycan had been freeze-dried.

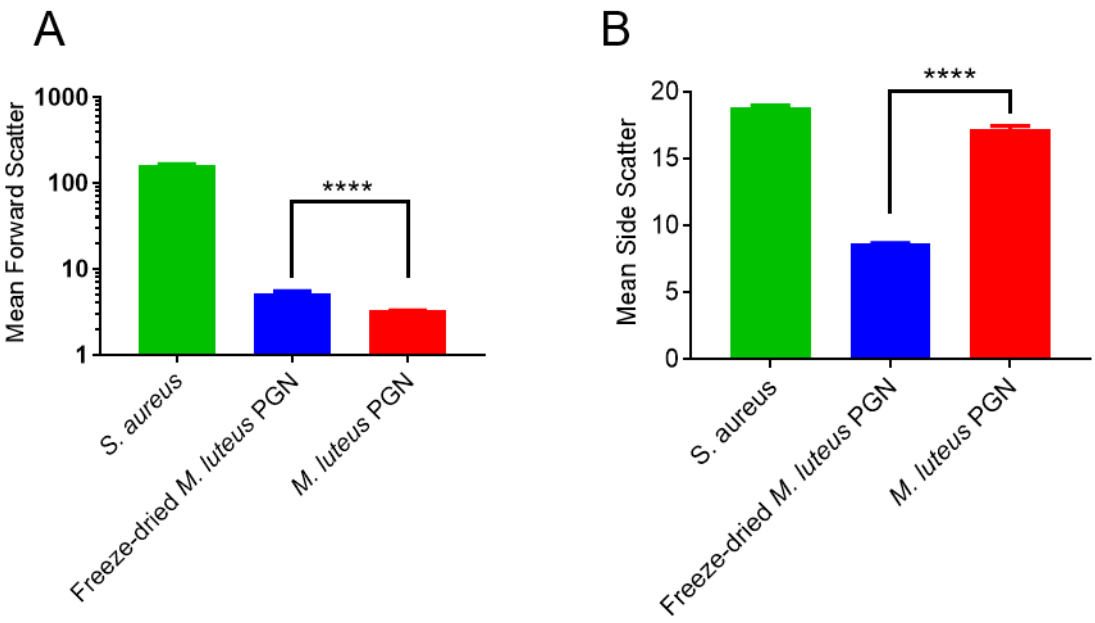

Figure 4.3 Freeze drying *M. luteus* peptidoglycan increases particle size but reduces granularity.

M. luteus peptidoglycan preparations were compared to *S. aureus* cells by flow cytometry to assess forward and side scatter. (n=3). Forward and Side scatter shown as mean with Std Dev. **** p<0.0001

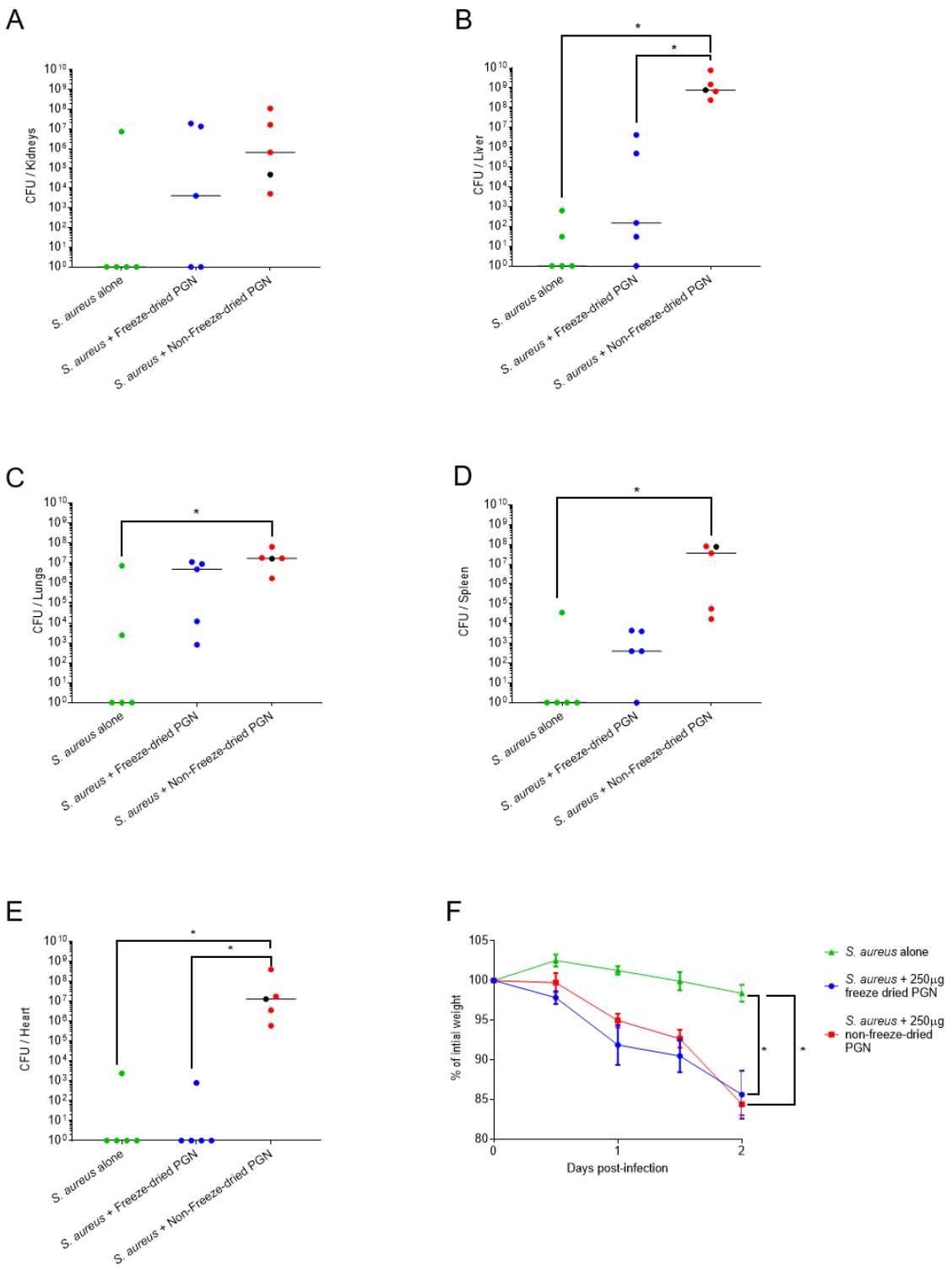

Figure 4.4 Freeze-drying *M. luteus* peptidoglycan reduces its ability to augment intravenous *S. aureus* infection

Mice were intravenously injected with 1x10^6 CFU *S. aureus* (NewHG) alone (green) or with untreated (red) or freeze dried (blue) *M. luteus* peptidoglycan. On day 2 post-infection mice were culled and kidneys (A), livers (B), lungs (C), spleens (D) and hearts (E) were harvested for CFU enumeration. Mice were weighed twice daily throughout the course of the infection (F). The black data-point in the non-freeze dried PGN group denotes a mouse that reached severity limits before the end of the protocol and was culled early, this mouse has therefore been left out of statistical analysis. CFU shown as median, weights shown as mean and Std Dev. * $p<0.05$, ** $p<0.01$.

4.3.3 Does augmentation require co-injection of *S. aureus* and peptidoglycan?

4.3.3.1 Injection of peptidoglycan prior to *S. aureus* infection

Augmentation of infection may occur due to peptidoglycan altering of the immunological milieu allowing greater infection. To test this, the requirement for co-injected was investigated. Mice were injected with 500µg of *M. luteus* peptidoglycan 24, 6 or 1 hour(s) before infection with $1x10^6$ CFU of *S. aureus* (NewHG). The positive control was co-injection of *S. aureus* and *M. luteus* peptidoglycan (Fig 4.5A). The negative control was infection with $1x10^6$ CFU of *S. aureus* (NewHG) alone. Mice were monitored and weighed daily throughout infection before being culled on day 3 post-infection when kidneys and livers were harvested for CFU enumeration. 500µg of peptidoglycan used as this was the standard lab dose and this experiment was performed before the data was gathered for Supplementary Figure 6, all further experiments use 250µg in their augmentative dose.

Compared to *S. aureus* alone there was no significant weight loss seen in any of the augmentation groups (Fig 4.5D). This was also found for CFU recovered from the kidneys. Co-injection of *S. aureus* and peptidoglycan significantly increased the CFU recovered from the livers compared to *S. aureus* alone. However, this was not observed if the augmenting material was injected prior to *S. aureus*. This does not conclusively show co-injection is required for augmentation as it could be that *S. aureus* needs to be present first for peptidoglycan to have its augmentative effect thus this was experimentally interrogated.

4.3.3.2 Injection of peptidoglycan after low dose *S. aureus* infection

To determine if peptidoglycan could augment *S. aureus* infection after the initial period, it was injected into pre-infected hosts. Mice were intravenously injected with $1x10^6$ CFU *S. aureus* (NewHG), the negative control had no more interventions, the positive control group also received *250µg M. luteus* peptidoglycan at the same time as the *S. aureus* inoculum. Experimental groups received peptidoglycan intravenously at 6, 24 or 48 hours after infection. Mice were monitored and weighed daily after infection. All groups were culled at 72 post-infection and their livers and kidneys were harvested for CFU enumeration.

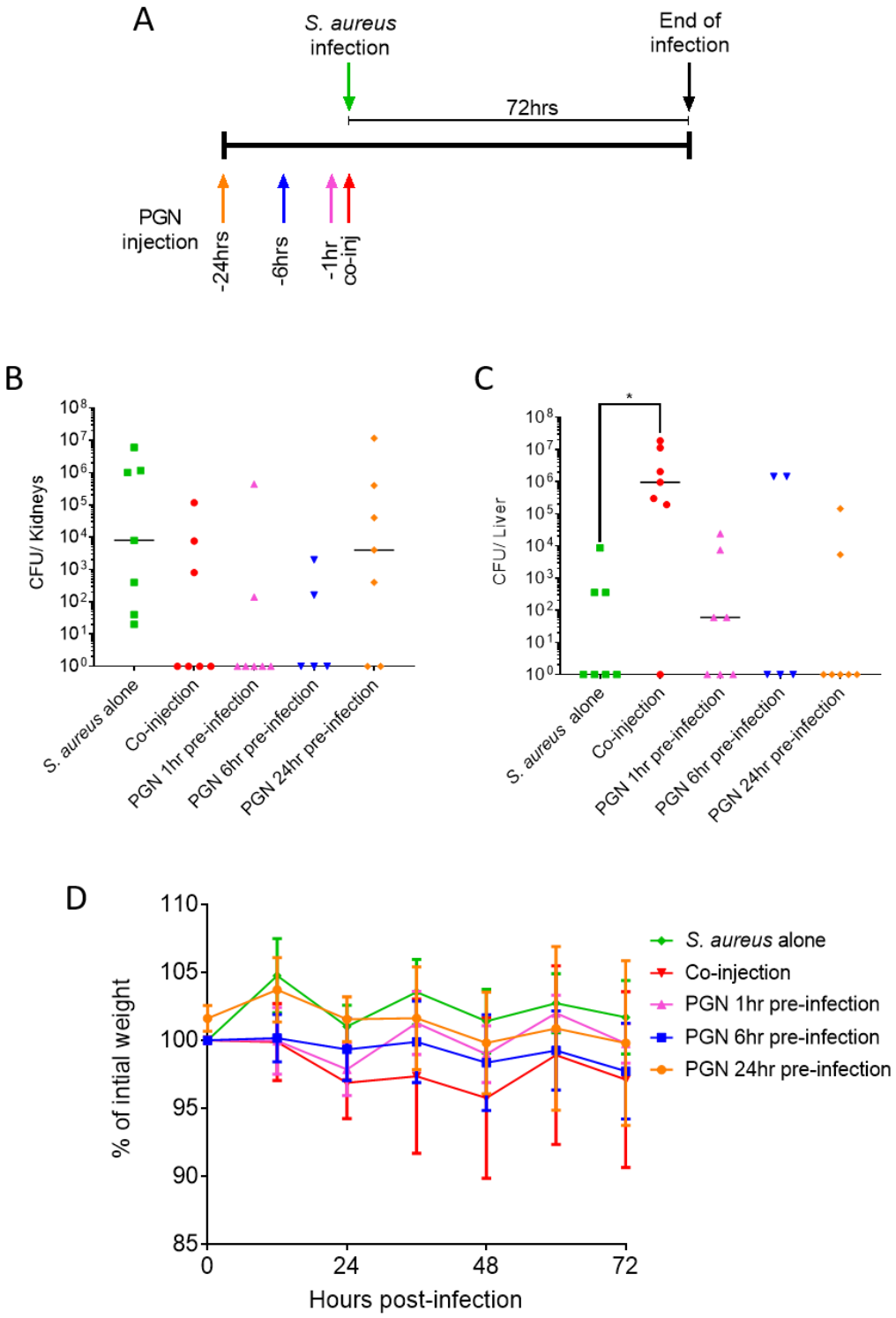

Figure 4.5 Effect of administration of *M. luteus* peptidoglycan before intravenous low dose *S. aureus* infection.
Mice were intravenously injected with 500µg *M. luteus* peptidoglycan 24 hours (orange), 6 hours (blue) or 1 hour (pink) before infection with $1x10^6$ CFU *S. aureus* (NewHG) (A). Control mice were intravenously injected at time = 0 with either $1x10^6$ CFU *S. aureus* (NewHG) alone (green) or $1x10^6$ CFU *S. aureus* (NewHG) and 500µg *M. luteus* peptidoglycan at the same time (red). CFU were measured in the kidneys (B) or livers (C) and mice were weighed throughout the infection (D). CFU shown as median, weights shown as mean and Std Dev. * $p<0.05$.

There is a trend whereby the closer in time that *S. aureus* and the peptidoglycan are injected the greater the pathology. The co-injection and peptidoglycan at 6 hours post-infection groups were the only groups with a significant weight loss on day 3 when compared to the *S. aureus* alone group (Fig 4.6D).

There was no significant difference in the CFU other than between the positive and negative control groups for augmentation in the liver CFU. However, there is the trend whereby the closer in time the two inocula were received the greater the number of CFU recovered. This could be confounded if, by the time of the peptidoglycan injection, the host had already cleared the *S. aureus* infection. To determine if this was the case a further experiment was carried out.

Mice were intravenously infected with $1x10^6$ CFU *S. aureus* (NewHG) and the positive control for augmentation also received 250µg of *M. luteus* peptidoglycan concomitantly. At 24 hours post-infection one group of mice was intravenously injected with 250µg of *M. luteus* peptidoglycan and another was culled to ascertain the level of infection present at 24 hours. All remaining mice were then culled 3 days after this timepoint (4 days post-infection). Mice were monitored and weighed daily throughout infection and the livers and kidneys were processed for CFU.

Both groups which received peptidoglycan had a greater weight loss than the *S. aureus* alone group, but this was insignificant at day 4 post-infection (Fig 4.7D). Only the co-injection group had significantly more CFU in the liver than the *S. aureus* alone group, indicating that administration of peptidoglycan at 24 hours post-infection was insufficient to augment *S. aureus* infection. Given the low levels of viable *S. aureus* seen in the organs of the mice which were culled at 24 hours this is unsurprising. There were very low CFU at the 24-hour time-point which implies that this infectious dose is mostly controlled by mice within 24 hours. Thus, an experiment was planned involving peptidoglycan given after a high dose infection.

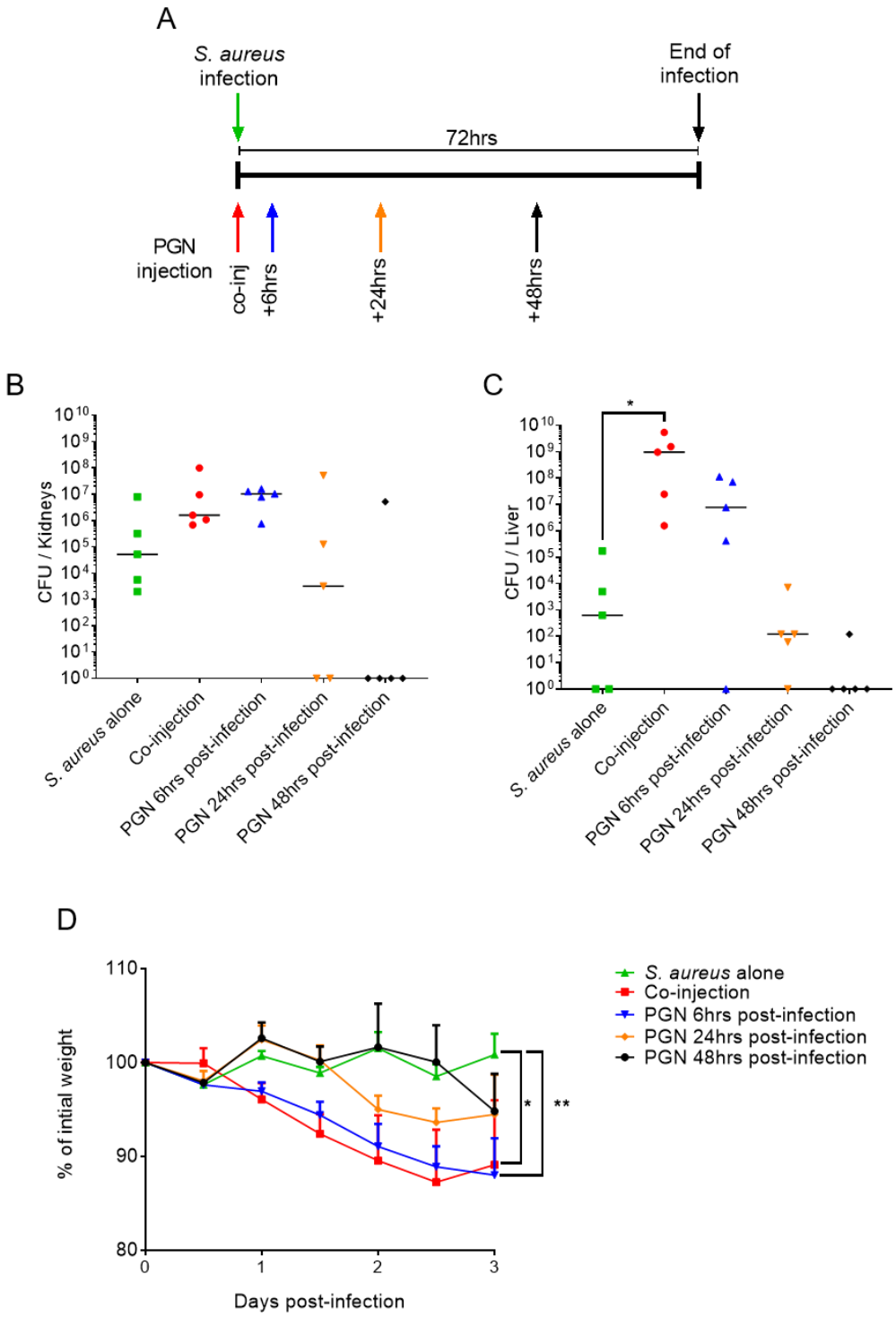

Figure 4.6 Effect of administration of *M. luteus* peptidoglycan after low dose *S. aureus* intravenous infection.
Mice were intravenously infected with 1x10^6 CFU of *S. aureus* (NewHG) alone (green) or co-injected with 250µg of *M. luteus* peptidoglycan at the same time as infection (red), 6 hours post-infection (blue), 24 hours post-infection (orange) or 48 hours post-infection (black). Mice were culled 3 days post-infection and the kidneys (B) and livers (C) were harvested for CFU enumeration. Mice were weighed twice daily throughout the course of infection (D). CFU shown as median, weights shown as mean and Std Dev. * $p<0.05$, ** $p<0.01$.

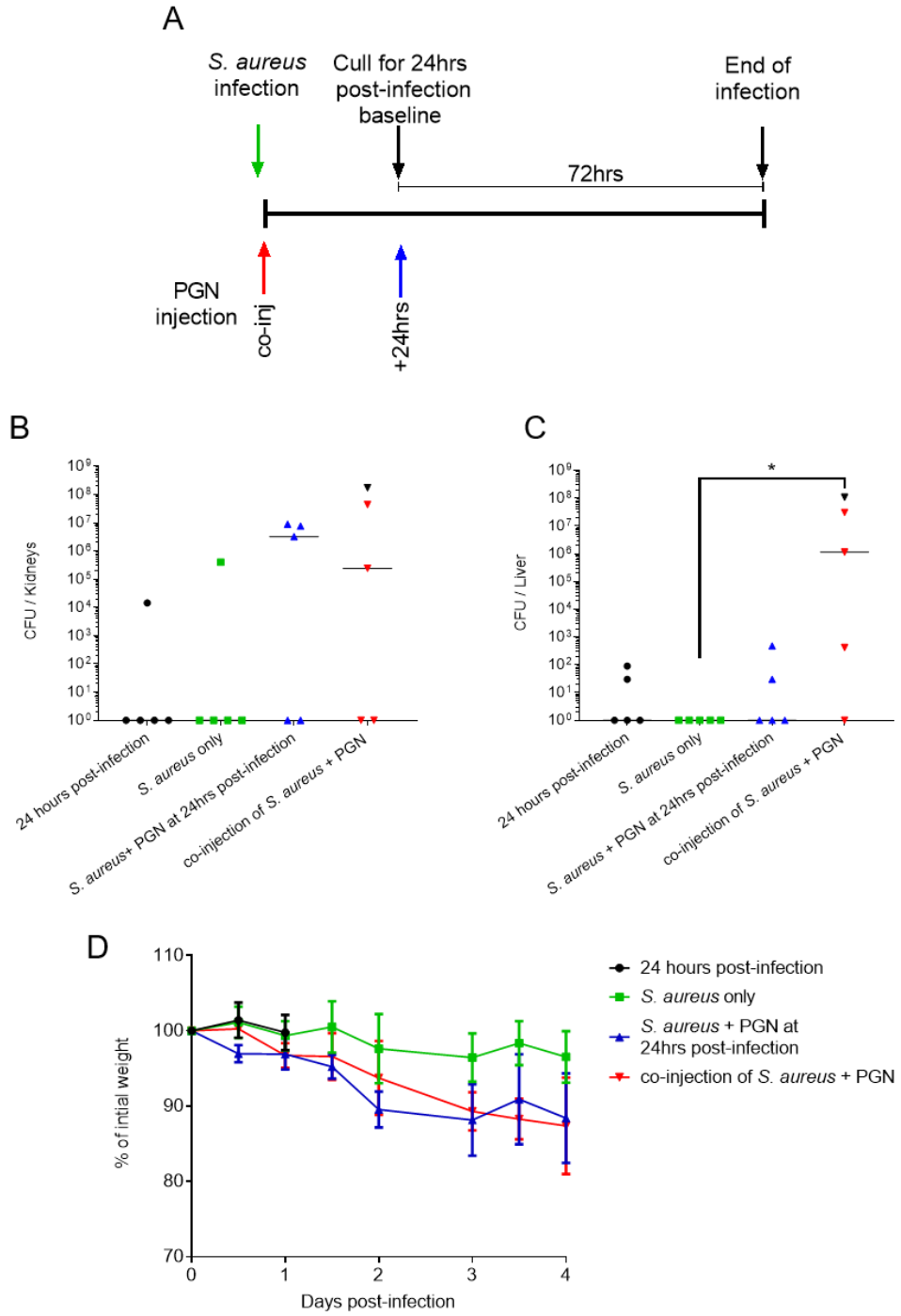

Figure 4.7 Intravenous administration of *M. luteus* peptidoglycan 24 hours after infection does not augment low dose intravenous *S. aureus* infection.
Mice were intravenously infected with 1x10^6 CFU *S. aureus* (NewHG). Mice received *S. aureus* alone (green), 250µg of *M. luteus* peptidoglycan injected at the same time as *S. aureus* (red) 250µg of *M. luteus* peptidoglycan intravenously 24 hours after infection with *S. aureus* (blue). One group of 5 mice were culled at 24 hours post-infection to provide a baseline level of the CFU present in the liver and kidneys at 24 hours (black), other mice were culled on day 4 post-infection and the kidneys (B) and livers (C) were harvested for CFU enumeration. Mice were weighed daily throughout the experiment (D). CFU shown as median, weights shown as mean and Std Dev. * p<0.05.

4.3.3.3 Effect of peptidoglycan injection after high dose *S. aureus* infection

The data in Figure 4.7 indicated that the majority of viable bacteria were cleared within 24 hours of infection when mice were intravenously infected with a low dose ($1x10^6$ CFU) of *S. aureus*. A high dose intravenous infection ($1x10^7$ CFU) leads to an established infection in the majority of mice[29]. Mice receiving this dose frequently present with severe pathology without addition of peptidoglycan. Therefore, giving peptidoglycan at the same time as this infectious dose has been previously avoided because it would likely cause rapid deterioration to the severity limits as defined by the Home Office project license P3BFD6DB9. 3 days post-infection most mice receiving the high dose of *S. aureus* have high recoverable CFU and kidney abscesses. Therefore, injecting peptidoglycan at 3 days or later in the high dose infection would ensure most mice had established infection for the peptidoglycan to potentially augment.

Four groups of mice were intravenously infected with $1x10^7$ CFU *S. aureus* (NewHG). On day 3 post-infection one group of mice was intravenously injected with 250µg *of M. luteus* peptidoglycan and another was intravenously injected with 100µl of etox PBS. On day 6 post-infection, the two groups of mice which had received a second inoculum were culled and their organs harvested for CFU enumeration. The remaining two groups of mice received their second inoculum (of 250µg of *M. luteus* peptidoglycan or etox PBS) on day 6 post-infection and were culled 3 days after this second inoculum (day 9 post-infection). Mice were monitored closely for adverse reactions and weighed daily throughout the experiment.

There was no significant difference in CFU recovered from mice which received peptidoglycan in the second inoculum compared to those mice that received PBS (Fig 4.8). This is regardless of which timepoint the mice received their second inoculum. The high number of CFU recovered from both groups which received PBS as a second inoculum demonstrates that lack of augmentation cannot be due to the fact there was no bacteria present. There was also no effect on overall weight loss due to the type of second inoculum received however all groups saw an appreciable weight loss by day 3 post-infection.

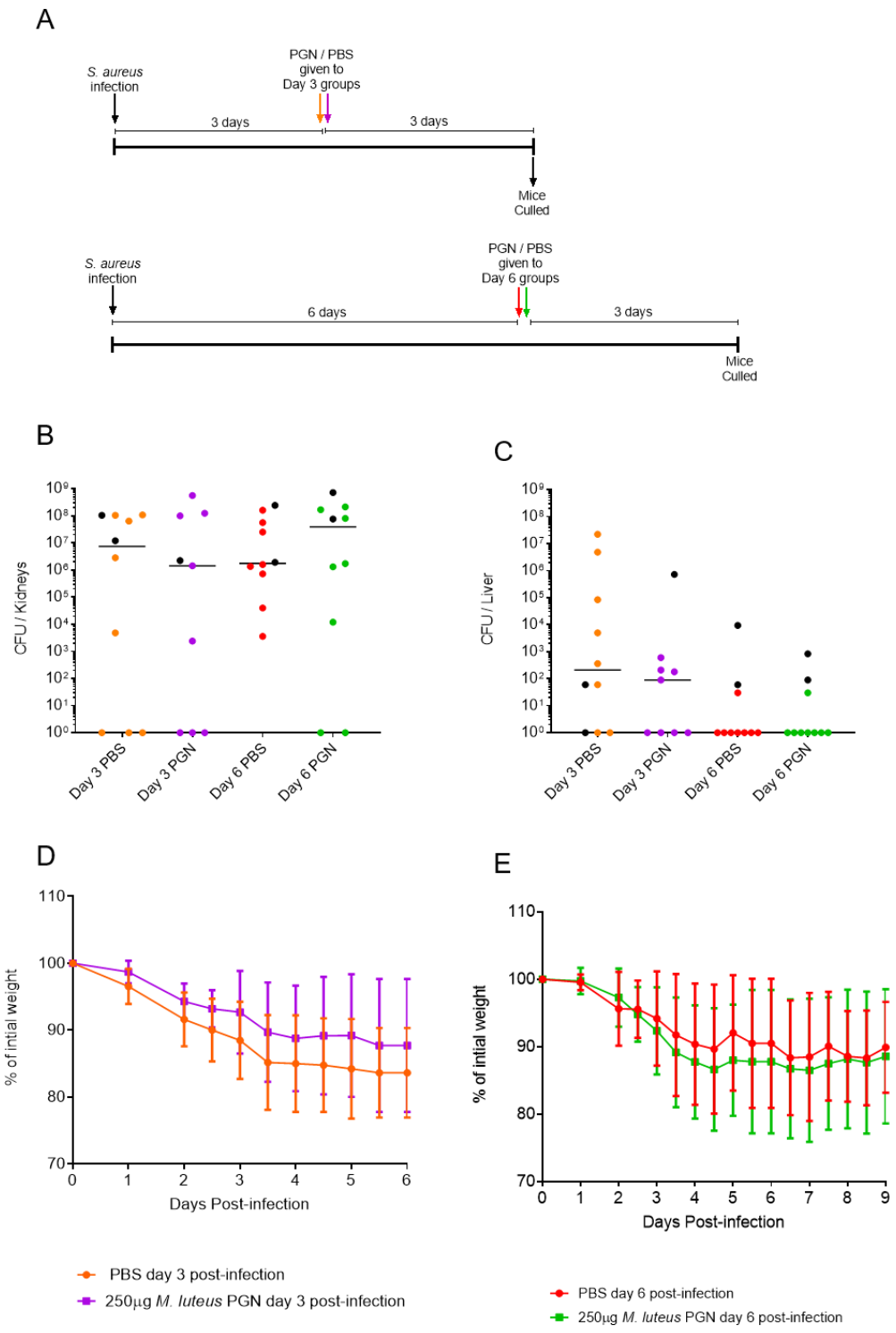

Figure 4.8. Effect of intravenous administration of *M. luteus* peptidoglycan in the late stages of high dose *S. aureus* infection.
Mice were intravenously challenged with $1x10^7$ CFU of *S. aureus* (NewHG). At day 3 (orange/purple) or day 6 (red/green) post-infection mice were intravenously injected with etox sterile PBS (orange/red) or 250µg of *M. luteus* peptidoglycan (purple/green). Mice were culled 3 days after this second injection and kidneys (B) and livers (C) were harvested for CFU enumeration. Mice were weighed daily throughout the course of the experiment (D and E). Black points on the CFU denote mice that reached protocol severity limits and were therefore culled before the end of protocol (these mice were excluded from statistical analysis). CFU shown as median, weights shown as mean and Std Dev. All results were found to be insignificant ($p>0.05$).

4.3.4 Use of augmented infection in vaccine development

Some of the major drawbacks in animal testing when it comes to vaccines and anti-infective therapeutics is the lack of reproducibility and applicability to human infections[318]. A prime example of these drawbacks is the fact that many animal infection models require large inocula to establish disease in animals with human pathogens. The augmentation model of infection as described by Boldock *et al.*[222] and recapitulated in this chapter allows for reproducible infection with a significantly lower dose of infectious material. The augmented infection model also more closely mimics real life infection which will rarely, come from homogenous monocultures in terms of bacterial species[319]. The applicability of this infection model to vaccine development was tested.

4.3.4.1 Vaccine formulation

First it was important to select the vaccine components for evaluation. Clumping factor A (ClfA) is a *S. aureus* sortase-linked, cell wall protein[320]. ClfA acts as a key virulence factor of *S. aureus* involved in the early stages of infection allowing dissemination throughout the host[79] through binding fibrinogen[321] allowing *S. aureus* to aggregate[322] and adhere to immobilised fibrinogen such as blood clots. ClfA also binds to complement factor I inducing greater cleavage of C3b into the inactive iC3b thereby protecting *S. aureus* from complement mediated opsonisation and increase phagosomal clearence[323,324] .

Although there is a current move towards multi-component vaccines including numerous antigens[325], ClfA was shown to be protective in preclinical models of infection as early as 2001[82]. Furthermore, in preclinical evaluations ClfA induced production of functional antibodies[326] and antibodies against ClfA have been shown to reduce severity of *S. aureus* endocarditis in the rabbit model of infection[327]. Vaccination with ClfA has been shown to protect against *S. aureus* sepsis[328] and septic arthritis[82] in the mouse model of infection and against endocarditis in the rat model of infection[329]. ClfA has also been included in some very high-profile clinical trials of *S. aureus* vaccines made by Pfizer and GSK[164,330,331] (Clinical trial numbers: NCT01018641, NCT01160172 and NCT02388165). None of these trials have resulted in a successful vaccine but the inclusion of ClfA in clinical trials alone indicates it was successful in preclinical trials of anti-*S. aureus* vaccination.

A vaccine which has been shown to be protective against intravenous infection included ClfA and CpG[190], which is a DNA-based adjuvant known to ligate TLR9 and direct the immune response towards a Th1 response[332]. ClfA in the presence of Alum has been shown to be protective against intravenous infection with *S. aureus* in mice[328]. Therefore, the vaccine composition and vaccination schedule were based on these publications. The vaccine dose used here contained 1µg ClfA, 50µg CpG and 1%(w/v) Alum (Alhydrogel®).

Recombinant 6xHis tagged ClfA (residues 40-559) was produced using XL1 blue *E. coli*, this is the same protein antigen used in many ClfA experimental vaccines[190,326,328]. The protein was purified from cell lysates via nickel affinity chromatography, size exclusion chromatography and then tested for and purified from endotoxin (section 2.24.7). To ensure the recombinant protein was exactly the antigen it was thought to be before it was injected into the mice, this recombinant protein was also verified as ClfA (40-559) by mass spectrometry (2.24.8) (Supplementary Figure 6). The addition of Alum was because ClfA in the presence of Alum protected mice against intravenous infection with the Newman[328] strain of *S. aureus* which is very closely related to the NewHG strain used for challenge here therefore there was definite precedent. Alhydrogel® was chosen over Adju-phos® as Alhydrogel® has a net positive charge at pH 5-7, therefore at physiological pH Alhydrogel® would bind our ClfA better as the recombinant ClfA used here had a calculated isoelectric point of 4.37 (ExPASy).

4.3.4.2 A vaccine consisting of ClfA, CpG and Alum is safe

Mice were subcutaneously injected with the vaccine or etox PBS on day 0, 14 and 21. On day 28 post-vaccination mice were intravenously infected with $1x10^6$ CFU *S. aureus*, $1x10^7$ CFU *S. aureus* or $1x10^6$ CFU *S. aureus* with 250µg *M. luteus* peptidoglycan. Mice were culled at day 3 post-infection (day 31 post-vaccination) and organs were harvested for CFU enumeration. Blood samples were also taken

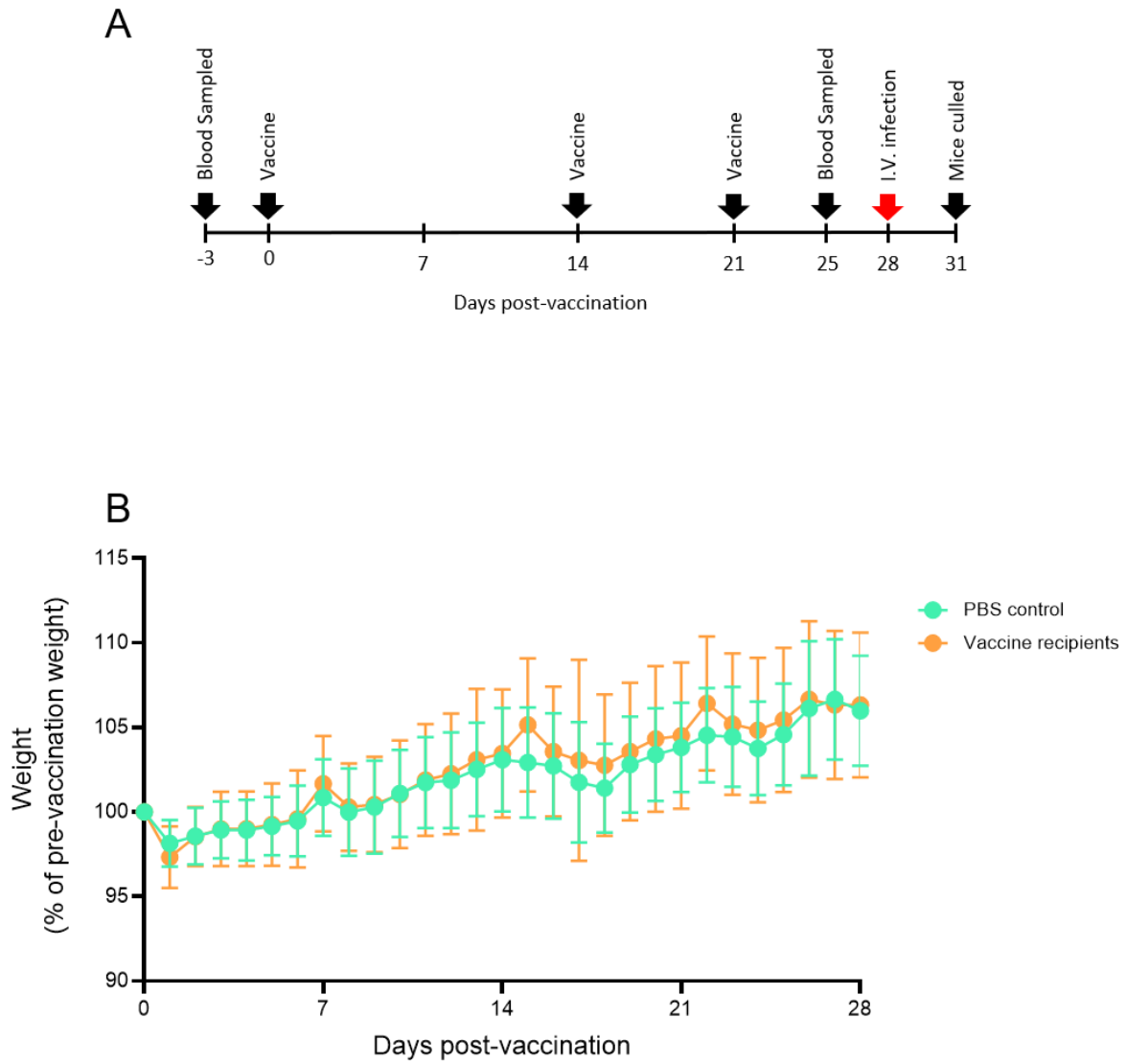

Figure 4.9 Schedule and effect of A vaccine consisting of ClfA, CpG and Alum.
Mice were vaccinated subcutaneously with 1µg ClfA, 50µg CpG and 1%(w/v) Alum or sterile, etox PBS on day 0, 14 and 21 with blood taken via tail venesection 3 days prior to vaccination and 3 days prior to infection as shown by the timeline diagram (A). Mice receiving vaccine (orange) and PBS control (green) had no significant difference in weight and no significant weight loss as a result of vaccination (B). Weights are shown as mean and Std Dev. ($p>0.05$).

A

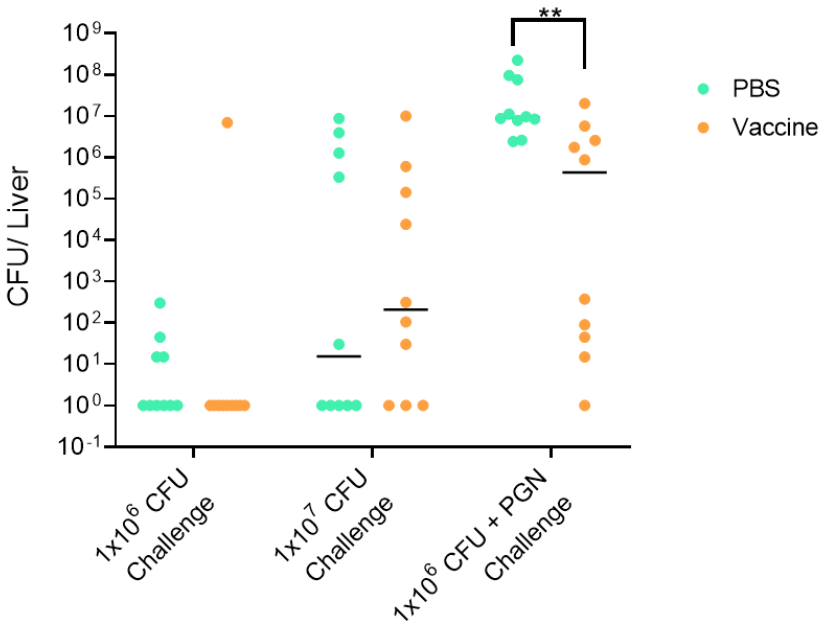
**
CFU/ Liver
10^9
10^8
10^7
10^6
10^5
10^4
10^3
10^2
10^1
10^0
10^{-1}
PBS
Vaccine
$1x10^6$ CFU Challenge
$1x10^7$ CFU Challenge
$1x10^6$ CFU + PGN Challenge

B

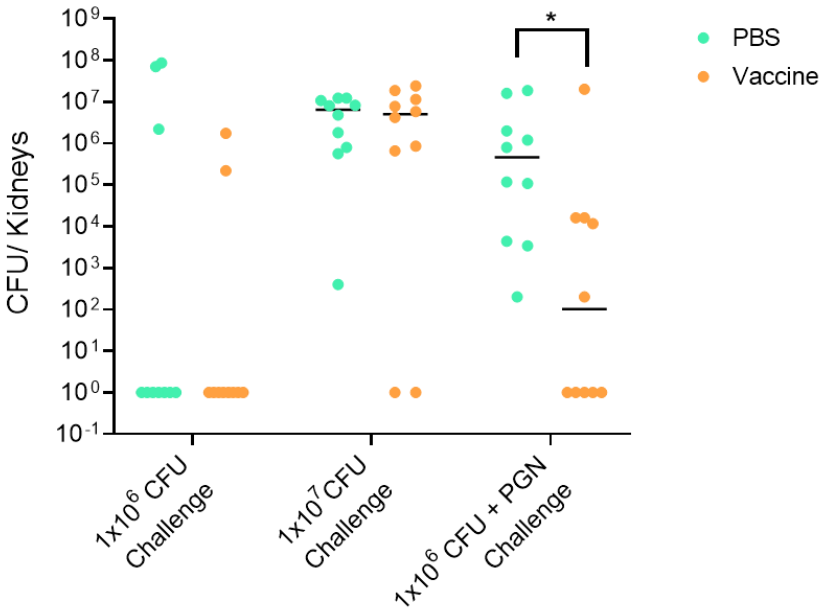
*
CFU/ Kidneys
10^9
10^8
10^7
10^6
10^5
10^4
10^3
10^2
10^1
10^0
10^{-1}
PBS
Vaccine
$1x10^6$ CFU Challenge
$1x10^7$ CFU Challenge
$1x10^6$ CFU + PGN Challenge

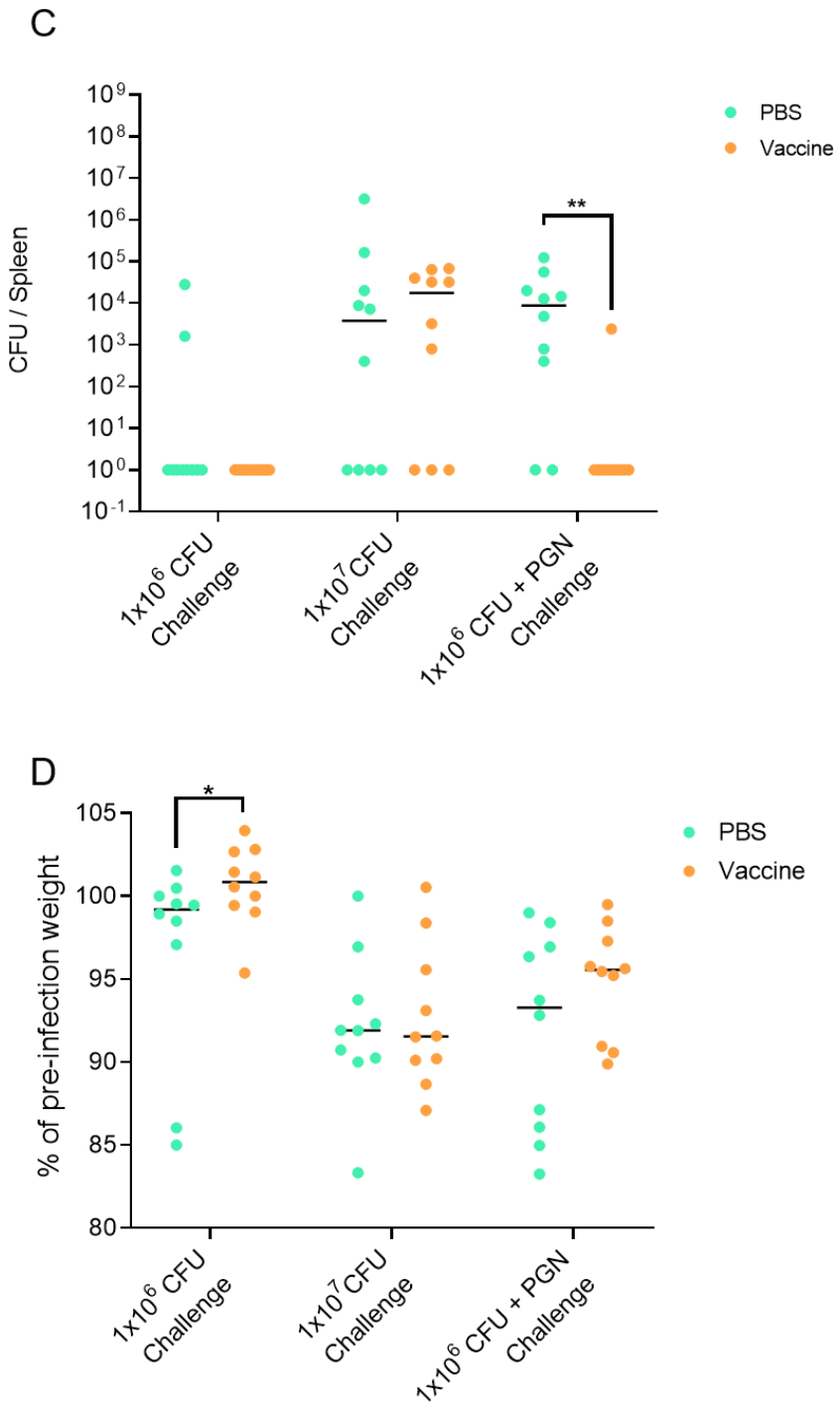

Figure 4.10 Vaccine efficacy in the murine sepsis model of *S. aureus* infection

Mice were vaccinated subcutaneously on day 0, 14 and 21 with a vaccine consisting of 1µg ClfA, 50µg CpG and 1%(w/v) Alum (orange) or subcutaneously injected with sterile, endotoxin free PBS as a negative control (green). On day 28 post-vaccination mice were intravenously injected with low dose *S. aureus* ($1x10^6$ CFU), high dose *S. aureus* ($1x10^7$ CFU) or a mixture of low dose *S. aureus* and 250µg *M. luteus* peptidoglycan. Mice were weighed daily and on day 3 post-infection mice were sacrificed and livers (A), kidneys (B) and spleens (C) were harvested for CFU enumeration. CFU and final day weight averages (D) shown as median. A: Liver CFU (** p=0.0015), B: Kidney CFU (* p=0.0187), C: Spleen CFU (** p=0.0019) D: Percentage of initial weight on day 3 post-infection (* p=0.0455).

through venesection of the tail vein 3 days before vaccination and 3 days before infection. The vaccination and challenge schedule is depicted in Figure 4.9A. Mice were weighed daily and checked for adverse reactions throughout the course of vaccination and the weight change is shown in Figure 4.9B. There was no significant difference between the weights of vaccine recipients and PBS control mice and the vast majority of mice gained weight throughout the course of vaccination thereby indicating that the vaccine itself is safe.

4.3.4.3 Efficacy of the ClfA, CpG & Alum Vaccine.

The CFU recovered and post-infection weight loss from the vaccination experiment are shown in Figure 4.10. The vaccine had no significant protective effect against high dose ($1x10^7$ CFU) challenge as measured by CFU or weight loss. The vaccine provided significant protection against weight loss in the low dose ($1x10^6$ CFU) challenge group (Fig 4.10C) but not for CFU in any organ. At this infectious dose the weight loss and CFU recovered are low which makes evaluating protective efficacy difficult, but it is clear the vaccine does not worsen infectious outcomes from this. The vaccine protected against challenge with the augmented infection ($1x10^6$ CFU & 250µg *M. luteus* peptidoglycan), with significantly fewer CFU were recovered from the livers, kidneys and spleens of vaccine recipients compared to PBS recipients.

4.3.4.4 Effect of vaccination on cytokine production before infection

Blood was taken from the mice, via tail venesection, 3 days before vaccination and 3 days before infection. The blood was centrifuged at 14000 x g to separate the haematocrit and serum. The serum was then sent to the Flow cytometry unit (Core services, University of Sheffield) analysed for cytokines with BD™ cytometric bead analysis Flex sets using a FACSArray Bioanalyzer (BD BioSciences, USA). Serum was measured for IFN-γ, IL-1β, IL-4, IL-6, IL-12p70, IL-17A, TNF-α, CXCL1, CCL2 and CCL4.

Over the four weeks of treatment all mice demonstrated a small but significant increase in all cytokines regardless of whether they received vaccine or PBS placebo (Fig 4.11). There was no significant difference between the cytokine levels between the two treatment groups.

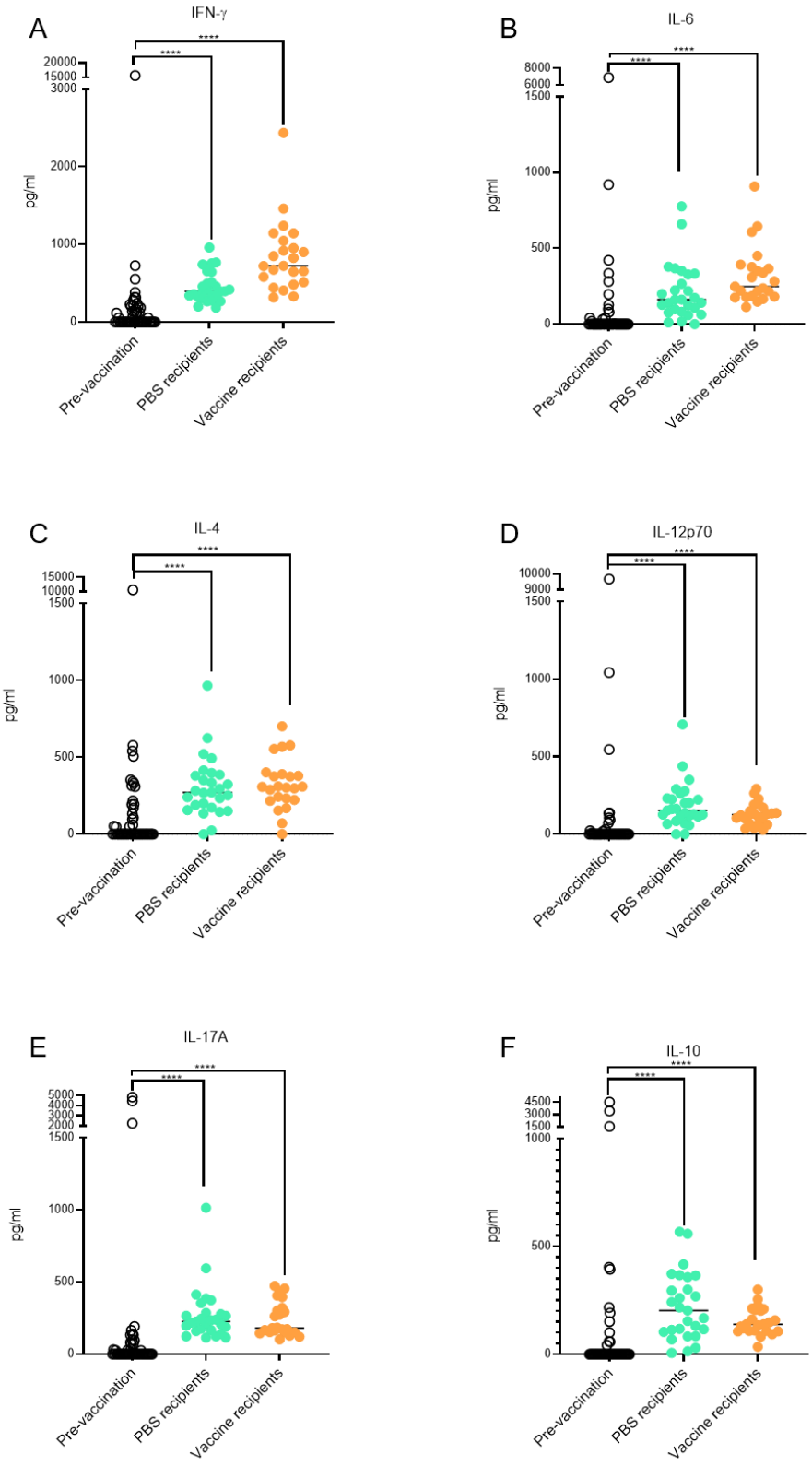
A
IFN-γ
pg/ml
20000
15000
3000
2000
1000
0
****
****
Pre-vaccination
PBS recipients
Vaccine recipients
B
IL-6
pg/ml
8000
6000
1500
1000
500
0
****
****
Pre-vaccination
PBS recipients
Vaccine recipients
C
IL-4
pg/ml
15000
10000
1500
1000
500
0
****
****
Pre-vaccination
PBS recipients
Vaccine recipients
D
IL-12p70
pg/ml
10000
9000
1500
1000
500
0
****
****
Pre-vaccination
PBS recipients
Vaccine recipients
E
IL-17A
pg/ml
5000
4000
3000
2000
1500
1000
500
0
****
****
Pre-vaccination
PBS recipients
Vaccine recipients
F
IL-10
pg/ml
4500
3000
1500
1000
500
0
****
****
Pre-vaccination
PBS recipients
Vaccine recipients

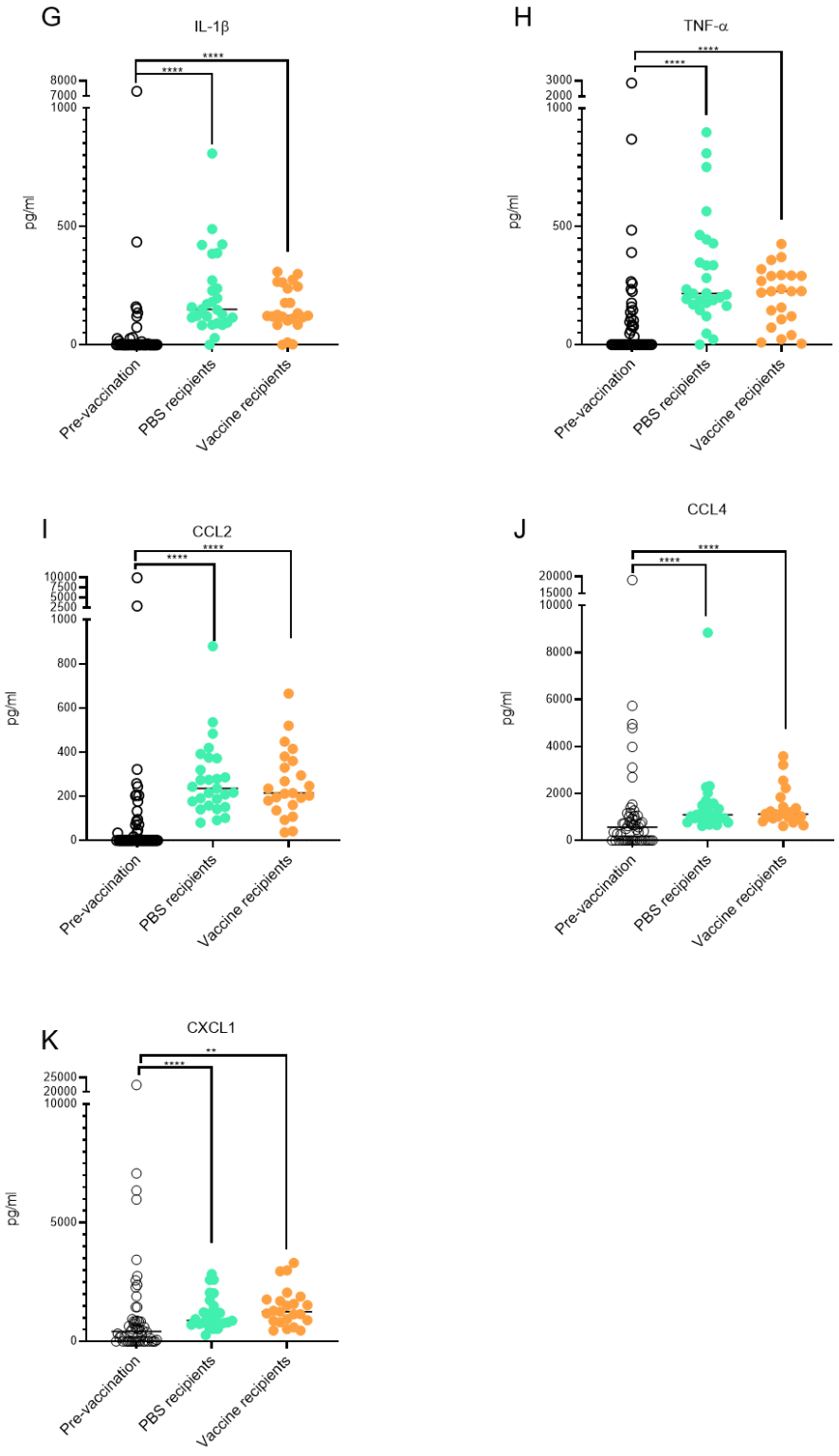

Figure 4.11 Cytokine measurements from mouse serum before and after vaccination or PBS placebo injections.
Mice (n=30) were subcutaneously injected with vaccine (orange) or etox PBS (green) at Day 0, 14 and 21 before intravenous infection at day 28. Blood sampling via the tail vein was carried out 3 days prior to vaccination (clear circles) and again 3 days prior to infection. Serum was measured for cytokines (A-K): IFN-γ, IL-6, IL-4, IL-12-p70, IL-17A, IL-10, IL-1β, TNF-α, CCL2, CCL4 and CXCL1. Average bars indicate the median value. **** p<0.0001.

4.3.4.5 Peptidoglycan as an adjuvant

M. luteus peptidoglycan is a key component that can augment *S. aureus* infection therefore it was tested as an adjuvant. Immunisation with peptidoglycan[313] and peptide mimics of peptidoglycan[315] have been shown to protect against *S. aureus* infection yet immunisation with whole bacterial cells have been shown not to protect against invasive *S. aureus* disease[333]. Furthermore, addition of the Sigma Adjuvant System, which contains bacterial cell wall components, provided better protection in mice against *S. aureus* when included in an Alum adsorbed ClfA vaccine compared to vaccination with Alum adsorbed ClfA alone[328].

As peptidoglycan with the vaccine constituted a new formulation this was first checked with a dosing study. A vaccine consisting of 1µg ClfA, 50µg CpG and 1%(w/v) Alum was given subcutaneously to mice alone or in conjunction with 100µg of 250µg of *M. luteus* peptidoglycan. Mice were monitored for adverse reactions and weight loss for 3 days. Some weight loss was seen in response to the vaccine with 250µg of peptidoglycan (Supplementary Figure 7). As a result, the concentration of peptidoglycan added to each dose of vaccine was set to 100µg.

On days 0, 14 and 21, 20 mice were subcutaneously injected with vaccine, 20 mice were subcutaneously injected with vaccine and peptidoglycan and 20 mice were injected with PBS. On day 28, half of each immunisation group (n=10) were intravenously infected with $5x10^6$ CFU of *S. aureus* (NewHG) and the other half (n=10) were intravenously infected with $5x10^5$ CFU of *S. aureus* (NewHG) and 250µg of *M. luteus* peptidoglycan. This was half the desired inoculum due to error, but it was sufficient to cause disease. On day 3 post-infection (day 31 post-vaccination) mice were culled, and organs harvested for CFU enumeration. Blood samples were taken by tail venesection 3 days before vaccination (day -3) and again on day 2 post-infection (day 30 post-vaccination). A timeline of this experimental design is shown in Figure 4.12A.

There was no significant weight loss in any group due to immunisation with all groups having a greater average weight than their starting weight by day 28 post-vaccination (Fig 4.12B). This shows that the vaccine with peptidoglycan included is largely well tolerated.

A

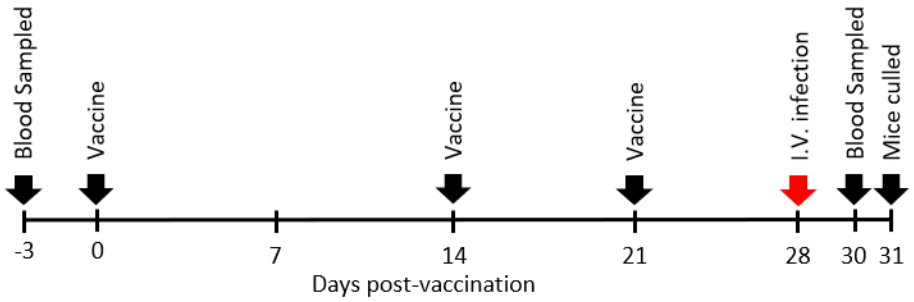

B

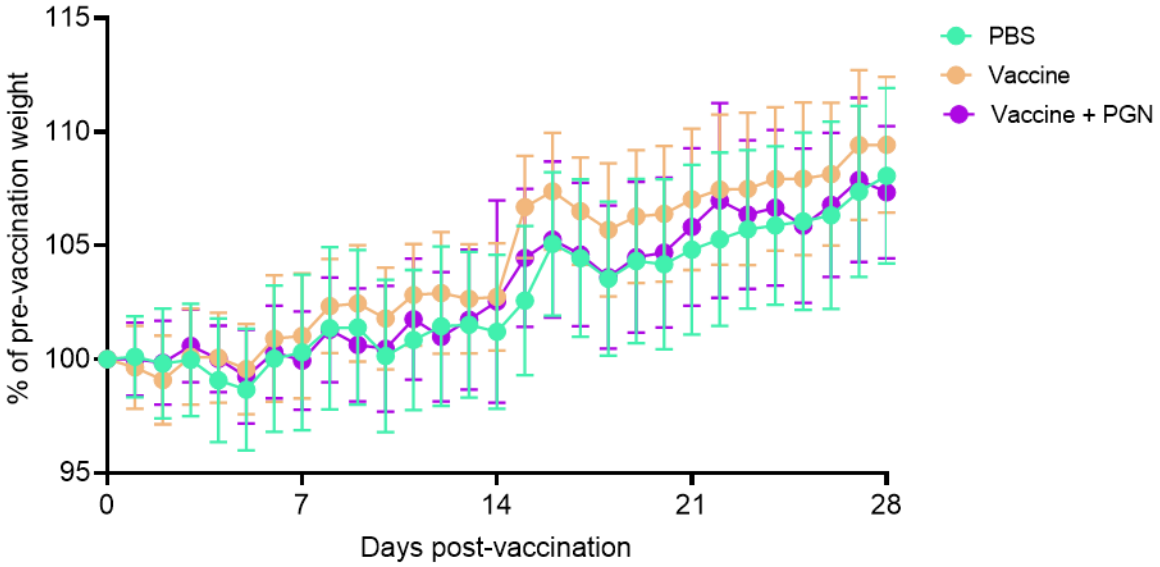

Figure 4.12 Schedule and effect of addition of peptidoglycan to the vaccine formulation

Mice were vaccinated subcutaneously with 1µg ClfA, 50µg CpG and 1%(w/v) Alum with or without 100µg *M. luteus* peptidoglycan or with sterile, etox PBS as a mock vaccine on day 0, 14 and 21 with blood taken via tail venesection 3 days prior to vaccination and on day 2 post-infection as shown on the timeline diagram (A). Mice receiving vaccine (orange), vaccine with peptidoglycan (purple) and mice receiving PBS control (green) had no significant difference in weight and no significant weight loss as a result of vaccination (B). Weight displayed at mean and Std Dev.

4.3.4.6 Effect of peptidoglycan on vaccine efficacy

Overall symptomatic disease was measured by weight loss after challenge (Fig 4.13D). Here the PBS recipients lost approximately 10% of their pre-infection weight in response to either high dose *S. aureus* only challenge ($5x10^6$ CFU) or augmented infection ($5x10^5$ CFU + 250µg *M. luteus* peptidoglycan). The vaccine adjuvanted with peptidoglycan significantly protected against weight loss induced by the high dose *S. aureus* (p=0.0031) whereas vaccine with or without the peptidoglycan adjuvant was significantly protective against augmented challenge (p=0.0267 & 0.0034 respectively).

This protection was supported in part by the CFU enumeration in the organs. In the liver the vaccine without peptidoglycan gave significant protection against the augmented challenge (p=0.0003). No significant protection was observed in the kidneys. Conversely, in the spleen the vaccine with peptidoglycan protected against the high dose challenge (p=0.0274) and the vaccine alone protected in the augmented infection model (p=0.0018).

A

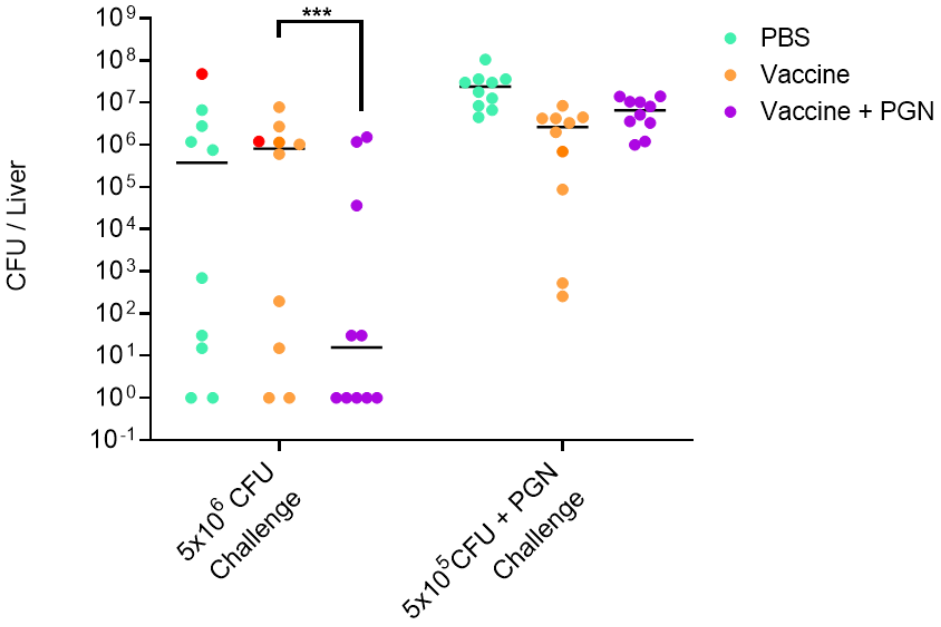
***
CFU / Liver
10^9
10^8
10^7
10^6
10^5
10^4
10^3
10^2
10^1
10^0
10^{-1}
PBS
Vaccine
Vaccine + PGN
$5x10^6$ CFU Challenge
$5x10^5$CFU + PGN Challenge

B

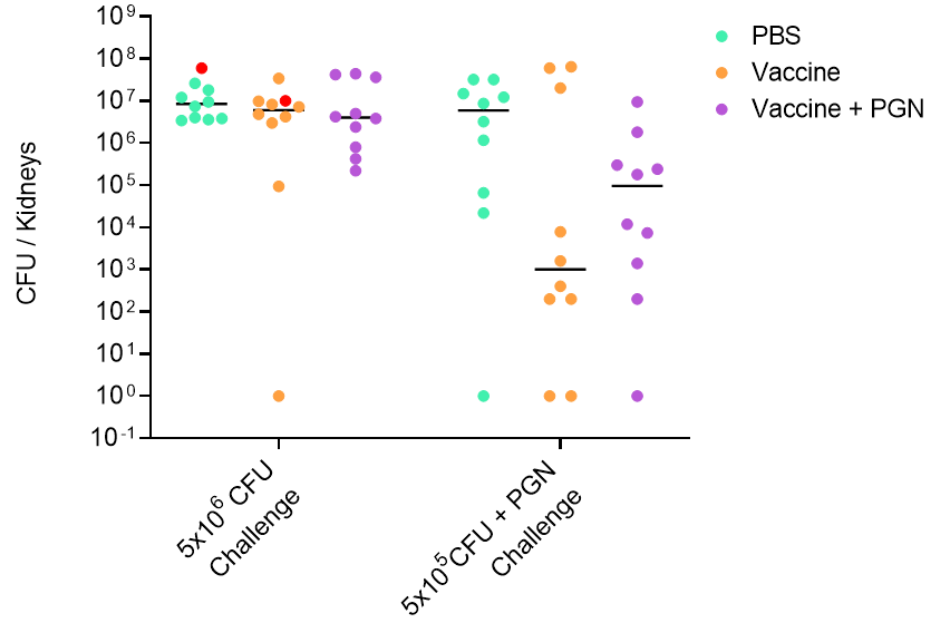
CFU / Kidneys
10^9
10^8
10^7
10^6
10^5
10^4
10^3
10^2
10^1
10^0
10^{-1}
PBS
Vaccine
Vaccine + PGN
$5x10^6$ CFU Challenge
$5x10^5$CFU + PGN Challenge

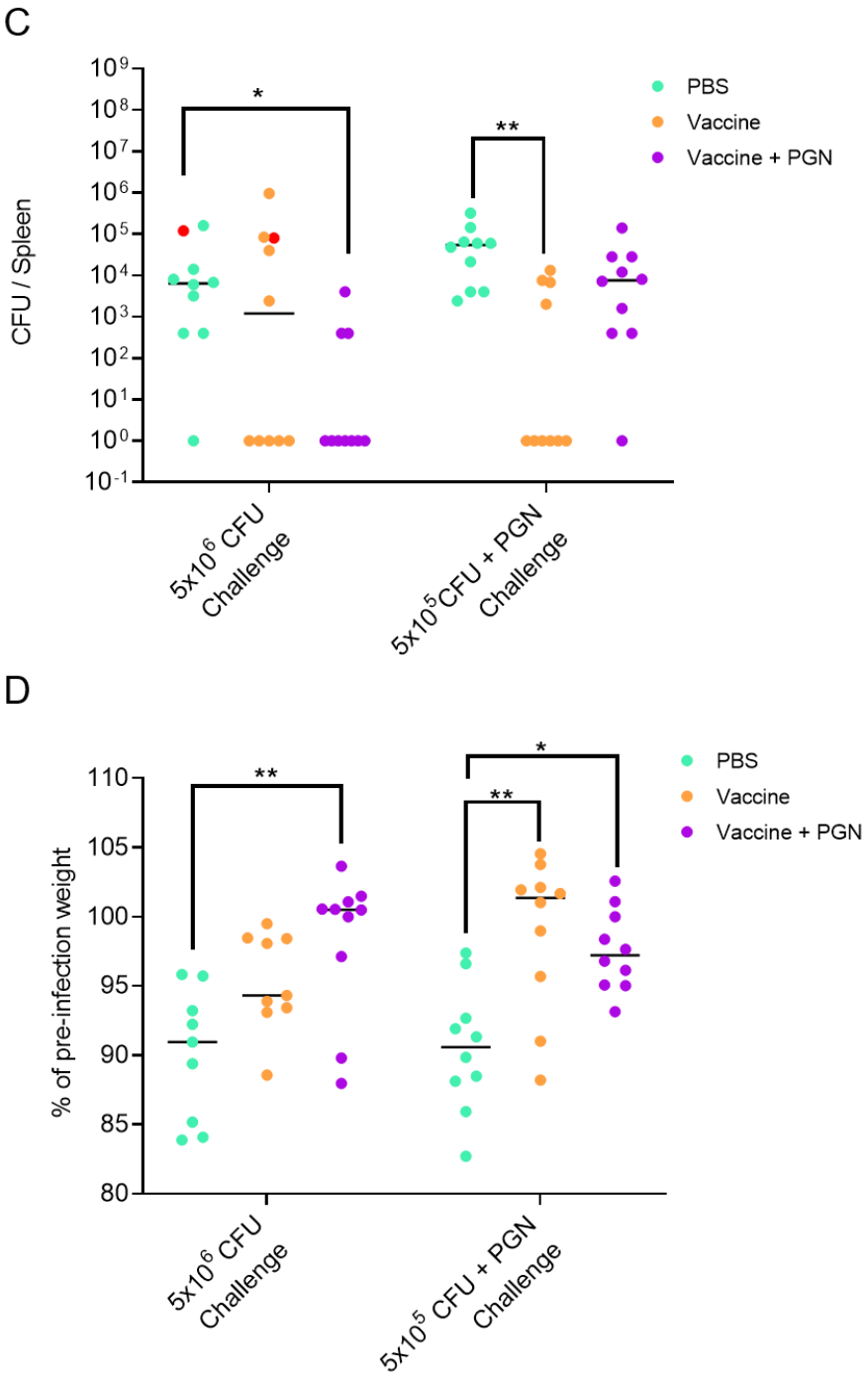

Figure 4.13. Effect of peptidoglycan addition on vaccine efficacy in the mouse sepsis model. Mice were vaccinated subcutaneously on day 0, 14 and 21 with sterile endotoxin free PBS as a negative control (green), a vaccine consisting of 1µg ClfA, 50µg CpG and 1%(w/v) Alum (orange) or the same vaccine with an additional 100µg of *M. luteus* peptidoglycan (purple). On day 28 post-vaccination mice were intravenously injected with *S. aureus* alone ($5x10^6$ CFU) or a mixture of low dose *S. aureus* ($5x10^5$ CFU) and 250µg *M. luteus* peptidoglycan. Mice were weighed daily and on day 3 post-infection mice were sacrificed and livers (A), kidneys (B) and spleens (C) were harvested for CFU enumeration. CFU and weight on the final day averages are displayed as medians. A: Liver CFUs (*** $p<0.005$), C: Spleen CFU * $p<0.05$, ** $p<0.01$), D: Percentage of initial weight on final day of infection (* $p<0.05$, ** $p<0.01$). Red data points denote mice which were culled early and subsequently excluded from statistical analysis due to reaching humane endpoints.

4.3.4.7 Effects of vaccination with and without peptidoglycan adjuvant on cytokine production post-infection

Blood was taken from the mice, via tail venesection, 3 days before vaccination and 2 days after infection. The blood was centrifuged at 14000 x g to separate the haematocrit and serum. The serum was then sent to the Flow cytometry unit (Core services, University of Sheffield) analysed for cytokines with BD™ cytometric bead analysis Flex sets using a FACSArray Bioanalyzer (BD BioSciences, USA). Serum was measured for IFN-γ, IL-1β, IL-4, IL-6, IL-12p70, IL-17A, TNF-α, CXCL1, CCL2 and CCL4 (Fig 4.14).

No significant change was seen in IL-10 production in any group. CXCL1 was significantly upregulated in those groups challenged with $5x10^6$ CFU of *S. aureus* and in the vaccine recipients challenged with the augmented dose of $5x10^5$ CFU and 250μg of peptidoglycan. CCL2 and TNF-α were also significantly increased in recipients of the vaccine with PGN that were also challenged with the augmented dose. IFN-γ was significantly increased from pre-vaccination baseline in all groups challenged the augmented infection, including placebo recipients, thereby implicating this immunological response in augmentation.

Administration of peptidoglycan at any point be that in vaccination, challenge inoculum or both had polarising effects on the levels of certain cytokines. Any group receiving peptidoglycan has significantly increased IL-17A, IL-1β, IL-4 and CCL4 whereas those mice which never received peptidoglycan showed no significant increase in these cytokines. Peptidoglycan administration also significantly downregulated IL-6 and IL-12p70 compared to mice that did not receive peptidoglycan. This indicates that administration of peptidoglycan at any point before or during infection establishes an immunological milieu that would predispose to a Th2 and Th17 response and precludes Th1 polarisation. The chemokine data would also suggest that peptidoglycan administration predisposes to greater macrophage recruitment. There was no significant difference between PBS and vaccine recipients within challenge groups thus there is no indication as to the mechanism of protection induced by the vaccine.

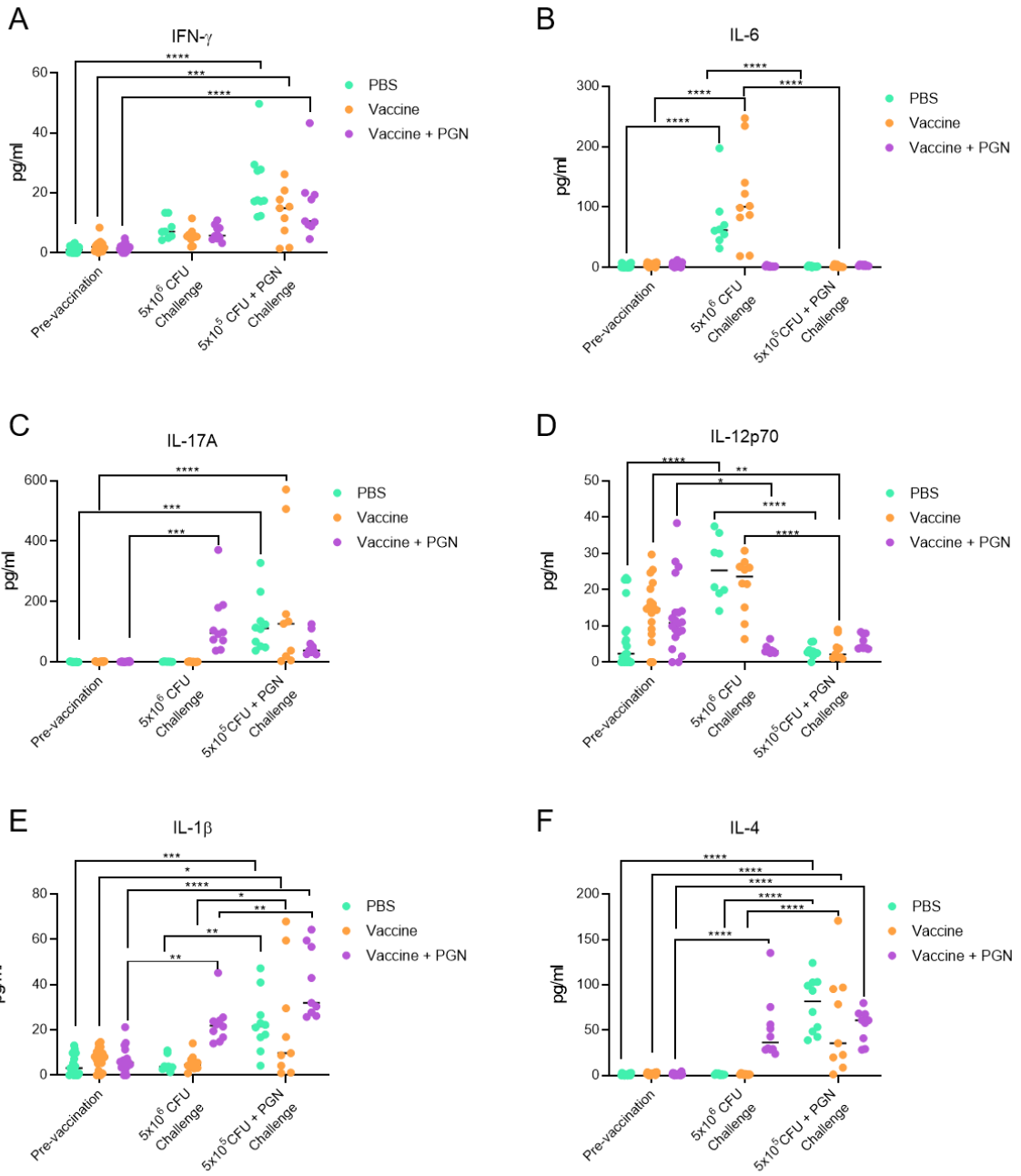
A
IFN-γ
pg/ml
PBS
Vaccine
Vaccine + PGN
Pre-vaccination
5x10^6 CFU Challenge
5x10^5 CFU + PGN Challenge
B
IL-6
C
IL-17A
D
IL-12p70
E
IL-1β
F
IL-4

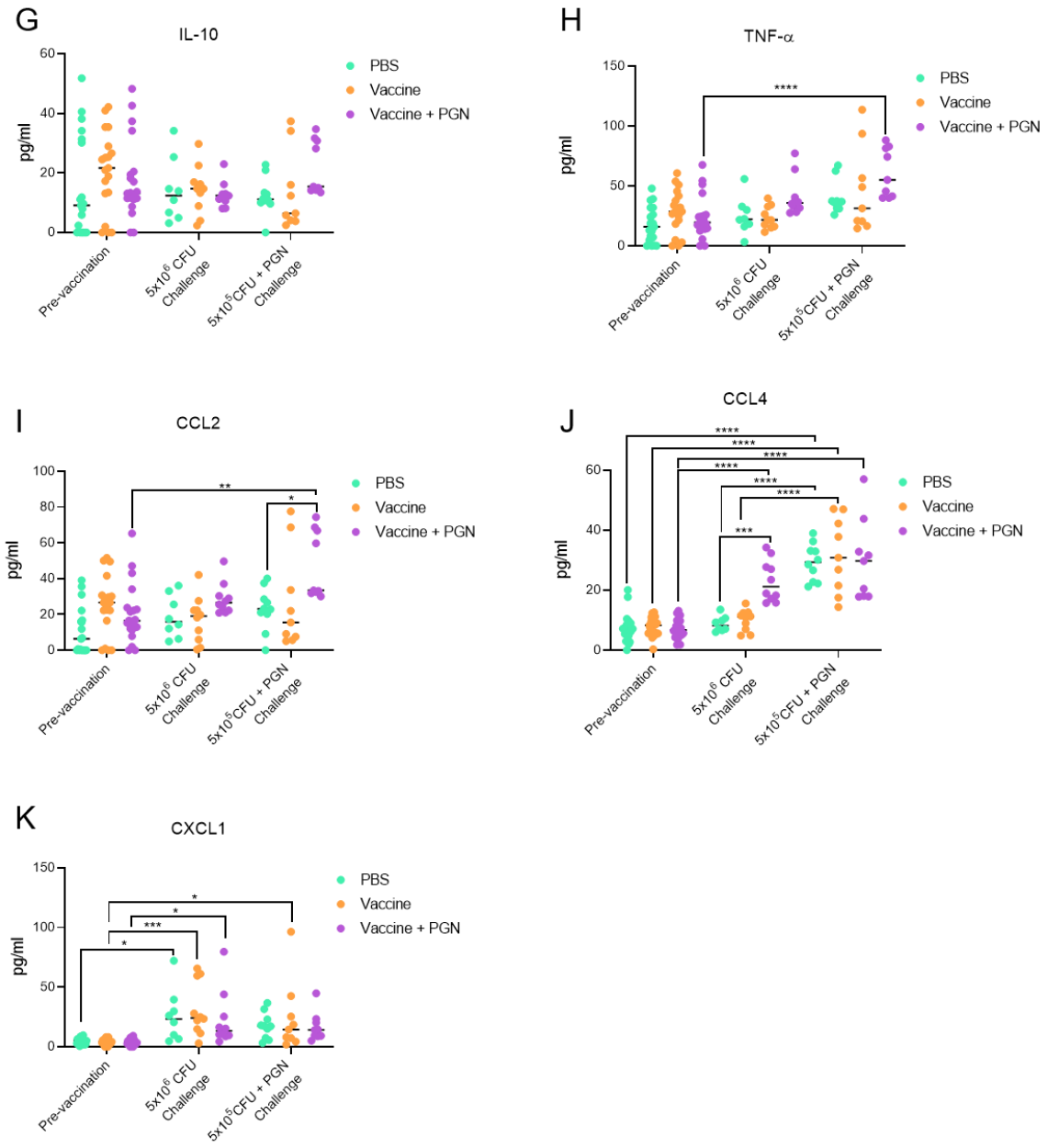

Figure 4.14: Cytokine measurements from mouse serum before vaccination and after vaccination and infection

Mice (n=20) were subcutaneously injected with vaccine (orange), vaccine with 100µg of *M. luteus* peptidoglycan (purple) or etox PBS (green) as a placebo control on day 0, 14 and 21 before intravenous infection with $5x10^6$ CFU *S. aureus* or $5x10^5$ CFU *S. aureus* and 250µg of *M. luteus* peptidoglycan at day 28. Blood sampling via the tail vein was carried out 3 days prior to vaccination and again 2 days post-infection. Serum was measured for cytokines (A-K): IFN-γ, IL-6, IL-17A, IL-12-p70, IL-1β, IL-4, IL-10, TNF-α, CXCL1, CCL2 and CCL4. Average bars indicate the median value. * p<0.05, ** p<0.01, *** p<0.005, **** p<0.0001.

4.4 Discussion

Our current understanding of *S. aureus* pathogenesis is complicated by the numerous infectious niches that it inhabits. This chapter has utilised the intravenous model of infection which mimics *S. aureus* bloodstream infections and sepsis. Our understanding of infection dynamics in this setting come from studies which outline how circulating *S. aureus* is first phagocytosed by the Kupffer cells of the liver[29,222]. Few *S. aureus* survive this initial immunological bottleneck (a seemingly stochastic process)[29,236] but those which do, seed clonal infections and abscesses around the body with infections tending to predominate in the kidneys[29,31,236].

Further work has shown that addition of commensal bacteria or their cell wall products can augment *S. aureus* infection leading to a smaller dose being required to establish infection in the mouse model of infection. In this model the infection is far more reliable and reproducible with the majority of mice becoming profoundly septic with infection predominating in the liver[222]. The work presented in this chapter tested how this new understanding could be applied to further elucidate infection dynamics and be used in vaccine development.

4.4.1 Mechanism of augmentation

4.4.1.1 Same place same time

As mice were not more susceptible to *S. aureus* infection alone when they received intravenous inocula of peptidoglycan before or after bacterial infection, it seems that the infectious and pro-infectious inocula (such as peptidoglycan) need to be co-administered. The lack of augmentation in the high dose challenged mice (Fig 4.8) leaves no concern that *S. aureus* may have been cleared before peptidoglycan was able to augment infection. The requirement for concomitant inoculation for augmentation suggests that *S. aureus* and pro-infectious agents are spatially linked in the host. The lack of augmentation when inocula were temporally separated and the fact it has been shown that intravenously injected peptidoglycan colocalises with intravenously injected *S. aureus* within the Kupffer cells[222] implies these stimuli need to be at the same place at the same time. The hypothesis follows that augmentation occurs within the phagocyte at the initial stage of infection.

4.4.1.2 Greater immune recruitment

If the pro-infectious effect is exerted in the phagosome then it stands to reason that greater uptake into phagosomes would benefit *S. aureus*. Therefore, activating the immune system especially phagocytes might be of benefit to *S. aureus*. Particulate peptidoglycan has been reported to increase the production of CXCL1 and CCL2[317] (the chemokines for neutrophils and monocytes). This agrees to an extent with cytokine data from mouse sera presented here which shows a significant increase in CCL4 in all mice challenged with augmented infection and lesser but still significant increases in CXCL1 and CCL2 in some groups receiving peptidoglycan (Fig 4.14). Therefore, it could be that peptidoglycan is causing greater recruitment of these immune cells which *S. aureus* can utilise as an intracellular niche in which to survive and disseminate.

4.4.1.3 Augmentation increases *S. aureus* survival within and escape from phagolysosomes

The flow cytometry and accompanying *in vivo* data showed that peptidoglycan which had not been freeze-dried, with a smaller particle size and was better at augmenting infection. This means that per µg of peptidoglycan administered there were more particles thereby allowing the augmentative effect to be present in more places/phagocytes at the same time. This would allow more *S. aureus* cells to pass through this initial immunological bottleneck. Furthermore, smaller particles of peptidoglycan may be phagocytosed more easily, this could easily be ascertained through labelling peptidoglycan and doing an *in vitro* macrophage uptake assay.

The flow cytometry also revealed that the peptidoglycan that was better at augmenting infection was more granular. This could be as the material was more particulate therefore more able to activate particulate-responsive NLRP3 inflammatory processes. Reports have indicated that one mechanism of inflammasome activation by particulates is induced due to physical lysosomal damage/perturbation[334]. If this were the case with peptidoglycan the augmented *S. aureus* dose and co-ingestion by macrophages would result in a greater number of *S. aureus* escaping phagosomal digestion. Evidence does suggest the particulate nature of peptidoglycan is required for it to properly activate the immune response[317] thereby lending credence to this argument. It has been shown that augmentation

happens in *nlrp3*$^{-/-}$ mice[222], indicating this inflammasome is unnecessary for augmentation to occur. However, the activation of the NLRP3 response wouldn't strictly be necessary for particulates such as peptidoglycan to aid intra-phagocyte survival of *S. aureus* by physically perturbing the phagosome and allowing for greater escape into the cytosol as suggested here.

In addition, intravital microscopy of the Kupffer cells during infection of mice with *S. aureus* with or without peptidoglycan showed a significant decrease in Kupffer cell ROS production[222] when peptidoglycan was present. It could be that peptidoglycan is soaking up ROS thereby protecting *S. aureus*. However, this data would also fit with the aforementioned, particulate-induced phagosome damage, as a leaky phagosome would be unable to concentrate ROS[335] sufficiently to kill *S. aureus* or induce measurable changes in fluorescent dyes.

4.4.1.4 Protecting *S. aureus* from immune-mediated damage via pro-infectious agents

Peptidoglycan could simply act to mop up antimicrobial defences which recognise bacteria via peptidoglycan. Given the 3-day timescale in our augmented infection experiments it would likely need to be an innate immune mechanism. An example of such a mechanism involves the mammalian peptidoglycan binding proteins which have been shown to induce cell death in *B. subtilis* through binding their peptidoglycan and activating the CssR-CssS two-component system. This system is involved in management of misfolded protein stress and activation by peptidoglycan binding proteins leads to membrane depolarisation, inactivation of synthesis pathways and upregulation of bacterial ROS which all ultimately lead to bacterial death[70]. If addition of peptidoglycan protects bacteria against host-defences mechanisms such as these it would be clear to see why it augments infection. This explanation becomes even more plausible given that the mammalian peptidoglycan recognition protein 2 has amidase activity[68] and is primarily expressed in the liver[69]. This matches that the epicentre of infection/tropism of infection in augmented infection shifts from the kidneys to the liver compared to *S. aureus* alone challenge. Knock out mice in these peptidoglycan binding proteins exist and show no increased susceptibility to challenge with *S. aureus* alone compared to wildtype mice[336]. However, augmented infection has not been tested in this host background.

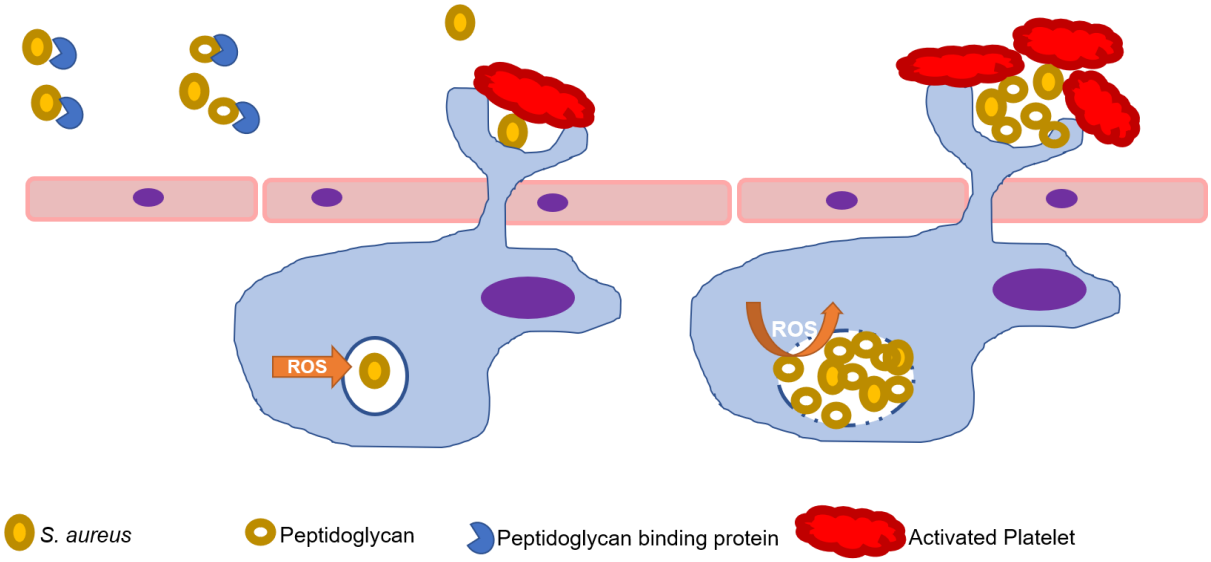

Figure 4.15. Conceptual diagram of how peptidoglycan could augment *S. aureus* infection within the liver sinusoid.
The addition of peptidoglycan (empty circles) to an inoculum could protect *S. aureus* (yellow filled circles) from degradation by host peptidoglycan binding proteins (blue). Peptidoglycan could also increase clotting factors and thereby increasing platelet (Red) activation and aggregation which would increase the amount of peptidoglycan and *S. aureus* engulfed by liver resident Kupffer cells (light blue with purple nucleus). Particulates such as insoluble peptidoglycan might physically disrupt the phagolysosome causing an inability to properly concentrate ROS in the phagolysosome and allowing greater numbers of *S. aureus* escape into the cytoplasm.

4.4.1.5 Peptidoglycan may act as a clotting agent

S. aureus peptidoglycan has been shown previously to induce pro-coagulation behaviour in monocytes in a concentration dependent and Tissue factor dependent fashion[337]. Tissue factor is a protein that starts the coagulation cascade and can be expressed by endothelia and monocytes. Furthermore, insoluble *S. aureus* peptidoglycan has been shown to induce pro-coagulation activity in whole blood to a greater extent than purified LTA[338]. This pro-coagulation activity takes place in a time-frame of seconds. In addition, platelet-dependent clots in MRSA bloodstream infections have been shown to aggregate in liver sinusoids and colocalise *S. aureus*-containing thrombi with Kupffer cells[339].

Given *S. aureus* is known to actively induce platelet aggregation and blood clotting through its alpha toxin[340] and bind to fibrin of clots through ClfA[321], blood clotting might benefit *S. aureus*. Peptidoglycan induce a greater amount of coagulation thereby allowing more *S. aureus* to survive in the bloodstream, resulting in a greater number passing to the liver and overwhelming the Kupffer cells. Addition of an anti-coagulant with the augmentation co-inoculation or infecting mice with mutations in their blood clotting cascade could test this.

4.4.1.6 Immune dysregulation

Although the cytokine data from the vaccine experiment with peptidoglycan showed a skewing towards Th17 polarising cytokines in mice receiving peptidoglycan, this is unlikely to be the mechanism for augmentation. Not only is the 3 day augmentation experiment a short time in which to mount a full adaptive response, the temporal experiments in which peptidoglycan was given before infection, which might be expected to affect the immune system similarly, did not augment infection.

However, IFN-γ was only significantly upregulated in those mice receiving the augmented infection, regardless of vaccination, implying that this cytokine may be involved in augmentation. IFN-γ has pleiotropic functions, acting on both the innate and adaptive immune system but based on the time-course of augmentation the focus should be on its innate effects. IFN-γ is produced in response to *S. aureus* antigens[341] and activates macrophages to a more pro-inflammatory state thereby being more able to phagocytose and kill bacteria. The importance of IFN-γ in sepsis is shown in IFN-γ receptor knockout mice which have much worse outcomes[342]. IFN-

γ is produced in the main by T cells and natural killer (NK) cells[343], therefore it might be interesting to look at NK cell knockout or knocked down mice as it is thought that overactivation of NK cells and excessive IFN-γ production may contribute to the cytokine storm of sepsis and predispose to poor outcomes of bacteraemia[344]. Interrogating natural killer cell involvement in augmentation is made even more prudent by the fact that the liver, the supposed site of augmentation, is enriched with natural killer cells with these making up to 50% of the hepatic lymphocyte population[345]. Therefore, it is entirely plausible that the excessive uptake of peptidoglycan by Kupffer cells leads to deleterious amounts of IFN-γ signalling from hepatic natural killer cells and this could contribute to the onset of severe sepsis.

Furthermore, the lack of IL-12 and the increased IL-4 indicates a greater Th2 type response compared to Th1 type response. This was the case even with PBS recipients indicating this is not response to vaccination. This response is interesting as an IFN-γ driven Th1 type response, which peptidoglycan seems to be precluding, has been shown to be protective against experimental *S. aureus* sepsis[190]. Furthermore, the low IFN-γ and high IL-4 of those mice receiving peptidoglycan is similar to immune milieu seen in atopic dermatitis patients who get recurrent *S. aureus* infections[346].

4.4.2 Vaccine testing

There is yet to be an *S. aureus* vaccine to successfully get through clinical trials. This is despite many pre-clinical trials in animal infection models showing protective effects such as those induced, in numerous models, by the ClfA antigen with various adjuvant combinations[190,328,329,347,348]. Therefore, there is either a disconnect between human disease and animal models or the animal models of infection are being improperly used/interpreted for informing decisions about clinical testing. Clinical trials for vaccines cost millions to billions of dollars[349], therefore, refining preclinical testing is a major drive within the pharmaceutical industry to reduce overall costs of clinical testing.

4.4.2.1 One organism, numerous pathologies

S. aureus can cause a variety of diseases, yet vaccines tend to treat *S. aureus* infections as a single entity. It has previously been shown that vaccines which protected against one route of infection such as intravenous infection may not be protective against another route such as skin infection[328,333]. A limitation of the work presented here is that only one route of infection was tested in terms of the efficacy of the vaccine-mediated protection. However, augmented infection is closer to the natural process due to the lower infectious inoculum used. Interestingly, the vaccine protected against the augmented infectious dose of live *S. aureus* and *M. luteus* peptidoglycan and was not significantly protective against challenge with *S. aureus* alone (Fig 4.10, 4.13). This emphasizes the importance of considering alternative infectious challenges when assessing vaccine-mediated protection during preclinical testing. Both the *S. aureus* alone challenge and the augmented challenge were intravenous challenges yet had different outcomes in terms of protection. Therefore, a separate type of protection seems to be necessary for each of these arguably similar intravenous challenges. Given *S. aureus* can cause such a wide variety of diseases in a range of niches[3], the difference in required protection should be unsurprising. Table 4.1 shows the range of disease caused by *S. aureus* compared to those diseases caused by other bacteria for which there are vaccines available.

The majority of these bacterial pathogens cause one or two types of disease or there is a clear virulence mechanism that can be targeted such as a toxin (e.g. tetanus, diphtheria). *S. aureus* causes a variety of diseases in different niches and has a varied armoury of immune evasion techniques[306]. Those organisms that do cause disease in more than one niche and have some commensal carriage such as *H. influenzae*, *S. pneumoniae* and *N. meningitidis* are preventable via immunisation with capsule derived vaccines[350]. However, capsule is not a protective silver bullet for *S. aureus* infections as it has been used in many potential *S. aureus* vaccines that have failed in clinical trials[163,331,351–353] and one vaccine with capsule led to worse outcomes[160].

A well-known, confounding factor in *S. aureus* vaccine development is that there are no defined correlates of protection for *S. aureus* from natural infection. However, this might suffer from the same issue as described above with different *S. aureus*

Bacterial pathogen	Vaccine(s)	Disease caused by bacteria	Commensal niche
S. aureus	N/a	Sepsis, bacteraemia, pneumonia, skin & soft tissue infection, endocarditis, meningitis, osteomyelitis, toxic shock syndrome, food poisoning[3,4,7]	Nares Skin
M. tuberculosis	BCG (attenuated mycobacterium inducing cross-protection)[354]	Tuberculosis (respiratory infection)	Latent respiratory infection/carriage[354,355]
V. cholerae	Oral, killed whole cell & toxin sub-unit[356]	Cholera (gastrointestinal infection)	N/a
B. pertussis	DTaP (Acellular pertussis antigen)[357]	Whooping cough (respiratory infection)[357]	Asymptomatic nasal carriage[358]
C. diptheriae	DTaP (toxin)[357]	Diptheria (upper respiratory infection) Cutaneous diptheria [357]	N/a
C. tetani	DTaP (toxin)[357]	Tetanus (neurotoxin induced disease)[357]	N/a
S. typhi	Ty21a (oral, attenuated) Vi polysaccharide (parenteral)[359]	Typhoid fever (systemic infection)	Asymptomatic gall bladder carriage possible[360]
N. meningitidis	Capsular vaccine or capsule polysaccharide conjugate vaccine[361]	Meningitis, sepsis[361]	Nares[361]
S. pneumoniae	Capsular polysaccharide or capsular conjugate[362]	Pneumonia, meningitis, sepsis, otitis media[362]	Nares [363]
H. influenzae	Capsular polysaccharide conjugate[364]	Pneumonia, epiglottitis, bacteraemia, meningitis[364]	Asymptomatic pharyngeal carriage[364]
B. anthracis	Anthrax vaccine Adsorbed (avirulent cell-free filtrate)[365]	Anthrax (cutaneous, respiratory, gastrointestinal)[365]	N/a

Table 4.1. Disease and commensal niche caused by *S. aureus* and bacteria for which there are commercially available vaccines

S. aureus causes a wider variety of diseases and has a large amount of commensal carriage compared to other bacteria for which successful vaccines have been developed. Of those that also cause numerous diseases and have some commensal carriage, vaccines based on capsular polysaccharides and their conjugates have proved protective which has not proven to be the case for *S. aureus*.

infections requiring different responses. For instance IL-10 has been shown to be beneficial in acute systemic *S. aureus* disease but detrimental in localised infections[193]. IL-9 and the Th9 response has been shown to be induced during *S. aureus* pneumonia in the mouse model[192] whereas IL-17 has been shown to be induced (and protective) in the murine *S. aureus* sepsis model[366,367] and surgical site infection[199]. Furthermore, IFN-γ and the Th1 response has been shown to be protective in mice during *S. aureus* intraperitoneal infection[190] but this immune response has also been suggested to be detrimental during intravenous infection[155].

Given all the differences discussed here regarding protection against different staphylococcal challenges it might be time to suggest that more than one type of vaccine may be necessary for an organism that can cause more than one type of infection. A vaccine wouldn't necessarily need to one-size fits all against all *S. aureus* infection in order to be useful. Protecting against any type of *S. aureus* infection would be beneficial in terms of saving lives and relieving economic costs of disease and burden on healthcare systems for instance protecting against *S. aureus* bacteraemia which can lead to up to 54% mortality[368,369].

4.4.2.2 Peptidoglycan as an adjuvant/vaccinogen

The function of an adjuvant is to improve immune activation by an antigen through increasing antigen persistence/presentation within the host or provide a disease context to an otherwise innocuous immunological stimulus thereby guiding the immune response. Freund's adjuvant contains mycobacterial cell wall and has been extensively demonstrated to be potently immunogenic but also toxic[370]. Therefore, there is rationale at looking at safer, more well-defined bacterial cell wall components and their potential in adjuvant or vaccinogen design. The cytokine data presented here indicate that peptidoglycan has a distinct immunomodulatory effect both when peptidoglycan is received before or when received in conjunction with the infectious stimulus (Fig 4.14). The data show that Th1 polarising cytokine IL-12p70 is downregulated and IL-4 and IL-17, which polarise a Th2 response and indicate a Th17 response respectively, were upregulated in relation to peptidoglycan administration. This data is corroborated in human immune cells by published evidence as it was recently shown that preincubation of cocultures of human dendritic cells and T cells with *S. aureus* peptidoglycan reduced the expression of IL-

12 in response to live *S. aureus* and increased Th17 polarisation[371]. Given this clear polarising ability, there is huge potential to further assess peptidoglycan as a novel form of adjuvant.

4.4.3 Limitations & Future work

The single route of infection used here gives preliminary data. Future work could assess vaccine efficacy against different routes of infection modelling different *S. aureus* pathologies. Whilst cytokines measured during the vaccine studies implied peptidoglycan induced a milleu which predisposed to a Th2/Th17 response there was no T cell phenotyping. This would be especially interesting in the augmentation experiments given the ability of NOD2 ligation by peptidoglycan to increase $CD8^+$ T cell polarisation[372]. Furthermore, measurements of specific antibody titres and class types would allow the effect of peptidoglycan to be determined. Such analyses would begin to determine the immunological mechanisms leading to protection against infection. Future work would phenotype the immune response to the vaccine used, including exposure to adjuvant or peptidoglycan alone.

One of the key benefits of the augmented infection model is that it is more representative of bloodstream infections due to the lower infectious inoculum required to establish an infection. However, the intravenous inoculum is given as a bolus dose as this does not require sedation of the mice and allows for greater numbers to be used. A steady intravenous infusion might be more representative of sepsis which would have a steady supply of bacteria in the bloodstream from an colonised cannula or infected wound[373,374]. Intravenous infusion would not be amenable to large experiments as performed here but it would be interesting to determine if the augmentation effect is also seen in this model of intravenous infection.

Whilst vaccination has always focused on inducing protection via priming the adaptive immune system there is increasing evidence that the innate immune system can be primed through epigenetic changes[375] and this has been shown to directly influence resistance to *S. aureus* skin and soft tissue infections[376]. Given the augmented infection overcomes the innate immunological bottleneck in the form of the Kupffer cells, priming of innate immunity as a new form of prophylaxis could be

interrogated with this model. Therefore, it would be interesting to assess the effect of the vaccine or even adjuvant alone as a single dose shortly before infection. If this was protective it could pave the way for a new form of prophylactic treatment to prevent *S. aureus* and other infections contracted during planned procedures such as elective surgery.

4.5 Conclusion

This work shows that peptidoglycan needs to be co-administered at the same time as the infectious inoculum to augment *S. aureus* infection and that smaller, more granular peptidoglycan is better at producing this augmentation phenomenon. Taken together this supports the argument that peptidoglycan and *S. aureus* need to co-localise within a phagocyte for augmentation to occur and this points towards several possible mechanisms for augmentation. The fact that vaccine-induced protection differed between the augmented infection challenge and challenge with *S. aureus* alone demonstrates these represent distinct and separate challenges to the host immune system despite the same intravenous administration route. Therefore, augmented infection is a useful tool for testing vaccine protective efficacy.

Chapter 5:
Use of murine models of infection to establish the role of the TrkA/p75^{NTR}-NGF-β pathway in *S. aureus* infection

5.1 Introduction

There is a current lack of knowledge as to what constitutes a beneficial immune response to *S. aureus*, with some experimental vaccinations leading to worse outcomes than placebo[160]. Follow up investigations and analysis of this vaccine data found that low IL-2 levels pre-vaccination correlated with poor outcome on receipt of the vaccine[161]. These two findings alone clearly demonstrate that an inappropriate immune response to *S. aureus* can contribute to pathology. Therefore, a greater knowledge of the interaction between *S. aureus* and the host immune system is necessary in order to generate better vaccines and treatments for *S. aureus* infection.

Phagocytes and antigen presenting cells such as neutrophils, macrophages and dendritic cells often present the first line of defence once a pathogen has gained access to the body. These are the first sentinels of the immune system with which a pathogen such as *S. aureus* will interact. *In vitro* and even *ex vivo* cell culture investigations into this interaction will always be somewhat limited as the cells have been removed to a much simpler immunological milieu. *In vivo* studies can help delineate the dynamics of an actual infection. This process can be further dissected by ablating entire cell subsets with chemical methods such as clodronate liposomes, which selectively remove macrophages within animal models of infection[377]. However, this is a blunt experimental instrument; although this showed that macrophages are important in *S. aureus* infection[223] it cannot tell us why macrophages are important or which pathways are involved in macrophage-dependent *S. aureus* control.

It is possible to identify important factors in disease pathogenesis by looking for increased susceptibility due to genetic mutations seen within a population. For example, it was recently found that diabetic patients are at an increased risk of *S. aureus* bacteraemia[378] which might indicate there is good rationale to look at the pathways dysregulated in diabetes for clues on important mechanisms in immunity aginst *S. aureus*. In addition patients with congenital insensitivity to pain with

anhidrosis (CIPA) have an increased susceptibility to *S. aureus* infections[379]. The genetic basis for CIPA is deleterious or missense mutations of the tyrosine kinase domain of the TrkA receptor[380] thereby implicating this receptor and its associated pathways in *S. aureus* disease. Hepburn *et al.*[214] also noticed that patients with hereditary sensory and autonomic neuropathy 4 and 5, due to biallelic mutations in nerve growth factor beta (NGF-β) or tropomyosine receptor kinase A (TrkA), were prone to recurrent *S. aureus* infections. This gave an impetus to study NGF-β signalling and its involvement in anti-*S. aureus* immunity and a clear signalling pathway to target through experimentation.

NGF-β is more commonly studied in its role in neural development as this is the role for which it was named[381]. But it was discovered that NGF-β levels increase in inflamed tissues[382,383] thereby implicating NGF-β in inflammatory processes and potentially immune regulation. The first evidence of direct action of NGF-β on the immune system was in 1977 when NGF-β injected into rats caused an increase in size and number of mast cells observed[384].

Subsequent study has revealed that NGF-β along with its high-affinity, specific receptor TrkA and its low-affinity, unspecific receptor p75-neurotrophin receptor ($p75^{NTR}$) have roles in the immune system (Fig 5.1) with monocytes/macrophages[385], granulocytes[386,387], T cells[388] and B cells[389] expressing these factors. These receptors and their signalling are dynamically regulated with regards to disease/inflammation state; for instance macrophages express less TrkA in the blood of those with chronic arthritis compared to those of healthy donors[390]. Garaci *et al.*[391] found that HIV infected macrophages increased NGF-β production. However, blocking this from acting in an autocrine fashion with anti-NGF-β caused a decrease in TrkA expression, an increase in $p75^{NTR}$ expression and an increase in apoptotic cell death. This may be beneficial in HIV infection as apoptotic cells released less HIV antigen, as measured by supernatant ELISA but it demonstrates the role NGF-β signalling might have in both immune cell survival and immune cell apoptosis. This signalling pathway clearly regulates immune function and deficiencies in this pathway lead to increased susceptibility to *S. aureus* in the human population, this justifies investigation of NGF-β in the context of *S. aureus* infection.

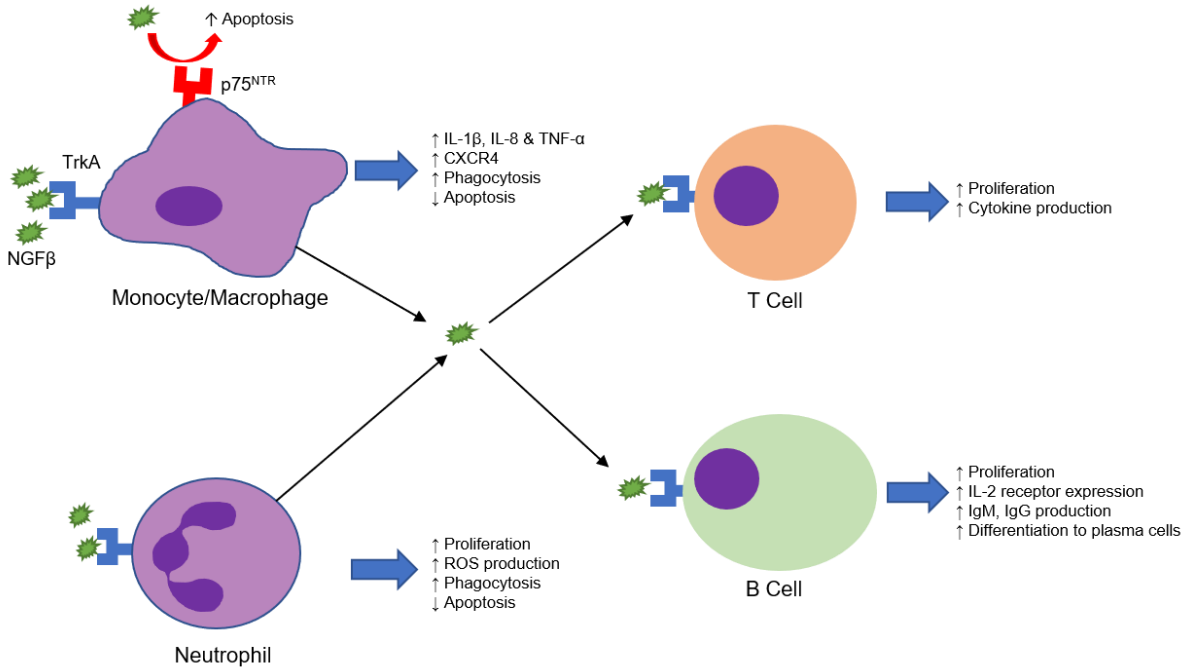

Figure 5.1. Simple diagram of some NGF-β immune functions.
NGF-β (green) acts on its specific receptor TrkA (blue) and its non-specific, low affinity receptor p75^{NTR} (red) on immune cells. This ligation causes a variety of effects such as decreased apoptosis and increased ROS production in innate immune cells and increased proliferation and antibody production in lymphocytes.

Hepburn *et al.*[214] showed NGF-β expression in human macrophages was triggered by *S. aureus* exoproteins and NGF-β treatment of human macrophages benefited their clearance of *S. aureus* infection *in vitro.* Furthermore, they demonstrated the importance of the NGF-β TrkA signalling pathway in anti-*S. aureus* immunity on an organism level through knocking down the TrkA receptor in zebrafish embryos with morpholinos. Zebrafish embryos with interrupted TrkA-NGF-β signalling succumbed to *S. aureus* infection significantly quicker than wildtype embryos.

This data is impressive but the shortcomings of the zebrafish embryo model should not be overlooked; whilst jawed fish do possess adaptive immune systems, at this stage of development zebrafish embryos only have neutrophils and macrophages[392]. However, these findings were supported in the mammalian system by Wirz *et al.*[393]. They found that mRNA transcripts encoding NGF-β and TrkA were significantly upregulated in the spleens of mice 4 hours after intraperitoneal infection with *S. aureus*. This demonstrates there is an *S. aureus*-induced activation of NGF-β signalling but does not display the importance of this pathway or its effects in anti-staphylococcal immunity in mice. Therefore, more in-depth study of the NGF-β pathway and its effect on *S. aureus* infection in the mammalian context was required.

Due to the importance of NGF-β in neuronal development a knockout at embryonic stage would have differing and potentially confounding physiology to wildtype systems. For instance mice lacking $p75^{NTR}$ lack defined white pulp areas due to dysregulated NGF-β signalling in splenic development[394]. It might be impossible to separate effects arising specifically from immune dysregulation from effects due to larger physiological abnormalities. Therefore, a selective mutation system would be beneficial to specifically knockout the NGF-β signalling capability in immune cells. One approach to making selective genetic mutations in eukaryotes is the *Cre/loxP* system.

The *Cre/loxP* system makes use of the Cre recombinase from the P1 phage. This recombinase selectively cleaves at *loxP* sites, then excises and circularises DNA between these sites. By flanking a gene with *loxP* sites and placing the Cre enzyme (which excises *loxP* flanked sites in DNA) under the control of a specific promotor, it is possible to knockout a gene only in cells expressing that specific gene thereby allowing tissue-specific knockouts, first accomplished by Gu *et al.* in 1994[395]. Cre

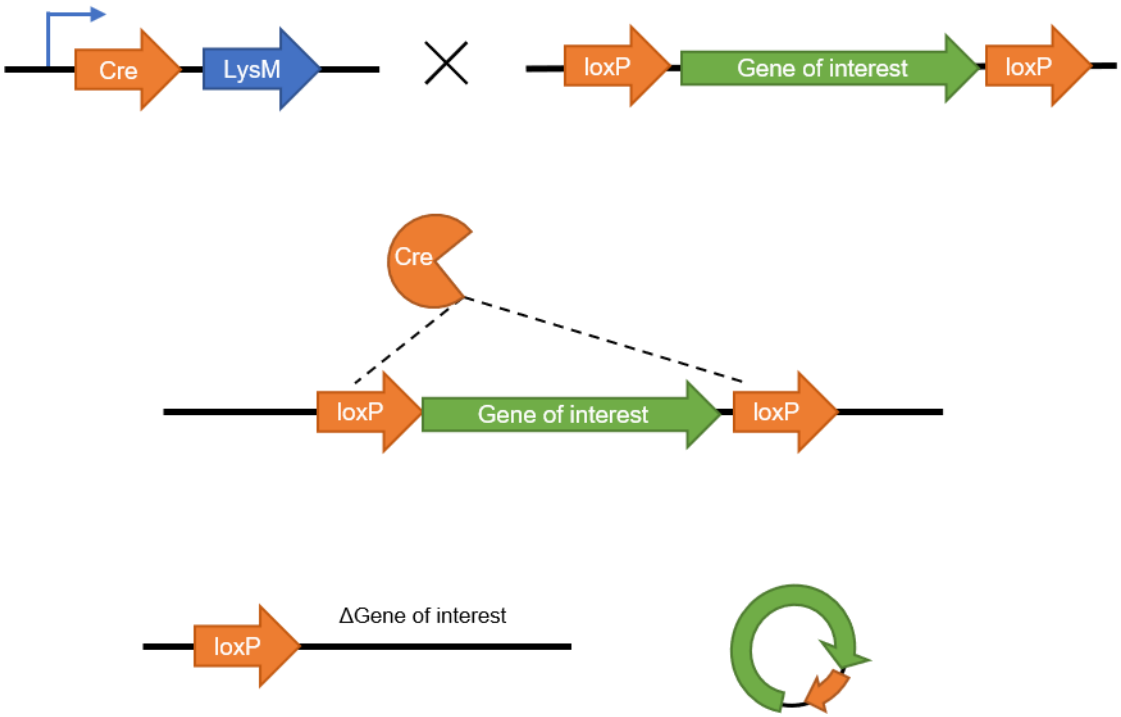

Figure 5.2 Diagram demonstrating the principles of *LysM-Cre* recombination.

Mice with Cre recombinase under the *LysM* promotor are crossed with mice which have a gene flanked with *loxP* sequences. In the resulting progeny *Cre* is expressed in cells that express *LysM* and the recombinase excises the gene of interest creating a knockout phenotype in only those cells expressing *LysM*.

was then put under the control of the *LysM* promotor by Clausen *et al.* in 1999 who reported recombination/knockout efficiency in almost 100% of granulocytes and 83-98% in mature macrophages[396]. The general principle of *LysM* Cre recombination is shown in Figure 5.2.

The Minichiello group at the University of Oxford generated transgenic mice using this *LysM-Cre* system. Mice with Cre under the control of the *LysM* promotor were crossed with mice which had genes involved in NGF-β signalling flanked by *loxP* sites. The following transgenic mice were generated:

- *Trka$^{lox/lox}$; LysM Cre* (*Trka^{LysMCre}*)
- *p75$^{NTR\ lox/lox}$; LysM Cre* (*p75$^{NTR\text{-}LysMCre}$*)
- *Trka$^{lox/lox}$ & p75$^{NTR\ lox/lox}$; LysM Cre* (*Trka/p75 $^{NTR\text{-}LysMCre}$*)
- *NGF-β$^{lox/lox}$; LysM Cre* (*NGF-β^{LysMCre}*)

These mice were sent to our lab at the University of Sheffield and challenged with *S. aureus* to assess the involvement of phagocyte NGF-β signalling in *S. aureus* infection and the resulting data is discussed in this chapter.

5.2 Aims

The overarching aim of this chapter was to determine the importance of the Trka/p75^{NTR}-NGF-β pathway in *S. aureus* infection in the mammalian system through use of the *Cre/loxP* system of knockout mice. The sub-aims were to:

- Assess the involvement of components of the NGF-β signalling pathway in *S. aureus* sepsis.
- Examine the contribution of NGF-β reception by TrkA and p75^{NTR} in the immune response to *S. aureus* skin and soft tissue infection (SSTI).

5.3 Results

5.3.1 The sepsis model

5.3.1.1 Determining the correct inoculum

The Minichiello lab had created mouse strains through crossbreeding transgenic mice from C57BL/6 and 129 backgrounds of mice to make a C57BL/6-129 hybrid which has not been used in Sheffield before. As per the Home Office project license (P3BFD6DB9); when infecting new mice strains a dosing study is required. A dosing study was also needed as different mouse backgrounds are known to have a range of susceptibilities to *S. aureus* infection[220]. Therefore, *Trka*^{LysMCre} mice and their wild type littermates were injected intravenously with increasing doses ($5x10^5$, $1x10^6$, $1x10^7$ and $3.5x10^7$ CFU) of *S. aureus* (NewHG) in groups of 2 (Fig 5.3). Mice were weighed daily throughout infection and at day 3 post-infection mice were culled and organs harvested for CFU enumeration.

There was no symptomatic pathology despite some weight loss seen in the groups challenged with the higher infectious dose (Fig 5.3E, 5.3F), which is perhaps understandable given that C57BL/6 mice are known to be more resistant to *S. aureus* infection than the Balb/C strain[220] which is more commonly used in our lab. The groups challenged with $5x10^5$ or $1x10^6$ CFU were trending towards clearance of the infection with high CFU in the kidneys of only one mouse in these groups. High CFU in the livers and kidneys were seen in the groups challenged with $1x10^7$ and $3.5x10^7$ CFU with only one set of kidneys (in the 1 $x10^7$ CFU challenge group) showing recoverable CFU below $1x10^5$.

An infectious inoculum of $1x10^7$ CFU/mouse was chosen as in C57BL/6-129 mice, this dose gave recoverable bacteria at day 3 post-infection (Fig 5.3A, 5.3B). The $3.5x10^7$ CFU/mouse dose led to pronounced weight loss approaching the severity limits of our license in all but one of the mice (Fig 5.3F), suggesting the immune system is being overwhelmed by bacterial numbers.

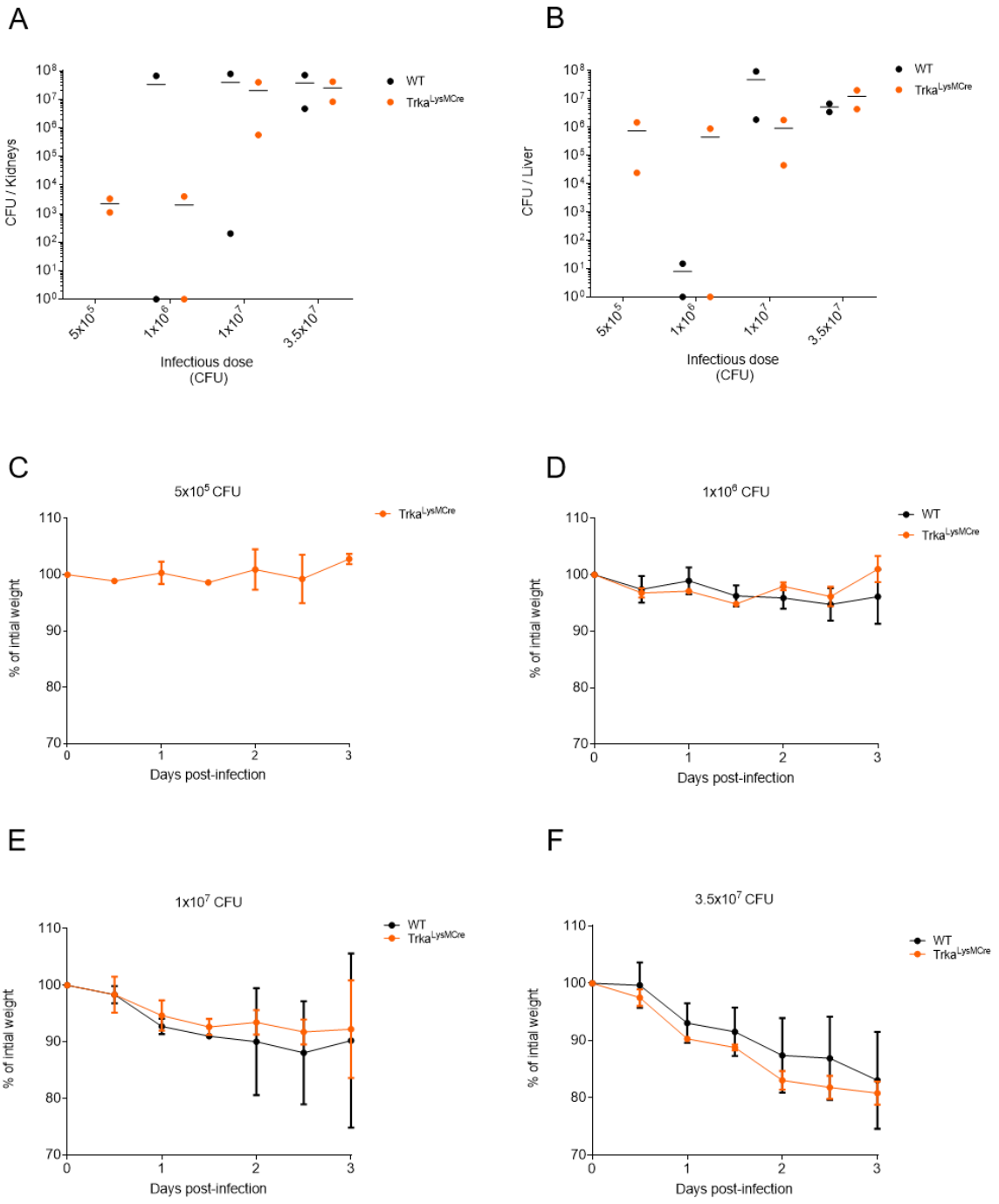

Figure 5.3 Dosing analysis for *S. aureus* (NewHG) in Trka^{LysMCre} mice using the sepsis model of infection

Mice were infected intravenously with 5x10^5, 1x10^6, 1x10^7 or 3.5x10^7 CFU of *S. aureus* (NewHG). On day 3 post-infection mice were culled and kidneys (A) and liver (B) were taken for CFU enumeration. Mice were also weighed throughout the course of their infection (C-F). CFU shown as median, weights shown as mean and Std Dev.

5.3.1.2 Involvement of TrkA in *S. aureus* sepsis

The infectious dose to be used in C57BL/6-129 background mice had been established as $1x10^7$ CFU/mouse based on the data from *Trka*^{LysMCre} mice in Figure 5.3. This was repeated with greater host numbers to grant sufficient statistical power to assess any differences. Once again *Trka*^{LysMCre} mice were intravenously infected with $1x10^7$ CFU *S. aureus* (NewHG) alongside wildtype homozygous Cre-negative littermates and all mice were culled on day 3 post-infection. Weight loss and CFU/organ are shown in Figure 5.4. There were no significant differences in CFU recovered from any organ or in weight loss between wildtype and *Trka*^{LysMCre} mice. It was concluded that the TrkA-NGF-β pathway is not important in staphylococcal sepsis or that NGF-β might be acting on another target, as NGF-β can also bind to $p75^{NTR}$ on immune cells (Fig 5.1).

5.3.1.3 Involvement of $p75^{NTR}$ in *S. aureus* sepsis

To assess the involvement of the alternative NGF-β receptor $p75^{NTR}$, *p75*$^{NTR\text{-}LysMCre}$ mice were used. *p75*$^{NTR\text{-}LysMCre}$ mice had their *p75*^{NTR} gene flanked by *loxP* sites and therefore had this excised in phagocyte cells expressing LysM and subsequently expressing Cre. The mice were intravenously infected with *S. aureus* (NewHG) at a dose of $1x10^7$ CFU/mouse alongside wildtype littermates. Mice were weighed daily throughout infection and on day 3 post-infection mice were culled and organs harvested for CFU enumeration.

There was no significant difference seen in the CFU recovered from any of the organs and no significant difference in weight loss between mutant and wildtype mice. As with the *Trka*^{LysMCre} mice (Fig 5.4) the *p75*$^{NTR\text{-}LysMCre}$ mice had no significant resistance or susceptibility to intravenous *S. aureus* challenge when compared to their wildtype littermates (Fig 5.5). Both TrkA and $p75^{NTR}$ are receptors for NGF-β[397] so it is possible that there is some functional redundancy in their ability to signal NGF-β presence in the context of immune cells such as LysM-expressing phagocytes. Functional redundancy would explain seeing no difference when each receptor was knocked out individually.

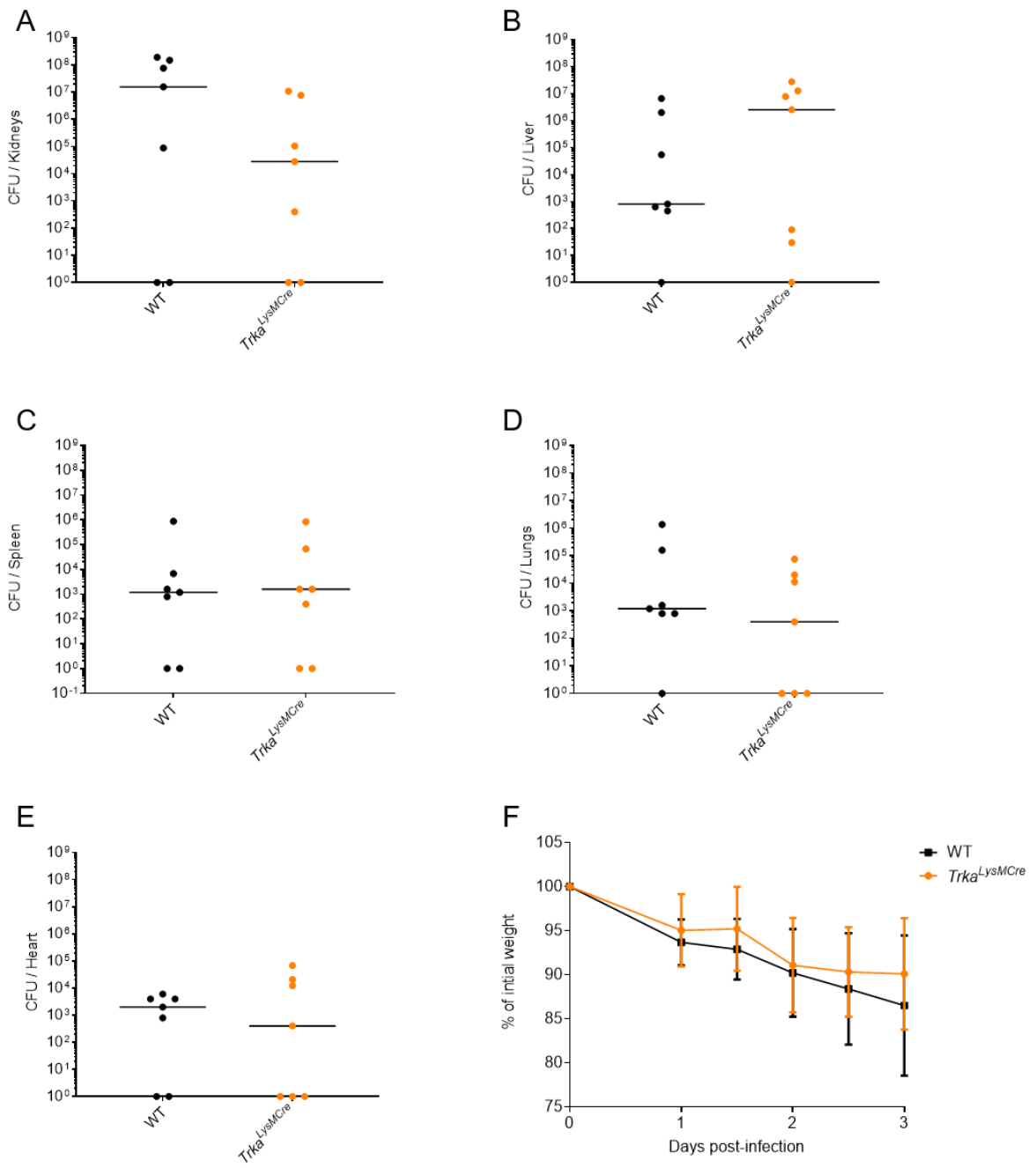

Figure 5.4 **Role of TrkA in intravenous *S. aureus* infection.**

Trka^{LysMCre} mice (orange) and litter matched wildtype controls (black) were intravenously infected with 1x10^{7} CFU *S. aureus* (NewHG). On day 3 post-infection mice were culled and kidneys (A), livers (B), spleens (C), lungs (D) and hearts(E) were harvested for CFU enumeration. Mice were weighed daily throughout the course of the experiment (F). CFU shown as median, weights shown as mean Std Dev. All p values>0.05.

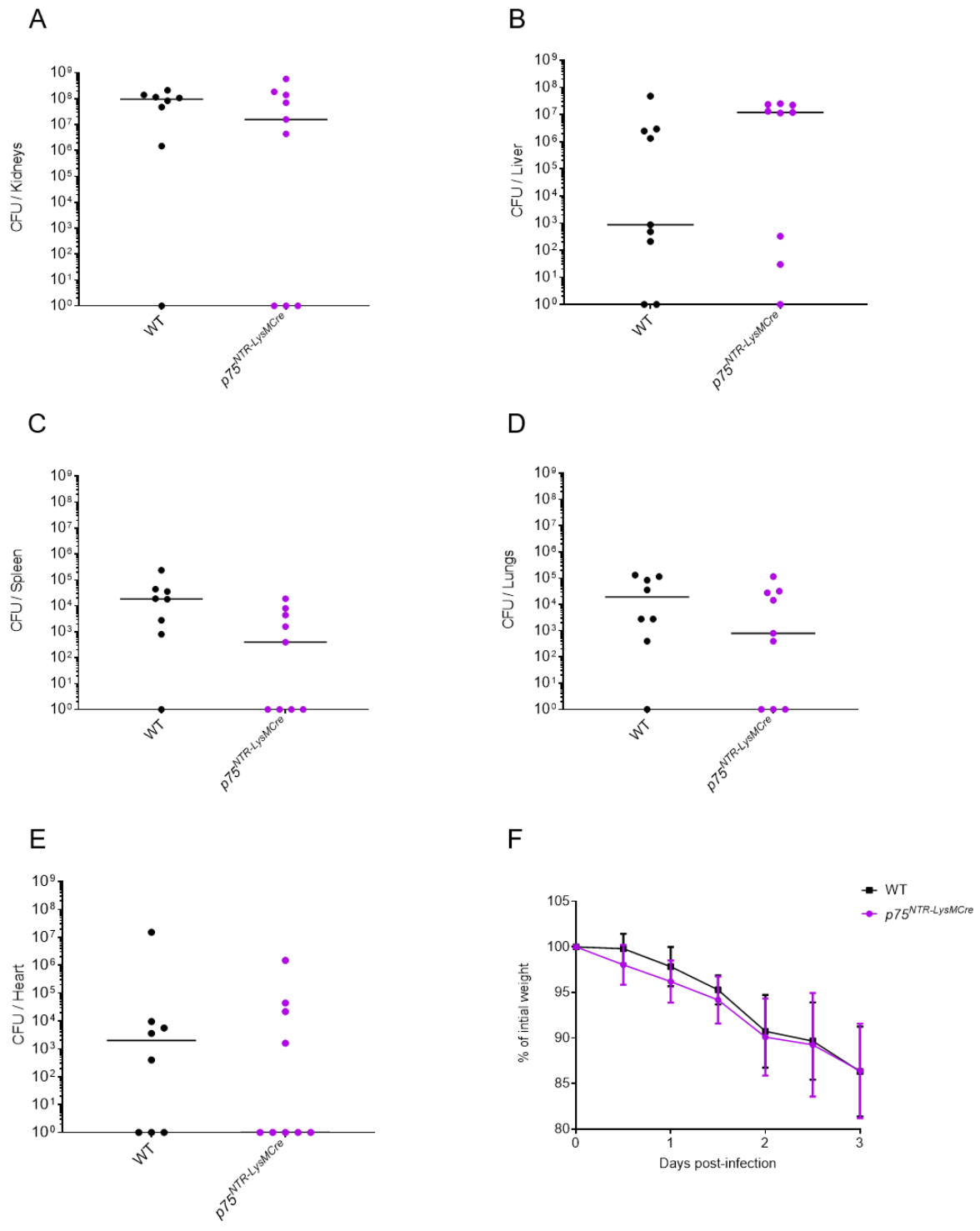

Figure 5.5 Role of p75^{NTR} in intravenous *S. aureus* infection.

p75$^{NTR\text{-}LysMCre}$ mice (purple) and litter matched wildtype controls (black) were intravenously infected with 1x10^{7} CFU *S. aureus* (NewHG). On day 3 post-infection mice were culled and kidneys (A), livers (B), spleens (C), lungs (D) and hearts (E) were harvested for CFU enumeration. Mice were weighed daily throughout the course of the experiment (F). CFU shown as median, weights shown as mean and Std Dev. All p values>0.05.

5.3.1.4 Involvement of NGF-β receptors in *S. aureus* sepsis

Given the potential for functional redundancy between TrkA and $p75^{NTR}$ in how LysM-expressing immune cells perceive NGF-β, a double conditional knockout was produced. Both *Trka* and $p75^{NTR}$ genes were flanked by *loxP* and this mouse was bred with a mouse line expressing Cre under the *LysM* promotor producing mice where both receptors would be knocked out in *LysM* expressing phagocytes. These, doubly deficient mice were each intravenously challenged with $1x10^7$ CFU of *S. aureus* (NewHG) as were their wildtype littermates. All mice were weighed daily throughout infection and culled on day 3 post-infection.

There was no significant difference in clearance of bacteria between *Trka/p75* $^{NTR\text{-}LysMCre}$ mice and their wildtype littermates as shown by CFU counts in each organ (Fig 5.6). There was also no difference seen in weight loss between the two groups (Fig 5.6F) indicating no difference in pathogenesis. It can be concluded from these data that the ability of the phagocytes to respond to NGF-β is not important for significant anti-*S. aureus* immunity.

The impetus to investigate the anti-staphylococcal utility of the TrkA-NGF-β pathway in mice came from the Hepburn *et al.* paper which showed the pathways involvement in anti-staphylococcal immunity in zebrafish[214]. That study used morpholinos to knock down *Trka,* which as a genetic approach has much less specificity than the *Cre/loxP* system. They also showed that human neutrophils produce large amounts of NGF-β in response to *S. aureus*. It is feasible that the *Trka* was knocked down in other cells and the NGF-β in the system was coming from the phagocytes rather than the important target of the NGF-β being the phagocytes themselves. Therefore, it was important to look at NGF-β-LysM Cre mice where the phagocytes specifically would be unable to produce NGF-β in response to *S. aureus* infection.

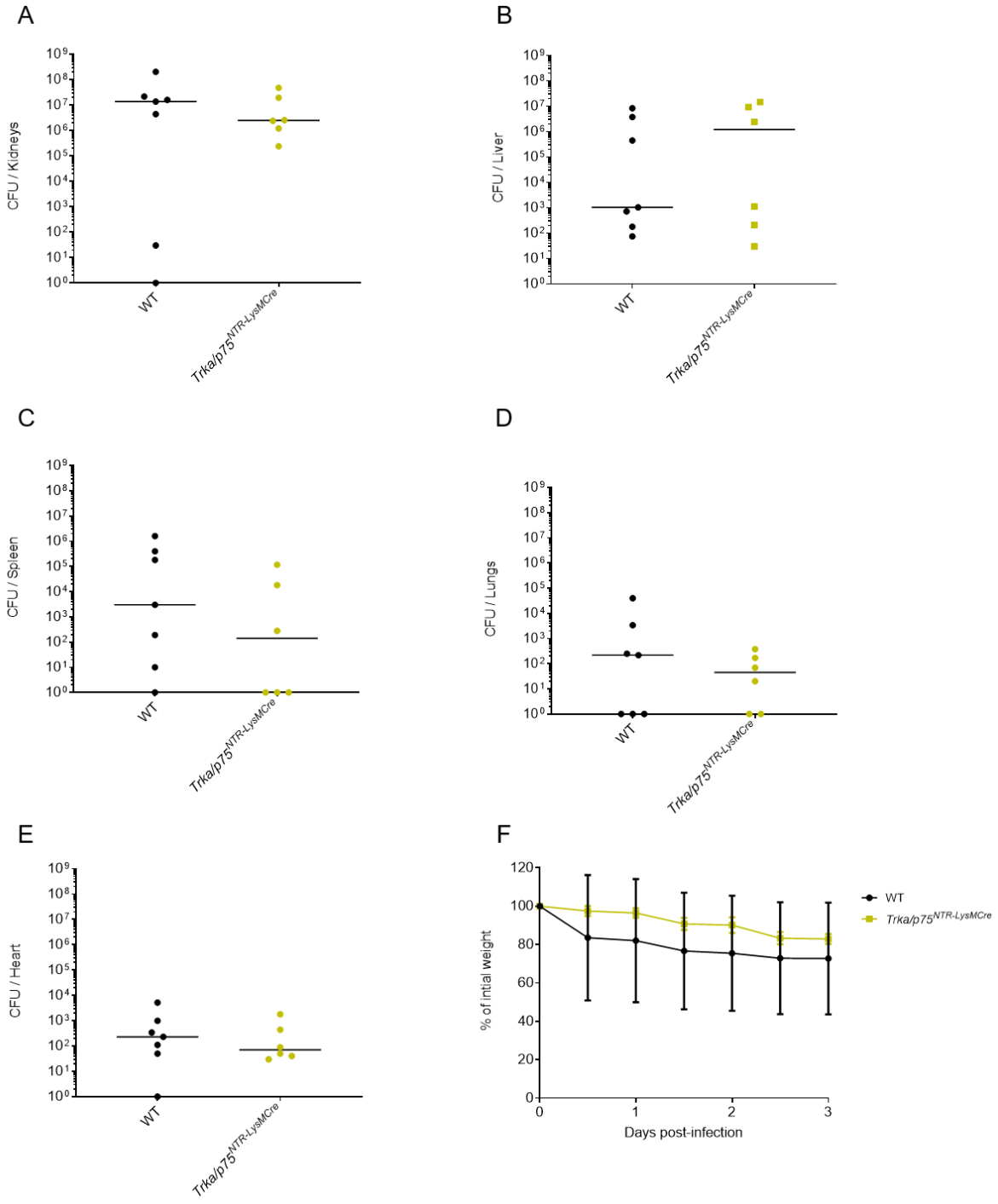

Figure 5.6 Combined role of TrkA and p75^{NTR} receptors in intravenous *S. aureus*.

Trka/p75 $^{NTR\text{-}LysMCre}$ mice (green) and litter matched wildtype controls (black) were intravenously infected with 1x10^{7} CFU *S. aureus* (NewHG). On day 3 post-infection mice were culled and kidneys (A), livers (B), spleens (C), lungs (D) and hearts (E) were harvested for CFU enumeration. Mice were weighed daily throughout the course of the experiment (F). CFU shown as median, weights shown as mean and Std Dev. All p values>0.05.

5.3.1.5 Involvement of phagocyte-derived NGF-β in *S. aureus* sepsis

The involvement of the NGF-β signalling in anti-staphylococcal immunity could be due to phagocyte production of NGF-β rather than response to NGF-β. Therefore *NGF-β^{LysMCre}* mice and their wildtype littermates were intravenously infected with 1x10^{7} CFU of *S. aureus* (NewHG). The mice were weighed daily throughout infection and organs were harvested for CFU enumeration after culling on day 3 post-infection.

There was no significant difference between *NGF-β^{LysMCre}* mice and wildtype mice based on bacterial clearance or weight loss (Fig 5.7). Coupled with the data from the NGF-β-receptor knock out mice these data would suggest that NGF-β is not important in the murine model of *S. aureus* sepsis. However, that does not mean NGF-β signalling is not important in other *S. aureus* infections*. S. aureus* causes a wide range of disease in several host tissues[3] and the immune milieu might be quite different in each setting.

Intravenous infection mimics sepsis, whereby the *S. aureus* have direct access to the blood stream. The data of *S. aureus* infection in this sepsis setting in the murine model suggest that the majority of *S. aureus* is taken up by Kupffer cells in the liver before seeding other parts of the body, particularly the kidneys[29]. However, the skin constitutes a vastly different immune environment to the blood, liver and kidneys[398,399]. Therefore, it was decided to examine the contributions of this signalling pathway in a model of skin and soft tissue infection with the subcutaneous infection model[222,309].

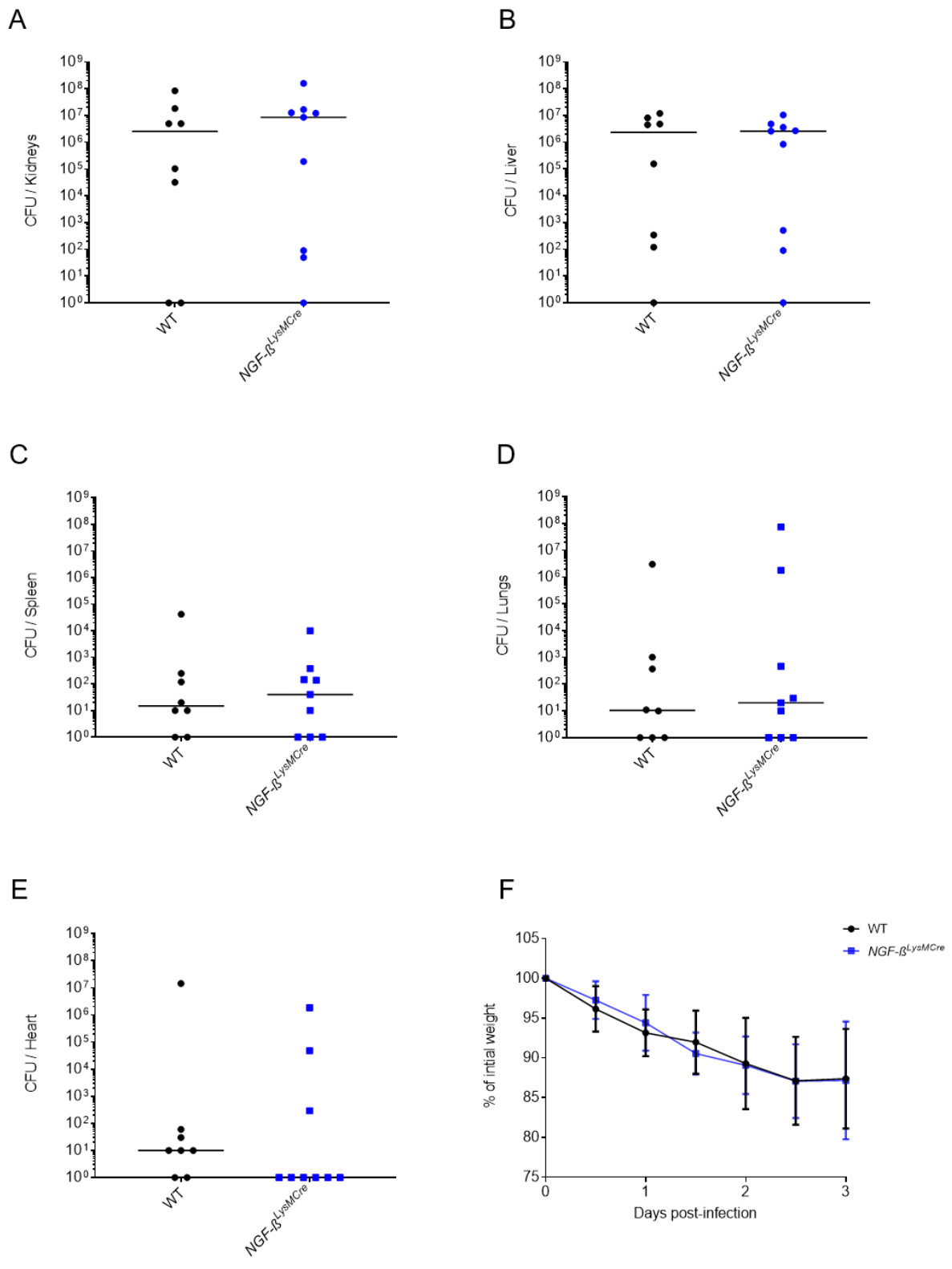

Figure 5.7 Role of phagocyte derived NGF-β in intravenous *S. aureus* infection.

NGF-β^{LysMCre} mice (blue) and litter matched wildtype controls (black) were intravenously infected with 1x10^7 CFU *S. aureus* (NewHG). On day 3 post-infection mice were culled and kidneys (A), livers (B), spleens (C), lungs (D) and hearts (E) were harvested for CFU enumeration. Mice were weighed daily throughout the course of the experiment (F). CFU shown as median, weights shown as mean and Std Dev. All p values>0.05.

5.3.2 Skin and soft tissue infection model

5.3.2.1 Dosing of subcutaneous infection in C57BL/6-129 mice

To assess the effects of *Trka*^{LysMCre} and *p75*$^{NTR\text{-}LysMCre}$ the subcutaneous *S. aureus* infection was used which models skin and soft tissue infections (SSTI). As with the initial intravenous infection of these mice (Fig 5.3) the subcutaneous route of infection in a new background of mice constituted a new infection which required a dosing study. Therefore, five groups of two C57BL/6-129 wildtype mice were subcutaneously infected with increasing doses ($1x10^5$, $1x10^6$, $5x10^6$, $1x10^7$ and $1x10^8$ CFU) of *S. aureus* (NewHG). Mice were weighed and monitored for 4 days post-infection as this was the length of infection used previously (Boldock *et al.*[222]). On day 4 post-infection mice were culled and the tissue at and surrounding the injection site was excised for CFU enumeration (2.38.5).

Pronounced weight loss above expected levels was seen on day 1 in the group challenged with $1x10^8$ CFU therefore this dose was discounted for further study. There was no significant weight loss in any other group. The CFU recovery was low in all the other groups. The second highest infectious dose $1x10^7$ CFU was chosen to take forward as this gave the highest recoverable CFU without a large drop in weight. Furthermore, to aid in CFU recovery the length of infection was reduced to 3 days for further subcutaneous infection work.

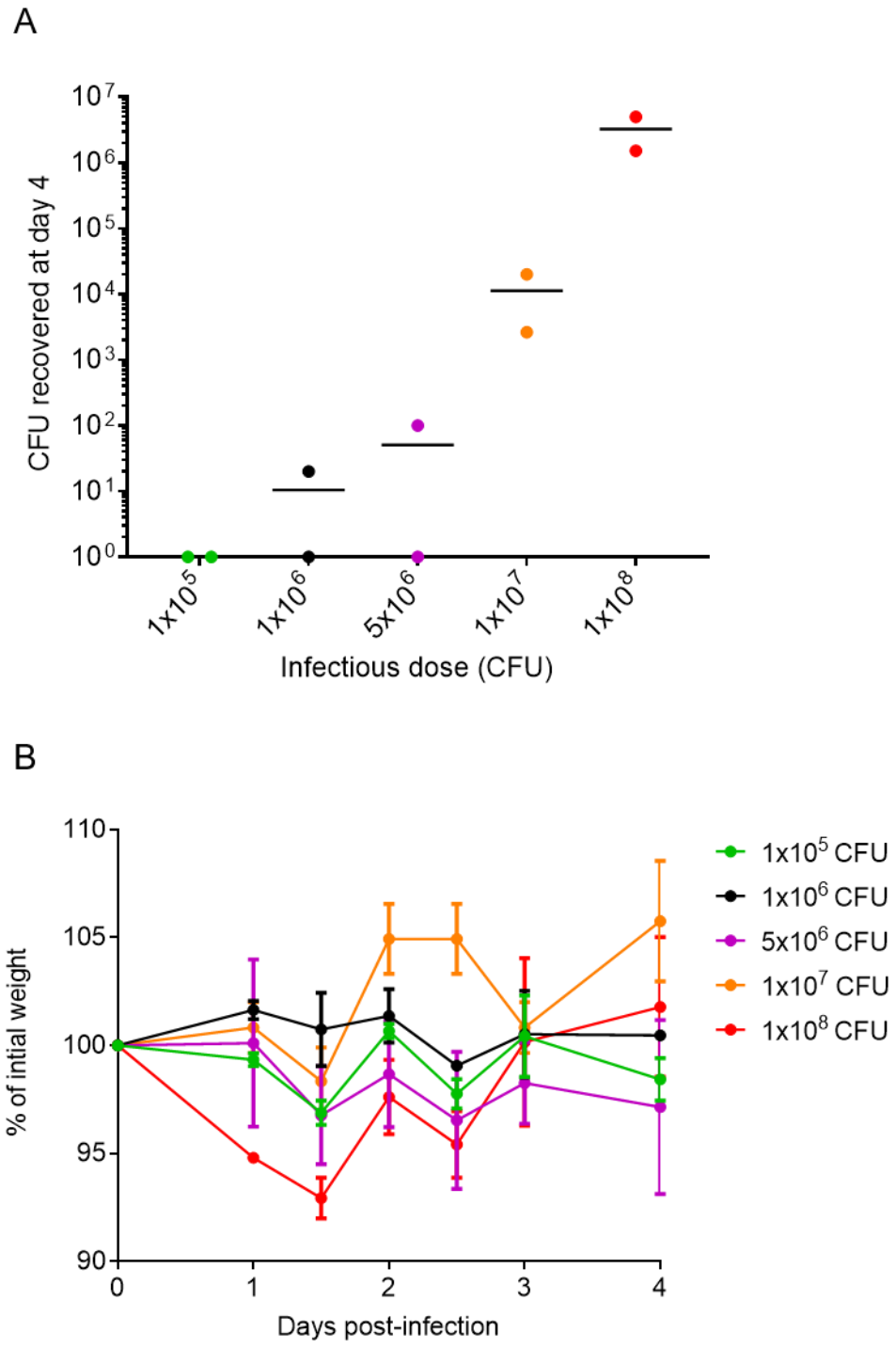

Figure 5.8 Determining the appropriate infectious dose for subcutaneous *S. aureus* infection of LysM-Cre background mice

Wildtype control mice of the LysM-Cre background were infected subcutaneously with $1x10^5$, $1x10^6$, $5x10^6$, $1x10^7$ or $1x10^8$ CFU of *S. aureus* (NewHG). On day 4 post-infection mice were culled and tissue excised for CFU enumeration (A). Mice were weighed throughout the course of their infection (B). CFU shown as median, weights shown as mean and Std Dev. All p values>0.05.

5.3.2.2 Involvement of phagocyte NGF-β receptors in *S. aureus* skin and soft tissue infection

Trka^{LysMCre}, *p75*$^{NTR\text{-}LysMCre}$ and wildtype mice were subcutaneously infected with 1x10^{7} CFU of *S. aureus* (NewHG). Mice were weighed daily before being culled on day 3 post-infection when tissue surrounding the injection site was excised for CFU enumeration. It was found that, whilst there was no significant difference in weight loss (Fig 5.9B), significantly fewer CFU were recovered from *p75*$^{NTR\text{-}LysMCre}$ mice compared to wildtype mice (Fig 5.9A). However, there was no significant difference seen between wildtype and *Trka*^{LysMCre} mice. Therefore, it might be that p75^{NTR}-NGF-β pathway is important in anti-staphylococcal immunity in skin and soft tissue infections.

This experiment was repeated with just *p75*$^{NTR\text{-}LysMCre}$ mice to confirm the difference seen in CFU in Figure 5.9B and to strengthen the conclusion that *p75*$^{NTR\text{-}LysMCre}$ mice are more resistant to *S. aureus* skin infections than wildtype mice. However, as seen in Figure 5.10 there was no significant difference in CFU recovered between wildtype and *p75*$^{NTR\text{-}LysMCre}$ mice. Furthermore, the significant difference in weight loss seen in Fig 5.10 would indicate that wildtype mice were more resistant to *S. aureus* skin infection than *p75*$^{NTR\text{-}LysMCre}$ mice, in complete contradiction of the findings of Figure 5.9. It was concluded that the contradicting significant results likely indicated there was no substantial difference and none of the tested mutants responded differently to *S. aureus* skin infection compared to wildtype mice.

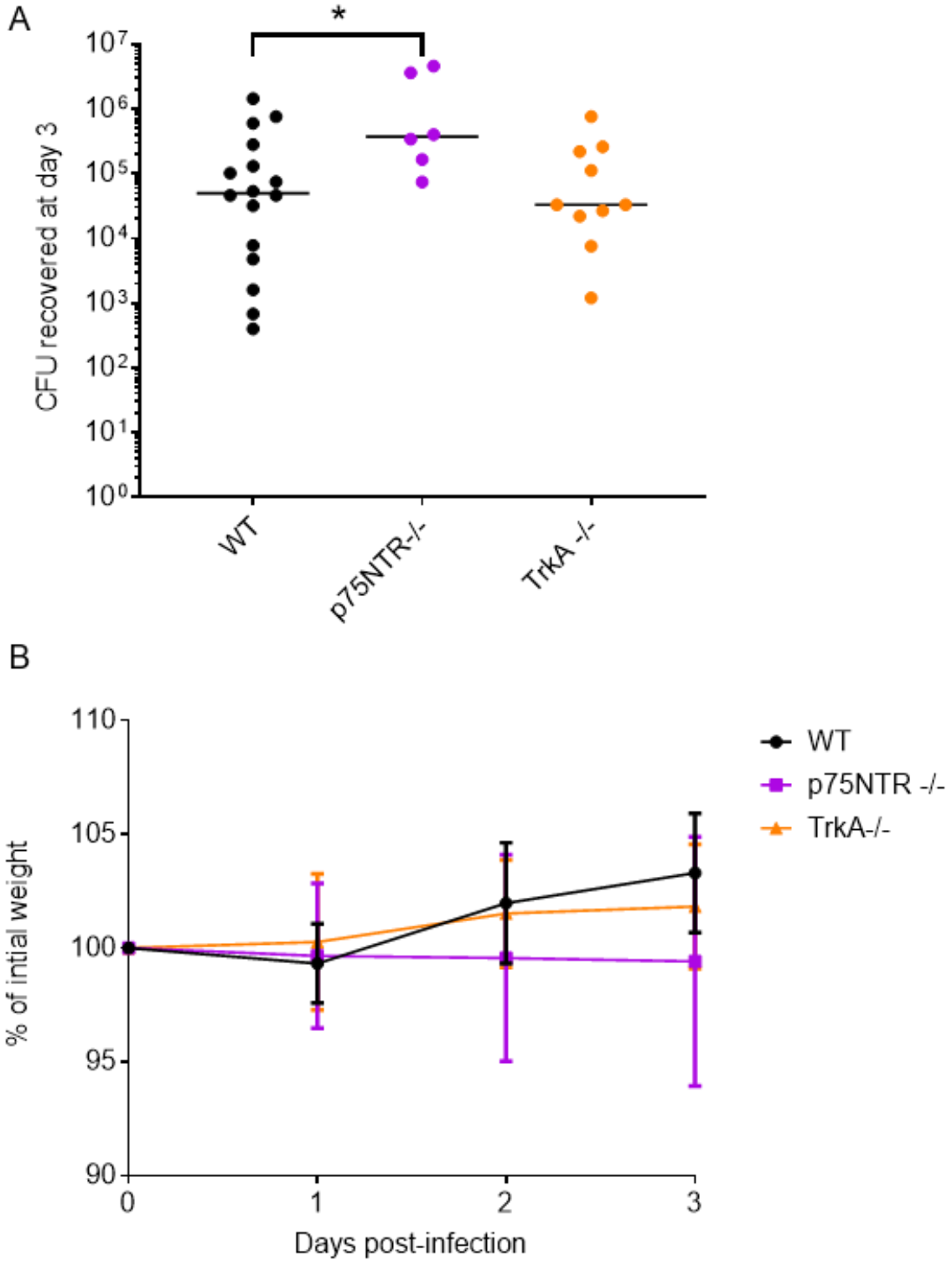

Figure 5.9 The role of TrkA and p75^{NTR} receptors in subcutaneous *S. aureus* infection.

Wildtype mice (black), *p75$^{NTR\text{-}LysMCre}$* mice (purple) and *Trka^{LysMCre}* mice (orange) were infected subcutaneously with 1x10^7 CFU of *S. aureus* (NewHG). On day 3 post-infection mice were culled and tissue excised for CFU enumeration (A). Mice also weighed throughout the course of their infection (B). CFU shown as median, weights shown as mean and Std Dev. * p<0.05 CFU.

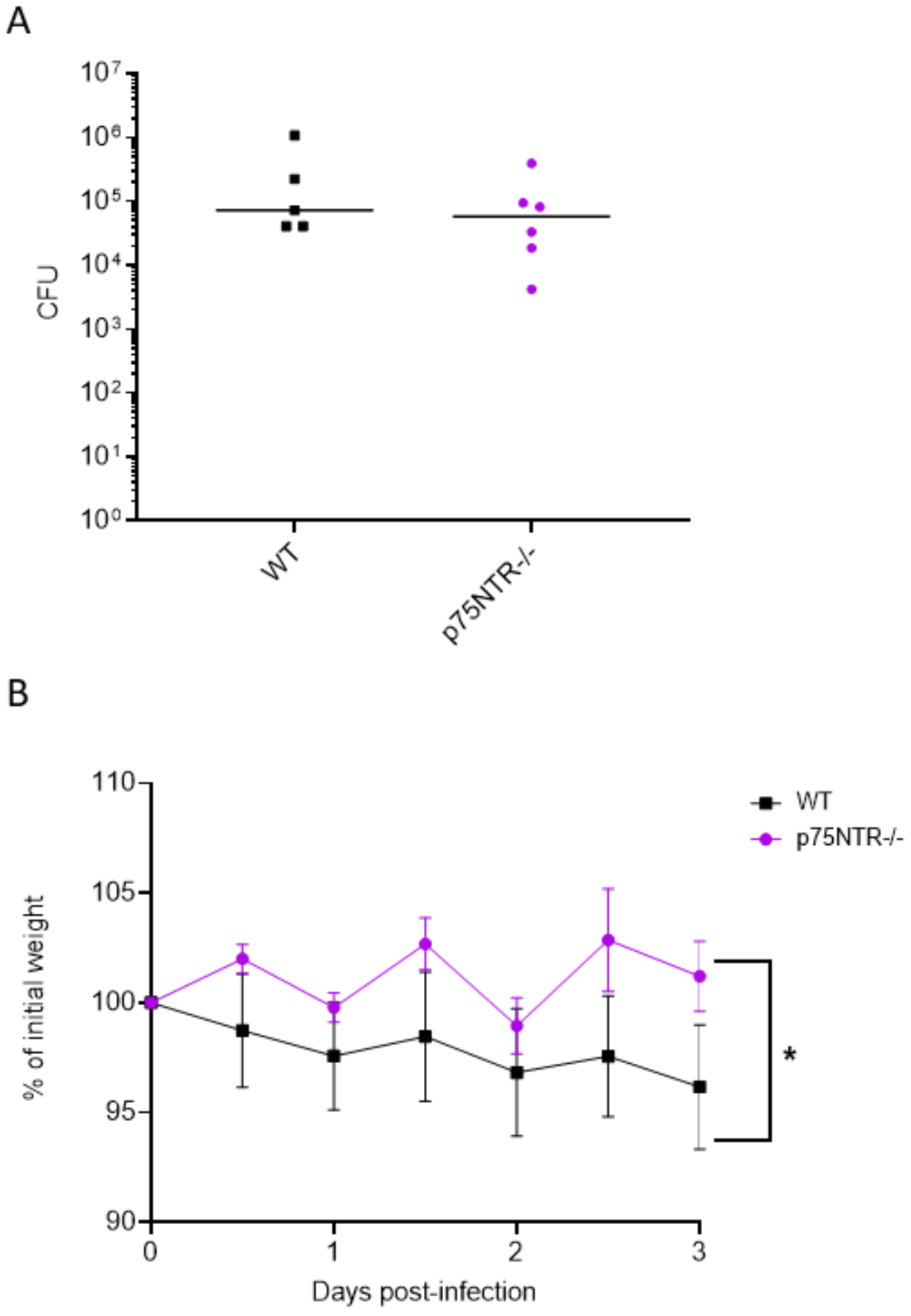

Figure 5.10 Role of p75*NTR* in subcutaneous *S. aureus* infection.

Wildtype mice (black) and *p75*$^{NTR\text{-}LysMCre}$ mice (purple) were infected subcutaneously with 1x10^7 CFU of *S. aureus* (NewHG). On day 3 post-infection mice were culled and tissue excised for CFU enumeration (A). Mice also weighed throughout the course of their infection (B). CFU shown as median, weights shown as mean and Std Dev. * $p<0.05$.

5.4 Discussion

NGF-β has numerous effects on both innate and adaptive immune cells (Fig 5.1). Given the increased susceptibility to *S. aureus* of patients with mutations in the NGF-β receptor TrkA[380] and the propensity of NGF-β to enhance phagosomal activity in neutrophils and macrophages[397] (Fig 5.1) there has been an increased interest in the role of this signalling pathway in anti-*S. aureus* immunity. This resulted in a publication by Hepburn *et al.* which showed that interrupting this signalling pathway led to increased susceptibility to *S. aureus* in zebrafish embryos[214]. The work presented in this chapter attempted to ascertain whether these results translate to the mouse model of infection by using mice engineered through the *Cre/lox* system to lack components of this signalling pathway in phagocytes.

At first glance this work contradicts the findings of Hepburn *et al.* 2014[214]; the reality is likely much more nuanced. They found that injecting zebrafish embryos with morpholinos to knockdown *Trka* reduced the ability of the zebrafish embryos to clear *S. aureus* infection. This implies that TrkA-NGF-β signalling is important in anti-*S. aureus* responses in neutrophils and macrophages as these are the immune cells present in a zebrafish embryo[392]. In contrast, the data shown in my study initially indicates that NGF-β perception in phagocytes via TrkA or/and $p75^{NTR}$ is not important during *S. aureus* sepsis or SSTI in mice and NGF-β production by phagocytes is also not important during *S. aureus* sepsis in mice.

The simplest explanation for the disparity between these findings is the differences between mouse and zebrafish embryo immune systems. Day 2 post-fertilisation zebrafish embryos only have primitive macrophages and neutrophils[216,218,392] whereas the mice used were all 7-8 weeks or older and therefore had mature innate and adaptive immune systems[400,401]. Not only does this mean the mouse will be better able to deal with infection due to a more competent immune system but there are also more potential sources of NGF-β-mediated immune communication. Furthermore, the potential for adaptive immunity to have a significant role here cannot be ruled out due to the potential for pre-exposure of laboratory mice[402].

The LysM Cre model used here assumes that genes of interest are knocked out in phagocytes due to their *LysM* expression. However, to suggest that all phagocytes express *LysM* equally would be an oversimplification. LysM-controlled Cre-

recombination was initially shown to be effective in almost 100% of granulocytes and 83-98% in mature macrophages[396], however, this does not necessarily account for recruited monocytes and immature macrophages. In addition, our understanding of immune cell ontogeny has vastly improved since 1999. It is now widely understood that macrophages are not a homogenous population and exist in M1 and M2 phenotypes[403] with more data becoming available to suggest even this dichotomy underestimates the diversity of macrophage phenotypes[404].

Even within the M1-M2 paradigm of macrophage phenotype there are differing levels of LysM expression. Whilst tissue resident macrophages are thought to largely be an M1 phenotype which have high level LysM expression, alternatively activated M2 macrophages can have low levels of LysM expression[405]. This low level LysM expression would subsequently cause low Cre production and a concomitant loss of efficient recombination resulting in unreliable knockouts in these cells. This M1 vs M2 dichotomy and incomplete recombination might explain why I found a slightly greater difference in the subcutaneous challenge compared to intravenous challenge. As there would be more M1 macrophages in the dermal tissue than in the liver where Kupffer cells are known to have M1/M2 plasticity[406].

It is also possible that the LysM-Cre knockouts used here were successful in tissue resident (M1) macrophages, but alternatively activated macrophages were recruited to each infected tissue and provided a sufficient source of NGF-β signalling in to ensure mutant mice were no more susceptible to *S. aureus* infection than wildtype mice. Instances of this incomplete recombination phenomenon have been published. For instance, Vannella *et al*. took advantage of this incomplete/differential Cre-mediated recombination to characterise a new subset of M2 macrophages that are important in schistosomiasis[405]. Furthermore, there is *in vitro* and *in vivo* evidence that *S. aureus* can promote M2 macrophage polarisation[407] thus making the incomplete recombination hypothesis due to a prominent recombination resistant M2 population of macrophages a more feasible explanation. Incomplete recombination would also be compatible with the findings of Hepburn *et al.*[214] as the anti-*Trka* morpholino would work on M2 macrophages as it is not dependent on LysM expression.

Whilst there was no reliable significant difference in the CFU measured it is interesting to note that there was often a relative increase in the liver CFU in the intravenous model of infection. The hepatic tissue and even some Kupffer cells have been shown to express NGF-β and TrkA under some conditions[408]. Therefore, an interesting avenue of future work would be to assess whether augmentation, which also shifts the focus of infection to the liver, occurs in these transgenic mice and to assess how the expression of these factors changes in the liver during *S. aureus* infection.

Future work should examine recombination efficiency in these mice via flow assisted cell sorting to sort different macrophage populations and PCR to determine the level of Cre-mediated recombination in these distinct populations in the context of *S. aureus* infection. This could shed light on the shortcomings of our model and the importance of M1/M2 polarisation in mammalian *S. aureus* infection. However, it is likely that macrophage polarisation one way or the other will not be a one size fits all rule. As is becoming increasingly apparent due to the wide range of infectious niches *S. aureus* can inhabit and cause different diseases, an appropriate immune response in one tissue would be unhelpful in another[409] and different vaccines/immune responses might be required for different types of infection[410]. Therefore, the involvement of NGF-β signalling and macrophage subsets in *S. aureus* pathogenesis should be investigated in various routes of infection.

Chapter 6:
General discussion

Developing therapeutics for *S. aureus* has stalled due to increasing antibiotic resistance[50] and an increasing number of failed clinical vaccine trials[175]. To overcome these obstacles new antibiotic targets, greater understanding of *S. aureus* pathogenesis and animal models which translate better to clinical *S. aureus* disease in humans are needed. The main findings of this thesis help to address these needs.

Chapter 3 convincingly demonstrates that *S. aureus* DivIC is interacting with WTA in the bacterial cell wall and lays the groundwork for establishing the binding site of this interaction. If this is proven to be an important interaction it could be one of the many checkpoints required for the extensive coordination of *S. aureus* cell division (Fig 6.1). Cell division requires cell growth and replication of intracellular components such as DNA and proteins and it is the synthesis of these components that antibiotics such as macrolides, aminoglycosides, fluoroquinolones and tetracyclines target[411].

The formation of the “piecrust” which denotes the beginning of septum formation in *S. aureus* is an apparent division checkpoint given that *ΔdivIB* mutations arrest cell division at this stage[150]. The *ΔdivIC* mutation in *S. coelicolor*[243] suggests a similar defect to the *ΔdivIB* mutation would be seen in a *ΔdivIC* in *S. aureus*. This coupled with the data presented in this thesis makes a strong argument for further work to define the role of DivIC and the associate FtsL, DivIB heterotrimer to subsequently target these division proteins for logical antibiotic design. Targeting well characterised divisome components is beginning to show therapeutic promise, as candidates that interfere with FtsZ ring formation have shown good antibiotic activity against Gram-positive bacteria such as *B. subtilis* and *S. aureus*[412–414]. This approach to antibiotic design is particularly promising as the essentiality of division proteins leads to less chance or resistance by mutation without concomitant fitness costs.

The other potential therapeutic target of the interaction demonstrated in Chapter 3 is WTA. The interaction with DivIC adds to the growing evidence in the literature that immunogenic, surface localised, targetable teichoic acids play a role in coordinating cell division. Mutants lacking WTA or LTA display pleiotropic phenotypes

characterised by aberrant septum placement/poor cell wall hydrolysis and multiple parallel septa respectively[119,268,415]. In addition, these molecules are mutually essential whereby double mutants are not viable[118] and pharmacological inhibition of both pathways leads to cell death[119] implying a redundancy in an essential function. Currently the exact mechanism of how teichoic acids regulate cell division is unknown.

There is evidence that LTA synthesis may act as a nutrient sensor in *B. subtilis*[416]. This would provide impetus for the initiation of cell division and explain why *ypfP* mutants in *S. aureus* grow much larger before the initiation of septum formation[116,417], this potentially presents a targetable cell cycle checkpoint. WTA have been implicated in controlling peptidoglycan cross-linking through PBP localisation[292] and in inhibition of peptidoglycan hydrolysis[98,99]. Daughter cell separation by peptidoglycan hydrolysis is another possible cell cycle breakpoint to target as mutants of the *walKR* operon, which controls cell wall hydrolysis, are non-viable unless exogenous peptidoglycan hydrolases are added[418]. Therefore, inhibiting hydrolysis could be an antibiotic target either through targeting *walKR*, murein hydrolases or ascertaining exactly how WTA coordinate the process.

Small molecules that disrupt teichoic acid synthesis already exist. Congo red inhibits LtaS activity but has carcinogenic toxicity to mammalian cells[419]. Tunicamycin and tarocin inhibit TarO[97,303,420] and targocil is an inhibitor of the WTA exporter TarGH[415]. TarO-inhibiting drugs have been shown to re-sensitize resistant strains to β-lactams and could therefore be used in combination therapy[97,268]. However, tunicamycin has not yet been pursued as an antibiotic for clinical use as it displays toxicity in eukaryotic cells[97,420]. Tarocin was shown to be less toxic than tunicamycin[97] but efforts are still underway to find tunicamycin derivatives that are less toxic to mammalian cells due to the ability of tunicamycin to also inhibit MraY and peptidoglycan synthesis[421]. Furthermore, resistance against targocil rapidly develops unless sub-inhibitory levels of β-lactams are also used[415]. Further study of the role of teichoic acids in the cell cycle of *S. aureus* could provide other angles from which to therapeutically target teichoic acids such as the interaction between WTA and DivIC demonstrated in this thesis.

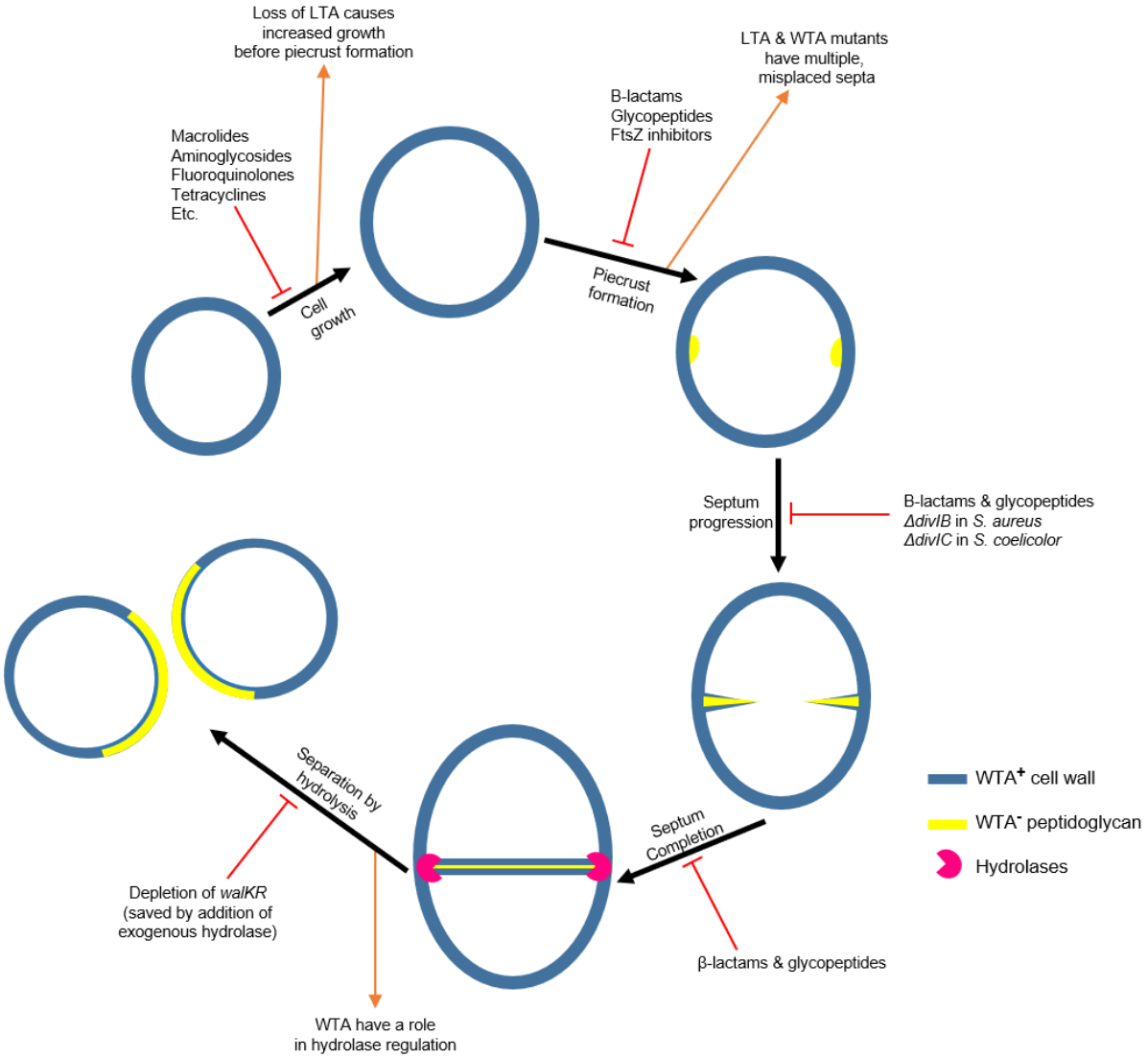

Figure 6.1 Diagram depicting points of the *S. aureus* cell cycle that are and could feasibly be targeted by antibiotics
The *S. aureus* cell cycle has many stages which can be inhibited (Red) by known antibiotics or genetic mutations which indicate potential targets for novel antibiotic development. Teichoic acids have numerous potential roles which have been implicated at numerous stages of the cell cycle (Orange).

Other points of intervention could focus not on the bacterial cell cycle but on the pathogenic mechanisms of *S. aureus,* thereby breaking the cycle of carriage and disease. Divisome proteins and WTA which interacts with DivIC could potentially be useful vaccine antigens. This is clearly a view shared at least in part by Sanofi Pasteur who are investigating a WTA-conjugate vaccine (patent: WO2017064190A1). A WTA based vaccine could potentially reduce carriage of *S. aureus* as WTA is involved in *S. aureus* colonisation of the nares (via interaction with SREC-I[422] which might be involved in uptake and invasion) and the GI tract[423]. Nasal colonisation is dependent on GlcNAc modifications[424] to which antibodies can be raised[425,426], thereby implicating GlcNAc modified WTA as a possible polysaccharide antigen with cross-strain protectivity.

Given the previously mentioned stochasticity of infection[29] there is likely to be a CFU threshold required to establish infection. A required threshold was even shown in the much more reproducible augmented infection model[222] used in Chapter 4. Reducing carriage below this threshold could be enough to protect the majority of hosts from *S. aureus* sepsis or reduce the chance of sepsis thereby lowering the incidence of sepsis across the population. Meta-analyses has previously shown that decolonisation via mupirocin before surgery reduces overall surgical site infection[427] but mupirocin resistance is on the rise with more topical antibacterial agents needed[428].

Vaccination is a viable method of reducing carriage, as demonstrated by the capsular vaccines which have reduced nasal carriage of *H. influenzae*[364] and *S. pneumoniae*[429]. However, reducing carriage can have various unintended consequences. Reducing carriage can open a niche for another bacteria for instance *S. pneumoniae* capsular conjugate vaccine recipients have been shown to have a higher carriage of *S. aureus*[430,431]. Furthermore, given the high rates of *S. aureus* colonisation, eliciting an immune reaction against carriage could potentially cause adverse reactions in the nares and on the skin through excessive inflammation due to commensal *S. aureus*.

Prevention of disease rather than carriage/colonisation requires knowledge of disease dynamics to identify critical points where *S. aureus* pathogenesis may be curtailed. Vaccines have attempted to target *S. aureus* survival within the blood and

adherence to endothelium by targeting virulence factors associated with these such as ClfA. Interestingly, endothelial adhesion is another process in which WTA have been implicated in *in vivo*[104]. One of the main findings of Chapter 4 was that the pro-infectious inoculum such as peptidoglycan needs to be administered concomitantly to augment infection. Vaccination to potentiate barrier immunity might help in this instance however it would be impossible (and ill advised) to completely ablate the commensal flora that might potentiate *S. aureus* infections. Therefore, it would potentially be prudent to focus on dressings or cannulation techniques that further reduce the presence of not only live commensal bacteria but also their remaining cell wall material such as a lysozyme-containing wash.

Based on the current understanding of the infection dynamics of *S. aureus* bacteraemia/sepsis another obvious target would be the immunological bottleneck of the Kupffer cells. *S. aureus* survival in Kupffer cells to seed further infections is a stochastic process which might be shifted through immunomodulation further toward control of infection by potentiating the innate immune capacity. Though the work in this Chapter 5 came about serendipitously via a collaboration with the Minichiello group is does demonstrate that the focus should not be on priming the NGF-β response based on its apparent lack of importance in mammalian anti-*staphylococcal* immunity.

It is clear that greater understanding is required on the pathogenic mechanisms of both host and bacterial factors that lead to severe *S. aureus* disease. However, even if we improve our understanding these areas, we still need to be able to translate these findings from animal models to the clinical setting. One of the most interesting findings of Chapter 4 is that augmented infection represents an immunologically distinct intravenous infection to infection with *S. aureus* alone. It might be optimistically argued that this finding delineates a sepsis model from a bacteraemia model but at the very least it shows that greater appreciation is needed of which pathology our animal models actually imitate. These data from Chapter 4 also strengthens the growing argument that different protections are necessary for different *S. aureus* pathologies. Only through honest scrutiny of the applicability of animal models and systematically assessing vaccine protection against different forms of *S. aureus* infection will we successfully progress the translation of preclinical *S. aureus* vaccines to the clinical setting.

This thesis has shown that NGF-β signalling is not important in phagocytes for mammalian, anti-*Staphylococcal* immunity through infections of *LysM Cre* mice. My work also increases understanding of *S. aureus* cell division by thoroughly demonstrated that the integral division protein DivIC binds to the cell wall through WTA. This provides insight into the role of DivIC and rationale for further study on how teichoic acids contribute to the coordination of cell division and an avenue to target these factors in antibiotic design. In addition, I have further characterised the murine intravenous model of sepsis in demonstrating pro-infectious agents need to be co-administered to augment infection and that co-administration of peptidoglycan predisposes to much greater immune activation. This proves that augmented infection represents a distinct immunological challenge and may delineate models of bacteraemia from models of sepsis therefore increasing the utility of the mouse model in vaccine research.

References

1. Clauditz, A., Resch, A., Wieland, K. P., Peschel, A. & Götz, F. Staphyloxanthin plays a role in the fitness of Staphylococcus aureus and its ability to cope with oxidative stress. *Infect. Immun.* (2006). doi:10.1128/IAI.00204-06

2. Crossley, K. B., Jefferson, K. K., Archer, G. L. & Fowler, V. G. *Staphylococci in Human Disease: Second Edition*. *Staphylococci in Human Disease: Second Edition* (2009). doi:10.1002/9781444308464

3. Lowy, F. D. Staphylococcus aureus infections. *N. Engl. J. Med.* **339**, 520–32 (1998).

4. Argudín, M. Á., Mendoza, M. C. & Rodicio, M. R. Food Poisoning and Staphylococcus aureus Enterotoxins. *Toxins (Basel).* **2**, 1751–1773 (2010).

5. D *et al.* Osteomyelitis. *N. Engl. J. Med.* **336**, 999–1007 (1997).

6. Shi, S. & Xianlong, Z. Interaction of Staphylococcus aureus with osteoblasts (Review). *Experimental and Therapeutic Medicine* (2012). doi:10.3892/etm.2011.423

7. Tong, S. Y. C., Davis, J. S., Eichenberger, E., Holland, T. L. & Fowler, V. G. Staphylococcus aureus infections: Epidemiology, pathophysiology, clinical manifestations, and management. *Clin. Microbiol. Rev.* (2015). doi:10.1128/CMR.00134-14

8. Kim, C. J. *et al.* The burden of nosocomial staphylococcus aureus bloodstream infection in South Korea: A prospective hospital-based nationwide study. *BMC Infect. Dis.* (2014). doi:10.1186/s12879-014-0590-4

9. Wisplinghoff, H. *et al.* Nosocomial bloodstream infections in US hospitals: Analysis of 24,179 cases from a prospective nationwide surveillance study. *Clin. Infect. Dis.* (2004). doi:10.1086/421946

10. Kollef, M. H. *et al.* Epidemiology and outcomes of health-care-associated pneumonia: Results from a large US database of culture-positive pneumonia. *Chest* (2005). doi:10.1378/chest.128.6.3854

11. Reddy, P. N., Srirama, K. & Dirisala, V. R. An Update on Clinical Burden , Diagnostic Tools , and Therapeutic Options of Staphylococcus aureus. (2017). doi:10.1177/1179916117703999

12. Pallin, D. J. *et al.* Increased US Emergency Department Visits for Skin and Soft Tissue Infections, and Changes in Antibiotic Choices, During the Emergence of Community-Associated Methicillin-Resistant Staphylococcus aureus. *Ann. Emerg. Med.* (2008). doi:10.1016/j.annemergmed.2007.12.004

13. Hayward, A. *et al.* Increasing hospitalizations and general practice prescriptions for community-onset staphylococcal disease, England. *Emerg. Infect. Dis.* (2008). doi:10.3201/eid1405.070153

14. Cribier, B. *et al.* Staphylococcus aureus leukocidin: A new virulence factor in cutaneous infections?: An epidemiological and experimental study. *Dermatology* (1992). doi:10.1159/000247443

15. Li, M. *et al.* Comparative analysis of virulence and toxin expression of global community-associated methicillin-resistant Staphylococcus aureus strains. *J. Infect. Dis.* (2010). doi:10.1086/657419

16. Voyich, J. M. *et al.* Is Panton-Valentine leukocidin the major virulence determinant in community-associated methicillin-resistant Staphylococcus aureus disease? *J. Infect. Dis.* (2006). doi:10.1086/509506

17. Löffler, B. *et al.* Staphylococcus aureus panton-valentine leukocidin is a very potent cytotoxic factor for human neutrophils. *PLoS Pathog.* (2010). doi:10.1371/journal.ppat.1000715

18. Soong, G., Chun, J., Parker, D. & Prince, A. Staphylococcus aureus activation of caspase 1/calpain signaling mediates invasion through human keratinocytes. *J. Infect. Dis.* (2012). doi:10.1093/infdis/jis244

19. Chua, K. Y. L. *et al.* Hyperexpression of -hemolysin explains enhanced virulence of sequence type 93 community-associated methicillin-resistant Staphylococcus aureus. *BMC Microbiol.* (2014). doi:10.1186/1471-2180-14-31

20. Cheung, G. Y. C., Joo, H. S., Chatterjee, S. S. & Otto, M. Phenol-soluble modulins - critical determinants of staphylococcal virulence. *FEMS Microbiology Reviews* (2014). doi:10.1111/1574-6976.12057

21. Wang, R. *et al.* Identification of novel cytolytic peptides as key virulence determinants for community-associated MRSA. *Nat. Med.* (2007). doi:10.1038/nm1656

22. Kobayashi, S. D. *et al.* Comparative analysis of USA300 virulence determinants in a rabbit model of skin and soft tissue infection. *J. Infect. Dis.* (2011). doi:10.1093/infdis/jir441

23. Berlon, N. R. *et al.* Clinical MRSA isolates from skin and soft tissue infections show increased in vitro production of phenol soluble modulins. *J. Infect.* (2015). doi:10.1016/j.jinf.2015.06.005

24. Johnson, A. P. *et al.* Mandatory surveillance of methicillin-resistant Staphylococcus aureus (MRSA) bacteraemia in England: The first 10 years. *J. Antimicrob. Chemother.* (2012). doi:10.1093/jac/dkr561

25. Stone, S. P. *et al.* Evaluation of the national Cleanyourhands campaign to reduce Staphylococcus aureus bacteraemia and Clostridium difficile infection in hospitals in England and Wales by improved hand hygiene: Four year, prospective, ecological, interrupted time series stud. *BMJ* (2012). doi:10.1136/bmj.e3005

26. Woll, C. *et al.* Epidemiology and Etiology of Invasive Bacterial Infection in Infants ≤60 Days Old Treated in Emergency Departments. *J. Pediatr.* (2018). doi:10.1016/j.jpeds.2018.04.033

27. Antonio, M. *et al.* Current etiology, clinical features and outcomes of bacteremia in older patients with solid tumors. *J. Geriatr. Oncol.* (2019). doi:10.1016/j.jgo.2018.06.011

28. Munro, A. P. S., Blyth, C. C., Campbell, A. J. & Bowen, A. C. Infection characteristics and treatment of Staphylococcus aureus bacteraemia at a tertiary children's hospital. *BMC Infect. Dis.* (2018). doi:10.1186/s12879-018-3312-5

29. Pollitt, E. J. G., Szkuta, P. T., Burns, N. & Foster, S. J. Staphylococcus aureus infection dynamics. *PLoS Pathog.* (2018). doi:10.1371/journal.ppat.1007112

30. Thwaites, G. E. & Gant, V. Are bloodstream leukocytes Trojan Horses for the metastasis of Staphylococcus aureus? *Nature Reviews Microbiology* (2011). doi:10.1038/nrmicro2508

31. Jorch, S. K. *et al.* Peritoneal GATA6+ macrophages function as a portal for

Staphylococcus aureus dissemination. *J. Clin. Invest.* (2019). doi:10.1172/JCI127286

32. Cheng, A. G. *et al.* Contribution of coagulases towards Staphylococcus aureus disease and protective immunity. *PLoS Pathog.* (2010). doi:10.1371/journal.ppat.1001036

33. Powers, M. E., Kim, H. K., Wang, Y. & Wardenburg, J. B. ADAM10 mediates vascular injury induced by staphylococcus aureus α-hemolysin. *J. Infect. Dis.* (2012). doi:10.1093/infdis/jis192

34. Kwiecinski, J. M. & Horswill, A. R. Staphylococcus aureus bloodstream infections: pathogenesis and regulatory mechanisms. *Current Opinion in Microbiology* (2020). doi:10.1016/j.mib.2020.02.005

35. Theuretzbacher, U. *et al.* Analysis of the clinical antibacterial and antituberculosis pipeline. *The Lancet Infectious Diseases* (2019). doi:10.1016/S1473-3099(18)30513-9

36. O'Neill, J. Antimicrobial Resistance : Tackling a crisis for the health and wealth of nations. *Rev. Antimicrob. Resist.* (2016).

37. Wright, G. D. Something old, something new: Revisiting natural products in Antibiotic drug discovery. *Can. J. Microbiol.* (2014). doi:10.1139/cjm-2014-0063

38. Perros, M. A sustainable model for antibiotics. *Science* (2015). doi:10.1126/science.aaa3048

39. Lowy, F. D. Antimicrobial resistance: The example of Staphylococcus aureus. *Journal of Clinical Investigation* (2003). doi:10.1172/JCI18535

40. Harkins, C. P. *et al.* Methicillin-resistant Staphylococcus aureus emerged long before the introduction of methicillin into clinical practice. *Genome Biol.* (2017). doi:10.1186/s13059-017-1252-9

41. Enright, M. C. *et al.* The evolutionary history of methicillin-resistant Staphylococcus aureus (MRSA). *Proc. Natl. Acad. Sci. U. S. A.* (2002). doi:10.1073/pnas.122108599

42. Cosgrove, S. E. *et al.* Comparison of Mortality Associated with Methicillin-Resistant and Methicillin-Susceptible Staphylococcus aureus Bacteremia: A Meta-analysis. *Clin. Infect. Dis.* **36**, 53–59 (2003).

43. Zeng, D. *et al.* Approved glycopeptide antibacterial drugs: Mechanism of action and resistance. *Cold Spring Harb. Perspect. Med.* (2016). doi:10.1101/cshperspect.a026989

44. Foster, T. J. Antibiotic resistance in Staphylococcus aureus. Current status and future prospects. *FEMS Microbiology Reviews* (2017). doi:10.1093/femsre/fux007

45. Arthur, M., Molinas, C., Depardieu, F. & Courvalin, P. Characterization of Tn1546, a Tn3-related transposon conferring glycopeptide resistance by synthesis of depsipeptide peptidoglycan precursors in Enterococcus faecium BM4147. *J. Bacteriol.* (1993). doi:10.1128/jb.175.1.117-127.1993

46. Ling, L. L. *et al.* A new antibiotic kills pathogens without detectable resistance. *Nature* (2015). doi:10.1038/nature14098

47. Öster, C. *et al.* Structural studies suggest aggregation as one of the modes of action for teixobactin. *Chem. Sci.* (2018). doi:10.1039/c8sc03655a

48. Dcosta, V. M. *et al.* Antibiotic resistance is ancient. *Nature* (2011). doi:10.1038/nature10388

49. Perry, J., Waglechner, N. & Wright, G. The prehistory of antibiotic resistance. *Cold Spring Harb. Perspect. Med.* (2016). doi:10.1101/cshperspect.a025197

50. Hutchings, M., Truman, A. & Wilkinson, B. Antibiotics: past, present and future. *Current Opinion in Microbiology* (2019). doi:10.1016/j.mib.2019.10.008

51. Lipinski, C. A., Lombardo, F., Dominy, B. W. & Feeney, P. J. Experimental and computational approaches to estimate solubility and permeability in drug discovery and development settings. *Advanced Drug Delivery Reviews* (1997). doi:10.1016/S0169-409X(96)00423-1

52. Pidot, S. J. *et al.* Increasing tolerance of hospital Enterococcus faecium to handwash alcohols. *Sci. Transl. Med.* (2018). doi:10.1126/scitranslmed.aar6115

53. Vollmer, W., Blanot, D. & Pedro, M. A. De. Peptidoglycan structure and architecture. **32**, 149–167 (2008).

54. Vollmer, W. Structural variation in the glycan strands of bacterial peptidoglycan. *FEMS Microbiology Reviews* (2008). doi:10.1111/j.1574-6976.2007.00088.x

55. Monteiro, J. M. *et al.* Peptidoglycan synthesis drives an FtsZ-treadmilling-independent step of cytokinesis. *Nature* **554**, 528–532 (2018).

56. Typas, A., Banzhaf, M., Gross, C. A. & Vollmer, W. From the regulation of peptidoglycan synthesis to bacterial growth and morphology. *Nature Reviews Microbiology* (2012). doi:10.1038/nrmicro2677

57. Scheffers, D. J. & Tol, M. B. LipidII: Just Another Brick in the Wall? *PLoS Pathogens* (2015). doi:10.1371/journal.ppat.1005213

58. Pinho, M. G., Kjos, M. & Veening, J. W. How to get (a)round: Mechanisms controlling growth and division of coccoid bacteria. *Nature Reviews Microbiology* (2013). doi:10.1038/nrmicro3088

59. Reed, P. *et al.* Staphylococcus aureus Survives with a Minimal Peptidoglycan Synthesis Machine but Sacrifices Virulence and Antibiotic Resistance. *PLoS Pathog.* (2015). doi:10.1371/journal.ppat.1004891

60. Macheboeuf, P., Contreras-Martel, C., Job, V., Dideberg, O. & Dessen, A. Penicillin binding proteins: Key players in bacterial cell cycle and drug resistance processes. *FEMS Microbiology Reviews* (2006). doi:10.1111/j.1574-6976.2006.00024.x

61. Qamar, A. & Golemi-Kotra, D. Dual roles of FmtA in Staphylococcus aureus cell wall biosynthesis and autolysis. *Antimicrob. Agents Chemother.* (2012). doi:10.1128/AAC.00187-12

62. Zuber, B. *et al.* Granular layer in the periplasmic space of gram-positive bacteria and fine structures of Enterococcus gallinarum and Streptococcus gordonii septa revealed by cryo-electron microscopy of vitreous sections. *J. Bacteriol.* (2006). doi:10.1128/JB.00391-06

63. Sauvage, E., Kerff, F., Terrak, M., Ayala, J. A. & Charlier, P. The penicillin-binding proteins: Structure and role in peptidoglycan biosynthesis. *FEMS Microbiology Reviews* (2008). doi:10.1111/j.1574-6976.2008.00105.x

64. Wolf, A. J. & Underhill, D. M. Peptidoglycan recognition by the innate immune system. *Nat. Rev. Immunol.* **18**, 243–254 (2018).

65. Girardin, S. E. *et al.* Nod2 is a general sensor of peptidoglycan through muramyl dipeptide (MDP) detection. *J. Biol. Chem.* (2003). doi:10.1074/jbc.C200651200

66. Shimada, T. *et al.* Staphylococcus aureus Evades Lysozyme-Based Peptidoglycan Digestion that Links Phagocytosis, Inflammasome Activation, and IL-1β Secretion. *Cell Host Microbe* (2010). doi:10.1016/j.chom.2009.12.008

67. Wolf, A. J. *et al.* Hexokinase Is an Innate Immune Receptor for the Detection of Bacterial Peptidoglycan. *Cell* (2016). doi:10.1016/j.cell.2016.05.076

68. Wang, Z. M. *et al.* Human peptidoglycan recognition protein-L is an N-acetylmuramoyl-L-alanine amidase. *J. Biol. Chem.* (2003). doi:10.1074/jbc.M307758200

69. Liu, C., Xu, Z., Gupta, D. & Dziarski, R. Peptidoglycan recognition proteins: A novel family of four human innate immunity pattern recognition molecules. *J. Biol. Chem.* (2001). doi:10.1074/jbc.M105566200

70. Kashyap, D. R. *et al.* Peptidoglycan recognition proteins kill bacteria by activating protein-sensing two-component systems. *Nat. Med.* (2011). doi:10.1038/nm.2357

71. Schneewind, O., Mihaylova-Petkov, D. & Model, P. Cell wall sorting signals in surface proteins of Gram-positive bacteria. *EMBO J.* (1993). doi:10.1002/j.1460-2075.1993.tb06169.x

72. Mazmanian, S. K., Ton-That, H. & Schneewind, O. Sortase-catalysed anchoring of surface proteins to the cell wall of Staphylococcus aureus. *Molecular Microbiology* (2001). doi:10.1046/j.1365-2958.2001.02411.x

73. Schneewind, O., Model, P. & Fischetti, V. A. Sorting of protein a to the staphylococcal cell wall. *Cell* (1992). doi:10.1016/0092-8674(92)90101-H

74. Mazmanian, S. K., Ton-That, H., Su, K. & Schneewind, O. An iron-regulated sortase anchors a class of surface protein during Staphylococcus aureus pathogenesis. *Proc. Natl. Acad. Sci. U. S. A.* (2002). doi:10.1073/pnas.032523999

75. DeDent, A., Bae, T., Missiakas, D. M. & Schneewind, O. Signal peptides direct surface proteins to two distinct envelope locations of Staphylococcus aureus. *EMBO J.* (2008). doi:10.1038/emboj.2008.185

76. Que, Y. A. *et al.* Fibrinogen and fibronectin binding cooperate for valve infection and invasion in Staphylococcus aureus experimental endocarditis. *J. Exp. Med.* (2005). doi:10.1084/jem.20050125

77. Moreillon, P. *et al.* Role of Staphylococcus aureus coagulase and clumping factor in pathogenesis of experimental endocarditis. *Infect. Immun.* (1995). doi:10.1128/iai.63.12.4738-4743.1995

78. Kwiecinski, J., Jin, T. & Josefsson, E. Surface proteins of Staphylococcus aureus play an important role in experimental skin infection. *APMIS* (2014). doi:10.1111/apm.12295

79. Cheng, A. G. *et al.* Genetic requirements for Staphylococcus aureus abscess formation and persistence in host tissues. *FASEB J.* (2009). doi:10.1096/fj.09-135467

80. Jonsson, I. M., Mazmanian, S. K., Schneewind, O., Bremell, T. & Tarkowski, A. The role of Staphylococcus aureus sortase A and sortase B in murine arthritis. *Microbes Infect.* (2003). doi:10.1016/S1286-4579(03)00143-6

81. Lacey, K. A., Geoghegan, J. A. & McLoughlin, R. M. The role of staphylococcus aureus virulence factors in skin infection and their potential as vaccine antigens. *Pathogens* (2016). doi:10.3390/pathogens5010022

82. Josefsson, E., Hartford, O., O'Brien, L., Patti, J. M. & Foster, T. Protection against

Experimental Staphylococcus aureus Arthritis by Vaccination with Clumping Factor A, a Novel Virulence Determinant . *J. Infect. Dis.* **184**, 1572–1580 (2002).

83. Brown, S., Santa Maria, J. P. & Walker, S. Wall Teichoic Acids of Gram-Positive Bacteria. *Annu. Rev. Microbiol.* (2013). doi:10.1146/annurev-micro-092412-155620

84. Soldo, B., Lazarevic, V. & Karamata, D. tagO is involved in the synthesis of all anionic cell-wall polymers in Bacillus subtilis 168. *Microbiology* (2002). doi:10.1099/00221287-148-7-2079

85. Swoboda, J. G., Campbell, J., Meredith, T. C. & Walker, S. Wall teichoic acid function, biosynthesis, and inhibition. *ChemBioChem* (2010). doi:10.1002/cbic.200900557

86. Tiwari, K. B., Gatto, C., Walker, S. & Wilkinson, B. J. Exposure of staphylococcus aureus to targocil blocks translocation of the major autolysin atl across the membrane, resulting in a significant decrease in autolysis. *Antimicrob. Agents Chemother.* (2018). doi:10.1128/AAC.00323-18

87. Gale, R. T., Li, F. K. K., Sun, T., Strynadka, N. C. J. & Brown, E. D. B. subtilis LytR-CpsA-Psr Enzymes Transfer Wall Teichoic Acids from Authentic Lipid-Linked Substrates to Mature Peptidoglycan In Vitro. *Cell Chem. Biol.* **24**, 1537-1546.e4 (2017).

88. Dengler, V. *et al.* Deletion of hypothetical wall teichoic acid ligases in Staphylococcus aureus activates the cell wall stress response. (2012). doi:10.1111/j.1574-6968.2012.02603.x

89. Over, B. *et al.* LytR-CpsA-Psr proteins in Staphylococcus aureus display partial functional redundancy and the deletion of all three severely impairs septum placement and cell separation. *FEMS Microbiol. Lett.* (2011). doi:10.1111/j.1574-6968.2011.02303.x

90. Brown, S., Meredith, T., Swoboda, J. & Walker, S. Staphylococcus aureus and bacillus subtilis W23 make polyribitol wall teichoic acids using different enzymatic pathways. *Chem. Biol.* (2010). doi:10.1016/j.chembiol.2010.07.017

91. Brown, S., Santa Maria, J. P. & Walker, S. Wall teichoic acids of gram-positive bacteria. *Annu. Rev. Microbiol.* (2013). doi:10.1146/annurev-micro-092412-155620

92. Mistretta, N. *et al.* Glycosylation of Staphylococcus aureus cell wall teichoic acid is influenced by environmental conditions. *Sci. Rep.* (2019). doi:10.1038/s41598-019-39929-1

93. Winstel, V., Xia, G. & Peschel, A. Pathways and roles of wall teichoic acid glycosylation in Staphylococcus aureus. *Int. J. Med. Microbiol.* **304**, 215–221 (2014).

94. Peschel, A. *et al.* Inactivation of the dlt operon in Staphylococcus aureus confers sensitivity to defensins, protegrins, and other antimicrobial peptides. *J. Biol. Chem.* (1999). doi:10.1074/jbc.274.13.8405

95. D'Elia, M. A. *et al.* Lesions in teichoic acid biosynthesis in Staphylococcus aureus lead to a lethal gain of function in the otherwise dispensable pathway. *J. Bacteriol.* (2006). doi:10.1128/JB.00197-06

96. Neuhaus, F. C. & Baddiley, J. A Continuum of Anionic Charge: Structures and Functions of d-Alanyl-Teichoic Acids in Gram-Positive Bacteria. *Microbiol. Mol. Biol. Rev.* (2003). doi:10.1128/mmbr.67.4.686-723.2003

97. Lee, S. H. *et al.* TarO-specific inhibitors of wall teichoic acid biosynthesis restore β-lactam efficacy against methicillin-resistant staphylococci. *Sci. Transl. Med.* (2016).

doi:10.1126/scitranslmed.aad7364

98. Schlag, M. *et al.* Role of staphylococcal wall teichoic acid in targeting the major autolysin Atl. *Mol. Microbiol.* (2010). doi:10.1111/j.1365-2958.2009.07007.x

99. Biswas, R. *et al.* Proton-binding capacity of staphylococcus aureus wall teichoic acid and its role in controlling autolysin activity. *PLoS One* (2012). doi:10.1371/journal.pone.0041415

100. Eugster, M. R. & Loessner, M. J. Wall teichoic acids restrict access of bacteriophage endolysin Ply118, Ply511, and Plyp40 cell wall binding domains to the Listeria monocytogenes peptidoglycan. *J. Bacteriol.* (2012). doi:10.1128/JB.00808-12

101. Soldo, B., Lazarevic, V. & Karamata, D. tagO is involved in the synthesis of all anionic cell-wall polymers in Bacillus subtilis 168 a aThe EMBL accession number for the nucleotide sequence reported in this paper is AJ004803. *Microbiology* (2002). doi:10.1099/00221287-148-7-2079

102. Lazarevic, V. & Karamata, D. The tagGH operon of Bacillus subtilis 168 encodes a two-component ABC transporter involved in the metabolism of two wall teichoic acids. *Mol. Microbiol.* (1995). doi:10.1111/j.1365-2958.1995.tb02306.x

103. Atilano, M. L. *et al.* Teichoic acids are temporal and spatial regulators of peptidoglycan cross-linking in Staphylococcus aureus. *Proc. Natl. Acad. Sci.* **107**, 18991–18996 (2010).

104. Weidenmaier, C. *et al.* Lack of Wall Teichoic Acids in Staphylococcus aureus Leads to Reduced Interactions with Endothelial Cells and to Attenuated Virulence in a Rabbit Model of Endocarditis . *J. Infect. Dis.* (2005). doi:10.1086/429692

105. Jung, Y.-C. *et al.* Synthesis and Biological Activity of Tetrameric Ribitol Phosphate Fragments of *Staphylococcus aureus* Wall Teichoic Acid. *Org. Lett.* acs.orglett.8b01725 (2018). doi:10.1021/acs.orglett.8b01725

106. Weidenmaier, C., Mcloughlin, R. M. & Lee, J. C. The Zwitterionic Cell Wall Teichoic Acid of Staphylococcus aureus Provokes Skin Abscesses in Mice by a Novel CD4 + T-Cell-Dependent Mechanism. **5**, (2010).

107. Jung, Y. C. *et al.* Synthesis and Biological Activity of Tetrameric Ribitol Phosphate Fragments of Staphylococcus aureus Wall Teichoic Acid. *Org. Lett.* (2018). doi:10.1021/acs.orglett.8b01725

108. van Dalen, R. *et al.* Langerhans cells sense Staphylococcus aureus wall teichoic acid through langerin to induce inflammatory responses. *MBio* (2019). doi:10.1128/mBio.00330-19

109. Kurokawa, K. *et al.* Glycoepitopes of Staphylococcal Wall Teichoic Acid Govern Complement-mediated Opsonophagocytosis via Human Serum Antibody and Mannose-binding Lectin * □ S. (2013). doi:10.1074/jbc.M113.509893

110. Wanner, S. *et al.* Wall teichoic acids mediate increased virulence in Staphylococcus aureus. *Nat. Microbiol.* (2017). doi:10.1038/nmicrobiol.2016.257

111. Gerlach, D. *et al.* Methicillin-resistant Staphylococcus aureus alters cell wall glycosylation to evade immunity. *Nature* (2018). doi:10.1038/s41586-018-0730-x

112. Rajagopal, M. & Walker, S. Envelope structures of gram-positive bacteria. in *Current Topics in Microbiology and Immunology* (2017). doi:10.1007/82_2015_5021

113. Gründling, A. & Schneewind, O. Synthesis of glycerol phosphate lipoteichoic acid in Staphylococcus aureus. *Proc. Natl. Acad. Sci. U. S. A.* (2007).

doi:10.1073/pnas.0701821104

114. Kiriukhin, M. Y. & Neuhaus, F. C. D-alanylation of lipoteichoic acid: Role of the D-alanyl carrier protein in acylation. *J. Bacteriol.* (2001). doi:10.1128/JB.183.6.2051-2058.2001

115. Arakawa, H., Shimada, A., Ishimoto, N. & Ito, E. Occurrence of ribitol-containing lipoteichoic acid in Staphylococcus aureus h and its glycosylation. *J. Biochem.* (1981). doi:10.1093/oxfordjournals.jbchem.a133349

116. Hesser, A. R. *et al.* The Length of Lipoteichoic Acid Polymers Controls Staphylococcus aureus Cell Size and Envelope Integrity . *J. Bacteriol.* (2020). doi:10.1128/jb.00149-20

117. Weart, R. B. *et al.* A Metabolic Sensor Governing Cell Size in Bacteria. *Cell* (2007). doi:10.1016/j.cell.2007.05.043

118. Oku, Y. *et al.* Pleiotropic roles of polyglycerolphosphate synthase of lipoteichoic acid in growth of Staphylococcus aureus cells. *J. Bacteriol.* (2009). doi:10.1128/JB.01221-08

119. Santa Maria, J. P. *et al.* Compound-gene interaction mapping reveals distinct roles for Staphylococcus aureus teichoic acids. *Proc. Natl. Acad. Sci. U. S. A.* (2014). doi:10.1073/pnas.1404099111

120. Bæk, K. T. *et al.* The cell wall polymer lipoteichoic acid becomes nonessential in staphylococcus aureus cells lacking the ClpX chaperone. *MBio* (2016). doi:10.1128/mBio.01228-16

121. Fournier, B. & Philpott, D. J. Recognition of Staphylococcus aureus by the innate immune system. *Clin. Microbiol. Rev.* **18**, 521–40 (2005).

122. Pohlmann-Dietze, P. *et al.* Adherence of Staphylococcus aureus to endothelial cells: Influence of capsular polysaccharide, global regulator agr, and bacterial growth phase. *Infect. Immun.* (2000). doi:10.1128/IAI.68.9.4865-4871.2000

123. Thakker, M., Park, J. S., Carey, V. & Lee, J. C. Staphylococcus aureus serotype 5 capsular polysaccharide is antiphagocytic and enhances bacterial virulence in a murine bacteremia model. *Infect. Immun.* (1998). doi:10.1128/iai.66.11.5183-5189.1998

124. Nanra, J. S. *et al.* Capsular polysaccharides are an important immune evasion mechanism for Staphylococcus aureus. in *Human Vaccines and Immunotherapeutics* (2013). doi:10.4161/hv.23223

125. Boyle-Vavra, S. *et al.* USA300 and USA500 clonal lineages of Staphylococcus aureus do not produce a capsular polysaccharide due to conserved mutations in the cap5 locus. *MBio* (2015). doi:10.1128/mBio.02585-14

126. Wann, E. R., Dassy, B., Fournier, J. M. & Foster, T. J. Genetic analysis of the cap5 locus of Staphylococcus aureus. *FEMS Microbiol. Lett.* (1999). doi:10.1016/S0378-1097(98)00528-X

127. O'Riordan, K. & Lee, J. C. Staphylococcus aureus Capsular Polysaccharides. *Clinical Microbiology Reviews* (2004). doi:10.1128/CMR.17.1.218-234.2004

128. Watts, A. *et al.* Staphylococcus aureus strains that express serotype 5 or serotype 8 capsular polysaccharides differ in virulence. *Infect. Immun.* (2005). doi:10.1128/IAI.73.6.3502-3511.2005

129. Renata Arciola, C. *et al.* Polysaccharide intercellular adhesin in biofilm: structural and

regulatory aspects. *Front. Cell. Infect. Microbiol.* **5**, (2015).

130. O'Gara, J. P. ica and beyond: Biofilm mechanisms and regulation in Staphylococcus epidermidis and Staphylococcus aureus. *FEMS Microbiology Letters* (2007). doi:10.1111/j.1574-6968.2007.00688.x

131. Vuong, C. *et al.* A crucial role for exopolysaccharide modification in bacterial biofilm formation, immune evasion, and virulence. *J. Biol. Chem.* (2004). doi:10.1074/jbc.M411374200

132. Maira-Litrán, T. *et al.* Immunochemical properties of the Staphylococcal poly-N-acetylglucosamine surface polysaccharide. *Infect. Immun.* (2002). doi:10.1128/IAI.70.8.4433-4440.2002

133. Maira-Litrán, T. *et al.* Synthesis and Evaluation of a Conjugate Vaccine Composed of Staphylococcus aureus Poly-N-Acetyl-Glucosamine and Clumping Factor A. *PLoS One* (2012). doi:10.1371/journal.pone.0043813

134. Steele, V. R., Bottomley, A. L., Garcia-Lara, J., Kasturiarachchi, J. & Foster, S. J. Multiple essential roles for EzrA in cell division of Staphylococcus aureus. *Mol. Microbiol.* (2011). doi:10.1111/j.1365-2958.2011.07591.x

135. Pinho, M. G. & Errington, J. Recruitment of penicillin-binding protein PBP2 to the division site of Staphylococcus aureus is dependent on its transpeptidation substrates. *Mol. Microbiol.* **55**, 799–807 (2005).

136. Eswara, P. J. *et al.* An essential staphylococcus aureus cell division protein directly regulates ftsz dynamics. *Elife* (2018). doi:10.7554/eLife.38856

137. Loose, M. & Mitchison, T. J. The bacterial cell division proteins ftsA and ftsZ self-organize into dynamic cytoskeletal patterns. *Nat. Cell Biol.* (2014). doi:10.1038/ncb2885

138. Pichoff, S. & Lutkenhaus, J. Unique and overlapping roles for ZipA and FtsA in septal ring assembly in Escherichia coli. *EMBO J.* (2002). doi:10.1093/emboj/21.4.685

139. Veiga, H. & G. Pinho, M. Staphylococcus aureus requires at least one FtsK/SpoIIIE protein for correct chromosome segregation. *Mol. Microbiol.* (2017). doi:10.1111/mmi.13572

140. Pereira, S. F. F., Henriques, A. O., Pinho, M. G., De Lencastre, H. & Tomasz, A. Evidence for a dual role of PBP1 in the cell division and cell separation of Staphylococcus aureus. *Mol. Microbiol.* (2009). doi:10.1111/j.1365-2958.2009.06687.x

141. Pinho, M. G., Filipe, S. R., De Lencastre, H. & Tomasz, A. Complementation of the essential peptidoglycan transpeptidase function of penicillin-binding protein 2 (PBP2) by the drug resistance protein PBP2A in Staphylococcus aureus. *J. Bacteriol.* (2001). doi:10.1128/JB.183.22.6525-6531.2001

142. Reichmann, N. T. *et al.* SEDS–bPBP pairs direct lateral and septal peptidoglycan synthesis in Staphylococcus aureus. *Nat. Microbiol.* (2019). doi:10.1038/s41564-019-0437-2

143. WYKE, A. W., WARD, J. B., HAYES, M. V. & CURTIS, N. A. C. A Role in vivo for Penicillin-Binding Protein-4 of Staphylococcus aureus. *Eur. J. Biochem.* (1981). doi:10.1111/j.1432-1033.1981.tb05620.x

144. Hamilton, S. M. *et al.* High-level resistance of staphylococcus aureus to β-Lactam antibiotics mediated by penicillin-binding protein 4 (PBP4). *Antimicrob. Agents Chemother.* (2017). doi:10.1128/AAC.02727-16

145. Noirclerc-savoye, M. *et al.* In vitro reconstitution of a trimeric complex of DivIB , DivIC and FtsL , and their transient co-localization at the division site in Streptococcus pneumoniae. **55**, 413–424 (2005).

146. Buddelmeijer, N. & Beckwith, J. A complex of the Escherichia coli cell division proteins FtsL, FtsB and FtsQ forms independently of its localization to the septal region. *Mol. Microbiol.* **52**, 1315–1327 (2004).

147. Glas, M. *et al.* The Soluble Periplasmic Domains of Escherichia coli Cell Division Proteins FtsQ / FtsB / FtsL Form a Trimeric Complex with Submicromolar Affinity * □. **290**, 21498–21509 (2015).

148. Katis, V. L. & Wake, R. G. Membrane-bound division proteins DivIB and DivIC of Bacillus subtilis function solely through their external domains in both vegetative and sporulation division. *J. Bacteriol.* (1999). doi:10.1128/jb.181.9.2710-2718.1999

149. Daniel, R. A. & Errington, J. Intrinsic instability of the essential cell division protein FtsL of Bacillus subtilis and a role for DivlB protein in FtsL turnover. *Mol. Microbiol.* (2000). doi:10.1046/j.1365-2958.2000.01857.x

150. Bottomley, A. L. *et al.* Staphylococcus aureusDivIB is a peptidoglycan-binding protein that is required for a morphological checkpoint in cell division. *Mol. Microbiol.* **94**, 1041–1064 (2014).

151. Boes, A., Olatunji, S., Breukink, E. & Terrak, M. Regulation of the peptidoglycan polymerase activity of PBP1b by antagonist actions of the core divisome proteins FtsBLQ and FtsN. *MBio* **10**, 1–16 (2019).

152. den Blaauwen, T. & Luirink, J. Checks and Balances in Bacterial Cell Division. *MBio* **10**, 1–5 (2019).

153. Pasquina-Lemonche, L. *et al.* The architecture of the Gram-positive bacterial cell wall. *Nature* (2020). doi:10.1038/s41586-020-2236-6

154. Holmes, K. K. *et al.* Major Infectious Diseases: Key Messages from Disease Control Priorities, Third Edition. in *Disease Control Priorities, Third Edition (Volume 6): Major Infectious Diseases* (2017). doi:10.1596/978-1-4648-0524-0_ch1

155. Karauzum, H. *et al.* Lethal CD4 T cell responses induced by vaccination against Staphylococcus aureus bacteremia. *J. Infect. Dis.* (2017). doi:10.1093/infdis/jix096

156. Kuchar, E., Karlikowska-Skwarnik, M., Han, S. & Nitsch-Osuch, A. Pertussis: History of the disease and current prevention failure. *Adv. Exp. Med. Biol.* (2016). doi:10.1007/5584_2016_21

157. IPSEN, J. Circulating antitoxin at the onset of diphtheria in 425 patients. *J. Immunol.* (1946).

158. Plotkin, S. A. Correlates of vaccine-induced immunity. *Clinical Infectious Diseases* (2008). doi:10.1086/589862

159. MCCOMB, J. A. THE PROPHYLACTIC DOSE OF HOMOLOGOUS TETANUS ANTITOXIN. *N. Engl. J. Med.* (1964). doi:10.1056/NEJM196401232700404

160. Fowler, V. G. *et al.* Effect of an investigational vaccine for preventing Staphylococcus aureus infections after cardiothoracic surgery: A randomized trial. *JAMA - J. Am. Med. Assoc.* (2013). doi:10.1001/jama.2013.3010

161. McNeely, T. B. *et al.* Mortality among recipients of the Merck V710 Staphylococcus aureus vaccine after postoperative S. aureus infections: An analysis of possible contributing host factors. *Hum. Vaccines Immunother.* (2014). doi:10.4161/hv.34407

162. Creech, C. B. *et al.* Safety, tolerability, and immunogenicity of a single dose 4-antigen or 3-antigen Staphylococcus aureus vaccine in healthy older adults: Results of a randomised trial. *Vaccine* **35**, 385–394 (2017).

163. Inoue, M. *et al.* Safety, tolerability, and immunogenicity of a novel 4-antigen Staphylococcus aureus vaccine (SA4Ag) in healthy Japanese adults. *Hum. Vaccines Immunother.* **14**, 2682–2691 (2018).

164. Frenck, R. W. *et al.* Safety, tolerability, and immunogenicity of a 4-antigen Staphylococcus aureus vaccine (SA4Ag): Results from a first-in-human randomised, placebo-controlled phase 1/2 study. *Vaccine* (2017). doi:10.1016/j.vaccine.2016.11.010

165. Anderson, A. S. *et al.* Development of a multicomponent Staphylococcus aureus vaccine designed to counter multiple bacterial virulence factors. *Human Vaccines and Immunotherapeutics* (2012). doi:10.4161/hv.21872

166. Stranger-Jones, Y. K., Bae, T. & Schneewind, O. Vaccine assembly from surface proteins of Staphylococcus aureus. *Proc. Natl. Acad. Sci. U. S. A.* (2006). doi:10.1073/pnas.0606863103

167. Dagan, R. *et al.* Serum serotype-specific pneumococcal anticapsular immunoglobulin G concentrations after immunization with a 9-valent conjugate pneumococcal vaccine correlate with nasopharyngeal acquisition of pneumococcus. *J. Infect. Dis.* (2005). doi:10.1086/431679

168. Whitney, C. G. *et al.* Decline in invasive pneumococcal disease after the introduction of protein-polysaccharide conjugate vaccine. *N. Engl. J. Med.* (2003). doi:10.1056/NEJMoa022823

169. Fernandez, J. *et al.* Prevention of Haemophilus influenzae type b colonization by vaccination: Correlation with serum anti-capsular IgG concentration. *J. Infect. Dis.* (2000). doi:10.1086/315870

170. Fattom, A. *et al.* Safety and immunogenicity of a booster dose of Staphylococcus aureus types 5 and 8 capsular polysaccharide conjugate vaccine (StaphVAX ®) in hemodialysis patients. *Vaccine* (2004). doi:10.1016/j.vaccine.2004.06.043

171. Schaffer, A. C. & Lee, J. C. Vaccination and passive immunisation against Staphylococcus aureus. *Int. J. Antimicrob. Agents* (2008). doi:10.1016/j.ijantimicag.2008.06.009

172. Pfizer Inc (Jessica Smith). Independent Data Monitoring Committee Recommends Discontinuation of the Phase 2b STRIVE Clinical Trial of Staphylococcus aureus Vaccine Following Planned Interim Analysis. *Businesswire A Berkshire Hathaway compay* (2019). Available at: https://www.businesswire.com/news/home/20181220005911/en/. (Accessed: 10th August 2020)

173. Plotkin, S. A. Correlates of Vaccine-Induced Immunity. **18902**, (2008).

174. Wertheim, H. F. *et al.* Risk and outcome of nosocomial Staphylococcus aureus bacteraemia in nasal carriers versus non-carriers. *Lancet* **364**, 703–705 (2004).

175. Redi, D., Raffaelli, C. S., Rossetti, B., De Luca, A. & Montagnani, F. Staphylococcus aureus vaccine preclinical and clinical development: Current state of the art. *New Microbiol.* (2018).

176. Levy, J. *et al.* Safety and immunogenicity of an investigational 4-component Staphylococcus aureus vaccine with or without AS03 B adjuvant : Results of a

randomized phase I trial. **11**, 620–631 (2015).

177. Schmidt, C. S. *et al.* NDV-3, a recombinant alum-adjuvanted vaccine for Candida and Staphylococcus aureus, is safe and immunogenic in healthy adults. *Vaccine* (2012). doi:10.1016/j.vaccine.2012.10.038

178. Giersing, B. K., Dastgheyb, S. S., Modjarrad, K. & Moorthy, V. Status of vaccine research and development of vaccines for Staphylococcus aureus. *Vaccine* (2016). doi:10.1016/j.vaccine.2016.03.110

179. Roetzer, A., Jilma, B. & Eibl, M. M. Vaccine against toxic shock syndrome in a first-in-man clinical trial. *Expert Review of Vaccines* (2017). doi:10.1080/14760584.2017.1268921

180. Chen, W. H. *et al.* Safety and immunogenicity of a parenterally administered, structure-based rationally modified recombinant staphylococcal enterotoxin B protein vaccine, STEBVax. *Clin. Vaccine Immunol.* (2016). doi:10.1128/CVI.00399-16

181. Landrum, M. L. *et al.* Safety and immunogenicity of a recombinant Staphylococcus aureus α-toxoid and a recombinant Panton-Valentine leukocidin subunit, in healthy adults. *Hum. Vaccines Immunother.* (2017). doi:10.1080/21645515.2016.1248326

182. Fattom, A. *et al.* Efficacy profile of a bivalent Staphylococcus aureus glycoconjugated vaccine in adults on hemodialysis: Phase III randomized study. *Hum. Vaccines Immunother.* (2015). doi:10.4161/hv.34414

183. Verkaik, N. J. *et al.* Induction of antibodies by Staphylococcus aureus nasal colonization in young children. *Clin. Microbiol. Infect.* **16**, 1312–1317 (2010).

184. Forsgren, A. & Quie, P. G. Effects of staphylococcal protein A on heat labile opsonins. *J. Immunol.* (1974).

185. Hoernes, M., Seger, R. & Reichenbach, J. Modern management of primary B-cell immunodeficiencies. *Pediatric Allergy and Immunology* (2011). doi:10.1111/j.1399-3038.2011.01236.x

186. Dhalla, F. & Misbah, S. A. Secondary antibody deficiencies. *Current Opinion in Allergy and Clinical Immunology* (2015). doi:10.1097/ACI.0000000000000215

187. Spellberg, B. *et al.* The antifungal vaccine derived from the recombinant N terminus of Als3p protects mice against the bacterium Staphylococcus aureus. *Infect. Immun.* **76**, 4574–80 (2008).

188. Gjertsson, I., Hultgren, O. H., Stenson, M., Holmdahl, R. & Tarkowski, A. Are B lymphocytes of importance in severe Staphylococcus aureus infections? *Infect. Immun.* (2000). doi:10.1128/IAI.68.5.2431-2434.2000

189. Romagnani, S. T-cell subsets (Th1 versus Th2). *Annals of Allergy, Asthma and Immunology* (2000). doi:10.1016/S1081-1206(10)62426-X

190. Brown, A. F. *et al.* Memory Th1 Cells Are Protective in Invasive Staphylococcus aureus Infection. *PLoS Pathog.* **11**, 1–32 (2015).

191. Nippe, N. *et al.* Subcutaneous infection with S. aureus in mice reveals association of resistance with influx of neutrophils and Th2 response. *J. Invest. Dermatol.* (2011). doi:10.1038/jid.2010.282

192. Xu, W., Tian, K., Li, X. & Zhang, S. IL-9 blockade attenuates inflammation in a murine model of methicillin-resistant Staphylococcus aureus pneumonia. *Acta Biochim. Biophys. Sin. (Shanghai).* (2020). doi:10.1093/abbs/gmz149

193. Leech, J. M., Lacey, K. A., Mulcahy, M. E., Mcloughlin, R. M. & Mcloughlin, R. M. IL-10 Plays Opposing Roles during Staphylococcus aureus Systemic and Localized Infections. (2018). doi:10.4049/jimmunol.1601018

194. Prajsnar, T. K. *et al.* A privileged intraphagocyte niche is responsible for disseminated infection of Staphylococcus aureus in a zebrafish model. **14**, 1600–1619 (2012).

195. Miller, L. S., Fowler, V. G., Shukla, S. K., Rose, W. E. & Proctor, R. A. Development of a vaccine against Staphylococcus aureus invasive infections: Evidence based on human immunity, genetics and bacterial evasion mechanisms. *FEMS Microbiology Reviews* (2019). doi:10.1093/femsre/fuz030

196. O'Brien, E. C. & McLoughlin, R. M. Considering the 'Alternatives' for Next-Generation Anti-Staphylococcus aureus Vaccine Development. *Trends Mol. Med.* **25**, 171–184 (2019).

197. Nielsen, M. M., Witherden, D. A. & Havran, W. L. γδ T cells in homeostasis and host defence of epithelial barrier tissues. *Nature Reviews Immunology* (2017). doi:10.1038/nri.2017.101

198. Lalor, S. J. & McLoughlin, R. M. Memory γδ T Cells–Newly Appreciated Protagonists in Infection and Immunity. *Trends in Immunology* (2016). doi:10.1016/j.it.2016.07.006

199. Maher, B. M. *et al.* Nlrp-3-driven interleukin 17 production by γδT cells controls infection outcomes during staphylococcus aureus surgical site infection. *Infect. Immun.* **81**, 4478–4489 (2013).

200. Sutton, C. E. *et al.* Interleukin-1 and IL-23 Induce Innate IL-17 Production from γδ T Cells, Amplifying Th17 Responses and Autoimmunity. *Immunity* (2009). doi:10.1016/j.immuni.2009.08.001

201. Murphy, A. G. *et al.* Staphylococcus aureus Infection of Mice Expands a Population of Memory γδ T Cells That Are Protective against Subsequent Infection . *J. Immunol.* (2014). doi:10.4049/jimmunol.1303420

202. Dillen, C. A. *et al.* Clonally expanded γδ T cells protect against Staphylococcus aureus skin reinfection. *J. Clin. Invest.* (2018). doi:10.1172/JCI96481

203. Cheng, P. *et al.* Role of gamma-delta T cells in host response against Staphylococcus aureus-induced pneumonia. *BMC Immunol.* (2012). doi:10.1186/1471-2172-13-38

204. Bambery, B., Selgelid, M., Weijer, C., Savulescu, J. & Pollard, A. J. Ethical criteria for human challenge studies in infectious diseases. *Public Health Ethics* (2016). doi:10.1093/phe/phv026

205. Waddington, C. S. *et al.* An outpatient, ambulant-design, controlled human infection model using escalating doses of salmonella typhi challenge delivered in sodium bicarbonate solution. *Clin. Infect. Dis.* (2014). doi:10.1093/cid/ciu078

206. Sweeney, E., Lovering, A. M., Bowker, K. E., MacGowan, A. P. & Nelson, S. M. An in vitro biofilm model of Staphylococcus aureus infection of bone. *Lett. Appl. Microbiol.* (2019). doi:10.1111/lam.13131

207. Sifri, C. D., Begun, J., Ausubel, F. M. & Calderwood, S. B. Caenorhabditis elegans as a model host for Staphylococcus aureus pathogenesis. *Infect. Immun.* (2003). doi:10.1128/IAI.71.4.2208-2217.2003

208. Pollitt, E. J. G., West, S. A., Crusz, S. A., Burton-Chellew, M. N. & Diggle, S. P. Cooperation, quorum sensing, and evolution of virulence in Staphylococcus aureus. *Infect. Immun.* (2014). doi:10.1128/IAI.01216-13

209. Needham, A. J., Kibart, M., Crossley, H., Ingham, P. W. & Foster, S. J. Drosophila melanogaster as a model host for Staphylococcus aureus infection. *Microbiology* (2004). doi:10.1099/mic.0.27116-0

210. Zhang, X. *et al.* A rabbit model of implant-related osteomyelitis inoculated with biofilm after open femoral fracture. *Exp. Ther. Med.* (2017). doi:10.3892/etm.2017.5138

211. Reinoso, E., Magnano, G., Giraudo, J., Calzolari, A. & Bogni, C. Bovine and rabbit models for the study of a Staphylococcus aureus avirulent mutant strain, RC122. *Can. J. Vet. Res.* **66**, 285–288 (2002).

212. Watts, J. L. Etiological agents of bovine mastitis. *Vet. Microbiol.* **16**, 41–66 (1988).

213. Soge, O. O. *et al.* Transmission of MDR MRSA between primates, their environment and personnel at a United States primate centre. *J. Antimicrob. Chemother.* (2016). doi:10.1093/jac/dkw236

214. Hepburn, L. *et al.* A Spaetzle-like role for nerve growth factor β in vertebrate immunity to Staphylococcus aureus. *Science (80-.).* (2014). doi:10.1126/science.1258705

215. Gomes, M. C. & Mostowy, S. The Case for Modeling Human Infection in Zebrafish. *Trends in Microbiology* (2020). doi:10.1016/j.tim.2019.08.005

216. Herbomel, P., Thisse, B. & Thisse, C. Ontogeny and behaviour of early macrophages in the zebrafish embryo. *Development* (1999).

217. Crowhurst, M. O., Layton, J. E. & Lieschke, G. J. Developmental biology of zebrafish myeloid cells. *Int. J. Dev. Biol.* (2002). doi:10.1387/ijdb.12141435

218. Prajsnar, T. K., Cunliffe, V. T., Foster, S. J. & Renshaw, S. A. A novel vertebrate model of Staphylococcus aureus infection reveals phagocyte-dependent resistance of zebrafish to non-host specialized pathogens. *Cell. Microbiol.* (2008). doi:10.1111/j.1462-5822.2008.01213.x

219. Trede, N. S., Langenau, D. M., Traver, D., Look, A. T. & Zon, L. I. The use of zebrafish to understand immunity. *Immunity* (2004). doi:10.1016/S1074-7613(04)00084-6

220. Von Köckritz-Blickwede, M. *et al.* Immunological mechanisms underlying the genetic predisposition to severe staphylococcus aureus infection in the mouse model. *Am. J. Pathol.* **173**, 1657–1668 (2008).

221. Waterston, R. H. *et al.* Initial sequencing and comparative analysis of the mouse genome. *Nature* (2002). doi:10.1038/nature01262

222. Boldock, E. *et al.* Human skin commensals augment Staphylococcus aureus pathogenesis. *Nat. Microbiol.* **3**, 881–890 (2018).

223. Tanaka, H., Miyazaki, S., Sumiyama, Y. & Kakiuchi, T. Role of macrophages in a mouse model of postoperative MRSA enteritis. *J. Surg. Res.* (2004). doi:10.1016/S0022-4804(03)00355-X

224. Becker, R. E. N., Berube, B. J., Sampedro, G. R., Dedent, A. C. & Bubeck Wardenburg, J. Tissue-specific patterning of host innate immune responses by staphylococcus aureus α-Toxin. *J. Innate Immun.* (2014). doi:10.1159/000360006

225. Holtfreter, S. *et al.* Characterization of a mouse-adapted Staphylococcus aureus strain. *PLoS One* **8**, (2013).

226. Shultz, L. D., Ishikawa, F. & Greiner, D. L. Humanized mice in translational biomedical research. *Nature Reviews Immunology* (2007). doi:10.1038/nri2017

227. Prince, A., Wang, H., Kitur, K. & Parker, D. Humanized mice exhibit increased susceptibility to staphylococcus aureus pneumonia. *J. Infect. Dis.* (2017). doi:10.1093/infdis/jiw425

228. Horsburgh, M. J. *et al.* δb modulates virulence determinant expression and stress resistance: Characterization of a functional rsbU strain derived from Staphylococcus aureus 8325-4. *J. Bacteriol.* (2002). doi:10.1128/JB.184.19.5457-5467.2002

229. Kreiswirth, B. N. *et al.* The toxic shock syndrome exotoxin structural gene is not detectably transmitted by a prophage. *Nature* (1983). doi:10.1038/305709a0

230. Weiss, W. J. *et al.* Effect of srtA and srtB gene expression on the virulence of Staphylococcus aureus in animal models of infection. *J. Antimicrob. Chemother.* (2004). doi:10.1093/jac/dkh078

231. Streker, K., Freiberg, C., Labischinski, H., Hacker, J. & Ohlsen, K. Staphylococcus aureus NfrA (SA0367) is a flavin mononucleotide-dependent NADPH oxidase involved in oxidative stress response. *J. Bacteriol.* (2005). doi:10.1128/JB.187.7.2249-2256.2005

232. Viana, D. *et al.* A single natural nucleotide mutation alters bacterial pathogen host tropism. *Nat. Genet.* (2015). doi:10.1038/ng.3219

233. Fey, P. D. *et al.* A genetic resource for rapid and comprehensive phenotype screening of nonessential Staphylococcus aureus genes. *MBio* (2013). doi:10.1128/mBio.00537-12

234. Valle, J. *et al.* SarA and not σB is essential for biofilm development by Staphylococcus aureus. *Mol. Microbiol.* (2003). doi:10.1046/j.1365-2958.2003.03493.x

235. Vergara-Irigaray, M. *et al.* Wall teichoic acids are dispensable for anchoring the PNAG exopolysaccharide to the Staphylococcus aureus cell surface. *Microbiology* (2008). doi:10.1099/mic.0.2007/013292-0

236. Mcvicker, G. *et al.* Clonal Expansion during Staphylococcus aureus Infection Dynamics Reveals the Effect of Antibiotic Intervention. **10**, (2014).

237. O'Connell, D. P. *et al.* The fibrinogen-binding MSCRAMM (clumping factor) of staphylococcus aureus Has a Ca2+-dependent inhibitory site. *J. Biol. Chem.* **273**, 6821–6829 (1998).

238. Minichiello, L. *et al.* Essential role for TrkB receptors in hippocampus-mediated learning. *Neuron* (1999). doi:10.1016/S0896-6273(00)80853-3

239. Schito, G. C. The importance of the development of antibiotic resistance in Staphylococcus aureus. *Clinical Microbiology and Infection* (2006). doi:10.1111/j.1469-0691.2006.01343.x

240. Chambers, H. F. & DeLeo, F. R. Waves of resistance: Staphylococcus aureus in the antibiotic era. *Nature Reviews Microbiology* (2009). doi:10.1038/nrmicro2200

241. Chaudhuri, R. R. *et al.* Comprehensive identification of essential Staphylococcus aureus genes using Transposon-Mediated Differential Hybridisation (TMDH). *BMC Genomics* (2009). doi:10.1186/1471-2164-10-291

242. Daniel, R. A., Noirot-Gros, M.-F., Noirot, P. & Errington, J. Multiple Interactions between the Transmembrane Division Proteins of Bacillus subtilis and the Role of FtsL Instability in Divisome Assembly. *J. Bacteriol.* **188**, 7396–7404 (2006).

243. Bennett, J. A., Aimino, R. M. & McCormick, J. R. Streptomyces coelicolor genes ftsL and divIC play a role in cell division but are dispensable for colony formation. *J.*

Bacteriol. (2007). doi:10.1128/JB.01303-07

244. Levin, P. A. & Losick, R. Characterization of a cell division gene from Bacillus subtilis that is required for vegetative and sporulation septum formation. *J. Bacteriol.* (1994). doi:10.1128/jb.176.5.1451-1459.1994

245. Kent, V. Cell wall architecture and the role of wall teichoic acid in Staphylococcus aureus. 242 (2013).

246. Reichmann, N. T. *et al.* Differential localization of LTA synthesis proteins and their interaction with the cell division machinery in Staphylococcus aureus. *Mol. Microbiol.* (2014). doi:10.1111/mmi.12551

247. Kabli, A. F. Identification and Characterisation of Cell Division Proteins in Staphylococcus aureus. 284 (2013).

248. Pasquina-Lemonche, L. *et al.* The architecture of the Gram-positive bacterial cell wall. *Nature* 1–4 (2020). doi:10.1038/s41586-020-2236-6

249. De Jonge, B. L. M., Chang, Y. S., Gage, D. & Tomasz, A. Peptidoglycan composition of a highly methicillin-resistant Staphylococcus aureus strain. The role of penicillin binding protein 2A. *J. Biol. Chem.* (1992).

250. Jurgens, U. J. & Weckesser, J. Polysaccharide covalently linked to the peptidoglycan of the cyanobacterium Synechocystis sp. strain PCC6714. *J. Bacteriol.* (1986). doi:10.1128/jb.168.2.568-573.1986

251. Larson, T. R. & Yother, J. Streptococcus pneumoniae capsular polysaccharide is linked to peptidoglycan via a direct glycosidic bond to β-D-N-acetylglucosamine. *Proc. Natl. Acad. Sci. U. S. A.* (2017). doi:10.1073/pnas.1620431114

252. Endl, J., Seidl, H. P., Fiedler, F. & Schleider, K. H. Chemical composition and structure of cell wall teichoic acids of staphylococci. *Arch. Microbiol.* (1983). doi:10.1007/BF00414483

253. Calamita, H. G., Ehringer, W. D., Koch, A. L. & Doyle, R. J. Evidence that the cell wall of Bacillus subtilis is protonated during respiration. *Proc. Natl. Acad. Sci. U. S. A.* (2001). doi:10.1073/pnas.261483798

254. Kemper, M. A., Urrutia, M. M., Beveridge, T. J., Koch, A. L. & Doyle, R. J. Proton motive force may regulate cell wall-associated enzymes of Bacillus subtilis. *J. Bacteriol.* (1993). doi:10.1128/jb.175.17.5690-5696.1993

255. Bottomley, A. L. Identification and characterisation of the cell division machinery in Staphylococcus aureus. 288 (2011).

256. Groisman, E. A. *et al.* Bacterial Mg 2+ Homeostasis, Transport, and Virulence . *Annu. Rev. Genet.* (2013). doi:10.1146/annurev-genet-051313-051025

257. Kurokawa, K., Takahashi, K. & Lee, B. L. The staphylococcal surface-glycopolymer wall teichoic acid (WTA) is crucial for complement activation and immunological defense against Staphylococcus aureus infection. *Immunobiology* (2016). doi:10.1016/j.imbio.2016.06.003

258. Xia, G., Kohler, T. & Peschel, A. The wall teichoic acid and lipoteichoic acid polymers of Staphylococcus aureus. *Int. J. Med. Microbiol.* **300**, 148–154 (2010).

259. Bera, A., Herbert, S., Jakob, A., Vollmer, W. & Götz, F. Why are pathogenic staphylococci so lysozyme resistant? The peptidoglycan O-acetyltransferase OatA is the major determinant for lysozyme resistance of Staphylococcus aureus. *Mol. Microbiol.* (2005). doi:10.1111/j.1365-2958.2004.04446.x

260. Li, H., Nooh, M. M., Kotb, M. & Re, F. Commercial peptidoglycan preparations are contaminated with superantigen-like activity that stimulates IL-17 production. *J. Leukoc. Biol.* (2008). doi:10.1189/jlb.0807588

261. S, B., Jr, S. M. J. & S, W. Wall Teichoic Acids of Gram-Positive Bacteria. *Annu. Rev. Microbiol.* **67**, 313–336 (2013).

262. Sadovskaya, I. *et al.* Another Brick in the Wall: a Rhamnan Polysaccharide Trapped inside Peptidoglycan of Lactococcus lactis . *MBio* **8**, 1–16 (2017).

263. Rachid, S. *et al.* Alternative transcription factor σB is involved in regulation of biofilm expression in a Staphylococcus aureus mucosal isolate. *J. Bacteriol.* (2000). doi:10.1128/JB.182.23.6824-6826.2000

264. Giachino, P., Engelmann, S. & Bischoff, M. σB activity depends on RsbU in Staphylococcus aureus. *J. Bacteriol.* (2001). doi:10.1128/JB.183.6.1843-1852.2001

265. Chan, Y. G. Y., Kim, H. K., Schneewind, O. & Missiakas, D. The capsular polysaccharide of Staphylococcus aureus is attached to peptidoglycan by the LytR-CpsA-Psr (LCP) family of enzymes. *J. Biol. Chem.* **289**, 15680–15690 (2014).

266. Rausch, M. *et al.* Coordination of capsule assembly and cell wall biosynthesis in Staphylococcus aureus. *Nat. Commun.* **10**, (2019).

267. Kneidinger, B. *et al.* Three highly conserved proteins catalyze the conversion of UDP-N-acetyl-D-glucosamine to precursors for the biosynthesis of O antigen in Pseudomonas aeruginosa O11 and capsule in Staphylococcus aureus type 5: Implications for the UDP-N-acetyl-L-fucosamine. *J. Biol. Chem.* (2003). doi:10.1074/jbc.M203867200

268. Campbell, J. *et al.* Synthetic lethal compound combinations reveal a fundamental connection between wall teichoic acid and peptidoglycan biosyntheses in staphylococcus aureus. *ACS Chem. Biol.* (2011). doi:10.1021/cb100269f

269. Li, X. *et al.* An accessory wall teichoic acid glycosyltransferase protects Staphylococcus aureus from the lytic activity of Podoviridae. *Sci. Rep.* (2015). doi:10.1038/srep17219

270. Endl, J., Seidl, P. H., Fiedler, F. & Schleifer, K. H. Determination of cell wall teichoic acid structure of staphylococci by rapid chemical and serological screening methods. *Arch. Microbiol.* (1984). doi:10.1007/BF00414557

271. Chen, Y. F., Yin, Y. N., Zhang, X. M. & Guo, J. H. Curtobacterium flaccumfaciens pv. beticola, a new pathovar of pathogens in sugar beet. *Plant Dis.* (2007). doi:10.1094/PDIS-91-6-0677

272. Schleifer, K. H. & Kandler, O. Peptidoglycan types of bacterial cell walls and their taxonomic implications. *Bacteriological reviews* (1972). doi:10.1128/mmbr.36.4.407-477.1972

273. Adams, N. B. P., Vasilev, C., Brindley, A. A. & Hunter, C. N. Nanomechanical and Thermophoretic Analyses of the Nucleotide-Dependent Interactions between the AAA+ Subunits of Magnesium Chelatase. *J. Am. Chem. Soc.* (2016). doi:10.1021/jacs.6b02827

274. Yahashiri, A., Jorgenson, M. A. & Weiss, D. S. The SPOR domain, a widely conserved peptidoglycan binding domain that targets proteins to the site of cell division. *J. Bacteriol.* (2017). doi:10.1128/JB.00118-17

275. Kirby, A. J. The lysozyme mechanism sorted - After 50 years. *Nature Structural*

Biology (2001). doi:10.1038/nsb0901-737

276. Pushkaran, A. C. *et al.* Understanding the structure-function relationship of lysozyme resistance in Staphylococcus aureus by peptidoglycan o-acetylation using molecular docking, dynamics, and lysis assay. *J. Chem. Inf. Model.* (2015). doi:10.1021/ci500734k

277. Gonzalez-Delgado, L. S. *et al.* Two-site recognition of Staphylococcus aureus peptidoglycan by lysostaphin SH3b. *Nat. Chem. Biol.* (2020). doi:10.1038/s41589-019-0393-4

278. Chan, Y. G. Y., Frankel, M. B., Missiakas, D. & Schneewind, O. SagB glucosaminidase is a determinant of Staphylococcus aureus glycan chain length, antibiotic susceptibility, and protein secretion. *J. Bacteriol.* (2016). doi:10.1128/JB.00983-15

279. Wheeler, R. *et al.* Bacterial cell enlargement requires control of cell wall stiffness mediated by peptidoglycan hydrolases. *MBio* (2015). doi:10.1128/mBio.00660-15

280. Kajimura, J. *et al.* Identification and molecular characterization of an N-acetylmuramyl-L- alanine amidase Sle1 involved in cell separation of Staphylococcus aureus. *Mol. Microbiol.* (2005). doi:10.1111/j.1365-2958.2005.04881.x

281. Cramton, S. E., Gerke, C., Schnell, N. F., Nichols, W. W. & Götz, F. The intercellular adhesion (ica) locus is present in Staphylococcus aureus and is required for biofilm formation. *Infect. Immun.* (1999). doi:10.1128/iai.67.10.5427-5433.1999

282. Rausch, M. *et al.* Coordination of capsule assembly and cell wall biosynthesis in Staphylococcus aureus. *Nat. Commun.* (2019). doi:10.1038/s41467-019-09356-x

283. Fitzgerald, S. N. & Foster, T. J. Molecular analysis of the tagF gene, encoding CDP-glycerol: Poly(glycerophosphate) glycerophosphotransferase of Staphylococcus epidermidis ATCC 14990. *J. Bacteriol.* (2000). doi:10.1128/JB.182.4.1046-1052.2000

284. Davison, A. L. & Baddiley, J. Teichoic acids in the walls of Staphylococci: Glycerol teichoic acids in walls of Staphylococcus epidermidis. *Nature* (1964). doi:10.1038/202874a0

285. Maity, S., Gundampati, R. K. & Kumar, T. K. S. NMR methods to characterize protein-ligand interactions. *Natural Product Communications* (2019). doi:10.1177/1934578X19849296

286. Choi, Y. *et al.* Structural Insights into the FtsQ/FtsB/FtsL Complex, a Key Component of the Divisome. *Sci. Rep.* (2018). doi:10.1038/s41598-018-36001-2

287. Danguole Kureisaite-Ciziene, A. V. *et al.* Structural Analysis of the Interaction between the Bacterial Cell Division Proteins FtsQ and FtsB. *MBio* **9**, 1–17 (2018).

288. Gonzalez, M. D. & Beckwith, J. Divisome under construction: Distinct domains of the small membrane protein ftsb are necessary for interaction with multiple cell division proteins. *J. Bacteriol.* (2009). doi:10.1128/JB.01597-08

289. Robert, X. & Gouet, P. Deciphering key features in protein structures with the new ENDscript server. *Nucleic Acids Res.* (2014). doi:10.1093/nar/gku316

290. Baumgart, M., Schubert, K., Bramkamp, M. & Frunzke, J. Impact of LytR-CpsA-Psr Proteins on Cell Wall Biosynthesis in Corynebacterium glutamicum. *J. Bacteriol.* **198**, 3045–3059 (2016).

291. Atilano, M. L., Yates, J., Glittenberg, M., Filipe, S. R. & Ligoxygakis, P. Wall teichoic acids of staphylococcus aureus limit recognition by the drosophila peptidoglycan

recognition protein-SA to promote pathogenicity. *PLoS Pathog.* (2011). doi:10.1371/journal.ppat.1002421

292. Atilano, M. L. *et al.* Teichoic acids are temporal and spatial regulators of peptidoglycan cross-linking in Staphylococcus aureus. *Proc. Natl. Acad. Sci. U. S. A.* (2010). doi:10.1073/pnas.1004304107

293. Gutiérrez-Fernández, J. *et al.* Modular Architecture and Unique Teichoic Acid Recognition Features of Choline-Binding Protein L (CbpL) Contributing to Pneumococcal Pathogenesis. *Sci. Rep.* (2016). doi:10.1038/srep38094

294. Jorge, A. M. *et al.* Staphylococcus aureus counters phosphate limitation by scavenging wall teichoic acids from other staphylococci via the teichoicase GlpQ. *J. Biol. Chem.* (2018). doi:10.1074/jbc.RA118.004584

295. Myers, C. L. *et al.* Identification of two phosphate starvation-induced wall teichoic acid hydrolases provides first insights into the degradative pathway of a key bacterial cell wall component. *J. Biol. Chem.* (2016). doi:10.1074/jbc.M116.760447

296. Holtje, J. V. & Tomasz, A. Specific recognition of choline residues in the cell wall teichoic acid by the N acetylmuramyl L alanine amidase of pneumococcus. *J. Biol. Chem.* (1975).

297. Giudicelli, S. & Tomasz, A. Attachment of pneumococcal autolysin to wall teichoic acids, an essential step in enzymatic wall degradation. *J. Bacteriol.* (1984). doi:10.1128/jb.158.3.1188-1190.1984

298. Herbold, D. R. & Glaser, L. Interaction of N acetylmuramic acid L alanine amidase with cell wall polymers. *J. Biol. Chem.* (1975).

299. Holtje, J.-V. & Tomasz, A. Lipoteichoic Acid: A Specific Inhibitor of Autolysin Activity in Pneumococcus. *Proc. Natl. Acad. Sci.* (1975).

300. Matias, V. R. F. & Beveridge, T. J. Cryo-electron microscopy of cell division in Staphylococcus aureus reveals a mid-zone between nascent cross walls. *Mol. Microbiol.* (2007). doi:10.1111/j.1365-2958.2007.05634.x

301. Formstone, A., Carballido-López, R., Noirot, P., Errington, J. & Scheffers, D. J. Localization and interactions of teichoic acid synthetic enzymes in Bacillus subtilis. *J. Bacteriol.* (2008). doi:10.1128/JB.01394-07

302. Bera, A. *et al.* Influence of wall teichoic acid on lysozyme resistance in Staphylococcus aureus. *J. Bacteriol.* (2007). doi:10.1128/JB.01221-06

303. Chan, Y. G. Y., Frankel, M. B., Dengler, V., Schneewind, O. & Missiakasa, D. Staphylococcus aureus mutants lacking the lytr-cpsa-Psr family of enzymes release cell wall teichoic acids into the extracellular medium. *J. Bacteriol.* **195**, 4650–4659 (2013).

304. Jenul, C. & Horswill, A. R. Regulation of Staphylococcus aureus Virulence. *Microbiol. Spectr.* (2018). doi:10.1128/microbiolspec.gpp3-0031-2018

305. Oliveira, D., Borges, A. & Simões, M. Staphylococcus aureus toxins and their molecular activity in infectious diseases. *Toxins* (2018). doi:10.3390/toxins10060252

306. Foster, T. J. Immune evasion by staphylococci. *Nature Reviews Microbiology* (2005). doi:10.1038/nrmicro1289

307. Kim, H. K., Missiakas, D. & Schneewind, O. Mouse models for infectious diseases caused by Staphylococcus aureus. *J. Immunol. Methods* (2014). doi:10.1016/j.jim.2014.04.007

308. Wade, C. M. & Daly, M. J. Genetic variation in laboratory mice. *Nature Genetics* (2005). doi:10.1038/ng1666

309. Malachowa, N., Kobayashi, S. D., Braughton, K. R. & DeLeo, F. R. Mouse model of Staphylococcus aureus skin infection. *Methods Mol. Biol.* (2013). doi:10.1007/978-1-62703-481-4_14

310. Reizner, W. *et al.* A systematic review of animal models for Staphylococcus aureus osteomyelitis. *European Cells and Materials* (2014). doi:10.22203/eCM.v027a15

311. Wertheim, H. F. L. *et al.* The role of nasal carriage in Staphylococcus aureus infections. *Lancet Infectious Diseases* (2005). doi:10.1016/S1473-3099(05)70295-4

312. Coates, R., Moran, J. & Horsburgh, M. J. Staphylococci: Colonizers and pathogens of human skin. *Future Microbiology* (2014). doi:10.2217/fmb.13.145

313. Capparelli, R. *et al.* The staphylococcus aureus peptidoglycan protects mice against the pathogen and eradicates experimentally induced infection. *PLoS One* **6**, (2011).

314. Vinod, N. *et al.* Generation of a novel staphylococcus aureus ghost vaccine and examination of its immunogenicity against virulent challenge in rats. *Infect. Immun.* (2015). doi:10.1128/IAI.00009-15

315. Chen, Y. *et al.* Peptide mimics of peptidoglycan are vaccine candidates and protect mice from infection with Staphylococcus aureus. *J. Med. Microbiol.* **60**, 995–1002 (2011).

316. Wang, X. Y. *et al.* A multiple antigenic peptide mimicking peptidoglycan induced T cell responses to protect mice from systemic infection with Staphylococcus aureus. *PLoS One* **10**, 1–17 (2015).

317. Kim, B. H. *et al.* In staphylococcus aureus, the particulate state of the cell envelope is required for the efficient induction of host defense responses. *Infect. Immun.* (2019). doi:10.1128/IAI.00674-19

318. Jameson, S. C. & Masopust, D. What Is the Predictive Value of Animal Models for Vaccine Efficacy in Humans? *Cold Spring Harb. Perspect. Biol.* (2018). doi:10.1101/cshperspect.a029132

319. Peters, B. M., Jabra-Rizk, M. A., O'May, G. A., William Costerton, J. & Shirtliff, M. E. Polymicrobial interactions: Impact on pathogenesis and human disease. *Clinical Microbiology Reviews* (2012). doi:10.1128/CMR.00013-11

320. McCormack, N., Foster, T. J. & Geoghegan, J. A. A short sequence within subdomain N1 of region A of the Staphylococcus aureus MSCRAMM clumping factor A is required for export and surface display. *Microbiology (United Kingdom)* (2014). doi:10.1099/mic.0.074724-0

321. Mcdevitt, D. *et al.* Characterization of the interaction between the Staphylococcus aureus clumping factor (ClfA) and fibrinogen. *Eur. J. Biochem.* (1997). doi:10.1111/j.1432-1033.1997.00416.x

322. McDevitt, D., Francois, P., Vaudaux, P. & Foster, T. J. Molecular characterization of the clumping factor (fibrinogen receptor) of Staphylococcus aureus. *Mol. Microbiol.* (1994). doi:10.1111/j.1365-2958.1994.tb00304.x

323. Hair, P. S. *et al.* Clumping factor A interaction with complement factor I increases C3b cleavage on the bacterial surface of Staphylococcus aureus and decreases complement-mediated phagocytosis. *Infect. Immun.* (2010). doi:10.1128/IAI.01065-09

324. Hair, P. S., Ward, M. D., Semmes, O. J., Foster, T. J. & Cunnion, K. M.

Staphylococcus aureus Clumping Factor A Binds to Complement Regulator Factor I and Increases Factor I Cleavage of C3b . *J. Infect. Dis.* (2008). doi:10.1086/588825

325. Giersing, B. K., Dastgheyb, S. S., Modjarrad, K. & Moorthy, V. Status of vaccine research and development of vaccines for Staphylococcus aureus. *Vaccine* **34**, 2962–2966 (2016).

326. Hall, A. E. *et al.* Characterization of a Protective Monoclonal Antibody Recognizing Staphylococcus aureus MSCRAMM Protein Clumping Factor A. *Infect. Immun.* (2003). doi:10.1128/IAI.71.12.6864-6870.2003

327. Vernachio, J. *et al.* Anti-Clumping Factor A Immunoglobulin Reduces the Duration of Methicillin-Resistant Staphylococcus aureus Bacteremia in an Experimental Model of Infective Endocarditis. *Antimicrob. Agents Chemother.* (2003). doi:10.1128/AAC.47.11.3400-3406.2003

328. Li, X. *et al.* Preclinical efficacy of clumping factor a in prevention of Staphylococcus aureus infection. *MBio* (2016). doi:10.1128/mBio.02232-15

329. Veloso, T. R. *et al.* Vaccination against Staphylococcus aureus experimental endocarditis using recombinant Lactococcus lactis expressing ClfA or FnbpA. *Vaccine* **33**, 3512–3517 (2015).

330. Levy, J. *et al.* Safety and immunogenicity of an investigational 4-component *Staphylococcus aureus* vaccine with or without AS03 $_B$ adjuvant: Results of a randomized phase I trial. *Hum. Vaccin. Immunother.* **11**, 620–631 (2015).

331. Inoue, M. *et al.* Safety, tolerability, and immunogenicity of a novel 4-antigen Staphylococcus aureus vaccine (SA4Ag) in healthy Japanese adults. *Hum. Vaccines Immunother.* (2018). doi:10.1080/21645515.2018.1496764

332. Bode, C., Zhao, G., Steinhagen, F., Kinjo, T. & Klinman, D. M. CpG DNA as a vaccine adjuvant. *Expert Review of Vaccines* (2011). doi:10.1586/erv.10.174

333. Zhang, F. *et al.* Antibody-mediated protection against Staphylococcus aureus dermonecrosis and sepsis by a whole cell vaccine. *Vaccine* (2017). doi:10.1016/j.vaccine.2017.05.085

334. Hornung, V. *et al.* Silica crystals and aluminum salts mediate NALP-3 inflammsome activation via phagosomal destabilization. *Nat. Immunol.* (2010). doi:10.1038/ni.1631.Silica

335. Joshi, G. N., Goetjen, A. M. & Knecht, D. A. Silica particles cause NADPH oxidase-independent ROS generation and transient phagolysosomal leakage. *Mol. Biol. Cell* (2015). doi:10.1091/mbc.E15-03-0126

336. Xu, M., Wang, Z. & Locksley, R. M. Innate Immune Responses in Peptidoglycan Recognition Protein L-Deficient Mice. *Mol. Cell. Biol.* (2004). doi:10.1128/mcb.24.18.7949-7957.2004

337. Mattsson, E., Herwald, H., Björck, L. & Egesten, A. Peptidoglycan from Staphylococcus aureus induces tissue factor expression and procoagulant activity in human monocytes. *Infect. Immun.* (2002). doi:10.1128/IAI.70.6.3033-3039.2002

338. Mattsson, E., Hartung, T., Morath, S. & Egesten, A. Highly purified lipoteichoic acid from Staphylococcus aureus induces procoagulant activity and tissue factor expression in human monocytes but is a weak inducer in whole blood: Comparison with peptidoglycan. *Infect. Immun.* (2004). doi:10.1128/IAI.72.7.4322-4326.2004

339. Wong, C. H. Y., Jenne, C. N., Petri, B., Chrobok, N. L. & Kubes, P. Nucleation of

platelets with blood-borne pathogens on Kupffer cells precedes other innate immunity and contributes to bacterial clearance. *Nat. Immunol.* (2013). doi:10.1038/ni.2631

340. Surewaard, B. G. J. *et al.* α-Toxin Induces Platelet Aggregation and Liver Injury during Staphylococcus aureus Sepsis. *Cell Host Microbe* (2018). doi:10.1016/j.chom.2018.06.017

341. Haller, D., Serrant, P., Granato, D., Schiffrin, E. J. & Blum, S. Activation of human NK cells by staphylococci and lactobacilli requires cell contact-dependent costimulation by autologous monocytes. *Clin. Diagn. Lab. Immunol.* (2002). doi:10.1128/CDLI.9.3.649-657.2002

342. Zhao, Y. X. & Tarkowski, A. Impact of interferon-gamma receptor deficiency on experimental Staphylococcus aureus septicemia and arthritis. *J. Immunol.* (1995).

343. Tau, G. & Rothman, P. Biologic functions of the IFN-γ receptors. *Allergy: European Journal of Allergy and Clinical Immunology* (1999). doi:10.1034/j.1398-9995.1999.00099.x

344. Guo, Y., Patil, N. K., Luan, L., Bohannon, J. K. & Sherwood, E. R. The biology of natural killer cells during sepsis. *Immunology* (2018). doi:10.1111/imm.12854

345. Mikulak, J., Bruni, E., Oriolo, F., Di Vito, C. & Mavilio, D. Hepatic natural killer cells: Organ-specific sentinels of liver immune homeostasis and physiopathology. *Frontiers in Immunology* (2019). doi:10.3389/fimmu.2019.00946

346. Campbell, D. E. & Kemp, A. S. Proliferation and production of interferon-gamma (IFN-γ) and IL-4 in response to Staphylococcus aureus and Staphylococcal superantigen in childhood atopic dermatitis. *Clin. Exp. Immunol.* (1997). doi:10.1111/j.1365-2249.1997.278-ce1172.x

347. Lacey, K. A., John M. Leech, Stephen J. Lalor, N. M., Geoghegan, J. A. & McLoughlin, R. M. The Staphylococcus aureus Cell Wall- Anchored Protein Clumping Factor A Is an Important T Cell Antigen. *Infect. Immun.* **85**, 1–12 (2017).

348. Hawkins, J. *et al.* A Recombinant Clumping Factor A-Containing Vaccine Induces Functional Antibodies to Staphylococcus aureus That Are Not Observed after Natural Exposure. **19**, 1641–1650 (2012).

349. Gouglas, D. *et al.* Estimating the cost of vaccine development against epidemic infectious diseases: a cost minimisation study. *Lancet Glob. Heal.* (2018). doi:10.1016/S2214-109X(18)30346-2

350. Mäkelä, P. H. Conjugate vaccines - A breakthrough in vaccine development. *Southeast Asian Journal of Tropical Medicine and Public Health* (2003).

351. Shinefield, H. *et al.* Use of a Staphylococcus aureus conjugate vaccine in patients receiving hemodialysis. *N. Engl. J. Med.* (2002). doi:10.1056/NEJMoa011297

352. Bloom, B. *et al.* Multicenter study to assess safety and efficacy of INH-A21, a donor-selected human staphylococcal immunoglobulin, for prevention of nosocomial infections in very low birth weight infants. *Pediatr. Infect. Dis. J.* (2005). doi:10.1097/01.inf.0000180504.66437.1f

353. DeJonge, M. *et al.* Clinical Trial of Safety and Efficacy of IHN-A21 for the Prevention of Nosocomial Staphylococcal Bloodstream Infection in Premature Infants. *J. Pediatr.* (2007). doi:10.1016/j.jpeds.2007.04.060

354. Daniel, T. M. The history of tuberculosis. *Respir. Med.* (2006). doi:10.1016/j.rmed.2006.08.006

355. Warner, D. F., Koch, A. & Mizrahi, V. Diversity and disease pathogenesis in mycobacterium tuberculosis. *Trends in Microbiology* (2015). doi:10.1016/j.tim.2014.10.005

356. Harris, J. B., LaRocque, R. C., Qadri, F., Ryan, E. T. & Calderwood, S. B. Cholera. in *The Lancet* (2012). doi:10.1016/S0140-6736(12)60436-X

357. Ogden, S. A., Ludlow, J. T. & Alsayouri, K. *Diphtheria Tetanus Pertussis (DTaP) Vaccine*. *StatPearls* (2020).

358. Locht, C. Live pertussis vaccines: will they protect against carriage and spread of pertussis? *Clinical Microbiology and Infection* (2016). doi:10.1016/j.cmi.2016.05.029

359. Gibani, M. M., Britto, C. & Pollard, A. J. Typhoid and paratyphoid fever: A call to action. *Current Opinion in Infectious Diseases* (2018). doi:10.1097/QCO.0000000000000479

360. Gonzalez-Escobedo, G., Marshall, J. M. & Gunn, J. S. Chronic and acute infection of the gall bladder by Salmonella Typhi: Understanding the carrier state. *Nat. Rev. Microbiol.* (2011). doi:10.1038/nrmicro2490

361. Dretler, A. W., Rouphael, N. G. & Stephens, D. S. Progress toward the global control of Neisseria meningitidis: 21st century vaccines, current guidelines, and challenges for future vaccine development. *Human Vaccines and Immunotherapeutics* (2018). doi:10.1080/21645515.2018.1451810

362. Kim, G. L., Seon, S. H. & Rhee, D. K. Pneumonia and Streptococcus pneumoniae vaccine. *Archives of Pharmacal Research* (2017). doi:10.1007/s12272-017-0933-y

363. Flasche, S. *et al.* Effect of pneumococcal conjugate vaccination on serotype-specific carriage and invasive disease in England: A cross-sectional study. *PLoS Med.* (2011). doi:10.1371/journal.pmed.1001017

364. Agrawal, A. & Murphy, T. F. Haemophilus influenzae infections in the H. influenzae type b conjugate vaccine era. *Journal of Clinical Microbiology* (2011). doi:10.1128/JCM.05476-11

365. Bienek, D. R., Loomis, L. J. & Biagini, R. E. The anthrax vaccine: No new tricks for an old dog. *Hum. Vaccin.* (2009). doi:10.4161/hv.5.3.7308

366. Narita, K., Asano, K. & Nakane, A. IL-17A plays an important role in protection induced by vaccination with fibronectin-binding domain of fibronectin- binding protein A against Staphylococcus aureus infection. *Med. Microbiol. Immunol.* **0**, 0 (2017).

367. Joshi, A. *et al.* Immunization with Staphylococcus aureus iron regulated surface determinant B (IsdB) confers protection via Th17/IL17 pathway in a murine sepsis model. *Hum. Vaccines Immunother.* (2012). doi:10.4161/hv.8.3.18946

368. Jacobsson, G., Gustafsson, E. & Andersson, R. Outcome for invasive Staphylococcus aureus infections. *Eur. J. Clin. Microbiol. Infect. Dis.* (2008). doi:10.1007/s10096-008-0515-5

369. Asgeirsson, H., Thalme, A. & Weiland, O. Staphylococcus aureus bacteraemia and endocarditis–epidemiology and outcome: a review. *Infectious Diseases* (2018). doi:10.1080/23744235.2017.1392039

370. Martiñón, S. *et al.* Chemical and immunological characteristics of aluminum-based, oil-water emulsion, and bacterial-origin adjuvants. *Journal of Immunology Research* (2019). doi:10.1155/2019/3974127

371. Balraadjsing, P. P. *et al.* The nature of antibacterial adaptive immune responses

against staphylococcus aureus is dependent on the growth phase and extracellular peptidoglycan. *Infect. Immun.* (2020). doi:10.1128/IAI.00733-19

372. Martinic, M. M. *et al.* The Bacterial Peptidoglycan-Sensing Molecules NOD1 and NOD2 Promote CD8 + Thymocyte Selection . *J. Immunol.* (2017). doi:10.4049/jimmunol.1601462

373. Fink, M. P. & Heard, S. O. Laboratory models of sepsis and septic shock. *J. Surg. Res.* (1990). doi:10.1016/0022-4804(90)90260-9

374. Poli-de-Figueiredo, L. F., Garrido, A. G., Nakagawa, N. & Sannomiya, P. Experimental models of sepsis and their clinical relevance. in *Shock* (2008). doi:10.1097/SHK.0b013e318181a343

375. Netea, M. G., Quintin, J. & Van Der Meer, J. W. M. Trained immunity: A memory for innate host defense. *Cell Host and Microbe* (2011). doi:10.1016/j.chom.2011.04.006

376. Chan, L. C. *et al.* Protective immunity in recurrent Staphylococcus aureus infection reflects localized immune signatures and macrophage-conferred memory. *Proc. Natl. Acad. Sci. U. S. A.* (2018). doi:10.1073/pnas.1808353115

377. Rooijen, N. Van & Sanders, A. Liposome mediated depletion of macrophages: mechanism of action, preparation of liposomes and applications. *J. Immunol. Methods* (1994). doi:10.1016/0022-1759(94)90012-4

378. Hansen, M. L. U. *et al.* Diabetes increases the risk of disease and death due to Staphylococcus aureus bacteremia. A matched case-control and cohort study. *Infect. Dis. (Auckl).* (2017). doi:10.1080/23744235.2017.1331463

379. Fruchtman, Y., Perry, Z. H. & Levy, J. Morbidity characteristics of patients with congenital insensitivity to pain with anhidrosis (CIPA). *J. Pediatr. Endocrinol. Metab.* (2013). doi:10.1515/jpem-2012-0151

380. Indo, Y. *et al.* Mutations in the TRKA/NGF receptor gene in patients with congenital insensitivity to pain with anhidrosis. *Nat. Genet.* (1996). doi:10.1038/ng0896-485

381. Levi-Montalcini, R. The nerve growth factor 35 years later. *Science (80-.).* (1987). doi:10.1126/science.3306916

382. Laudiero, L. B. *et al.* Multiple sclerosis patients express increased levels of β-nerve growth factor in cerebrospinal fluid. *Neurosci. Lett.* (1992). doi:10.1016/0304-3940(92)90762-V

383. Aloe, L., Tuveri, M. A., Carcassi, U. & Levi-Montalcini, R. Nerve growth factor in the synovial fluid of patients with chronic arthritis. *Arthritis Rheum.* (1992). doi:10.1002/art.1780350315

384. Aloe, L. & Levi-Montalcini, R. Mast cells increase in tissues of neonatal rats injected with the nerve growth factor. *Brain Res.* (1977). doi:10.1016/0006-8993(77)90772-7

385. Caroleo, M. C., Costa, N., Bracci-Laudiero, L. & Aloe, L. Human monocyte/macrophages activate by exposure to LPS overexpress NGF and NGF receptors. *J. Neuroimmunol.* (2001). doi:10.1016/S0165-5728(00)00441-0

386. Noga, O. *et al.* Activation of the specific neurotrophin receptors TrkA, TrkB and TrkC influences the function of eosinophils. *Clin. Exp. Allergy* (2002). doi:10.1046/j.1365-2745.2002.01442.x

387. Bürgi, B. *et al.* Basophil Priming by Neurotrophic Factors: Activation Through the trk Receptor. *J. Immunol.* (1996).

388. Lambiase, A. *et al.* Human CD4+ T cell clones produce and release nerve growth factor and express high-affinity nerve growth factor receptors. *J. Allergy Clin. Immunol.* (1997). doi:10.1016/S0091-6749(97)70256-2

389. Torcia, M. *et al.* Nerve growth factor is an autocrine survival factor for memory B lymphocytes. *Cell* (1996). doi:10.1016/S0092-8674(00)81113-7

390. Prencipe, G. *et al.* Nerve Growth Factor Downregulates Inflammatory Response in Human Monocytes through TrkA. *J. Immunol.* (2014). doi:10.4049/jimmunol.1300825

391. Garaci, E. *et al.* Nerve growth factor is an autocrine factor essential for the survival of macrophages infected with HIV. *Proc. Natl. Acad. Sci. U. S. A.* (1999). doi:10.1073/pnas.96.24.14013

392. Van Der Vaart, M., Spaink, H. P. & Meijer, A. H. Pathogen recognition and activation of the innate immune response in zebrafish. *Advances in Hematology* (2012). doi:10.1155/2012/159807

393. Wirz, S. A., Tobias, P. S., Ulevitch, R. J., Aribibe, L. & Bartfai, T. TLR2 is required for the altered transcription of p75NGF receptors in gram positive infection. *Neurochem. Res.* (2006). doi:10.1007/s11064-005-9020-8

394. Pérez-Pérez, M. *et al.* p75NTR in the spleen: Age-dependent changes, effect of NGF and 4-methylcatechol treatment, and structural changes in p75 NTR-deficient mice. *Anat. Rec. - Part A Discov. Mol. Cell. Evol. Biol.* (2003). doi:10.1002/ar.a.10010

395. Gu, H., Marth, J. D., Orban, P. C., Mossmann, H. & Rajewsky, K. Deletion of a DNA polymerase β gene segment in T cells using cell type-specific gene targeting. *Science (80-.).* (1994). doi:10.1126/science.8016642

396. Clausen, B. E., Burkhardt, C., Reith, W., Renkawitz, R. & Förster, I. Conditional gene targeting in macrophages and granulocytes using LysMcre mice. *Transgenic Res.* (1999). doi:10.1023/A:1008942828960

397. Minnone, G., De Benedetti, F. & Bracci-Laudiero, L. NGF and its receptors in the regulation of inflammatory response. *International Journal of Molecular Sciences* (2017). doi:10.3390/ijms18051028

398. Abdallah, F., Mijouin, L. & Pichon, C. Skin Immune Landscape: Inside and Outside the Organism. *Mediators of Inflammation* (2017). doi:10.1155/2017/5095293

399. Nguyen, A. V. & Soulika, A. M. The dynamics of the skin's immune system. *International Journal of Molecular Sciences* (2019). doi:10.3390/ijms20081811

400. Holladay, S. D. & Smialowicz, R. J. Development of the murine and human immune system: Differential effects of immunotoxicants depend on time of exposure. *Environ. Health Perspect.* (2000). doi:10.2307/3454538

401. Holsapple, M. P., West, L. J. & Landreth, K. S. Species comparison of anatomical and functional immune system development. *Birth Defects Research Part B - Developmental and Reproductive Toxicology* (2003). doi:10.1002/bdrb.10035

402. Schulz, D. *et al.* Laboratory mice are frequently colonized with Staphylococcus aureus and mount a systemic immune response-note of caution for in vivo infection experiments. *Front. Cell. Infect. Microbiol.* (2017). doi:10.3389/fcimb.2017.00152

403. Pozzi, C. *et al.* Phagocyte subsets and lymphocyte clonal deletion behind ineffective immune response to Staphylococcus aureus. *FEMS Microbiol. Rev.* **39**, 750–763 (2015).

404. Mosser, D. M. & Edwards, J. P. Exploring the full spectrum of macrophage activation.

Nature Reviews Immunology (2008). doi:10.1038/nri2448

405. Vannella, K. M. *et al.* Incomplete Deletion of IL-4Rα by LysMCre Reveals Distinct Subsets of M2 Macrophages Controlling Inflammation and Fibrosis in Chronic Schistosomiasis. *PLoS Pathog.* (2014). doi:10.1371/journal.ppat.1004372

406. Luo, W., Xu, Q., Wang, Q., Wu, H. & Hua, J. Effect of modulation of PPAR-γ activity on Kupffer cells M1/M2 polarization in the development of non-alcoholic fatty liver disease. *Sci. Rep.* (2017). doi:10.1038/srep44612

407. Peng, K. T. *et al.* Staphylococcus aureus biofilm elicits the expansion, activation and polarization of myeloid-derived suppressor cells in vivo and in vitro. *PLoS One* (2017). doi:10.1371/journal.pone.0183271

408. Rasi, G. *et al.* Nerve growth factor involvement in liver cirrhosis and hepatocellular carcinoma. *World J. Gastroenterol.* (2007). doi:10.3748/wjg.v13.i37.4986

409. Proctor, R. A. Recent developments for Staphylococcus aureus vaccines: Clinical and basic science challenges. *Eur. Cells Mater.* **30**, 315–326 (2015).

410. Luna, B. M. *et al.* Vaccines targeting Staphylococcus aureus skin and bloodstream infections require different composition. *PLoS One* (2019). doi:10.1371/journal.pone.0217439

411. Giedraitiene, A., Vitkauskiene, A., Naginiene, R. & Pavilonis, A. Antibiotic resistance mechanisms of clinically important bacteria. *Medicina* (2011). doi:10.3390/medicina47030019

412. Singh, D. *et al.* SB-RA-2001 inhibits bacterial proliferation by targeting FtsZ assembly. *Biochemistry* (2014). doi:10.1021/bi401356y

413. Groundwater, P. W. *et al.* A Carbocyclic Curcumin Inhibits Proliferation of Gram-Positive Bacteria by Targeting FtsZ. *Biochemistry* (2017). doi:10.1021/acs.biochem.6b00879

414. Haydon, D. J. *et al.* An inhibitor of FtsZ with potent and selective anti-staphylococcal activity. *Science (80-.).* (2008). doi:10.1126/science.1159961

415. Campbell, J. *et al.* An antibiotic that inhibits a late step in wall teichoic acid biosynthesis induces the cell wall stress stimulon in Staphylococcus aureus. *Antimicrob. Agents Chemother.* (2012). doi:10.1128/AAC.05938-11

416. Chien, A. C., Zareh, S. K. G., Wang, Y. M. & Levin, P. A. Changes in the oligomerization potential of the division inhibitor UgtP co-ordinate Bacillus subtilis cell size with nutrient availability. *Mol. Microbiol.* (2012). doi:10.1111/mmi.12007

417. Kiriukhin, M. Y., Debabov, D. V., Shinabarger, D. L. & Neuhaus, F. C. Biosynthesis of the glycolipid anchor in lipoteichoic acid of Staphylococcus aureus RN4220: Role of YpfP, the diglucosyldiacylglycerol synthase. *J. Bacteriol.* (2001). doi:10.1128/JB.183.11.3506-3514.2001

418. Delaune, A. *et al.* Peptidoglycan crosslinking relaxation plays an important role in staphylococcus aureus walkr-dependent cell viability. *PLoS One* (2011). doi:10.1371/journal.pone.0017054

419. Suzuki, T. *et al.* Wall teichoic acid protects Staphylococcus aureus from inhibition by Congo red and other dyes. *J. Antimicrob. Chemother.* (2012). doi:10.1093/jac/dks184

420. Heifetz, A., Keenan, R. W. & Elbein, A. D. Mechanism of Action of Tunicamycin on the UDP-GlcNAc:Dolichyl-Phosphate GlcNAc-1 -Phosphate Transferase. *Biochemistry* **18**, 2186–2192 (1979).

421. Price, N. P. J. *et al.* Modified tunicamycins with reduced eukaryotic toxicity that enhance the antibacterial activity of β-lactams. *J. Antibiot. (Tokyo).* (2017). doi:10.1038/ja.2017.101

422. Baur, S. *et al.* A Nasal Epithelial Receptor for Staphylococcus aureus WTA Governs Adhesion to Epithelial Cells and Modulates Nasal Colonization. *PLoS Pathog.* (2014). doi:10.1371/journal.ppat.1004089

423. Misawa, Y. *et al.* Staphylococcus aureus Colonization of the Mouse Gastrointestinal Tract Is Modulated by Wall Teichoic Acid, Capsule, and Surface Proteins. *PLoS Pathog.* (2015). doi:10.1371/journal.ppat.1005061

424. Winstel, V. *et al.* Wall teichoic acid glycosylation governs Staphylococcus aureus nasal colonization. *MBio* (2015). doi:10.1128/mBio.00632-15

425. Gerlach, D. *et al.* Methicillin-resistant Staphylococcus aureus alters cell wall glycosylation to evade immunity. *Nature* **563**, 705–709 (2018).

426. Fong, R. *et al.* Structural investigation of human S. aureus-targeting antibodies that bind wall teichoic acid. *MAbs* (2018). doi:10.1080/19420862.2018.1501252

427. Tang, J., Hui, J., Ma, J. & Mingquan, C. Nasal decolonization of Staphylococcus aureus and the risk of surgical site infection after surgery: a meta-analysis. *Ann. Clin. Microbiol. Antimicrob.* **19**, 33 (2020).

428. Shittu, A. O. *et al.* Mupirocin-resistant Staphylococcus aureus in Africa: A systematic review and meta-analysis. *Antimicrobial Resistance and Infection Control* (2018). doi:10.1186/s13756-018-0382-5

429. Kurugöl, Z. Pneumococcal vaccines. *Turk Pediatr. Ars.* **42**, 43–50 (2007).

430. Regev-Yochay, G. *et al.* Association between carriage of Streptococcus pneumoniae and Staphylococcus aureus in children. *J. Am. Med. Assoc.* (2004). doi:10.1001/jama.292.6.716

431. Bogaert, D. *et al.* Colonisation by Streptococcus pneumoniae and Staphylococcus aureus in healthy children. *Lancet* (2004). doi:10.1016/S0140-6736(04)16357-5

Appendix- Supplementary Figures

A

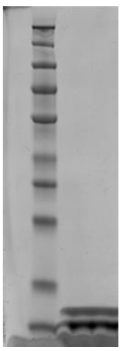

B

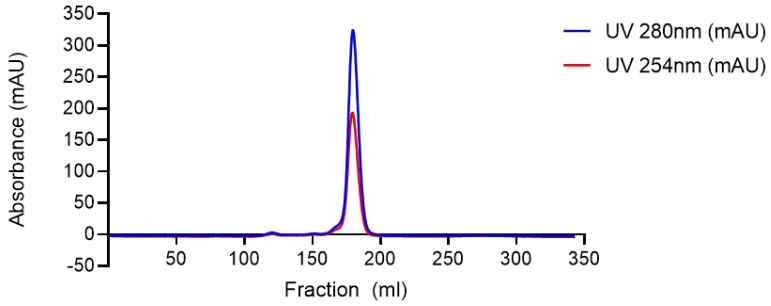

Supplementary Figure 1 Purity of recombinant DivIC as ascertained by SDS-PAGE & Size exclusion chromatography
Recombinant His-tagged DivIC (Lys56 to Lys130) was produced in *E. coli* and purified by Ni^{2+} affinity chromatography then analysed by 12%(w/v) SDS-PAGE to assess its purity (A). This was then further purified by size exclusion chromatography using a Superdex™ 200 10/300 GL column and protein elution was measured by UV absorbance (B).

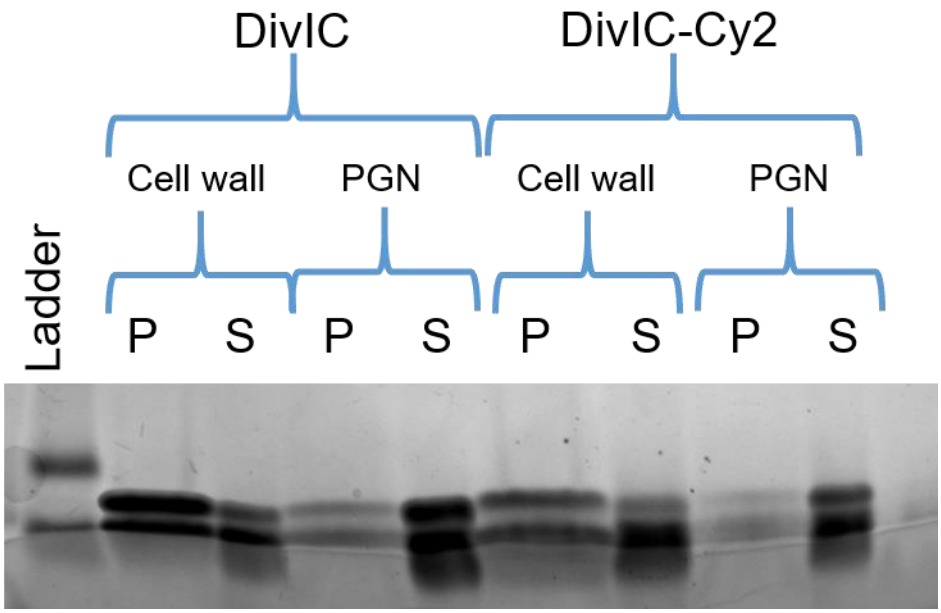

Supplementary Figure 2 DivIC-Cy2 preferentially binds cell wall as native DivIC

1mg/ml of SH1000 cell wall or peptidoglycan (PGN) was incubated with 0.1mg/ml (~10µM) DivIC or DivIC-Cy2 in binding buffer (20mM sodium citrate, 10mM $MgCl_2$, 0.1%(v/v) Tween, 10µg/ml BSA, pH 5). These mixtures were centrifuged and the insoluble pellet (P) and soluble supernatant (S) fractions were separated, boiled in SDS-PAGE loading buffer containing 10%(v/v) 2-mercaptoethanol and analysed by 12%(w/v) SDS-PAGE.

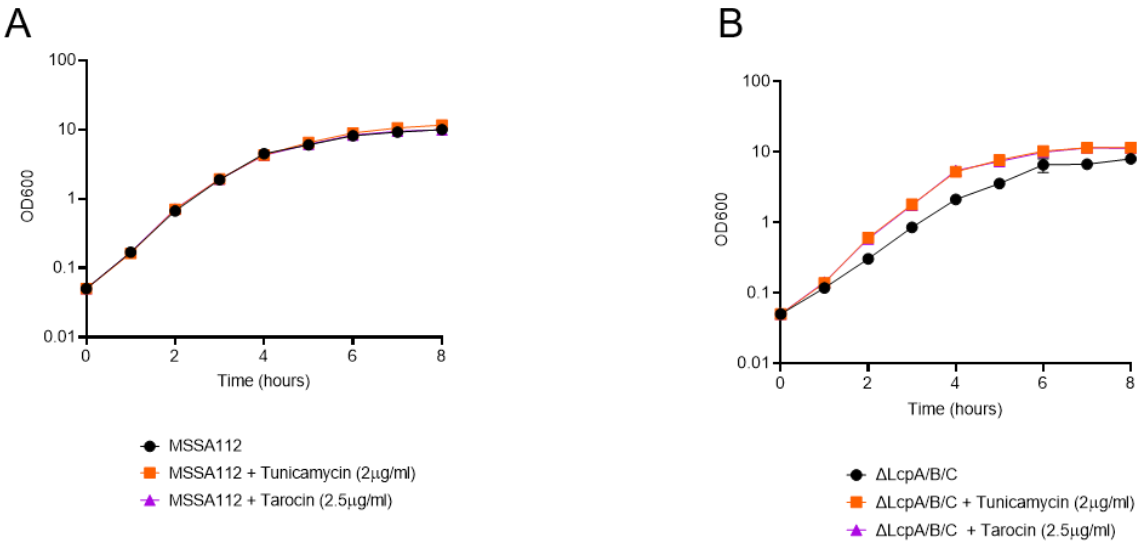

Supplementary Figure 3. Tunicamycin and Tarocin do not negatively affect the growth of MSSA112 or the *lcp* triple knockout

MSSA112 and triple *lcp* knockout cells were grown overnight then sub-cultured into pre-warmed media containing no drugs, 2µg/ml of tunicamycin or 2.5µg/ml of tarocin to an OD_{600} of 0.05. Cultures were grown at 37°C and 250rpm. OD_{600} was measured hourly. OD_{600} shown as mean.

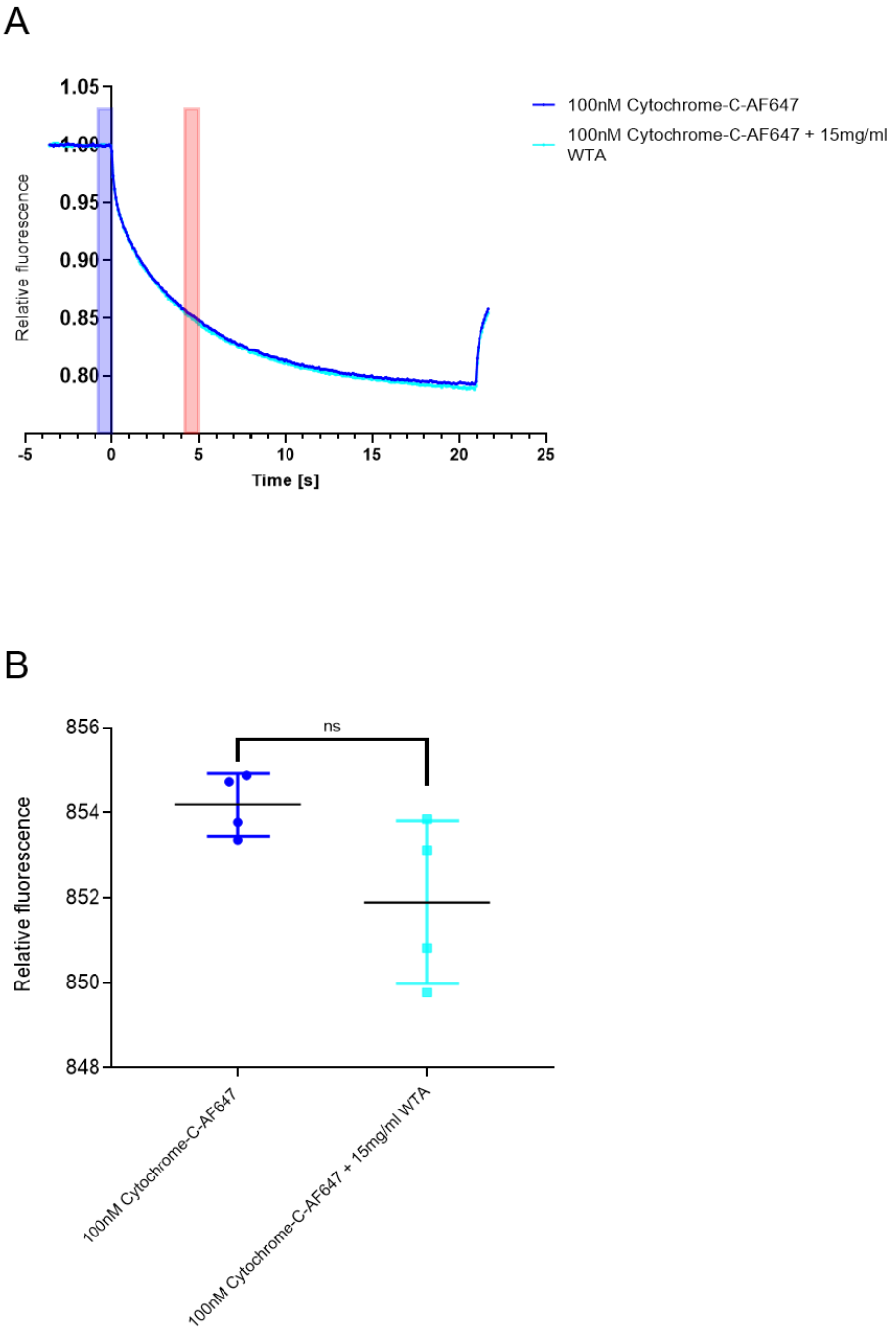

Supplementary Figure 4 Cytochrome C does not bind soluble WTA
100nM Cytochrome-C-AF647 was incubated in binding buffer (20mM sodium citrate, 10mM $MgCl_2$, 0.1%(v/v) Tween, 10µg/ml BSA, pH 5) with 15mg/ml (cyan) of LTA isolated from *S. aureus* (Sigma). This mixture and Cytochrome-C-AF647 alone in the same buffer were loaded into premium capillary tubes and loaded into a Nanotemper monolith microscale thermophoresis machine. The binding check

protocol was performed with the MST power at medium and red LED-mediated excitation set at 60%. The trace shows the difference between change in detected fluorescence of DivIC-AF647 alone (blue) and DivIC-AF647 with 15mg/ml WTA (cyan) over time (A) and the difference in the demarcated 5th second (red) plotted in B. Relative Fluorescence shown as mean with Std Dev in B.

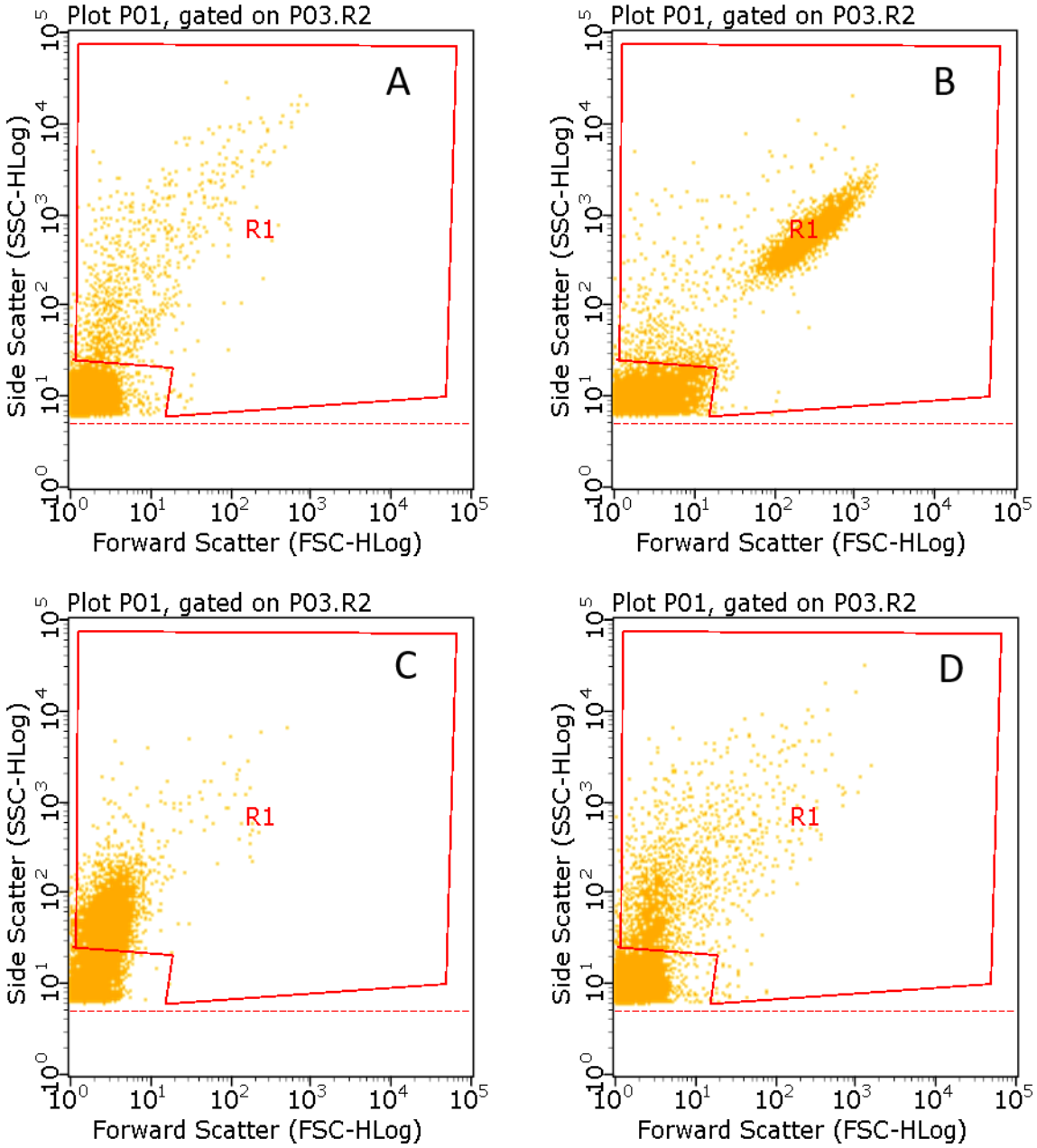

Supplementary Figure 5 Flow Cytometry gating plot for peptidoglycan
Flow Cytometry plots comparing Forward and Side Scatter of PBS (A), *S. aureus* cells (B) and *M. luteus* peptidoglycan preparations before (C) and after (D) freeze drying. Points outside the red gated area were excluded from further analysis as this was considered background noise.

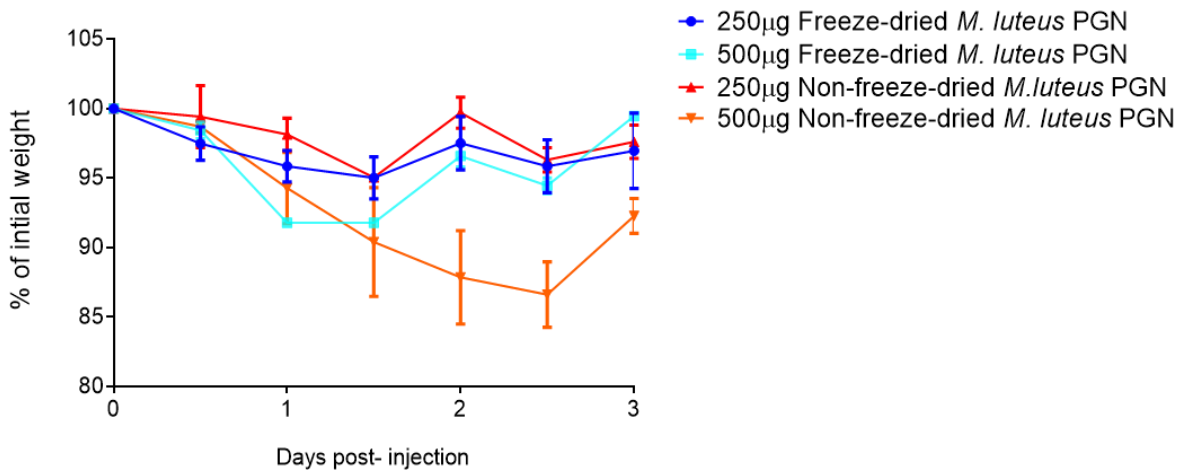

Supplementary Figure 6 Dosing analysis of freeze-dried vs non-freeze-dried *M. luteus* peptidoglycan
2 mice per group were intravenously injected with 250µg (dark blue & red) or 500µg (light blue & orange) of *M. luteus* peptidoglycan which had (blues) or had not (red & orange) been previously freeze-dried. Mice were weighted twice daily and culled on day 3 post-injection. Weights shown as mean and Std Dev.

Protein sequence coverage: 52%

Matched peptides shown in ***bold red***.

```
  1 HHHHHHENSV TQSDSASNES KSNDSSSVSA APKTDDTNVS DTKTSSNTNN
 51 GETSVAQNPA QQETTQSSST NATTEETPVT GEATTTTTNQ ANTPATTQSS
101 NTNAEELVNQ TSNETTSNDT NTVSSVNSPQ NSTNAENVST TQDTSTEATP
151 SNNESAPQST DASNKDVVNQ AVNTSAPRMR AFSLAAVAAD APVAGTDITN
201 QLTNVTVGID SGTTVYPHQA GYVKLNYGFS VPNSAVKGDT FKITVPKELN
251 LNGVTSTAKV PPIMAGDQVL ANGVIDSDGN VIYTFTDYVN TKDDVKATLT
301 MPAYIDPENV KKTGNVTLAT GIGSTTANKT VLVDYEKYGK FYNLSIKGTI
351 DQIDKTNNTY RQTIYVNPSG DNVIAPVLTG NLKPNTDSNA LIDQQNTSIK
401 VYKVDNAADL SESYFVNPEN FEDVTNSVNI TFPNPNQYKV EFNTPDDQIT
451 TPYIVVVNGH IDPNSKGDLA LRSTLYGYNS NIIWRSMSWD NEVAFNNGSG
501 SGDGIDKPVV PEQPDEPGEI EPIPE
```

Supplementary Figure 7 Mass spectrometry verification of recombinant ClfA
Recombinant, FPLC purified ClfA was analysed using liquid chromatography LC–MS/MS following tryptic digestion. The Mascot software search engine (Matrix Science) was employed to process the mass spectrometry data to identify proteins from the peptide sequence reference database for *Escherichia coli* (UniProt Proteome ID: UP000000625; 4391 entries; downloaded on 26/08/2020). The sequence of the recombinant ClfA protein was included as an additional entry to this reference proteome ClfA was identified and the matched peptides are shown in red against the full-length amino acid sequence of the recombinant protein.

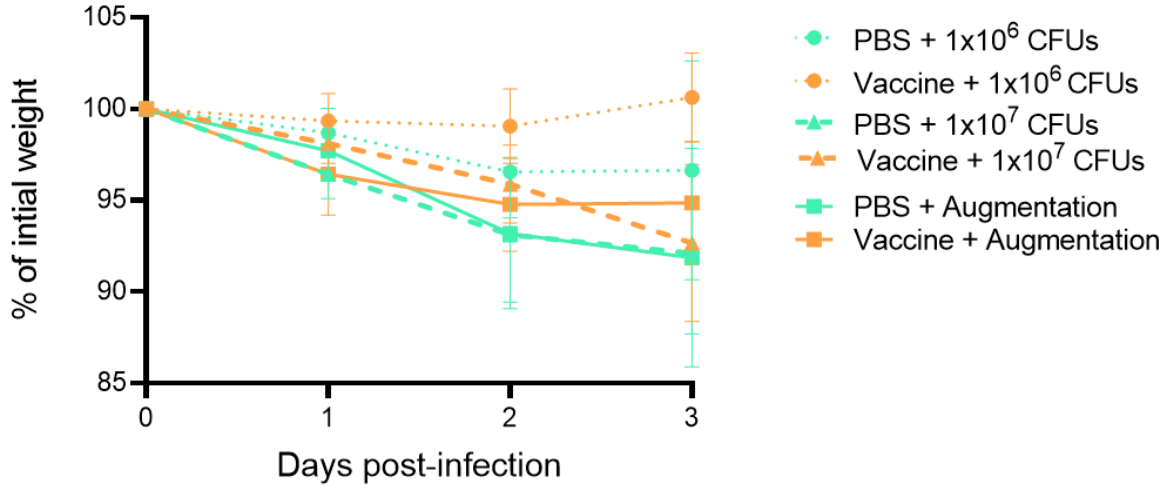

Supplementary Figure 8 Effect of vaccination with or without peptidoglycan on weight loss through the course of infection
Mice were vaccinated subcutaneously on day 0, 14 and 21 with sterile endotoxin free PBS as a negative control (green) or a vaccine consisting of 1µg ClfA, 50µg CpG and 1%(w/v) Alum (orange. On day 28 post-vaccination mice were intravenously injected with low dose *S. aureus* ($1x10^6$ CFU), high dose *S. aureus* ($1x10^7$ CFU) or a mixture of low dose *S. aureus* ($5x10^5$ CFU) and 250µg *M. luteus* peptidoglycan. Mice were weighed daily and on day 3 post-infection mice were sacrificed. Weights shown as mean and Std Dev.

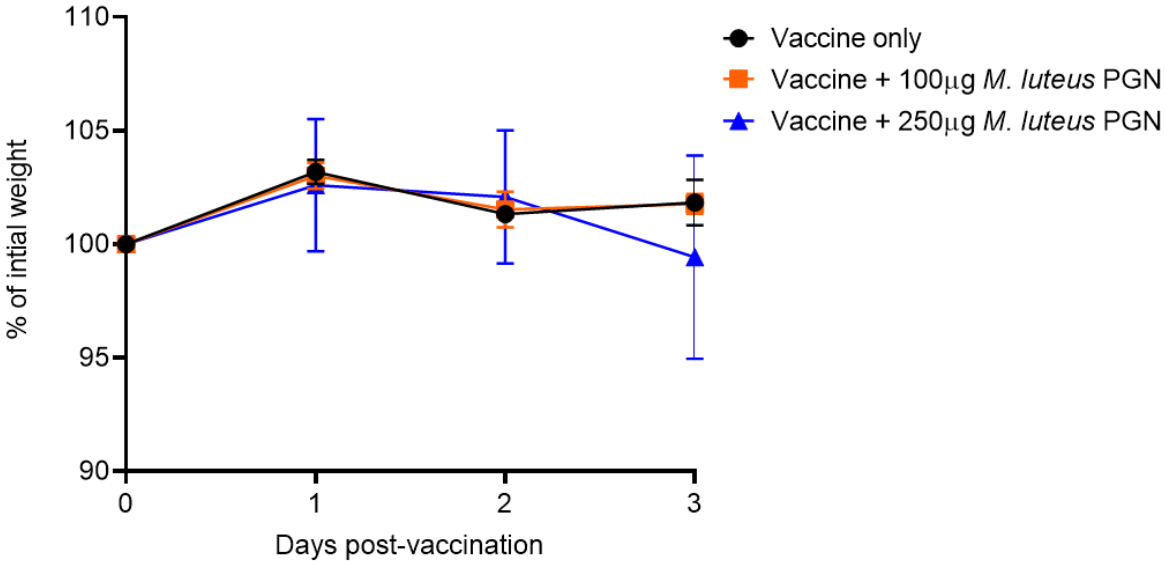

Supplementary Figure 9 Dosing analysis for peptidoglycan inclusion in vaccine
Female balb/C Mice were subcutaneously injected with a vaccine consisting of 1%(w/v) Alum, 1µg ClfA, 50µg CpG alone (black) or with the addition of 100µg (orange) or 250µg (blue) of *M. luteus* peptidoglycan. Mice were weighed daily and culled on day 3 post-injection. Weights shown as mean and Std Dev.

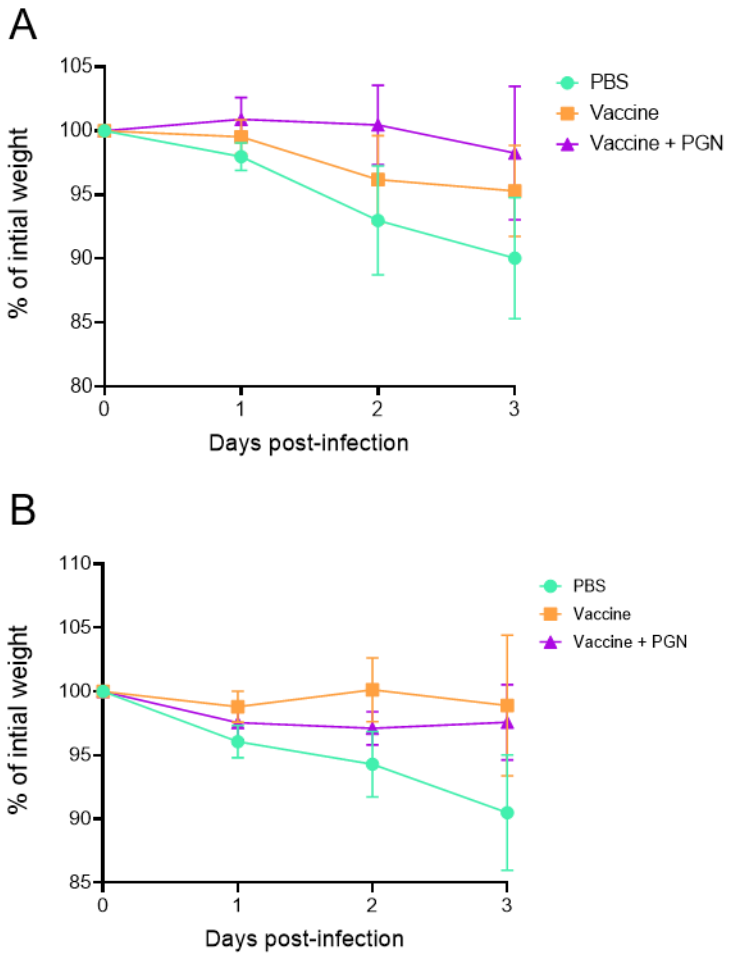

Supplementary Figure 10. Effect of vaccination with or without peptidoglycan on weight loss through the course of infection

Mice were vaccinated subcutaneously on day 0, 14 and 21 with sterile endotoxin free PBS as a negative control (green), a vaccine consisting of 1µg ClfA, 50µg CpG and 1%(w/v) Alum (orange) or the same vaccine with an additional 100µg of *M. luteus* peptidoglycan (purple) On day 28 post-vaccination mice were intravenously injected with (A) *S. aureus* alone ($5x10^6$ CFU) or (B) a mixture of low dose *S. aureus* ($5x10^5$ CFU) and 250µg *M. luteus* peptidoglycan. Mice were weighed daily and on day 3 post-infection mice were sacrificed. Weights shown as mean and Std Dev.